ISSN: 2958-8995. 2958-8987
Doi: 10.59799/APPP6605
No: 4 Val:1/December/ 2023

Journal of Natural and Applied Sciences URAL

A Quarterly Multidisciplinary Scientific Journal Issued by European Academy for Development and Research / Brussels and Center of Research and Human Resources Development Ramah- Jordan

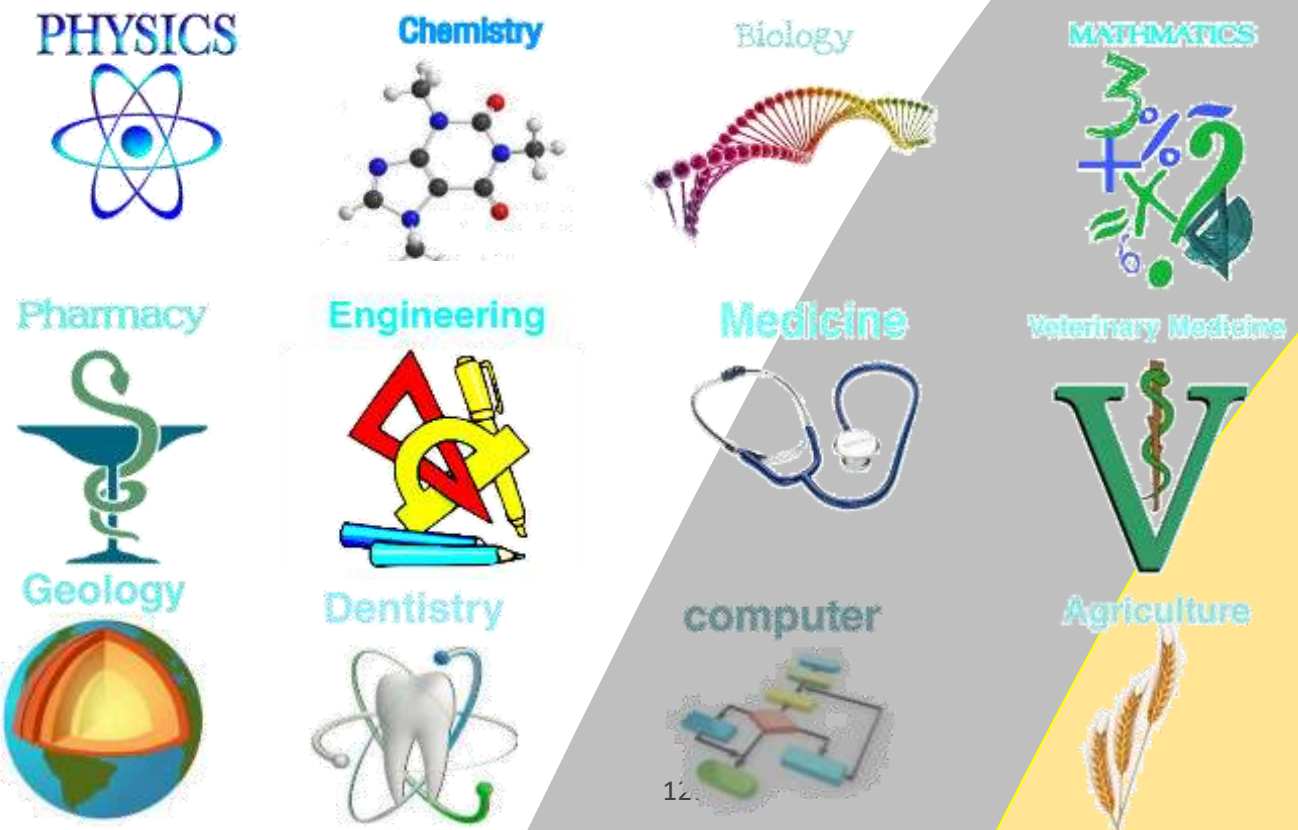

Focus & Scope:

Journal of Natural and Applied Sciences URAL

Journal welcomes high quality contributions investigating topics in the fields of Biology, physics, computer science, Engineering, chemistry, Geology, Agriculture, Medicine, Mathematics, Pharmacy, Veterinary, Nursing, Dentistry, and Environment.

Publication specializations in the journal	
Biology	**Chemistry**
Physics	**Geology**
Computer	**Agriculture**
Engineering	**Mathematics**
Medicine	**Pharmacy**
Veterinary	**Dentistry Veternity,**
Environment	**Nursing**

The Journal is Published in English and Arabic

General Supervisor of the Journal

Prof. Dr. Khalid Ragheb Ahmed Al-Khatib

Head of the Center for Research and Human

Resources Development Ramah – Jordan

Managing Director:

Dr. Mosaddaq Ameen Ateah AL – Doori

Linguistic Reviewer Team

Prof. Dr. Lamiaa Ahmed Rasheed

Tikrit University/College of Education for Women

Asst. Prof. Ahmed Khalid Hasoon

Tikrit University/ College of Education for Women

Asst. Prof. Dr. Mohammad Burjess

Tikrit University/ College of Education

Administrative Title of the Journal:

Amman\ Jordan\ Wasfi Al-Tal \ Gardens

Phone: +962799424774

Index

Certain programs of differential subordination to univalent functions determined by the integral operator

Mustafa I. Hameed [1*],
Shaheed Jameel al-Dulaimi [2],
Ismael I. Hameed [3],
Israa A. Ibrahim [4],
Hussaini Joshua [5]

[1] University of Anbar, College of Education for Pure Sciences, Department of Mathematics, Ramadi-Iraq
mustafa8095@uoanbar.edu.iq
[2] al- Maarif University College, Department of computer science, Ramadi, Iraq
[3] Ministry of Education, General Directorate of Education in Anbar Governorate, Anbar, Iraq
[4] Department of Science, College of Open Education, Kirkuk Education Directorate, Kirkuk, Iraq
[5] Department of Mathematical Sciences, Faculty of Science, University of Maiduguri, Nigeria

Certain programs of differential subordination to univalent functions determined by the integral operator

Mustafa I. Hameed [1*], Shaheed Jameel al-Dulaimi [2], Ismael I. Hameed [3], Israa A. Ibrahim [4], Hussaini Joshua [5]

[1] University of Anbar, College of Education for Pure Sciences, Department of Mathematics, Ramadi-Iraq
mustafa8095@uoanbar.edu.iq
[2] Department of computer science, al- Maarif University College, Ramadi, Iraq
[3] Ministry of Education, General Directorate of Education in Anbar Governorate, Anbar, Iraq
[4] Department of Science, College of Open Education, Kirkuk Education Directorate, Kirkuk, Iraq
[5] Department of Mathematical Sciences, Faculty of Science, University of Maiduguri, Nigeria

ABSTRACT

The goal of the article is to present certain uses of the differential subordination the idea on subclasses of univalent functions that include certain convolution as a operators. Numerous complicated mathematical investigators, such as Euler, Gauss, Riemann, Cauchy, as well as a number of others have grown throughout this period. Analysis as well as geometry come together or interact in geometric function theory. The above paper's primary goals are to study the dependence principle as well as to add an additional subset over polyvalent functions via an additional operator that is connected to derivatives products of higher order. In light of the different geometric properties, including coefficient estimation, deformation and expansion bounds, radii for strlikeness, convexity, as well as close-to-convexity, the results were significant. As an these classes of functions, that we investigate geometric characteristics such as coefficient bounds, distortion theorem, as well as radii of starlikeness as well as convexity. The integral operator and extreme points have been looked into.

Key words: Differential Subordination, Univalent Function, Extreme Points, Hadamard Product, Analytic Function, Convex and Starlike Functions, Distortion Theorem, Integral Operator.

1. INTRODUCTION

With the help provided by the Hadamard product that represents the fundamental higher-order products of differential subordination for diverse functions, the study's goal is to be able to investigate an additional category of multivalent functions referred to as a novel linear operator as well as start examining the fresh linear operator. As an higher-order products of variations subordination within the open unit disk, multiple outcomes will be obtained by utilizing the universal hypergeometric function as well as the characteristics associated with the generalized a byproduct operator.
The Bieberbach speculation, commonly referred to as the value of the coefficient issue, served as the main stimulus over this type of reasoning because it provided a ton of room for advancement between 1916 and De Branges's successful resolution of the issue in 1985, resulting in to an enormous number of conclusions centered on the speculation. that time then, Geometry Function Theory continues to be treated independently. One popular subject was geometric function theory. Regardless of that, it still finds new uses in a variety of disciplines, such as contemporary computational physics, medical science, engineering, and various other areas, as well as in more conventional physics areas such as fluid mechanics, not linear compatible systems theory, as well as the study of partial differential equation theory. The company geometric function is a function that's used within complex analysis outlines particular geometries.

We have demonstrated a correlation between the subclass and higher-order products of diverse functions. Results concerning harmonious multivalent functions determined by operators with differential properties are very interesting. The investigation of the analyzing univalent function subclass related to the notion of variations subordination. We looked at certain outcomes of variations subordination as well as superordination including a particular class that focuses upon the domain of univalent meromorphic functions within a wide unit disc.

Particularly, this area has caught the attention of several investigators in practical science within an assortment of circumstances. The precise solution over computational modeling, including in the analysis of physical, chemical, as well as engineering areas, is also determined in part by these concepts [1-3].

Many of the key ideas for complicated evaluation is the notion of harmonically along with analytical [4] univalent mathematical functions (bi or multi-types) [5-8]. In order to establish fresh, intriguing categories or subclasses of special functions associated to multiple operators [9-12] who could be optimized or improve a few actual issues by applying a particular functional household arising about the notion of conventional functions by means of specific characteristics of complicated functions [13-16], some special components have been described with this framework of theory.

Take $\mathcal{A}$ represent the function classℓ in the shape of

$$\ell(\nu) = \sum_{\iota=1}^{\infty} e_\iota \, \nu^\iota \, , (e_\iota > 0 \, , \nu \in \phi) \qquad (1)$$

that serves as analytic within the disk unit $\phi = \{\nu \in \mathbb{C} : |\nu| < 1\}$. A function ℓ being related to class $\mathcal{A}$ is believed to be starlike (convex) in shape $\phi(r)$ if: [17-20]

$$\Re e\left\{\frac{\nu\ell'(\nu)}{\ell(\nu)}\right\} > 0, \left(\Re e\left\{1 + \frac{\nu\ell''(\nu)}{\ell'(\nu)}\right\} > 0\right), \text{ respectively in which } \nu \in \phi(r), 0 < r \leq 1.$$

As an a specific set of analytic functions $\ell(\nu) = \sum_{\iota=0}^{\infty} e_\iota \, \nu^\iota$ and $\Gamma(\nu) = \sum_{\iota=0}^{\infty} b_\iota \, \nu^\iota$, we indicate by $\ell * \Gamma$ the convolution of ℓ and Γ according to by: [21-24]

$$(\ell * \Gamma)(\nu) = \sum_{\iota=0}^{\infty} e_\iota \, b_\iota \nu^\iota = (\Gamma * \ell)(\nu). \qquad (2)$$

presently, we provide the next operator means, which extends certain well-known operators.

Definition 1.1: In order to $\ell: \mathcal{A} \to \mathcal{A}$, the generalized operator $S_{\mu,\tau}^{\alpha\eta}: \mathcal{A} \to \mathcal{A}$ is defined by

$$S_{\mu,\tau}^{\alpha\eta}\ell(\nu) = \nu + \sum_{\iota=2}^{\infty} \frac{\left(\frac{2+e-\mu}{\iota+e-\tau}\right)^{\eta}}{(2\tau\iota - 2\tau + 2)^{\alpha}} e_\iota \nu^\iota, \qquad (3)$$

when $\alpha \in \mathbb{N}_0, \eta \in \mathbb{C},$ and $\tau \geq \mu \geq 0$.

Examples for this operator's special cases:

1- The Srivastava- Attiya operator $S_{0,0}^{\alpha\eta}$[25].
2- The Salagean operator $S_{1,0}^{\alpha+1,0}$[26].
3- The Generalized Salagean operator initiated by Al-Oboudi $S_{\mu,0}^{\alpha+1,0}$[27-28].

The researchers present a fresh subclass via the operator $S_{\mu,\tau}^{\alpha\eta}$as shown below:

Definition 1.2: In order to $\mathrm{SM}_{\mu,\tau}^{\alpha\eta}(e,X,Z,\xi)$ become a function class ℓ in the shape of

$$\ell(\nu)=\nu-\sum_{\iota=2}^{\infty}e_{\iota}\,\nu^{\iota}, \qquad (4)$$

as well as meeting the following requirements

$$\frac{\xi+2}{1-\xi}\left(\frac{\left(\nu^{2}\left(\mathrm{S}_{\mu,\tau}^{\alpha\eta}\ell(\nu)\right)'-\xi\mathrm{S}_{\mu,\tau}^{\alpha\eta}\ell(\nu)\right)}{\nu\mathrm{S}_{\mu,\tau}^{\alpha\eta}\ell(\nu)}-1\right)\prec\frac{2+X\nu}{1+Z\nu}, \qquad (5)$$

when $(0\leq\xi<1)$ and $(-1\leq Z<X\leq 1)$.

2. THE MAIN FINDINGS

On the following subsection, we come a condition that is both required and sufficient over the function ℓ about the class $\mathrm{SM}_{\mu,\tau}^{\alpha\eta}(e,X,Z,\xi)$.

Theorem 2.1: The function ℓ in the shape of (4) is enrolled in a class $\mathrm{SM}_{\mu,\tau}^{\alpha\eta}(e,X,Z,\xi)$ assuming and only assuming

$$\sum_{\iota=2}^{\infty}\big(Z(\iota-\xi)+X(1-\xi)+(\iota-1)\big)F_{\iota}e_{\iota}<\big(Z(\xi-1)+X(\xi-1)\big), \qquad (6)$$

at which

$$F_{\iota}=\frac{\big(2+\mu(\iota-1)\big)^{\alpha-1}}{\big(\tau(\iota-1)\big)^{\alpha}}\left(\frac{1+\iota}{2+\iota}\right)^{\eta},\quad \iota\in\mathbb{N} \qquad (7)$$

Proof: Allow $\ell\in\mathrm{SM}_{\mu,\tau}^{\alpha\eta}(e,X,Z,\xi)$, subsequently we're left with

$$\frac{\xi+2}{1-\xi}\left(\frac{\left(\nu^{2}\left(\mathrm{S}_{\mu,\tau}^{\alpha\eta}\ell(\nu)\right)'-\xi\mathrm{S}_{\mu,\tau}^{\alpha\eta}\ell(\nu)\right)}{\nu\mathrm{S}_{\mu,\tau}^{\alpha\eta}\ell(\nu)}-1\right)\prec\frac{2+Xh(\nu)}{1+Zh(\nu)}, \qquad (8)$$

at which $|h(\nu)|<1,\ h(0)=0$, for each $\nu\neq 0$, then

$$\left|\frac{\nu^{2}\left(\mathrm{S}_{\mu,\tau}^{\alpha\eta}\ell(\nu)\right)'-\xi\mathrm{S}_{\mu,\tau}^{\alpha\eta}\ell(\nu)}{(2+X\nu)(1-\xi)\nu\mathrm{S}_{\mu,\tau}^{\alpha\eta}\ell(\nu)-Z\left(\nu^{2}\left(\mathrm{S}_{\mu,\tau}^{\alpha\eta}\ell(\nu)\right)'-\xi\mathrm{S}_{\mu,\tau}^{\alpha\eta}\ell(\nu)\right)}\right|<1.$$

Thus,

$$\left|\frac{\sum_{\iota=2}^{\infty}(\iota-2)\,F_{\iota}e_{\iota}\nu^{\iota-1}}{\frac{(2+X\nu)(1-\xi)}{w}-\sum_{\iota=2}^{\infty}\big(Z(\iota-\xi)+X(1-\xi)+(\iota-1)\big)F_{\iota}e_{\iota}\nu^{\iota-1}}\right|<1.$$

establishing $\nu=r,\ (0<r<1)$, we receive

$$\sum_{\iota=2}^{\infty}(\iota-2)\,F_{\iota}e_{\iota}r^{\iota-1}<\frac{(2+Xv)(1-\xi)}{w}-\sum_{\iota=2}^{\infty}\big(Z(\iota-\xi)+X(1-\xi)+(\iota-1)\big)\,F_{\iota}e_{\iota}r^{\iota-1},$$

allowing $r\to 1^{-}$, Afterwards we receive the desired result.

In contrast, demonstrating that

$$\left|v^{2}\left(\mathrm{S}_{\mu,\tau}^{\alpha\eta}\ell(v)\right)^{'}-\xi\mathrm{S}_{\mu,\tau}^{\alpha\eta}\ell(v)\right|-\left|(2+Xv)(1-\xi)\mathrm{S}_{\mu,\tau}^{\alpha\eta}\ell(v)-Z\left[v^{2}\left(\mathrm{S}_{\mu,\tau}^{\alpha\eta}\ell(v)\right)^{'}-\xi\mathrm{S}_{\mu,\tau}^{\alpha\eta}\ell(v)\right]\right|<0.$$

Selecting $v=r,\ (0<r<1)$, we receive

$$\left|\sum_{\iota=2}^{\infty}(\iota-2)\,F_{\iota}e_{\iota}v^{\iota}\right|-\left|\frac{(2+Xv)(1-\xi)}{w}v-\sum_{\iota=2}^{\infty}\big(Z(\iota-\xi)+X(1-\xi)+(\iota-1)\big)\,F_{\iota}e_{\iota}v^{\iota}\right|$$

$$\leq\sum_{\iota=2}^{\infty}(\iota-2)\,F_{\iota}e_{\iota}r^{\iota}-\left(\frac{(2+Xv)(1-\xi)}{w}r-\sum_{\iota=2}^{\infty}\big(Z(\iota-\xi)+X(1-\xi)+(\iota-1)\big)\,F_{\iota}e_{\iota}r^{\iota}\right)$$

$$<\sum_{\iota=2}^{\infty}\big(Z(\iota-\xi)+X(1-\xi)+(\iota-1)\big)\,F_{\iota}e_{\iota}-\big((2+Xv)(1-\xi)\big)\leq 0,$$

as a result, we gain $\ell\in\mathrm{SM}_{\mu,\tau}^{\alpha\eta}(e,X,Z,\xi)$.

Now we provide our integral operator assets to identify the class's$\mathrm{SM}_{\mu,\tau}^{\alpha\eta}(e,X,Z,\xi)$ extreme points.

Theorem 2.2: Take $\ell(v)=v$ with

$$\ell_{\iota}(v)=\left(\frac{\big(v\xi(Z-X)+v\iota(1-Z)+v(X-1)\big)}{\big(\xi(Z-X)+\iota(1-Z)+(X-1)\big)}\right)F_{\iota}-\frac{\big(\xi(Z-X)+(X-Z)\big)v^{\iota}}{\big(\xi(Z-X)+(X-Z)\big)v^{\iota-1}}.\qquad(9)$$

Following that $\ell\in\mathrm{SM}_{\mu,\tau}^{\alpha\eta}(e,X,Z,\xi)$ if it is possible to express it in a manner

$$\ell(v)=\sum_{\iota=1}^{\infty}\mu_{\iota}\,\ell_{\iota}(v),\quad\left(\mu_{\iota}\geq 0\,,\sum_{\iota=1}^{\infty}\mu_{\iota}=1.\right)\qquad(10)$$

Proof: From (10), therefore,

$$\ell(v)=\left(\frac{v\mu_{\iota}\big(\xi(Z-X)+\iota(1-Z)+(X-1)\big)}{\big(\xi(Z-X)+\iota(1-Z)+(X-1)\big)}\right)F_{\iota}-\frac{v\mu_{\iota}\big(\xi(Z-X)+\iota(1-Z)+(X-1)\big)F_{\iota}}{\big(\xi(Z-X)+(X-Z)\big)v^{\iota-1}}.\quad(11)$$

presently, using (10), we receive

$$\sum_{\iota=2}^{\infty}\frac{\mu_{\iota}\big(\xi(Z-X)+(X-Z)\big)}{\big(\xi(Z-X)+\iota(1-Z)+(X-1)\big)F_{\iota}-\big(\xi(Z-X)+(X-Z)\big)v^{\iota-1}}\times$$

$$\left[\frac{\big(\xi(Z-X)+\iota(1-Z)+(X-1)\big)F_{\iota}}{\big(\xi(Z-X)+(X-Z)\big)}-v^{\iota-1}\right]=\sum_{\iota=2}^{\infty}\mu_{\iota}=1-\mu_{1}<1.$$

The following demonstrates $\ell\in\mathrm{SM}_{\mu,\tau}^{\alpha\eta}(e,X,Z,\xi)$.

However, how about $\ell\in\mathrm{SM}_{\mu,\tau}^{\alpha\eta}(e,X,Z,\xi)$, afterwards

$$e_{\iota}\leq\frac{\big(\xi(Z-X)+(X-Z)\big)}{\big(\xi(Z-X)+\iota(1-Z)+(X-1)\big)F_{\iota}-\big(\xi(Z-X)+(X-Z)\big)v^{\iota-1}},\qquad\iota\geq 2$$

Placing

$$\mu_\iota = \frac{\big(\xi(Z-X)+\iota(1-Z)+(X-1)\big)F_\iota - \big(\xi(Z-X)+(X-Z)\big)v^{\iota-1}}{\big(\xi(Z-X)+(X-Z)\big)}, \quad \iota \geq 2$$

and

$$\mu_\iota = 1 - \sum_{\iota=2}^{\infty} \mu_\iota ,$$

we receive,

$$\ell(v) = \sum_{\iota=1}^{\infty} \mu_\iota \, \ell_\iota(v).$$

Theorem 2.3: A function $p(v)$ specified by

$$p(v) = \frac{c+1}{v^c} \int_0^z u^{c-1} \ell(u) du, \qquad (12)$$

in which c belongs to the class $\mathrm{SM}_{\mu,\tau}^{\alpha\eta}(e,X,Z,\xi)$ whether the function $\ell \in \mathrm{SM}_{\mu,\tau}^{\alpha\eta}(e,X,Z,\xi)$, and an is c number that is real.

Proof: Take

$$p(v) = e_1 v - \textstyle\sum_{\iota=2}^{\infty} t_\iota v^\iota, \quad (t_\iota \geq 0), \qquad (13)$$

in which,

$$t_\iota = \frac{c+1}{c+\iota} e_\iota. \qquad (14)$$

Then,

$$\sum_{\iota=2}^{\infty} \big(\xi(Z-X)+\iota(1-Z)+(X-1)\big)F_\iota \, t_\iota = \sum_{\iota=2}^{\infty} \big(\xi(Z-X)+\iota(1-Z)+(X-1)\big)F_\iota \frac{c+1}{c+\iota} e_\iota$$
$$\leq \big(\xi(Z-X)+\iota(1-Z)+(X-1)\big)F_\iota e_\iota \leq \big(\xi(Z-X)+(X-Z)\big)e_1.$$

Assuming $\ell \in \mathrm{SM}_{\mu,\tau}^{\alpha\eta}(e,X,Z,\xi)$, it follows that $p(v) \in \mathrm{SM}_{\mu,\tau}^{\alpha\eta}(e,X,Z,\xi)$.

The radius of Starlikeness as well as Convexity have provided through the theorem.

Theorem 2.4: The radii of Starlikeness for the class$\mathrm{H}_{\lambda,\eta,\varepsilon}^{m,s}(a,A,B,\xi)$is give by

$$r_1 = ln\ell_{\iota\geq 2}\left(\frac{\big(\xi(Z-X)+\iota(1-Z)+(X-1)\big)F_\iota}{\iota\big(\xi(Z-X)+(X-Z)\big)}\right)^{\frac{1}{\iota-1}}, \quad \iota \geq 2\,. \qquad (15)$$

Proof. We need to show that

$$\left|\frac{v\ell'(v)}{\ell(v)} - 1\right| \leq 1. \quad (v = r_1\,; 0 < r_1 < 1)$$

Subsequently is simple to demonstrate if

$$\sum_{\iota=2}^{\infty} (\iota-1) e_\iota \, r_1^{\iota-1} \leq 1 + \sum_{\iota=2}^{\infty} e_\iota \, v^{\iota-1} - \sum_{\iota=2}^{\infty} e_\iota \, r_1^{\iota-1}, \qquad (16)$$

and

$$\sum_{\iota=2}^{\infty} \iota e_\iota r_1^{\iota-1} - e_\iota \nu^{\iota-1} \leq 1 . \qquad (17)$$

Through (10),

$$\sum_{\iota=2}^{\infty} a_n \left(\frac{\big(\xi(Z-X)+\iota(1-Z)+(X-1)\big)F_\iota}{\big(\xi(Z-X)+(X-Z)\big)} - \nu^{\iota-1} \right) \leq 1. \qquad (18)$$

As a result, (17) will be accurate if

$$\iota r_1^{\iota-1} - \nu^{\iota-1} \leq \left(\frac{\big(\xi(Z-X)+\iota(1-Z)+(X-1)\big)F_\iota}{\big(\xi(Z-X)+(X-Z)\big)} \right),$$

or

$$r_1 < \left(\frac{\big(\xi(Z-X)+\iota(1-Z)+(X-1)\big)F_\iota}{\big(\xi(Z-X)+(X-Z)\big)} \right)^{\frac{1}{\iota-1}}.$$

The outcome is precise for the function

$$\ell(\nu) = \left(\frac{\big(\nu\xi(Z-X)+\nu\iota(1-Z)+\nu(X-1)\big)}{\big(\xi(Z-X)+\iota(1-Z)+(X-1)\big)} \right) F_\iota - \frac{\big(\xi(Z-X)+(X-Z)\big)\nu^\iota}{\big(\xi(Z-X)+(X-Z)\big)\nu^{\iota-1}}.$$

Theorem 2.5: Allow a function ℓ for given create (4) in $\mathrm{SM}_{\mu,\tau}^{\alpha\eta}(e,X,Z,\xi)$, thus it

$$\psi(r) \leq |\ell(\nu)| \leq \left(\frac{r\big(2-3Z+X+\xi(Z-X)\big)}{2-3Z+X+\xi(Z-X)} \right) F_\iota - \frac{\big(\xi(Z-X)+(X-Z)\big)r^\iota}{\big(\xi(Z-X)+(X-Z)\big)\nu}, \qquad (19)$$

$$\psi(r) = \begin{cases} r & r \leq \nu \\ \left(\dfrac{r\big(2-3Z+X+\xi(Z-X)\big)}{2-3Z+X+\xi(Z-X)} \right) F_\iota - \dfrac{\big(\xi(Z-X)+(X-Z)\big)r^\iota}{\big(\xi(Z-X)+(X-Z)\big)\nu} & \text{otherwise} \end{cases} \qquad (20)$$

supplied the order

$$\left\{ \big(\xi(Z-X)+\iota(1-Z)+(X-1)\big)F_\iota - \big(\xi(Z-X)+(X-Z)\big)\nu^{\iota-1} \right\}_{\iota=2}^{\infty}, \qquad (21)$$

optimistic and not diminishing. Also,

$$e_1 - \frac{\big(\xi(Z-X)+(X-Z)\big)r}{\big(2-3Z+X+\xi(Z-X)\big)F_2 - \big(\xi(Z-X)+(X-Z)\big)\nu} \leq |\ell'(\nu)| \leq \left(\frac{2-3Z+X+\xi(Z-X)}{2-3Z+X+\xi(Z-X)} \right) rF_2 - \frac{2\big((X-Z)+\xi(Z-X)\big)r^2}{\big((X-Z)+\xi(Z-X)\big)r},$$

supplied the order

$$\left\{ \frac{\big(\xi(Z-X)+\iota(1-Z)+(X-1)\big)F_\iota - \big(\xi(Z-X)+(X-Z)\big)\nu^{\iota-1}}{\iota} \right\}_{\iota=2}^{\infty}, \qquad (22)$$

is beneficial and non-decreasing, ($|z| = r$, $0 < r < 1$) and F_ι is specified by (7)

Proof. Allow $\ell \in \mathrm{SM}_{\mu,\tau}^{\alpha\eta}(e,X,Z,\xi)$, then assumingly, we arrive at

$$\sum_{\iota=2}^{\infty} e_\iota \leq \frac{\big(\xi(Z-X)+(X-Z)\big)}{\big(2-3Z+X+\xi(Z-X)\big)F_2 - \big(\xi(Z-X)+(X-Z)\big)\nu}.$$

and,

$$\sum_{\iota=2}^{\infty} \iota e_\iota \leq \frac{3\big(\xi(Z-X)+(X-Z)\big)}{\big(2-3Z+X+\xi(Z-X)\big)F_2-3\big(\xi(Z-X)+(X-Z)\big)\nu}.$$

For $\nu = r, (0<r<1)$, we achieve

$$|\ell(\nu)| = \left|e_1\nu - \sum_{\iota=2}^{\infty} e_\iota \nu^\iota\right| \leq r\left(1+\sum_{\iota=2}^{\infty} e_\iota\, \nu^{\iota-1}+\sum_{\iota=2}^{\infty} e_\iota\, r^{\iota-1}\right) < r\left(1+(\nu+r)\sum_{\iota=2}^{\infty} e_\iota\right)$$

$$\leq \left(\frac{2-3Z+X+\xi(Z-X)}{2-3Z+X+\xi(Z-X)}\right) rF_2 - \frac{2\big(\xi(Z-X)+(X-Z)\big)r^2}{\big(\xi(Z-X)+(X-Z)\big)r},$$

and

$$r\left(e_1-\sum_{\iota=2}^{\infty} e_\iota\, r^{\iota-1}\right) = r\left(1+\sum_{\iota=2}^{\infty} e_\iota\,(\nu^{\iota-1}-r^{\iota-1})\right) \leq \left|e_1\nu-\sum_{\iota=2}^{\infty} e_\iota\nu^\iota\right| = |\ell(\nu)|,$$

hence , $|\ell(\nu)| \geq r$ if $r \leq \nu$, though if $r > \nu$, we achieve $\{\nu^{\iota-1}-r^{\iota-1}\}_{\iota=2}^{\infty}$ is unfavorable and declining, so the situation

$$|\ell(\nu)| \geq r\left(1+(\nu-r)\sum_{\iota=2}^{\infty} e_\iota\right) \geq \left(\frac{2-3Z+X+\xi(Z-X)}{2-3Z+X+\xi(Z-X)}\right) rF_2 - \frac{2\big(\xi(Z-X)+(X-Z)\big)r^2}{\big(\xi(Z-X)+(X-Z)\big)r},$$

and using the identical method, we arrive at the outcome (22). We can use the formulas $\ell(\nu) = \nu$ and

$$\ell_2(\nu) = \left(\frac{2-3Z+X+\xi(Z-X)}{2-3Z+X+\xi(Z-X)}\right)\nu F_2 - \frac{2\big(\xi(Z-X)+(X-Z)\big)\nu^2}{\big(\xi(Z-X)+(X-Z)\big)\nu}.$$

Theorem 2.6: Allow the function ℓ stated by (4) to take the class $\mathrm{SM}_{\mu,\tau}^{\alpha\eta}(e,X,Z,\xi)$, we get

$$e_1 r - \frac{\big(\xi(Z-X)+(X-Z)\big)e_1}{\big(2-3Z+X+\xi(Z-X)\big)F_2} r^2 \leq |\ell(\nu)| \leq e_1 r + \frac{\big(\xi(Z-X)+(X-Z)\big)e_1}{\big(2-3Z+X+\xi(Z-X)\big)F_2} r^2, \quad (23)$$

and

$$e_1 - \frac{\big(\xi(Z-X)+(X-Z)\big)e_1}{\big(2-3Z+X+\xi(Z-X)\big)F_2} r \leq |\ell'(\nu)| \leq e_1 + \frac{\big(\xi(Z-X)+(X-Z)\big)e_1}{\big(2-3Z+X+\xi(Z-X)\big)F_2} r. \quad (24)$$

Proof. Using supposition, we've obtained

$$\sum_{\iota=2}^{\infty} e_\iota \leq \frac{\big(\xi(Z-X)+(X-Z)\big)e_1}{\big(2-3Z+X+\xi(Z-X)\big)F_2},$$

and

$$\sum_{\iota=2}^{\infty} \iota e_\iota \leq \frac{2\big(\xi(Z-X)+(X-Z)\big)e_1}{\big(2-3Z+X+\xi(Z-X)\big)F_2}.$$

Then, through (4), we're left with

$$|\ell(\nu)| = \left|e_1\nu-\sum_{\iota=2}^{\infty} e_\iota\nu^\iota\right| \leq e_1 r + \sum_{\iota=2}^{\infty} e_n\, r^n \leq e_1 r + r^2 \sum_{\iota=2}^{\infty} e_\iota \leq e_1 r + \frac{\big(\xi(Z-X)+(X-Z)\big)e_1}{\big(2-3Z+X+\xi(Z-X)\big)F_2}$$

and

$$e_1 r - \frac{\big(\xi(Z-X)+(X-Z)\big)e_1}{\big(2-3Z+X+\xi(Z-X)\big)F_2} r^2 \leq |\ell(\nu)|$$

Further, there is

$$|\ell'(v)| \leq e_1 + r\sum_{\iota=2}^{\infty} \iota e_\iota\, r^{\iota-2} \leq e_1 + r\sum_{\iota=2}^{\infty} \iota e_\iota \leq e_1 + \frac{2\big(\xi(Z-X)+(X-Z)\big)e_1}{\big(2-3Z+X+\xi(Z-X)\big)F_2} r\,,$$

and

$$e_1 - \frac{2\big(\xi(Z-X)+(X-Z)\big)e_1}{\big(2-3Z+X+\xi(Z-X)\big)F_2} r \leq |\ell'(v)|.$$

Consider the following function to get clarity

$$\ell_2(v) = e_1 v - \frac{2\big(\xi(Z-X)+(X-Z)\big)e_1}{\big(2-3Z+X+\xi(Z-X)\big)F_2} v^2\,.$$

3. CONCLUSIONS

It was found in this paper some applications of the notion of differential subordination as it relates to subclasses of univalent functions that use specific convolution as operators. We did examine geometric properties of these kinds of functions, including coefficient bounds, distortion theorem, starlikeness and convexity radii, among others. Extreme points and the integral operator have both been studied.

We investigated a few of the characteristics of variations subordination of analytical univalent functions over an open unit disc as well as deduced specific subordination as well as superordination properties using the characteristics of the broader a byproduct operator. Additionally, it gave insight into geometrical traits like coefficient disparities and Hadamard product characteristics. There were installed certain intriguing findings for derivatives differential subordination as well as superordination of analytical univalent functions. Then, a few findings of variations subordination that involve linear operators have been presented employing the convolution with two linear operators. The convolution operator has been used to deal with a number of leads to over differential subordination within the unit disk with open edges employing broader hypergeometric function.

Through the use of an operator with linearity as well as variations subordination, we arrived at a few conclusions as well as a few sandwich theorems. As an a few convolution as a operators, we as a species provided a few variations subordination programs towards subclasses about univalent functions. Through the application of a straight-line operator, it was possible to achieve certain important outcomes in the variations subordination as well as variations superordination about meromorphic analyzing univalent functions of the second order. Lastly, we provided a few outcomes over 2nd-order differential subordination within the open section disk involving broader hypergeometric function employing the convexity operator.

4. UPCOMING STUDY

The next phase of investigation is broken down as follows:

- The ability to investigate a novel linear operator by employing the Hadamard the item as its fundamental hypergeometric function along with to study a novel category of multifaceted functions determined by the newly discovered parametric operator.
- As a 4th order differential subordination within the open unit disk, a number of leads to will be obtained through the broader hypergeometric function along with the characteristics associated with the broader a byproduct operator.
- Can create two brand-new bi-univalent function subclasses while getting notions to feed the class about functions projections.

REFERENCES

[1] Ruscheweyh, S. (1981). Neighborhoods of univalent functions, Proc. Amer. Math. Soc., 81, 521-527. https://www.ams.org/journals/proc/1981-081-04/S0002-9939-1981-0601721-6/.

[2] Ali, R., Ravichandran, V., Lee, S. (2009). Subclasses of multivalent starlike and convex functions, Bulletin of the Belgian Mathematical Society - Simon Stevin,16 385–394. https://doi.org/10.36045/bbms/1251832366.

[3] Hameed, M.I., Shihab, B.N., Jassim, K.A. (2021, September). Certain Geometric Properties of Meromorphic Functions Defined by a New Linear Differential Operator, In Journal of Physics: Conference Series (Vol. 1999, No. 1, p. 012090). IOP Publishing. DOI:https://10.1088/1742-6596/1999/1/012090.

[4] Elrifai, E., Darwish, H., Ahmed, A. (2012). On subordination for higher-order derivatives of multivalent functions associated with the generalized Srivastava-attiya operator, Demonstration Math XLV, (1), 40-49. https://doi.org/10.1515/dema-2013-0363..

[5] Hameed, M.I., Shihab, B.N., Jassim, K.A. (2022, November). Some properties of subclass of P-valent function with new generalized operator, In AIP Conference Proceedings (Vol. 2394, No. 1, p. 070006). AIP Publishing LLC. https://doi.org/10.1063/5.0120913

[6] Uzoamaka, A., Maslina, D., Olubunmi, A. (2020). The q-analogue of Sigmoid function in the space of univalent λ-Pseudo starlike functions, International Journal of Mathematics and Computer Science, 15 (2), 621–626. http://ijmcs.future-in-tech.net/15.2/R-DarusEF.pdf.

[7] Dziok J., Srivastava, H.M. (2003). Certain subclasses of analytic functions associated with the generalized hypergeometric function, Integral Transform. Spec. Funct.,vol.14,7–18. https://doi.org/10.1080/10652460304543.

[8] Kiryakova, V., Saigo M., Srivastava, H.M. (1998). Some criteria for univalence of analytic functions involving generalized fractional calculus operators, Fract. Calc. Appl. Anal., vol. 1, 79–104. https://cutt.us/ftpVp.

[9] Hameed, M.I., Al-Dulaimi, S.J., Jassim, K.A. (2023, January). Some applications of certain subclasses of meromorphic functions defined by certain differential operators, In AIP Conference Proceedings (Vol. 2554, No. 1, p. 020001). AIP Publishing LLC. https://doi.org/10.1063/5.0103963.

[10] Abelman, S, Selvakumaran, K.A., M. M. Rashidi, M.M., Purohit, S.D. (2017). Subordination conditions for a class of non-bazilevic type defined by using fractional q-Calculus operator, Facta universitatis(NIS) Math. Inform., Vol 32, No 2, 255-267. http://casopisi.junis.ni.ac.rs/index.php/FUMathInf/article/view/2151.

[11] Duren, P.L. (1983). Univalent functions, Grundlehren der Mathematischen Wissenschaften, Fundamental Principles of Mathematical Sciences, Springer-Verlag, New York./Users/Mustafa/Downloads/CHAPTER6.pdf.

[12] Miller, S.S., Mocanu, P.T. (1978). Second-order differential inequalities in the complex plane, J. Math. Anal. Appl., vol. 65, 298–305. https://doi.org/10.1016/0022-247X(78)90181-6.

[13] Hameed, M.I., Shihab, B.N. (2022, august). Some Classes of Univalent Function with Negative Coefficients. In Journal of Physics: Conference Series (Vol. 2322, No. 1, p. 012048). IOP Publishing. DOI:https://10.1088/1742-6596/2322/1/012048.

[14] Mocanu, P.T., Bulboaca T., Salagean, G.S. (1999). Geometric theory of univalent functions, Casa Cartii de Stiinta, Cluj-Napoca. https://cutt.us/7vk3s.

[15] Miller, S.S., Mocanu, P.T. (2000). Differential subordinations, Theory and applications, Monographs and Textbooks in Pure and applied Mathematics, Marcel Dekker, Inc., New York.https://10.12691/ajams-7-5-2.

[16] Hameed, M.I., Shihab, B.N. (2022). On Differential Subordination and Superordination for Univalent Function Involving New Operator. Iraqi Journal For Computer Science and Mathematics, 3(1), 22-31. DOI: https://doi.org/10.52866/ijcsm.2022.01.01.003.

[17] Irmak, H., Cho, N. (2007). A differential operator and its application to certain multivalently analytic functions, Hacettepe Journal of Mathematics and Statistics, 36(1), 1–6. https://dergipark.org.tr/en/download/article-file/86903.
[18] Ramachandran, C., Dhanalakshmi, K., Vanitha, L. (2016). Certain aspects of univalent function with negative coefficients defined by Bessel function, Brazilian archives of Biology and Technology, 2016, 59 (2), 1-14. https://doi.org/10.1590/1678-4324-2016161044.
[19] Hameed, M.I., Ali, M.H. (2021, July). Some Classes Of analytic Functions For The Third Hankel Determinant, In Journal of Physics: Conference Series (Vol. 1963, No. 1, p. 012080). IOP Publishing. DOI: https://10.1088/1742-6596/1963/1/012080.
[20] Oros, G., Oros, G.I. (2003). A class of holomorphic functions II, Miron Nicolescu (19031975) and Nicolae Cior˘anescu (19031957), Libertas Math., vol. 23, 65–68. https://cutt.us/MiBk4.
[21] Al-Oboudi, F.M. (2004). On univalent functions defined by a generalized S˘al˘agean operator, Int. J. Math. Math. Sci., No. 25-28, 1429–1436. https://doi.org/10.1155/S0161171204108090.
[22] Hameed, M.I., Shihab, B.N., Jassim, K.A. (2022, October). An application of subclasses of Goodman-Salagean-type harmonic univalent functions involving hypergeometric function, In AIP Conference Proceedings (Vol. 2398, No. 1, p. 060012). AIP Publishing LLC. https://doi.org/10.1063/5.0093392.
[23] Ravichandran, V., Ahuja, O., Ali, R. (2014). Analytic and harmonic univalent functions, abstract and applied analysis article ID 578214, 1-3. https://doi.org/10.1155/2014/578214.
[24] Hameed, M.I., Shihab, B.N. (2022). Several Subclasses of r-Fold Symmetric Bi-Univalent Functions possess Coefficient Bounds, Iraqi Journal of Science, vol. 63, no. 12, p. 5438-5446. https://doi.org/10.24996/ijs.2022.63.12.29.
[25] Sokół, J. (2008). On some applications of the Dziok-Srivastava operator, Appl. Math. Comput., vol. 201, 774–780. https://doi.org/10.1016/j.amc.2008.01.013.
[26] Salagean, G.S. (1981). Subclasses of univalent functions, in Complex analysis fifth Romanian-Finnish seminar, Part 1, 362–372, Lecture Notes in Math., 1013, Springer, Berlin. https://cutt.us/WZyTd.
[27] Dziok, J. (2007). On the convex combination of the Dziok-Srivastava operator, Appl. Math. Comput., vol. 188,1214–1220. https://doi.org/10.1016/j.amc.2006.10.081.
[28] Hameed, M.I., Ali, M.A., Shihab, B.N. (2022). A certain Subclass of Meromorphically Multivalent Q-Starlike Functions Involving Higher-Order Q-Derivatives, Iraqi Journal of Science, vol. 63, no. 1, p. 251-258. https://www.iasj.net/iasj/download/ea3445974dc36b83.

Detection of elements (pb, Cd, Cu, Cr)

in unrefined table salt

by atomic absorption spectrometer (AAS) in Iraqi salt sites

Prof. Hadi D. Alattabi1 **Hanan Kaayem Ghazi**

E-mail;hananalkazaali@gmail.com

Department of Physics, College of Science, Wasit University, Wasit, Iraq

Detection of elements (pb, Cd, Cu, Cr) in unrefined table salt by atomic absorption spectrometer (AAS) in Iraqi salt sites

Prof. Hadi D. Alattabi1 **Hanan Kaayem Ghazi**

Department of Physics, College of Science, Wasit University, Wasit, Iraq

E-mail;hananalkazaali@gmail.com

Abstract

Heavy metals that may be hazardous to one's health after consuming contaminated foods are lead, cadmium, copper and chromium. Table salt is one of the most widely used food additives with a unique position in food consumption. Although purified table salt is expected to obtain a lower level of contamination, this study aims to investigate the contamination of consumed table salt with heavy metals. Unwashed salt (from soil sites) was analyzed using an atomic absorption spectrophotometer to detect toxic heavy metals The result was a pb concentration equal to 1.325, 0.592, 0.279, 0.295, a Cd concentration of 9.103, 10.574, 17.191, and 18.294 for the samples, a Cu concentration of 43.545, 20.534, 7.182, and 17.693, and a Cr concentration of 11.926. 7.759, 12.389, 9.611 for samples A, B, C, D, in order, and in comparing the results of lead concentration (FAO/WHO), we note that the values are lower than those of FAO/WHO. Based on the findings, Cd, It was discovered that the values are much more than the (FAO/WHO) limit, as well as the concentration of Cu, which is a heavy metal and much of its consumption can be hazardous to one's health.

Keywords: table salt, atomic absorption spectrometry, heavy materials.

الكشف عن العناصر (pb, Cd, Cu, Cr) في ملح الطعام الغير مكرر بواسطة جهاز مطياف الامتصاص الذري (AAS) في مواقع الاملاح العراقية

أ.د. هادي دويج العتابي **م.م. حنان كعيم غازي**

جامعة واسط /كلية العلوم **جامعة واسط /كلية العلوم**

الخلاصة

المعادن الثقيلة التي قد تسبب المخاطر الصحية بعد استهلاك الأطعمة الملوثة هي الرصاص والكادميوم والنحاس والكروم يعتبر ملح الطعام هو أحد أكثر استخدامًا المضافات الغذائية مع مكانة فريدة في استهلاك الغذاء. على الرغم من

توقع ملح الطعام المنقى للحصول على مستوى أقل من التلوث، تهدف هذه الدراسة الى التحقيق في تلوث ملح الطعام المستهلك بالمعادن الثقيلة حيث تم تحليل الملح الغير مغسول (من مواقع التربة) باستخدام جهاز الامتصاص الذري الطيفي للكشف عن المعادن الثقيلة السامة. وكانت النتيجة تركيز pb يساوي 1.325، 0.592، 0.279, 0.295 وتركيز Cd للعينات هي 9.103، 10.574، 17.191 ,18.294 وتركيز Cu 43.545، 20.534 ,7.182, 17.693 وتركيز Cr 11.926، 7.759، 12.389 ,9.611 للعينات A، B،C ، D حسب الترتيب وفي مقارنة نتائج تركيز الرصاص مع منظمة الأغذية والزراعة/ منظمة الصحة العالمية (FAO/WHO) نلاحظ القيم أقل من تلك الخاصة FAO/WHO. اما الكادميوم من النتائج لوحظ أن القيم أكثر بكثير من حد FAO/WHO وكذلك تركيز Cu وهو معدن ثقيل وكثير يمكن أن يكون استهلاكه خطر على صحة الإنسان من المستحسن أن يحتوي الملح على كمية أقل من هذا المعدن أو إذا أمكن عدم احتوائه على الإطلاق اما الكروم كانت جميع النتائج في أكبر بكثير من الحد الأقصى الاستهلاك البشري الذي حدده الدستور الغذائي.

الكلمات المفتاحية: ملح الطعام، مطياف الامتصاص الذري، مواد ثقيلة.

Introduction

Heavy metals may be found in abundance in the Earth's crust, air, water, and a variety of man-made items. Heavy metals can be absorbed through the skin or inhaled. Contamination of food products with heavy metals makes the food chain and diet a major pathway for human exposure to heavy metals. Despite the normal state that foodborne, Food poisoning owing to hazardous and heavy metal concentrations should also be considered as a result of meals contaminated with microbes. [1, 2].

Salt is considered one of the natural products that emerge from the ground in areas with salt deposits in a specific season when the rainy season falls, the winter season in Iraq. When the rain water evaporates, the salt comes out naturally from the ground to the surface in the month (April, May and June). These months are called the salt harvest season in the central and southern regions of Iraq. Saline areas extend along the highway linking Baghdad and Basra in southern Iraq. Figure (1) shows a Google Maps satellite snapshot of saline locations.

Table salt is a major source in daily consumption, as it is included in all human food, and table salt is free from pollutants and heavy elements, which is very necessary for human health, and for this I found it necessary to reveal the percentage of minerals present in table salt.

Figure (1) picture from Google Maps of a salinity site in the city of Diwaniyah

Materials and devices used

Table salt (sodium chloride)

Molecular formula (NaCl) Molar mass 58.44 g/mol Appearance White crystalline powder Density 2.16 g/cm^3 Melting point 801 °C Boiling point 1465 °C Solubility in water 36 g/100 ml water. Figure (2) shows the Braves lattice of a sodium chloride crystal, a face-centered cube (FCC), the length of its sides (a = 5.63 Å). A single cell contains four lattice points, each point of which is accompanied by a base consisting of two ions, sodium Na and chlorine Cl. They are separated by a distance equal to the radius of the cubic unit cell. With the sides and the center of the cube or vice versa, a sodium chloride crystal can be depicted as consisting of two FCC-type lattices, one of which is a sodium lattice and the other a chlorine lattice, each one displaced from the other by (a = 1/2) [3,4].

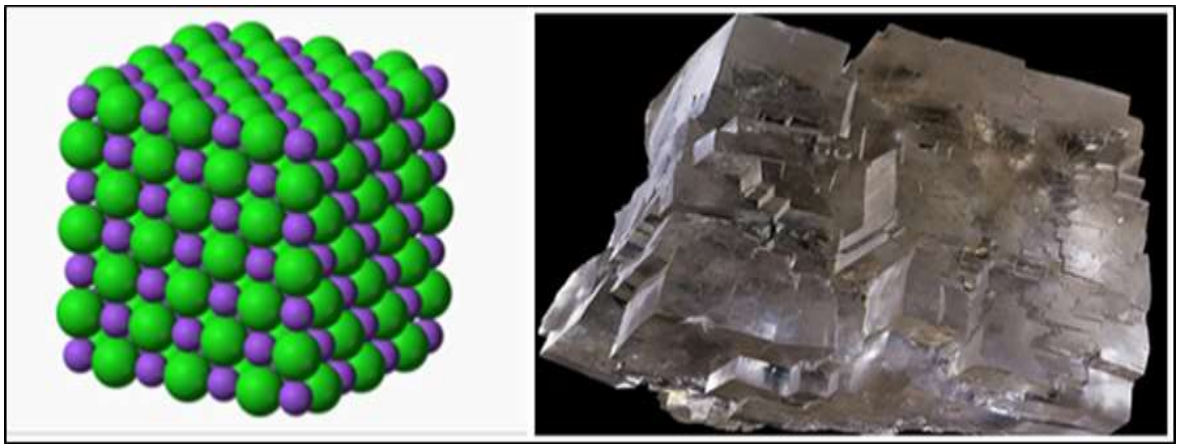

Figure (2) Crystal structure of sodium chloride (table salt) [4]

Atomic Absorption Spectrometer (AAS)

The term atomic spectroscopy is applied to the set of techniques that are used to determine the different elements in their atomic state, where the samples are exposed to a

thermal or electrical energy source to break the molecular bonds, and once these bonds are broken and free atoms are given, the analysis process is done using atomic absorption spectroscopy, atomic emission, or atomic fluorescence [5]. Fig. 3 shows an (AAS) device based on the principle of atomic absorption, based on the fact that most of the atoms of the substance are found in the ground energy level (E_o) that is not excited from the energy levels of the atom, and with the presence of a light source with a suitable wavelength λ, the electron in the ground energy level absorbs this light beam to move to a higher excited energy level. Thus, the intensity of the light beam (I_o) passing through the atomic fog Aerosol will decrease and escape from the fog with intensity I, and this decrease is proportional to The number of absorbent atoms has, and this is consistent with the Beer-Lambert law, where the absorbance is expressed by the symbol A and is given by the relationship: -

$A = \log (I_o/I) = \varepsilon\lambda.l.C$, this relationship is directly linear within a specific range of concentrations.

Where I_o is the intensity of the incoming light ray, I is the intensity of the transmitted light ray, l is the path length, C is the concentration, ελ is a qualitatively characteristic value of the atomic absorption at wavelength λ of the studied element [6,7].

Figure 3: The Atomic Absorption Spectrometer (AAS)

Studied Elements

Lead

a chemical element with the symbol Pb and atomic number 82. It belongs to the carbon group, which is the fourteenth group on the periodic chart and the fourth group overall. Lead is a heavy metal with a high density that is typically seen in the hue bluish-silver. However, when exposed to air, this color soon loses its brilliance and turns opaque gray. In addition to being a component of many alloys, lead is a soft, malleable metal that is ductile and

malleable. It's a stable metal as well, and three of its isotopes are towards the end of the decay sequence for radioactive heavy elements. It is a toxic metal, which led to limiting its applications in most countries after discovering its toxicity. Lead affects negatively inside vital bodies, where its effect is similar to neurotoxins in terms of the ability to harm the nervous system and disrupt the functional performance of some vital enzymes, causing neurological and movement disorders [8, 9].

The most effective way to find trace quantities of lead is to use AAS, either through a graphite or quartz tube. The 4.5 ng/mL lower limit of detection is possible. Typically, lead is treated with sodium borohydride to produce volatile lead (II) hydride, which is then collected in a lab beaker and electrically heated to temperatures above 900 °C. Lead can then be detected using a hollow cathode lamp because it exhibits an absorbance at 283.3 nm. [10,11].

Cadmium

It is an element in the periodic table of elements with the chemical symbol Cd, atomic number 48, and atomic weight 112.411. The element is poisonous, as are its salts, and Cd also endangers the environment. The kidneys, skeletal system, and respiratory system are all adversely affected by cd, which is classified as a human carcinogen. Although there are only little amounts of it in the environment, human activity has greatly increased those levels. Its color is blue to whitish. Cd dissolves in acids and does not dissolve in alkalis. Boiling cadmium produces toxic yellow fumes [11,12].

Copper

Copper (Cu) is characterized by its high conductivity and great ability to conduct heat and electricity. It has a reddish-brown color that has become covered with time with a green layer as a result of its exposure to moist air. It has an atomic number of 29, an atomic mass of (63.54 g/mol), a boiling point of (2567 ̊C), a melting point of (1083.4 ̊C), and a density of (8.96 g/cm^3). Copper helps in the synthesis of many enzymes. To extract energy from food and to absorb iron, it thus plays a role in preventing anemia, as an increase in its concentration in the body leads to many diseases, the most famous of which is Wilson’s disease [13,14].

Chromium

Chromium is a chemical element whose symbol is Cr, and it is of two types, the first is trivalent, which is safe for humans, and the second is hexavalent, which is a poison that causes health problems.The recommended daily dose (men 0.2-35, women 0.2-25, pregnant 29-30) micrograms [11, 15, 16].

Sample preparation and method of work

Samples were collected from different salt sites, where the samples were kept in polyethylene bags after being exposed to air and sunlight for a week for the purpose of drying them from moisture. Salt samples were crushed in the laboratory, then sifted into 80 mesh, after that they were transferred to sealed glass containers. Four elements were detected, namely lead, cadmium, chromium, and copper, by an atomic absorption instrument. Figure (4) shows the salt samples that were collected and examined.

Figure 4 shows the salt samples that were collected and examined

Using a desiccant and a previously distilled moisture plate, (0.05 g) of salt was put in an oven to determine its moisture content. The dish spent two hours in the oven, which was set to 110 degrees Celsius. In a desiccator, it was chilled after heating. This plate was weighed after cooling, and the formula below was used to determine the sample's moisture content:

Weight% Moisture = (A/B) ×100 where: - A = weight loss in grams after drying. B = weight in grams of the salt sample.

Use an AAS with an analytical model (Hitachi Z8000) that contains the details of the examined minerals indicated in Table 1. The volume of the sample was made (1 liter) by dissolving twice distilled water (DDW) in a 1000 ml beaker, heating this sample solution at 110 ° C for 15 minutes, and then condensing it for 30 minutes without boiling. The sample was made by dissolving (10 ml) of (HNO3) and (5 g) of the sample to make a mixture, and this mixture was covered with a glass for 30 minutes. chilling the sample solution, adding 5 ml of pure HNO3, and then reflowing it For 30 minutes, sample the remedy once again. Most of the samples did not emit any brown fumes during reflux, indicating the presence of HNO3, but those that did were added to 5 ml of concentrated HNO3 and mixed again for 30 minutes, until no brown fumes were detected.

Table (1) Features of Metal AAS

Metals	ʎ(max)nm	Flame gases	Sensitivity	Maximum lamp current
pb	283.3	Air-acetylene	20	15
Cd	228.8	Air-acetylene	1.5	8
Cu	324.8	Air-acetylene	4	10
Cr	367.9	Nitrous oxide	4	12

Results and discussion

It is well known that heavy metals have an active role and occupy an important place in many biological processes. Table No. (2) and Figure (5) show the results of the analysis of four samples of salt collected from different locations, where the sample A and B were collected from two different locations in the city of Samawah, and samples C and D were collected from two different locations in the city of Diwaniyah in central Iraq.

Table No. (2) Results of (AAS) analysis in table salt samples

no	Pb(ppm)	Cd(ppm)	Cu(ppm)	Cr(ppm)
A	1.325	9.103	43.545	11.926
B	0.592	10.574	20.534	7.759
C	0.279	17.191	7.182	12.389
D	0.295	18.294	17.693	9.611

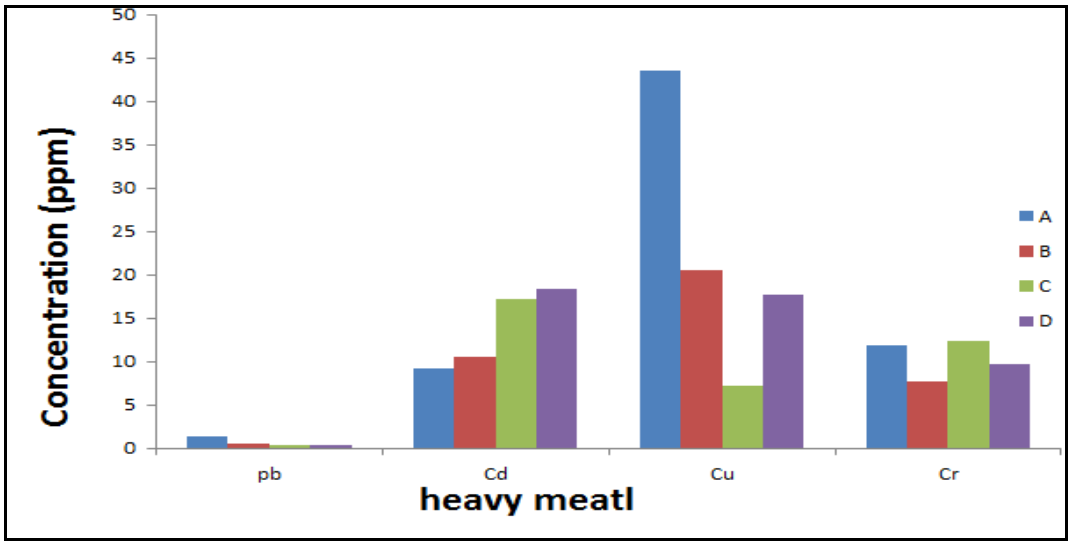

Figure (5) Results of (AAS) analysis in table salt samples

We note in Table (2) that the percentage of lead (pb) in salt was the lowest in all salt samples, and in comparing the results of lead concentration with the Food and Agriculture Organization / World Health Organization (FAO/WHO) as a result of the analyzes in Table (3), we note the values within the limits recommended by FAO/WHO, which is around 2 mg kg^{-1}. As for cadmium from the results, it was noted that the values are much more than the FAO/WHO equal 0.5 mg kg^{-1} [16]. The World Health Organization recommended that the maximum content of copper in salt be 2 mg / g. It is a heavy metal and much of its consumption can be dangerous to human health. It is recommended that the salt contain a smaller amount of this metal or if it is possible not to contain it at all [17]. As for chromium, all results were in much greater than the maximum human consumption specified by the Codex Alimentarius.

Table (3) average concentration of heavy metals in salt sites in Iraq compared to the maximum limit of the Codex Alimentarius

Tracer	Mean ± SD	Codex maximum limit
pb	0.6227∓0.021	1.0
Cd	13.7905∓0.002	0.25
Cu	22.2385∓0.80	2
Cr	10.42125∓0.143	0.5

Table (4) Comparing the concentration of heavy metals in salt sites in other countries by a group of researchers

location	Pb (ppm)	Cd (ppm)	Cu (ppm)	Cr (ppm)	References
Himalayan	0.06	ND	0.04	0.42	7
NIGERIA	0.36	0.50	0.03	ND	18
Iran	1.59	0.91	1.24	ND	19
Ghana	0.001	2.80	6.88	ND	20
Egypt	0.66	0.22	0.47	ND	21
KSA (Riyadh)	0.0114	0.0002	0.0009	0.0005	9
Sri Lanka	ND	4.07	ND	ND	22

ND=not detected

Conclusions

The purpose of the current study was to assess chemically unprocessed rock salt at significant salt producing sites in Iraq. During the research, the focus was on comparing the outcomes with regards to the upper limits set by the Codex Alimentarius Commission, the World Health Organization (WHO), and the Food and Agriculture Organization (FAO) for human consumption. In Codex the concentration of Cd, Cu and Cr was above their safety limits as stipulated in the SON and Codex regulations. These results indicate that some metallurgical processes should be performed the samples' salt purity should be increased. To increase their degree of purity, samples of unrefined rock salt must go through some sort of chemical or physical process. To increase the purity of salt samples to 97%, they must additionally go through rigorous refining and metallurgical operations. The mineral content just has to be below the limit for human consumption defined by the Codex Alimentarius Commission.

References

1) Lugendo, I. J., & Bugumba, J. (2021). Heavy metals and essential elements in table salt extracted from Bahi wetlands in Central Tanzania. *International Journal of Engineering, Science and Technology*, *13*(4), 21-31.

2) Ben Garali, A., Ouakad, M., & Gueddari, M. (2010). Contamination of superficial sediments by heavy metals and iron in the Bizerte lagoon, northern Tunisia. *Arabian Journal of Geosciences*, *3*, 295-306.

3) Trumbo, S. K., Brown, M. E., & Hand, K. P. (2019). Sodium chloride on the surface of Europa. *Science advances*, *5*(6), eaaw7123.

4) Lanaro, G., & Patey, G. N. (2016). Birth of NaCl crystals: Insights from molecular simulations. *The Journal of Physical Chemistry B*, *120*(34), 9076-9087.

5) ARAS N.K.; ATAMAN O.Y., Trace Element Analysis of Food and Diet. The Royal Society of Chemistry (2006)

6) EBDON L.; EVANS E.H.; FISHER A.S.; HILL S.J., An Introduction to Analytical Atomic Spectrometry. John Wiley & Sons (1996).

7) ul Hassan, A., Din, A. M. U., & Ali, S. (2017). Chemical characterisation of Himalayan rock salt. *Pakistan Journal of Scientific & Industrial Research Series A: Physical Sciences*, *60*(2), 67-71.

8) Amorim, F. A., & Ferreira, S. L. (2005). Determination of cadmium and lead in table salt by sequential multi-element flame atomic absorption spectrometry. *Talanta*, *65*(4), 960-964.

9) Al-Rajhi, M. A. (2014). Study of some heavy metals and trace elements. *Physics International*, *5*(2), 128-131.

10) Soylak, M., Narin, I., Elci, L., & Dogan, M. (2001). Atomic absorption spectrometric determination of copper, cobalt, cadmium, lead, nickel and chromium in table salt samples after preconcentration on activated carbon. *Kuwait Journal of Science and Engineering*, *28*, 361–370.

11) Almayahi, B. A., Hakeem, E., Alduhaidahawi, F. J., & Aqeela, H. (2014). Heavy metals concentration in different soil samples in Najaf city, Iraq. *International Journal of Engineering Trends and Technology (IJETT)*, *16*(2), 69-71.

12) Amorim, F. A., & Ferreira, S. L. (2005). Determination of cadmium and lead in table salt by sequential multi-element flame atomic absorption spectrometry. Talanta, 65(4), 960-964.

13) Sigel, A., Sigel, H., & Sigel, R. K. (Eds.). (2013). *Interrelations between essential metal ions and human diseases* (Vol. 13, pp. 81-137). Netherlands: Springer Netherlands.

14) Loef, M., & Walach, H. (2012). Copper and iron in Alzheimer's disease: a systematic review and its dietary implications. *British Journal of Nutrition*, *107*(1), 7-19.

15) Abdollahi, M., Farshchi, A., Nikfar, S., & Seyedifar, M. (2013). Effect of chromium on glucose and lipid profiles in patients with type 2 diabetes; a meta-analysis review of randomized trials. *Journal of Pharmacy & Pharmaceutical Sciences*, *16*(1), 99-114.

16)FAO/WHO Report of the fifth session of the Codex Committee on Contaminant in foods. FAO/WHO, Hague, Netherlands, 21–25. March 2011.

17) CODEX, A., & FORCE, I. T. (2006). Joint FAO/WHO food standards programme.

18) UKWO, S. P. (2021). Human health risk assessment of heavy metal contaminants in table salt from Nigeria. Food and Environment Safety Journal, 19(4).

19) Khaniki, G. R. J., Dehghani, M. H., Mahvi, A. H., & Nazmara, S. (2007). Determination of trace metal contaminants in edible salts in Tehran (Iran) by atomic absorption spectrophotometry. *J Biol Sci*, *7*(5), 811-814.

20) Affam, M., & Asamoah, D. N. (2011). Economic potential of salt mining in Ghana towards the oil find. Research journal of environmental and earth sciences, 3(5), 448-456.

21) Khalil, M., Elharairey, M., Atta, E., & Aboelkhair, H. (2021). Evaluation of salts in salt pans, Siwa Oasis, Egypt. Arabian Journal of Geosciences, 14, 1-10.

22) Wijekoon, W. M. C. J., Kaumal, M. N., & Perumpuli, P. A. B. N. Edible Salt: A Possible Source of Heavy Metal Intake in Sri Lanka.

Improving Convergence and Exploration in the Flower Pollination Algorithm: The Effective Local Flower Pollination Algorithm (ELFPA)

Shifaa N. Sahi[1], Nazar K. Hussein[2]

[1]Dept. of Mathematics, College of Computer Science and Mathematics,

Tikrit University, Iraq,

shafaanamh@gmail.com

[2]Dept. of Mathematics, College of Computer Science and Mathematics,

Tikrit University, Iraq,

nazar.dikhil@tu.edu.iq

Improving Convergence and Exploration in the Flower Pollination Algorithm: The Effective Local Flower Pollination Algorithm (ELFPA)

Shifaa N. Sahi[1], Nazar K. Hussein[2]

[1]*Dept. of Mathematics, College of Computer Science and Mathematics, Tikrit University, Iraq, shafaanamh@gmail.com*

[2]*Dept. of Mathematics, College of Computer Science and Mathematics, Tikrit University, Iraq, nazar.dikhil@tu.edu.iq*

Abstract

Another popular swarm intelligence technique for handling optimization issues is the Flower Pollination Algorithm (FPA). It has grown in prominence as a result of its straightforward architecture and powerful optimization skills. FPA shares some drawbacks with other swarm-based algorithms, including a propensity for local optima and slow rate of improvement for high-dimensional global optimization problems. The Effective Local Flower Pollination Algorithm (ELFPA), a modified version of FPA, has been offered as a solution to these problems. By employing a balanced exploitation and exploration approach, ELFPA seeks to improve exploitation capabilities and solution accuracy. In order to avoid local optima, it uses random operators. These tactics work best together, which improves FPA performance. Benchmark test functions, including those from the CEC 2017 test suite, were evaluated experimentally. The findings of comparing the performance of ELFPA to other swarm intelligence algorithms and sophisticated methodologies were quite positive and encouraging.

Keywords: Flower Pollination Algorithm, Swarm intelligence, Metaheuristic algorithm, Local optima, Optimization algorithm

1. Introduction

In a mathematics problem known as an optimization problem, a collection of variables is changed to reduce or increase an objective function while satisfying a set of constraints. In other words, it is the challenge of identifying the optimum solution from all those that satisfy the given constraints. There are two primary types of optimization issues: linear and nonlinear. The objective function and restrictions in linear optimization problems are both linear functions. The objective function, the restrictions, or both are nonlinear functions in nonlinear optimization problems. Numerous disciplines, including engineering, economics, finance, computer science, physics, and many others, encounter optimization issues [1]. Common instances of optimization problems include:

Find the shortest path between any two points on a graph, minimize the error in the regression model, maximize the accuracy in the classification model, and optimize the position of objects to minimize collisions in a three-dimensional environment. These tasks are all related to finding the minimum cost of producing a certain amount of product. Numerous optimization procedures, including graded ratios, Newton's method, simulated softening, genetic algorithms, and many others, can be utilized to address optimization problems. The particulars of the problem, the traits of the target function, and any constraints will determine which algorithm is used. There are numerous categories of optimization algorithms, each with a distinct methodology. However, the following are some broad groups of optimization algorithms: [2]

Deterministic optimization algorithms: These algorithms employ a particular strategy to locate the best outcome. Mathematical programming techniques including linear programming, quadratic programming, and accurate programming are typically used. Random optimization algorithms: These algorithms look for the best answer based on a set of probabilities. The majority of the time, they rely on metaheuristic techniques like simulated annealing, genetic algorithms, particle swarm optimization, and ant colony

optimization. Algorithms for gradient-based optimization: These algorithms iteratively search for the minimum value using the gradient of the target function. They are typically employed for objective functions that are smooth and distinct. Derivative-free optimization algorithms: These algorithms are capable of handling heterogeneous or non-differentiable objective functions since they do not rely on the objective function's derivative. The Nelder-Mead simplex approach, evolutionary algorithms, and pattern search are a few examples of methods that are commonly based on research. Algorithms for hybrid optimization: These techniques integrate two or more optimization algorithms to boost the potency of each and improve performance. An imperative technique and a random method, for instance, might be combined in a hybrid algorithm. The goal of cascading algorithms is to handle difficult optimization problems that are beyond the scope of conventional mathematical techniques. These algorithms, which are based on heuristics and research techniques, don't promise to find the best solution, but rather to do so in an acceptable amount of time.

Metaheuristic algorithms come in a variety of forms, but the following are the most popular:

Natural selection and evolution are the foundations of genetic algorithms (GAs). They begin with a variety of viable answers and then create new ones using genetic elements like intersection and mutation. The best solutions are chosen for the following generation [3], Particle Mobilization Optimization (PSO): These algorithms are based on the behavior of particle swarms, and solutions are evaluated based on their applicability. The Ant Colony Optimization (ACO) algorithms are based on how ants navigate to find the shortest path between their colony and a food source. Each particle represents a potential solution and moves through the search area, adjusting its position based on its best position and the best position of the swarm. These algorithms are based on the physical annealing process, where the material is gradually heated and cooled to obtain the least energy state. Each ant symbolizes a potential solution and travels across the search space, leaving the pheromones that draw the other ants to follow the same path. To explore the search space and escape the local Optima [6], Tabu Search (TS): These algorithms are built on the idea of retaining a list of recently visited prohibitions or disallowed solutions. The algorithm starts with a high temperature and gradually lowers it. The algorithm traverses the search space, dodging obstacles and venturing into uncharted territory.

2. Preliminaries

2.1 flower pollination algorithm (FPA)

One of the metaheuristic optimization algorithms, the flower pollination algorithm (FPA), was first put forth by Xin-She Yang, the same researcher who came up with the Firefly method. The Flower Pollination Algorithm, also known as FPA, is a brand-new optimization algorithm created based on the pollination process carried out by plants. It was first introduced in its paper "Flower Pollination Algorithm for Global Optimization," published in the journal "Unconventional Computation and Natural Computation" in 2012 [7]. This program applies the pollination process to the suggested solutions in each optimization cycle using a novel model [8]. The flower pollination algorithm is predicated on the idea that stronger candidates for solutions in the current generation tend to have genetic traits that are more likely to be handed down to succeeding generations. Since plants are pollinated at random, the algorithm makes use of this notion to produce a random pollination process that aids in diversity and encourages exploration throughout the solution's potential domain. Numerous example challenges, including concerns with numerical methods, performance optimization, data categorization, image analysis, artificial intelligence, and deep learning, can be solved using the flower pollination algorithm. The flower pollination algorithm (FPA) is a relatively new optimization technique, and Yang's initial algorithm from 2012 has undergone numerous modifications and extensions. The Binary Flower Pollination Algorithm (BFPA) is made for tackling binary optimization issues and is especially well suited for feature selection tasks. The following are some of the most recent versions of FPA along with their references. Implementation of the flower pollination algorithm This paper presents a new optimization approach based on the Flower Pollination Algorithm (FPA) to solve the

Economic Load Dispatch (ELD) and the Combined Economic Emission Dispatch (CEED) problems in power systems. This approach integrates economic and environmental objectives into the optimization process using the FPA algorithm. The suggested FPA is a meta-heuristic algorithm that draws inspiration from how flowers in nature pollinate one another [11]. The proposed DECD-FPA algorithm offers a promising approach for optimizing engineering design problems with multiple objectives and constraints. It is a modified version of the FPA algorithm that incorporates a new search strategy to improve its performance in solving mechanical engineering design problems. [12]. The invention of an adaptive version of the FPA algorithm that integrates self-adaptation techniques to increase its performance in resolving software test suite minimization issues is the contribution of this research. A viable method for optimizing software testing issues with intricate and sizable software systems is the AFPA algorithm [13]. The suggested AFPA algorithm offers a potential strategy for building antenna arrays with increased performance and decreased complexity and cost. Synthesis of linear antenna arrays. Other varieties of antenna arrays and other optimization issues in the field of antenna design and optimization can be addressed using the method [14]. The paper provides insights into the benefits and drawbacks of the FPA algorithm, which can help researchers and practitioners choose the best optimization algorithm for their particular problem. Flower pollination algorithm: a comprehensive review of the FPA algorithm, its variations, and its applications in various fields. The evaluation also identifies the areas that require more study if the FPA algorithm is to perform and operate more effectively [15]. The novel flower pollination algorithm suggestion is a novel modification of the FPA method that improves the algorithm's performance for continuous optimization issues. The suggested IFPA method provides a more effective search space exploitation while maintaining population variety, improving optimization results [16]. Tuning the flower pollination algorithm's parameters First, it offers a thorough evaluation of the impact of the various FPA algorithm's parameters on performance. Second, it suggests a fresh method for parameter adjustment that could result in better optimization outcomes [17]. The performance of a modified flower pollination algorithm in resolving global optimization issues is enhanced. The suggested approach, a flower pollination algorithm with pollination attraction, includes a new mutation operator and a new technique for updating the flower population [18]. a thorough examination of the suggested strategy, which compares the new flower pollination algorithm, the improved pollination mechanism, and the adaptive learning mechanism to other cutting-edge metaheuristic algorithms on a number of benchmark functions [19]. While the adaptive learning mechanism updates the step size and aids in balancing exploration and exploitation, the increased pollination mechanism enhances the search capability by introducing pollination with random flowers and nearby flowers. An improved method for discreate flower pollination was tested on several datasets [20], and the findings demonstrate that it performs better than previous algorithms in terms of both solution quality and convergence speed [21]. The approach is straightforward, simple to use, and in some circumstances outperforms competing optimization algorithms. To acquire the best outcomes for a particular optimization problem, it is advised to test out a few different optimization algorithms because it may not always be the best option. The flower pollination algorithm (FPA) has several disadvantages in addition to its benefits, such as the possibility of a lengthy processing time. The optimal solution may take an algorithm longer to find than it does for some other algorithms. The severity of the issue could be considerably impacted. Large-scale or high-dimensional problems might be challenging for the algorithm to handle, and these situations may necessitate adjusting the algorithm to improve performance. You might not always come up with the best answer. In some circumstances, the algorithm might have trouble locating the best solution, or it might come close to the best solution but fall short. To enhance its performance, you might have to make changes. By making various adjustments, such as modifying the values of some parameters or the update method for solutions, the algorithm's performance can be enhanced. You might experience the issue of settling for local answers. If the start is bad, the algorithm may struggle to avoid falling into local solutions and failing to find the best answer. The Flower Pollination Technique is a powerful optimization algorithm that offers a number of benefits, such as: Ease of application: The Flower Pollination Algorithm is easily applied to a variety of issues that call for numerical solutions. Speed of solution: Because the algorithm is based on the idea of probability and regular movement between options, it finds the best solution to the given problem fast and efficiently. A flower pollination algorithm is capable

of handling a wide range of issues and, in certain situations, outperforms other algorithms in locating the best solutions. Ability to avoid settling for local solutions: The algorithm's ability to settle for local solutions is what gives it a better chance of finding the ideal answer. Capacity to enhance existing solutions: The algorithm's ability to enhance current solutions rather than only find optimal answers distinguishes it and makes it valuable for resolving complicated issues. The algorithm's capacity to learn and adapt to its surroundings is used to enhance both its performance and the solutions it provides. The flower pollination algorithm, which is regarded as one of the best in the fields of optimization and data analysis, has a wide range of advantages and benefits. The local search process in the algorithm was modified in this study in order to avoid these flaws and try to discover solutions to them by increasing the randomness inside the equation and changing the updating process for the local solution rather than depending on a dominant factor. The comprehensive solution has undergone changes. the exploration and exploitation operations by including a control factor as a counterbalance in the modernization equation. Original Flower Pollination Algorithm There are two main types of pollination: biotic and abiotic. About 90% of flowering plants are biopollinated, which means that pollen is spread by pollinators like insects and animals. The remaining 10% of flowering plants are pollinated abiotically, which means that no pollinators are needed. With at least 200,000 different species of pollinators, including insects, bats, and birds, pollinators, also known as pollen carriers, can be extremely diverse. A notable example of a pollinator is the honey bee, which has the potential to develop a trait known as "flower stability" in which it favors particular flower kinds over others. Because it will improve the passage of flower pollen to the same plants and hence increase the reproduction of the same flower species, such floral stability has evolutionary benefits. Because pollinators can ensure nectar supply with their limited memory and at the lowest possible cost, rather than concentrating on some new, unpredictable, and potentially more rewarding flower species, this bloom constancy may also be advantageous for pollinators. The stability of flowering may call for a low initial outlay and, most likely, a nectar intake that is ensured. Self-pollination is the fertilization of one flower, such as peach flowers, from pollen of the same flower or different flowers of the same plant, and frequently takes place when there are no pollinators present. Pollination by cross-pollination, self-pollination, or cross-pollination means that pollination can occur from flower pollen from a different plant. Pollination can be seen as comprehensive because cross-pollination can take place over great distances and because pollinators like bees, bats, birds, and flies are capable of flying great distances. Additionally, bees and birds have been known to engage in a type of flight behavior known as fibrous flight, in which the steps of the jumping or flying distance are subject to a fibrous distribution and the stability of the flower can be used as an upward step by comparing or contrasting two flowers. The following four rules can be used to explain the stability of the bloom and the behavior of pollinators throughout the pollination process: Abiotic self-pollination is local pollination, but biocross-pollination is global pollination because pollinators make a lengthy journey. The likelihood of reproduction, which is inversely correlated with the resemblance of two different flowers, might be thought of as flower wandering. Additionally, it should be highlighted that A has the potential to influence the interaction between universal pollination and local pollination by adjusting p. [0,1]

2.1.1 Mathematical representation of mass vaccination and local pollination

global and local pollination represented mathematically the two key steps in the flower pollination algorithm are bulk and local pollination processes. Pollinators like insects spread pollen in large quantities, and since they can probably fly and move quickly, pollen can go great distances. The following is how they can be mathematically represented:

$$y_i^{t+1} = y_i^t + \gamma * l(\beta) * (y_i^t - y_{best}) \qquad \dots (1)$$

$$l(\beta) = 0.01 \times \frac{u \times \sigma}{|v|^{\frac{1}{\beta}}} \qquad (2)$$

$$\sigma = \left(\frac{\Gamma(1+\beta) \times \sin\left(\frac{\pi\beta}{2}\right)}{\Gamma(\frac{1+\beta}{2}) \times \beta \times 2^{\left(\frac{\beta-1}{2}\right)}} \right)^{\frac{1}{\beta}} \qquad (3)$$

Whereas, y_i^t the solution in the course:t, y_{best} the best solution obtained in the course t, γ Scaling factor to control step size, $l(\beta)$ levy distribution trace parameter, y_i^{t+1} the new solution.

As for local pollination, self-pollination, that is, between flowers on the plant itself, and it can be

Its mathematical representation is as follows

$$y_i^{t+1} = y_i^t + \epsilon * \left(y_j^t - y_k^t\right) \qquad \dots (4)$$

Whereas, y_i^t the current solution at iteration t, and y_i^{t+1} the new solution: y_j^t, y_k^t two different solutions j, k randomly selected values, ϵ random variable following a uniform distribution

Pseudo-code of Flower pollination algorithm

Objective min or max $f(X)$, $X = (X_1, X_2, \dots, X_N)$
Initialize a population of N flowers /pollen gametes with random solutions
Find the best solution g^* in the initial population
Define a switch probability $p \in [0,1]$
While ($t < Maxiter$)
    For (all N flowers in the population)
        If rand<p
            Calculate L which obeys a Levy distribution
            Global pollination via $x_i^{t+1} = x_i^t + l(\beta)\,(g^* - x_i^t)$
        Else
            Generate ϵ from a uniform distribution in $[0,1]$
            Randomly choose j and k from N
            local pollination via $x_i^{t+1} = x_i^t + \epsilon\,(x_j^t - x_k^t)$
        End if
        Evaluate new solutions
        Update the best solution
    End for
Find the current best solution g_*
End while

2.2 Proposed method

The Levy distribution is used to calculate the global search percentage in the original blossoming pollination method. This percentage represents the difference between the optimal solution and the current solution. By adding qualitative options that are far from the present optimal solution through uncertainty and unpredictability, which is given by the ratio that follows the Levy distribution, this update process may produce good results, but it may be constrained in variety for far solutions. Since the SSA technique's step size is dependent on the factor c_1, we added a step size based on the search space as a third term to the original equation to create the proposed approach. As a result, the original algorithm's global search can be

improved, and better results are attained. For example, in the equation below, the current solutions can be replaced with new solutions that cover a region that is very remote from the current solution and the best solution. This increases the likelihood of obtaining promising solutions that enable the algorithm to approach the best global solution.

$$x_i^{t+1} = x_i^t + l(\beta) * (g^* - x_i^t) + c_1 * \left((ub - lb) * c_2 + lb\right) \quad \dots (5)$$

the Levy distribution, and the original flower pollination algorithm updates the current solution by adding the proportion of tracking the normal distribution within the interval [0,1] from the difference between two sites within the current iteration that are randomly selected within the community, and this step is initially intended to aid the algorithm. If the community adopted a method of choosing three random solutions, and the percentage of addition between the two random solutions was the same percentage or value that we used in the global search process described above, c_1 and this percentage is not added to the current solution but added to the third random solution that is chosen, the search process will be faster and more accurate.

$$x_i^{t+1} = x_{r_1}^t + c_1 * \left(x_{r_2}^t - x_{r_3}^t\right) \quad \dots (6)$$

$$c_1 = 2e^{-(\frac{4t}{Maxiter})^2} \quad \dots (7)$$

Enhanced Local Flower pollination algorithm

Objective min or max $f(x)$, $X = (X_1, X_2, \dots, X_N)$

Initialize a population of N flowers /pollen gametes with random solutions

Find the best solution g^* in the initial population

Define a switch probability $p \in [0,1]$

While ($t < Maxiter$)

Compute the value of c_1 by eq(7)

Evaluate the objective function of each solution x_i^t as $Fitness(i)$

For (all N flowers in the population)

$Xnew = zeros(dim)$

If rand<p

Calculate L which obeys a Levy distribution

Global pollination via

$Xnew = x_i^t + l(\beta) * (g^* - x_i^t) + c_1 * ((ub - lb) * c_2 + lb)$

Else

Generate ϵ from a uniform distribution in [0,1]

Randomly choose r_1, r_2 and r_3 from N

local pollination via

$Xnew = x_{r_1}^t + c_1 * (x_{r_2}^t - x_{r_3}^t)$

End if

Evaluate the objective function F_{new} at the solution $Xnew$

If $F_{new} < Fitness(i)$

$x_i^{t+1} = Xnew$

End for

Update the best solution

End for

Find the current best solution g_*

End while

3. Experimental Results and Analysis

For replicating real-world issues, a wide range of unique test routines might be quite helpful. These functions are consistently used by researchers to gauge how effective random algorithms are. This contrasts the performance of the proposed algorithm with a number of sophisticated metaphysical algorithms, including as BAT [23], PSO [4], CSO [24], and SCA [25], and WOA [26], MFO [27], HHO [28], and SSA [29]. This compares ELFPA's performance with CEC2017 test functions [22]

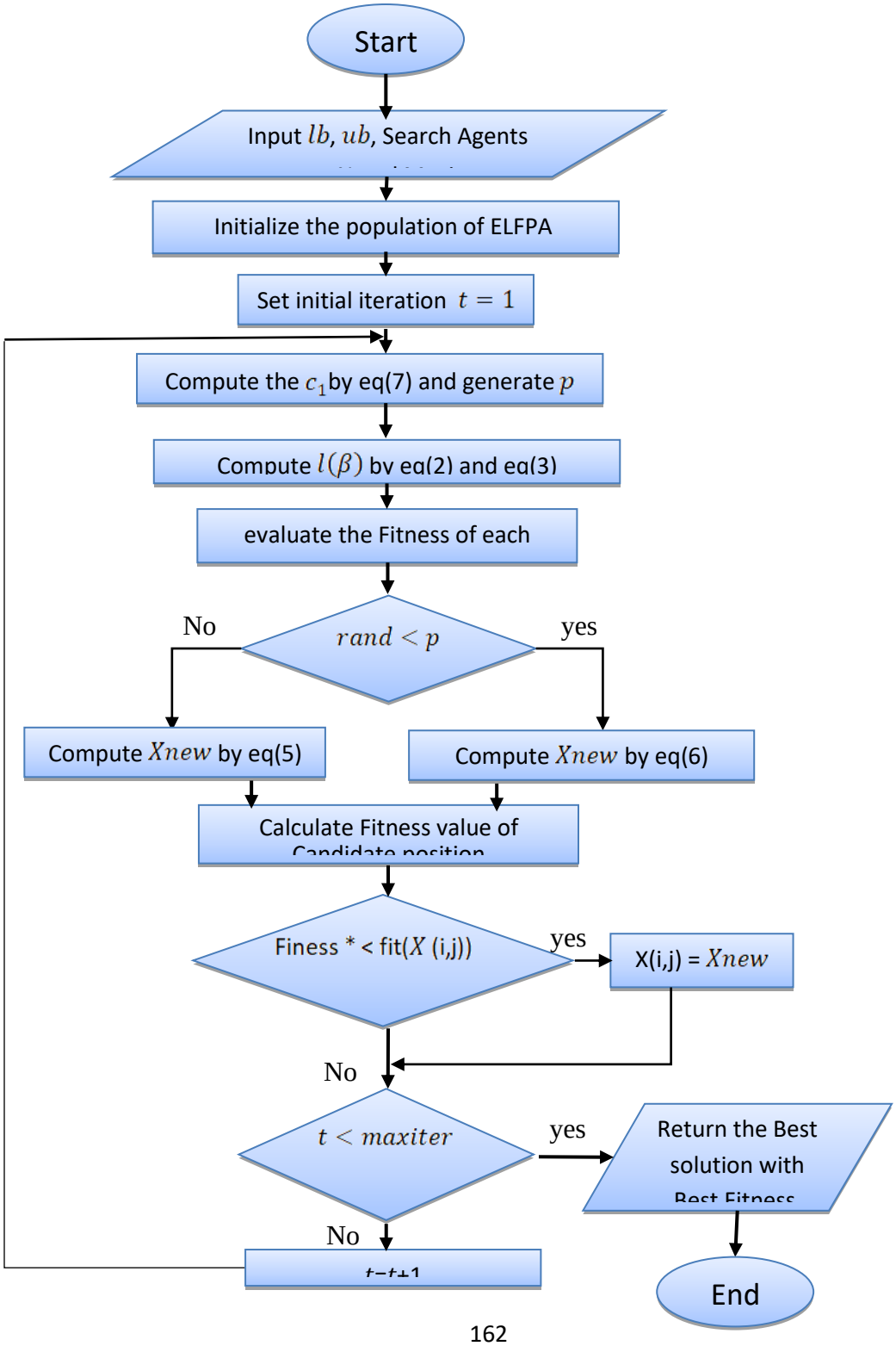

in 50 dimensions. Organize the test's setup. Using the CEC2017 test functions with a dimension of 50, which are described in Table 1, the effectiveness of the ELFPA algorithm will be evaluated in this section. It is intended to demonstrate how the ELFPA algorithm performs well with various test functions by evaluating the enhanced algorithm using this collection of test functions. When comparing the ELFPA algorithm to other optimization algorithms of the same type, which include Since metaphysical algorithms are random, it is best to assess and contrast them unbiasedly to ensure that testing procedures are fair. The trials were carried out on an Intel Core i5-7200U (2.50 GHz) processor with 4 GB of main memory, and all algorithms were created in Python 3. All forms of functions, including monotony, multimodality, hybridity, and compositeness, are covered by the test functions.

50 dimensions have been used with CEC 2017 issues and test functions as shown in Table.1. We repeat each test 30 times, concentrating on each distinct function, to make sure that all of our tests are accurate, performed consistently, and fairly. The maximum number of iterations and population size (N) are specific to each experiment (maximum).

Table 1. CEC 2017 benchmark function.

Type	**Fun**	**Function name**	**Fmin**
U	F1	Shifted and rotated bent cigar function	100
U	F2	Shifted and rotated Zakharov	300
M	F3	Shifted and rotated ROSENBROCKS	400
M	F4	Shifted and rotated restrains	500
M	F5	Shifted and rotated expanded scoffers f6	600
M	F6	Shifted and rotated Lunacek bi -restrains	700
M	F7	Shifted and rotated non-continuous restrains	800
M	F8	Shifted and rotated levy	900
M	F9	Shifted and rotated Schwefels	1000
H	F10	Hybrid function 1 (n=3)	1100
H	F11	Hybrid function 2 (n=3)	1200
H	F12	Hybrid function 3 (n=3)	1300
H	F13	Hybrid function 4 (n=4)	1400
H	F14	Hybrid function 5 (n=4)	1500
H	F15	Hybrid function 6 (n=4)	1600
H	F16	Hybrid function 6 (n=5)	1700
H	F17	Hybrid function 6(n=5)	1800

H	F18	Hybrid function 6 (n=5)	1900
H	F19	Hybrid function 6(n=6)	2000
C	F20	Composition function 1 (n=3)	2100
C	F21	Composition function 2 (n=3)	2200
C	F22	Composition function 3 (n=4)	2300
C	F23	Composition function 4 (n=4)	2400
C	F24	Composition function 5 (n=5)	2500
C	F25	Composition function 6 (n=5)	2600
C	F26	Composition function 7 (n=6)	2700
C	F27	Composition function 8 (n=6)	2800
C	F28	Composition function9 (n=3)	2900
C	F29	Composition function 10 (n=3)	3000

2. Measure performance and determine parameters

Metrics must be employed in order to compare and show the effectiveness of the ELFPA algorithm; thus, we will use three metrics to assess how well the suggested algorithm performs. The average of the results of the improvement is the first metric, and it is determined as follows:

$$\text{Mean} = \frac{1}{n}\sum_{i=1}^{n} X_i \qquad (8)$$

It stands for the outcome of each development. The improvement outcomes' second measure and standard deviation, X_i, are calculated as follows:

$$\text{Std} = \sqrt{\frac{1}{n-1}\sum_{i=1}^{n}(X_i - \text{Mean})^2} \qquad (9)$$

In addition to the third scale, the standard deviation and median (MED), in comparison, show how stable the method is. A more reliable and adaptable algorithm will have a lower standard deviation, according to science. Table **2** lists the parameters for the ELFPA and other algorithms. The comparisons made are accurate since each algorithm is set up to operate in a setting that is optimal for its parameters. Additionally, the bolded results are the best ones.

Table 2. Hyperparameter settings

Algorithm	**Parameter**	**range\value**
ELFPA	p Coefficient c_1	[0, 1] [2/e, 2]
FPA	p	[0, 1]
MFO	T	[-1, 1]
CSO	Phi	0
BAT	Loudness, Pulse rate Frequency minimum Frequency maximum	0.5, 0.5 0 2
PSO	Inertia weight (wmin, wmax) Cognitive coefficient	0.04, 0.09 2
HHO	Beta	1.5
WOA	Convergence constant (a) [0, 2] Coefficient (b) 1	2
SCA	Convergence constant r_1	[0, 2]
SSA	Coefficient c_1	[2/e, 2]

4. Numerical performance evaluation

The results are shown in the tables, with the best result shown in bold. The ultimate values of win (W), draw (T), and loss (L) for each algorithm are shown in the last row of each table. Using the CEC 2017 standard with 50 dimensions and a focus on the phases of exploration, exploitation, and the capacity to avoid local optimal solutions, the efficiency of the ELFPA was compared to the efficiency of various improvers. Additionally, the overall performance of ELFPA is contrasted with that of comparable algorithms.

Table 3. Results of Unimodal functions for the ELFPA vs some recent techniques.

Fun	**Criteria**	**CSO**	**SSA**	**PSO**	**WOA**	**BAT**	**HHO**	**SCA**	**MFO**	**FPA**	**ELFPA**
F1	avg	1.81E+12	3.08E+09	1.52E+11	1.16E+10	1.36E+12	7.10E+11	5.28E+11	4.88E+11	2.55E+12	**9950.32**
	std	2.192E+11	2.537E+09	4.952E+10	4.472E+09	3.237E+10	7.922E+10	5.719E+10	1.969E+11	3.180E+11	9.664E+03
	med	1.779E+12	3.430E+09	1.549E+11	1.010E+10	7.765E+10	7.318E+11	5.219E+11	5.181E+11	2.589E+12	4.980E+04

F2	avg	469217.6	**109430.5**	163000.6	193137.4	4181579	203536.7	145726.5	300850.9	615757.4	272714
	Std	1.585E+06	2.506E+04	2.967E+04	6.001E+04	1.505E+04	2.757E+04	2.341E+04	1.047E+05	7.499E+04	5.892E+04
	med	3.806E+05	1.095E+05	1.616E+05	1.825E+05	8.602E+04	2.003E+05	1.420E+05	2.793E+05	6.229E+05	2.596E+05
rank	W/T/L	0/0/2	1/0/1	0/0/2	0/0/2	0/0/2	0/0/2	0/0/2	0/0/2	0/0/2	1/0/1

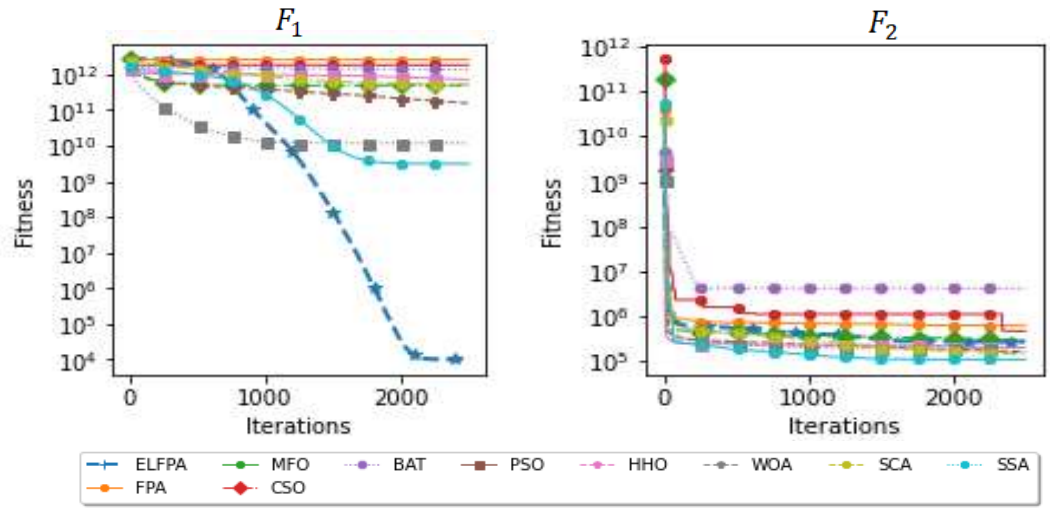

Fig. 2 ELFPA for F1 and F2 Convergence curves and other traditional algorithms during 2500 iterations

4.1 Capabilities for exploitation analyses and exploration

The test functions F1 and F2 are single-minimum value functions, and the efficiency of the proposed algorithm ELFPA is tested in the exploitation process by applying the algorithm to these two functions. The results showed the superiority of the algorithm in these functions, which confirms that the algorithm is very efficient in exploitation by achieving a strong ability to solve these Problems and reaching the optimal solution, and this is evident from Table 3 Also, Figure 2 shows the convergence of the algorithm compared to other algorithms.

As for testing the ability of the algorithm to solve multimodal optimization issues, which are the functions that include more than one minimum value, which are the F3_F9 functions, the results of the algorithm were very strong, and this can be seen in Table 4 as well as Figure 3, which shows the algorithm's convergence compared to other algorithms, and this shows the strength of the algorithm in exploration and obtaining new solutions.

Fun	**Criteria**	**CSO**	**SSA**	**PSO**	**WOA**	**BAT**	**HHO**	**SCA**	**MFO**	**FPA**	**ELFPA**
F3	avg	66998.4	800.18	4753.17	1153.63	52324.62	21138.93	8630.45	5358.94	126831.3	**587.44**
	std	1.402E+04	9.771E+01	1.296E+03	1.460E+02	4.641E+02	4.230E+03	1.756E+03	3.475E+03	2.009E+04	3.358E+01
	med	6.602E+04	7.918E+02	4.930E+03	1.123E+03	1.190E+03	2.077E+04	8.607E+03	4.342E+03	1.303E+05	5.969E+02
F4	avg	1464.14	846.29	973.99	976.4	1176.15	951.15	1091.82	990.8	1704.29	**579.93**
	std	6.610E+01	7.137E+01	6.156E+01	7.472E+01	4.057E+01	3.603E+01	3.351E+01	9.151E+01	7.674E+01	1.354E+01

	med	1.486E+03	8.457E+02	9.729E+02	9.589E+02	7.339E+02	9.484E+02	1.095E+03	9.703E+03	1.713E+03	5.671E+02
F5	avg	769.98	685.59	684.8	718.45	711.76	702.1	699.78	689.39	808.64	**604.84**
	std	1.194E+01	1.113E+01	8.197E+00	1.568E+01	1.041E+01	6.522E+00	5.907E+00	1.282E+01	1.147E+01	2.336E+01
	med	7.734E+02	6.834E+02	6.856E+02	7.190E+02	6.340E+02	7.025E+02	6.981E+02	6.871E+02	8.092E+02	6.050E+02
F6	avg	4193.63	1461.41	1514.89	1791.32	3002.68	1749.65	1707.13	2173.39	6170.34	**857.71**
	std	2.826E+02	1.626E+02	7.016E+01	9.950E+01	1.004E+02	5.799E+01	7.866E+01	5.200E+02	3.970E+02	2.179E+01
	med	4.111E+03	1.435E+03	1.496E+03	1.780E+03	1.098E+03	1.773E+03	1.714E+03	2.121E+03	6.237E+03	8.516E+02
F7	avg	1790.8	1182.11	1250.4	1253.28	1745.96	1205.97	1405.86	1403.36	2040.57	**879.49**
	std	7.072E+01	7.845E+01	5.276E+01	5.448E+01	8.739E+01	3.710E+01	3.010E+01	7.913E+01	8.556E+01	1.378E+01
	med	1.774E+03	1.179E+03	1.246E+03	1.255E+03	1.037E+03	1.200E+03	1.411E+03	1.373E+03	2.051E+03	8.788E+02
F8	avg	70048.41	15780.9	19896.09	28484.07	16486.89	14882.34	25728.7	18673.84	104988	**960.79**
	std	1.002E+04	3.043E+03	3.964E+03	8.005E+03	4.102E+03	1.171E+03	4.033E+03	5.450E+03	1.333E+04	3.800E+01
	med	7.268E+04	1.459E+04	2.026E+04	2.641E+04	1.189E+04	1.463E+04	2.542E+04	1.782E+04	1.043E+05	9.477E+02
F9	avg	15720.22	8708.89	14571.83	11940.56	11469.7	11395.55	15019.39	8900.26	15272.34	**7237.95**
	std	5.936E+02	8.483E+02	7.082E+02	1.400E+03	2.588E+03	1.303E+03	3.663E+02	1.228E+03	5.108E+02	8.830E+02
	med	1.578E+04	8.008E+03	1.469E+04	1.196E+04	7.076E+03	1.111E+04	1.506E+04	8.895E+03	1.529E+04	7.116E+03
rank	W/T/L	0/0/7	0/0/7	0/0/7	0/0/7	0/0/7	0/0/7	0/0/7	0/0/7	0/0/7	7/0/0

Table 4. Results of Multi-unimodal functions for the ELFPA vs some recent techniques.

As for testing the ability of the algorithm to solve multimodal optimization issues, which are the functions that include more than one minimum value, which are the F3_F9 functions, the results of the algorithm were very strong, and this can be seen in Table 4 as well as Figure 3, which shows the algorithm's convergence compared to other algorithms, and this shows the strength of the algorithm in exploration and obtaining new solutions.

In addition to testing the strength of the proposed algorithm in the process of exploitation and exploration, the capabilities of the algorithm were tested in the process of balancing between these two processes, and therefore the functions F10-F19 are the functions designated for this purpose. The results of the algorithm in these countries were very excellent compared to other algorithms as in Table 5 And also Figure 4, which shows the closeness ratio of the algorithm compared to other algorithms within these functions, which confirms the power of the algorithm in the balance between exploitation and exploration.

Fun	Criteria	CSO	SSA	PSO	WOA	BAT	HHO	SCA	MFO	FPA	ELFPA
F10	avg	50469.2	2449.69	4504.52	2782.58	92218.77	16365.74	8828.7	22276.62	93327.88	**1376.93**
	std	1.426E+04	5.261E+02	1.191E+03	6.232E+02	1.923E+03	2.679E+03	1.956E+03	1.646E+04	1.596E+04	6.071E+01
	med	4.817E+04	2.402E+03	4.120E+03	2.677E+03	4.662E+03	1.719E+04	8.579E+03	1.725E+04	9.404E+04	1.387E+03
F11	avg	9.00E+11	2.56E+09	3.76E+10	6.61E+09	7.07E+11	3.84E+11	1.22E+11	6.28E+10	1.13E+12	**3.47E+08**
	std	2.132E+11	2.641E+09	1.675E+10	3.649E+09	1.301E+10	1.112E+11	2.931E+10	4.455E+10	1.478E+11	3.012E+08
	Med	8.373E+11	1.834E+09	3.448E+10	5.755E+09	5.699E+09	3.967E+11	1.243E+11	4.834E+10	1.160E+12	2.814E+08
F12	avg	5.67E+11	147799.2	5.64E+09	1.8E+08	4.99E+11	1.70E+11	4.21E+10	2.33E+10	6.13E+11	**122560.5**
	std	2.047E+11	6.688E+04	3.459E+09	2.499E+08	1.131E+09	1.173E+11	1.563E+10	2.875E+10	7.107E+10	5.854E+04
	med	5.895E+11	9.423E+04	4.518E+09	1.125E+08	1.139E+09	1.409E+11	3.750E+10	7.490E+09	6.323E+08	2.814E+08
F13	avg	1.8E+08	687403	1178547	2291624	1.39E+08	30408952	4859968	2359651	39310857	**135729.5**
	std	9.520E+07	7.672E+05	1.201E+06	1.707E+06	8.484E+05	3.166E+07	3.373E+06	4.014E+06	1.400E+07	1.482E+05
	med	1.040E+08	5.727E+05	6.766E+05	2.127E+06	6.438E+05	1.999E+07	3.737E+06	1.033E+06	3.675E+07	1.110E+05
F14	avg	1.64E+11	**74358.9**	1.03E+08	26692289	1.08E+11	1.94E+10	6E+09	1.53E+09	2.55E+11	94143.94
	std	6.306E+10	3.138E+04	9.247E+07	4.638E+07	1.330E+09	1.468E+10	2.984E+09	2.910E+09	6.767E+10	4.442E+04
	med	1.464E+11	5.368E+04	6.167E+07	6.974E+06	5.678E+06	1.708E+10	5.575E+09	3.652E+05	2.625E+11	8.261E+04
F15	avg	11158.38	4037.96	4501.68	5515.57	10049.51	7402.1	5858.66	4471.31	12723.78	**2805.54**
	std	1.748E+03	5.624E+02	6.527E+02	8.221E+02	5.171E+02	1.753E+03	4.389E+02	5.127E+02	8.793E+02	3.704E+02
	med	1.087E+04	3.842E+03	4.574E+03	5.421E+03	3.145E+03	7.033E+03	5.916E+03	4.468E+03	1.281E+04	2.771E+03
F16	avg	61252.86	3683.91	3426.7	4192.94	148244.1	5216.22	4709.87	4534.96	2791807	**2532.01**
	std	1.634E+05	3.799E+02	3.704E+02	4.726E+02	2.495E+02	1.085E+03	2.911E+02	1.526E+03	1.943E+06	2.421E+02
	med	7.325E+04	3.568E+03	3.375E+03	4.113E+03	2.855E+03	4.952E+03	4.716E+03	4.182E+03	2.403E+06	2.527E+03
F17	avg	4.47E+08	5141403	7889465	16328707	4.53E+08	71212865	27543217	12940008	2.54E+08	**1762044**
	std	2.342E+08	4.167E+06	5.373E+06	1.274E+07	1.130E+07	4.117E+07	1.397E+07	1.501E+07	9.834E+07	1.464E+06
	med	3.408E+08	4.547E+06	6.203E+06	1.167E+07	3.500E+06	5.392E+07	2.351E+07	9.159E+06	2.455E+08	1.220E+06
F18	avg	6.1E+10	17053613	1.57E+08	29073092	**17754.6**	7.66E+09	3.74E+09	8.19E+08	1.12E+11	922549.4
	std	2.695E+10	1.984E+07	2.194E+08	6.049E+07	8.186E+07	8.203E+09	1.666E+09	2.304E+09	2.759E+10	8.978E+05
	med	7.234E+1	8.922E+0	6.868E+0	1.058E+0	5.009E+0	6.083E+0	3.407E+0	3.988E+0	1.187E+1	7.397E+0

		0	6	7	7	6	9	9	7	1	5
F19	avg	4560.53	3255.36	3812.37	3765.37	4237.13	3521.72	4007.32	3843.33	4703.76	**2734.93**
	std	2.392E+02	2.869E+02	3.241E+02	3.512E+02	4.889E+02	2.806E+02	1.611E+02	2.922E+02	1.384E+02	2.029E+02
	med	4.499E+03	3.235E+03	3.884E+03	3.813E+03	3.144E+03	3.596E+03	4.007E+03	3.797E+03	4.734E+03	2.732E+03
rank	w/t/l	0/0/10	1/0/9	0/0/9	0/0/10	1/0/9	0/0/10	0/0/10	0/0/10	0/0/10	8/0/2

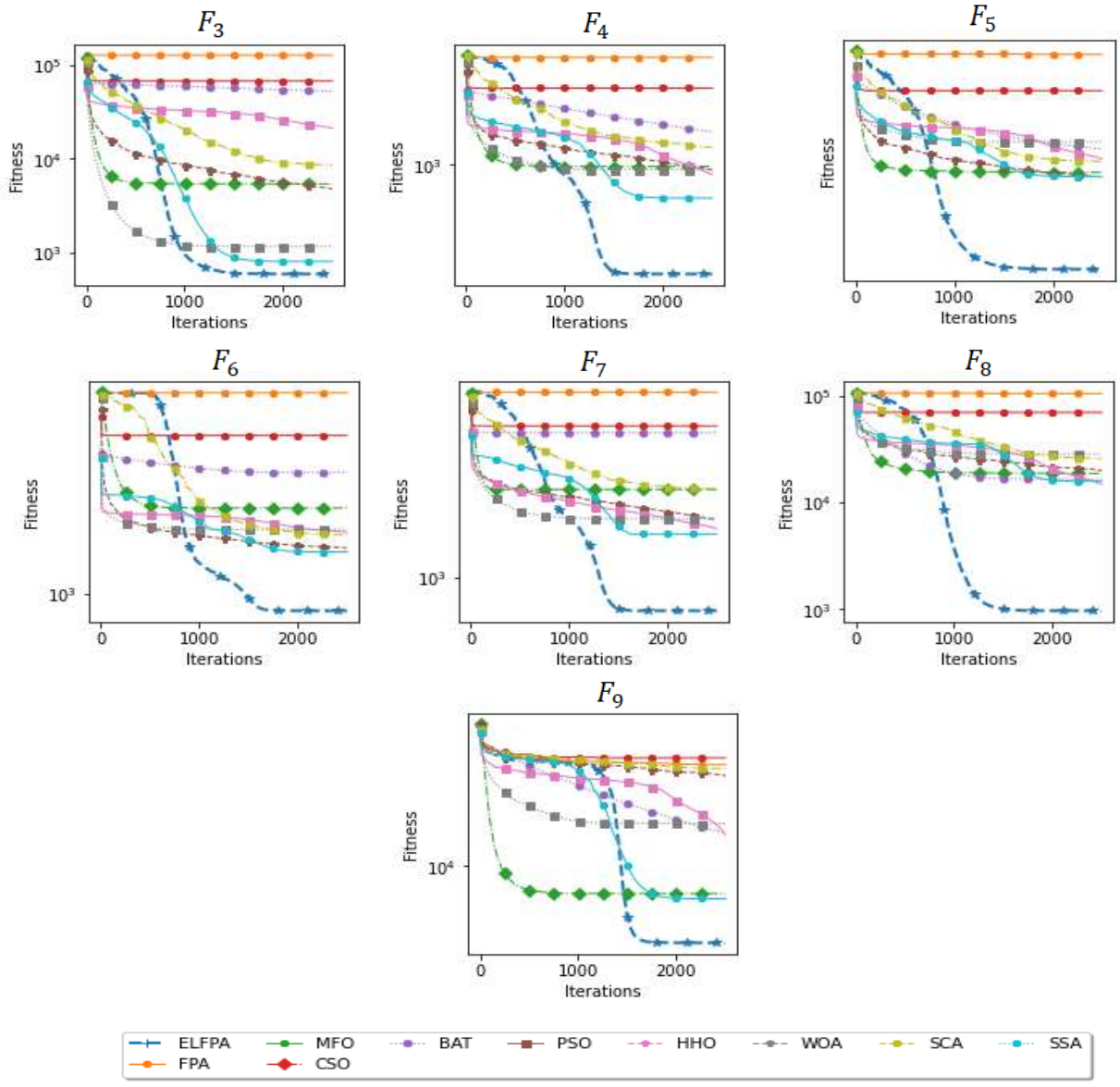

Fig. 3 ELFPA for F3 – F9 Convergence curves and other traditional algorithms during 2500 iterations

Table 5. Results of Hybrid functions for the ELFPA vs some recent techniques.

Table 6. Results of Composition functions for the ELFPA vs some recent techniques.

Fun	Criteria	CSO	SSA	PSO	WOA	BAT	HHO	SCA	MFO	FPA	ELFPA
F20	avg	3394.65	2631.47	2813.24	2959.14	3150.5	3035.39	2908.03	2787.96	3561.62	**2375.62**
	std	1.339E+02	6.514E+01	4.596E+01	1.013E+02	5.125E+01	8.516E+01	4.460E+01	7.420E+01	1.004E+02	1.291E+01
	Med	3.413E+03	2.646E+03	2.819E+03	2.953E+03	2.530E+03	3.014E+03	2.903E+03	2.781E+03	3.576E+03	2.377E+03
F21	avg	17427.72	9703.5	15929.13	13273.57	13899.39	13398.6	16654.28	10489.39	17047.9	**8449.81**
	std	6.786E+02	1.850E+03	1.745E+03	1.324E+03	2.528E+03	1.208E+03	4.319E+02	1.010E+03	3.105E+04	9.450E+02
	med	1.746E+04	1.031E+04	1.639E+04	1.348E+04	8.790E+03	1.333E+04	1.674E+04	1.068E+04	1.704E+04	8.517E+03
F22	avg	4962.48	3182.71	3442.9	3721.23	4617.8	4233.77	3590	3230.58	4369.76	**2813.23**
	std	3.582E+02	9.997E+01	8.097E+01	1.883E+02	9.548E+01	2.132E+02	7.492E+01	7.564E+01	7.429E+01	1.830E+01
	med	4.972E+03	3.147E+03	3.451E+03	3.751E+03	2.989E+03	4.207E+03	3.578E+03	3.219E+03	4.366E+03	2.811E+02
F23	avg	5568.49	3264.89	3663.53	3776.15	4863.85	4496.28	3774.79	3245.59	4246.09	**2989.85**
	std	5.384E+02	9.187E+01	7.984E+01	1.723E+02	1.376E+02	2.405E+02	6.064E+01	5.091E+01	5.547E+01	2.092E+01
	med	5.434E+03	3.270E+03	3.653E+03	3.773E+03	3.165E+03	4.486E+03	3.768E+03	3.243E+03	4.253E+03	2.990E+03
F24	avg	32360.55	3308.2	5747.74	3486.85	25086.01	10165.09	7382.41	6354.31	64870.05	**3052.49**
	std	6.108E+03	8.815E+01	6.977E+02	1.335E+02	4.286E+02	9.735E+02	7.762E+02	3.849E+03	1.022E+04	2.246E+01
	med	7.154E+04	6.000E+03	1.169E+04	5.534E+03	4.604E+04	1.981E+04	1.746E+04	1.161E+04	6.396E+04	3.048E+03
F25	avg	24868.14	8193.6	10853.3	13984.83	21653.95	14922.57	12815.13	9048.23	22207.85	**4637.71**
	std	2.820E+0+	2.675E+03	7.221E+02	1.215E+03	7.765E+02	7.011E+02	4.847E+02	8.458E+02	9.439E+02	1.651E+02
	med	2.562E+04	8.475E+03	1.081E+04	1.417E+04	6.629E+03	1.479E+04	1.277E+04	8.941E+03	2.235E+04	4.638E+03
F26	avg	8032.7	3809.11	4606.11	4285.97	**3200.01**	6350.56	4578.91	3646.24	5001.54	3432.73
	std	1.113E+03	1.688E+02	1.867E+02	4.691E+02	1.018E+02	9.094E+02	1.743E+02	1.230E+02	2.435E+02	9.904E+01
	med	8.130E+03	3.864E+03	4.684E+03	4.151E+03	3.640E+03	6.339E+03	4.608E+03	3.658E+03	4.992E+03	3.416E+03

F27	avg	18662.53	3790.64	5610.76	4264.04	**3300.01**	9890.64	7309.72	8507.42	17611.1	3358.69
	std	2.195E+03	2.585E+02	5.386E+02	2.741E+02	5.211E+02	8.839E+02	6.693E+02	1.117E+03	1.165E+03	3.264E+01
	med	1.847E+04	3.751E+03	5.717E+03	4.245E+03	40404E+03	9.849E+03	7.295E+03	8.865E+03	1.764E+04	3.359E+03
F28	avg	437524.5	6309.82	7034.7	8313.3	412148.1	28187.87	8006.84	5752.27	46046.67	**4238.84**
	std	1.062E+06	7.372E+02	8.103E+02	9.872E+02	3.547E+02	2.448E+04	8.454E+02	6.151E+02	3.324E+04	3.018E+02
	Med	2.641E+05	6.215E+03	7.157E+03	8.264E+03	4.812E+03	1.969E+04	7.943E+03	5.622E+03	3.178E+04	4.220E+03
F29	avg	1.09E+11	4.84E+08	8.97E+08	5.83E+08	8.86E+10	1.25E+10	6.1E+09	1.87E+09	1.29E+11	**88245992**
	std	4.397E+10	2.303E+08	5.753E+08	3.097E+08	2.399E+08	7.920E+09	1.983E+09	3.894E+09	2.765E+10	3.493E+07
	med	9.897E+10	5.117E+08	7.147E+08	5.299E+08	3.399E+08	9.554E+09	6.234E+09	1.181E+08	1.350E+11	7.980E+07
Rank	w/t/l	0/0/10	0/0/10	0/0/10	0/0/10	2/0/8	0/0/10	0/0/10	1/0/9	0/0/10	8/0/2

In addition to the above, it is necessary to test the strength of the algorithm in complex or complex functions, and these functions are F20-F29. The results of the proposed algorithm within these countries were very superior to other algorithms, which confirms that it is one of the strong algorithms, and this can be seen through Table 6 and Figure 5 as well, which Shows the algorithm's affinity compared to other algorithms

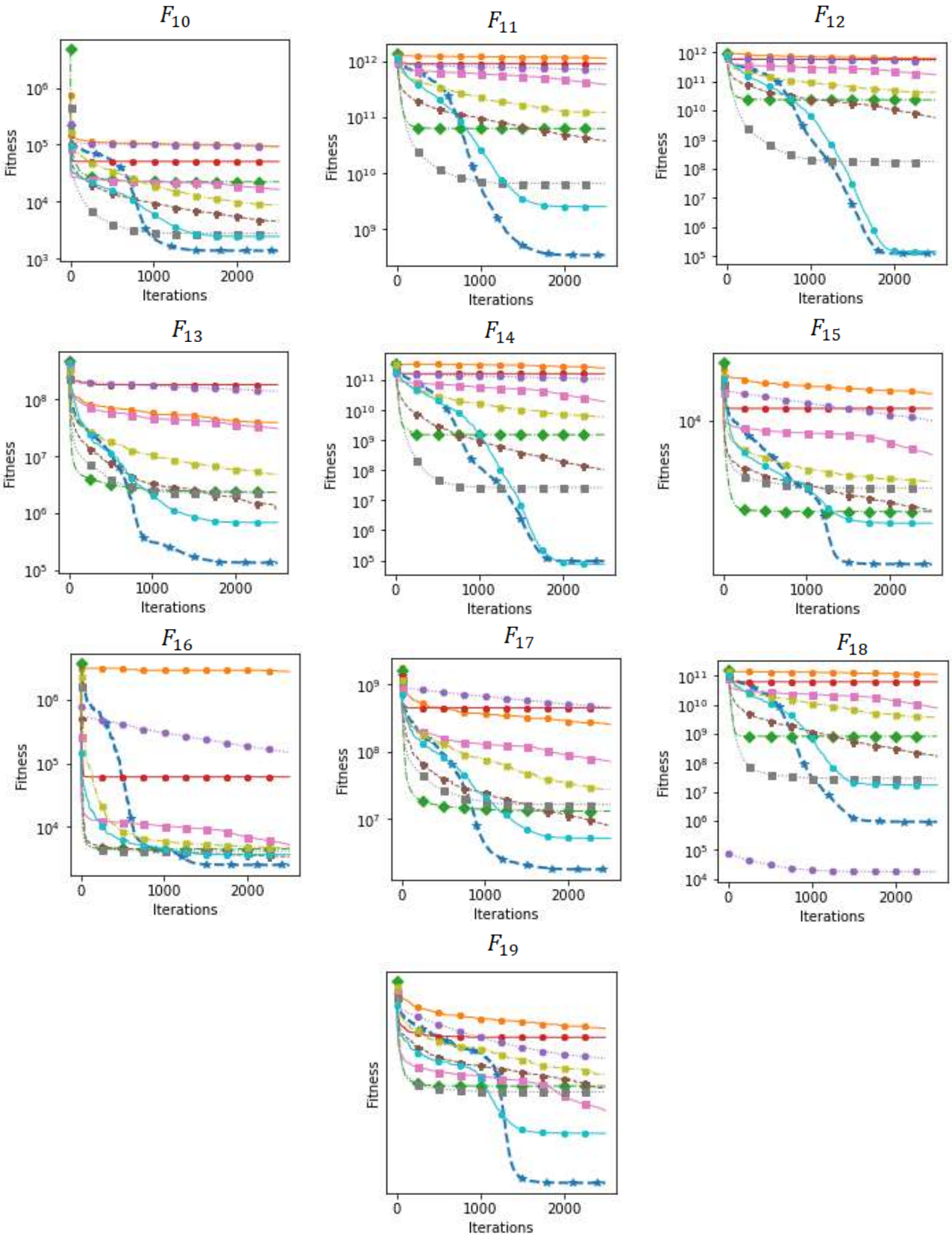

Fig. 4 ELFPA for F10 – F19 Convergence curves and other traditional algorithms during 2500 iterations

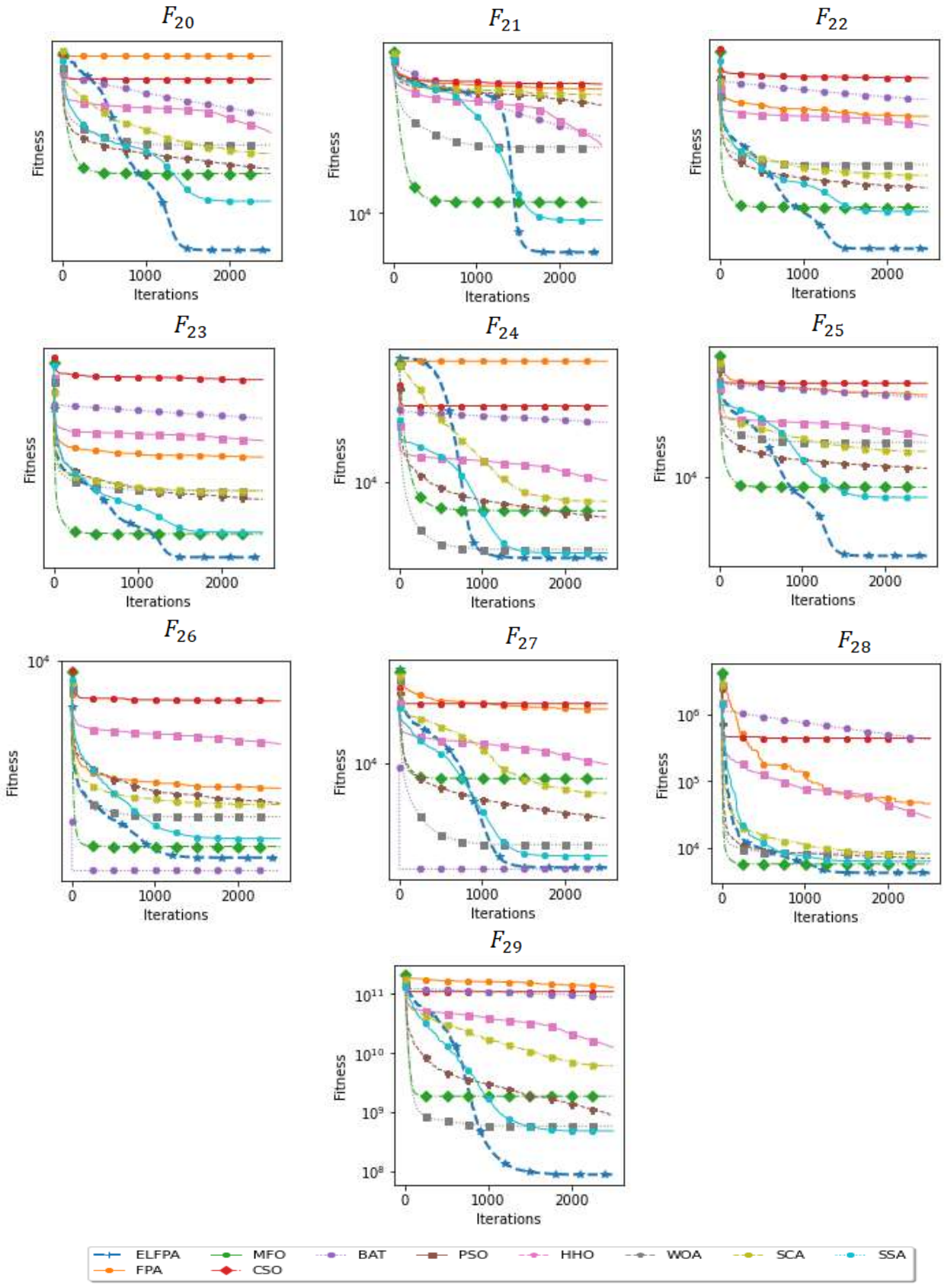

Fig. 3 ELFPA for F20 – F29 Convergence curves and other traditional algorithms during 2500 iterations

5. Conclusion and future work

An improved version of the Flower Pollination Algorithm has been presented, called the ELFPA (Effective Local Flower Pollination Algorithm). The ELFPA algorithm effectively addresses the shortcomings of FPA, such as premature convergence and a lack of exploration-exploitation balance, by incorporating efficient local search mechanisms, such as a parameter balanced between exploitation and exploration, and using the mechanism of the random solution.

The performance of ELFPA has been extensively evaluated experimentally on benchmark functions, including the CEC 2017 test suite, and compared to other cutting-edge metaheuristic algorithms. The results show that in terms of convergence speed, ability to escape local optima, and solution efficiency, ELFPA beats the original FPA and other methods. The suggested method demonstrates its superiority in handling complex global optimization issues, making it a potential optimizer for practical use.

The effective use of ELFPA as a feature selection algorithm emphasizes the algorithm's adaptability and efficiency in addressing a range of optimization problems. The suggested ELFPA algorithm can be tested and used to handle a variety of real-world issues in the future. The study's encouraging findings urge more research and possible ELFPA improvements to advance the field of swarm intelligence optimization.

References

[1] J. Nocedal, S. J. Wright, J. Nocedal, and S. J. Wright, *Numerical Optimization*. Springer, 2006.

[2] O. Özkaraca, J. Güç, Ü. Optimizasyon, Y. Kullanimina, and İ. İnceleme Öz, "A REVIEW ON USAGE OF OPTIMIZATION METHODS IN GEOTHERMAL POWER GENERATION," *Mugla Journal of Science and Technology*, vol. 130, doi: 10.22531/muglajsci.437340.

[3] J. H. Holland, "Genetic algorithms," *Sci Am*, vol. 267, no. 1, pp. 66–72, 1992, doi: 10.1038/SCIENTIFICAMERICAN0792-66.

[4] R. Eberhart and J. Kennedy, "New optimizer using particle swarm theory," *Proceedings of the International Symposium on Micro Machine and Human Science*, pp. 39–43, 1995, doi: 10.1109/MHS.1995.494215.

[5] M. Dorigo, M. Birattari, and T. Stutzle, "Ant colony optimization," *IEEE Comput Intell Mag*, vol. 1, no. 4, pp. 28–39, Nov. 2006, doi: 10.1109/MCI.2006.329691.

[6] E. Aarts, J. Korst, and W. Michiels, "Simulated annealing," *Search Methodologies: Introductory Tutorials in Optimization and Decision Support Techniques*, pp. 187–210, 2005, doi: 10.1007/0-387-28356-0_7/COVER.

[7] X. Huang, T. H. Klinge, J. I. L. B, X. Li, and J. H. Lutz, "Unconventional Computation and Natural Computation," *Lecture Notes in Computer Science (including subseries Lecture Notes in Artificial Intelligence and Lecture Notes in Bioinformatics)*, vol. 7445, pp. 29–40, 2012, doi: 10.1007/978-3-642-32894-7.

[8] Z. A. A. Alyasseri, A. T. Khader, M. A. Al-Betar, M. A. Awadallah, and X. S. Yang, "Variants of the flower pollination algorithm: A review," *Studies in Computational Intelligence*, vol. 744, pp. 91–118, 2018, doi: 10.1007/978-3-319-67669-2_5/COVER.

[9] D. Rodrigues, X. S. Yang, A. N. De Souza, and J. P. Papa, "Binary flower pollination algorithm and its application to feature selection," *Studies in Computational Intelligence*, vol. 585, pp. 85–100, 2015, doi: 10.1007/978-3-319-13826-8_5/COVER.

[10] A. Y. Abdelaziz, E. S. Ali, and S. M. Abd Elazim, "Combined economic and emission dispatch solution using Flower Pollination Algorithm," *International Journal of Electrical Power & Energy Systems*, vol. 80, pp. 264–274, Sep. 2016, doi: 10.1016/J.IJEPES.2015.11.093.

[11] A. Y. Abdelaziz, E. S. Ali, and S. M. Abd Elazim, "Implementation of flower pollination algorithm for solving economic load dispatch and combined economic emission dispatch problems in power systems," *Energy*, vol. 101, pp. 506–518, Apr. 2016, doi: 10.1016/J.ENERGY.2016.02.041.

[12] O. K. Meng, O. Pauline, S. C. Kiong, H. A. Wahab, and N. Jafferi, "Application of Modified Flower Pollination Algorithm on Mechanical Engineering Design Problem," *IOP Conf Ser Mater Sci Eng*, vol. 165, no. 1, p. 012032, Jan. 2017, doi: 10.1088/1757-899X/165/1/012032.

[13] M. N. Kabir, J. Ali, A. R. A. Alsewari, and K. Z. Zamli, "An adaptive flower pollination algorithm for software test suite minimization," *3rd International Conference on Electrical Information and Communication Technology, EICT 2017*, vol. 2018-January, pp. 1–5, Jan. 2018, doi: 10.1109/EICT.2017.8275215.

[14] U. Singh and R. Salgotra, "Synthesis of linear antenna array using flower pollination algorithm," *Neural Comput Appl*, vol. 29, no. 2, pp. 435–445, Jan. 2018, doi: 10.1007/S00521-016-2457-7/METRICS.

[15] M. Abdel-Basset and L. A. Shawky, "Flower pollination algorithm: a comprehensive review," *Artif Intell Rev*, vol. 52, no. 4, pp. 2533–2557, Dec. 2019, doi: 10.1007/S10462-018-9624-4/METRICS.

[16] Y. Chen and D. Pi, "An innovative flower pollination algorithm for continuous optimization problem," *Appl Math Model*, vol. 83, pp. 237–265, Jul. 2020, doi: 10.1016/J.APM.2020.02.023.

[17] P. E. Mergos and X. S. Yang, "Flower pollination algorithm parameters tuning," *Soft comput*, vol. 25, no. 22, pp. 14429–14447, Nov. 2021, doi: 10.1007/S00500-021-06230-1/TABLES/10.

[18] M. Abdel-Basset, R. Mohamed, S. Saber, S. S. Askar, and M. Abouhawwash, "Modified Flower Pollination Algorithm for Global Optimization," *Mathematics 2021, Vol. 9, Page 1661*, vol. 9, no. 14, p. 1661, Jul. 2021, doi: 10.3390/MATH9141661.

[19] P. E. Mergos and X. S. Yang, "Flower pollination algorithm with pollinator attraction," *Evol Intell*, pp. 1–17, Jan. 2022, doi: 10.1007/S12065-022-00700-7/METRICS.

[20] K. M. Ong, P. Ong, and C. K. Sia, "A new flower pollination algorithm with improved convergence and its application to engineering optimization," *Decision Analytics Journal*, vol. 5, p. 100144, Dec. 2022, doi: 10.1016/J.DAJOUR.2022.100144.

[21] F. Seghir and G. Khababa, "An improved discrete flower pollination algorithm for fuzzy QoS-aware IoT services composition based on skyline operator," *Journal of Supercomputing*, pp. 1–32, Feb. 2023, doi: 10.1007/S11227-023-05074-W/METRICS.

[22] R. Mallipeddi, P. S.-N. T. University, and undefined 2010, "Problem definitions and evaluation criteria for the CEC 2010 competition on constrained real-parameter optimization," *al-roomi.org*, 2010, Accessed: May 28, 2023. [Online]. Available: http://www.al-roomi.org/multimedia/CEC_Database/CEC2010/RealParameterOptimization/CEC2010_RealParameterOptimization_TechnicalReport.pdf

[23] X. S. Yang, "A new metaheuristic Bat-inspired Algorithm," *Studies in Computational Intelligence*, vol. 284, pp. 65–74, 2010, doi: 10.1007/978-3-642-12538-6_6.

[24] R. Cheng, Y. J.-I. transactions on cybernetics, and undefined 2014, "A competitive swarm optimizer for large scale optimization," *ieeexplore.ieee.org*, Accessed: May 28, 2023. [Online]. Available: https://ieeexplore.ieee.org/abstract/document/6819057/

[25] S. Mirjalili, "SCA: A Sine Cosine Algorithm for solving optimization problems," *Knowl Based Syst*, vol. 96, pp. 120–133, Mar. 2016, doi: 10.1016/J.KNOSYS.2015.12.022.

[26] S. Mirjalili and A. Lewis, “The Whale Optimization Algorithm,” *Advances in Engineering Software*, vol. 95, pp. 51–67, May 2016, doi: 10.1016/J.ADVENGSOFT.2016.01.008.

[27] S. Mirjalili, “Moth-flame optimization algorithm: A novel nature-inspired heuristic paradigm,” *Knowl Based Syst*, vol. 89, pp. 228–249, Nov. 2015, doi: 10.1016/J.KNOSYS.2015.07.006.

[28] A. A. Heidari, S. Mirjalili, H. Faris, I. Aljarah, M. Mafarja, and H. Chen, “Harris hawks optimization: Algorithm and applications,” *Future Generation Computer Systems*, vol. 97, pp. 849–872, Aug. 2019, doi: 10.1016/J.FUTURE.2019.02.028.

[29] S. Mirjalili, A. H. Gandomi, S. Z. Mirjalili, S. Saremi, H. Faris, and S. M. Mirjalili, “Salp Swarm Algorithm: A bio-inspired optimizer for engineering design problems,” *Advances in Engineering Software*, vol. 114, pp. 163–191, Dec. 2017, doi: 10.1016/J.ADVENGSOFT.2017.07.002.

Preparation And Characterization of Some New Quinazoline Derivatives From 2-(4-Nitrophenyl) Acetohydrazide and Biological Activity Evaluation

Khalid A. Al-Badrany and Abdul Wahid Khedhr Abdul Wahid
Department of Chemistry / College of Education for Pure Sciences / Tikrit University

Preparation And Characterization of Some New Quinazoline Derivatives From 2-(4-Nitrophenyl) Acetohydrazide and Biological Activity Evaluation

Khalid A. Al-Badrany and Abdul Wahid Khedhr Abdul Wahid
Department of Chemistry / College of Education for Pure Sciences / Tikrit University

Abstract
The research encompassed the synthesis of 2-(4-nitrophenyl) acetohydrazide through the reaction between ethyl 2-(4-nitrophenyl) acetate and hydrazine. Subsequently, Schiff bases were derived from the interaction between 2-(4-nitrophenyl) acetohydrazide and various aromatic aldehyde derivatives. Additionally, quinazoline was synthesized by reacting the Schiff bases with 2-aminobenzoic acid. The structural characterization of the compounds was achieved using an array of analytical techniques including melting point determination, color assessment, Nuclear Magnetic Resonance spectroscopy (^{1}H-NMR and ^{13}C-NMR), and Fourier-Transform Infrared (FT-IR) spectroscopy. These analyses were conducted to confirm the structural attributes of the compounds. Furthermore, the biological activity of the synthesized compounds was evaluated against two bacterial strains, namely Escherichia coli and Staphylococcus aureus.
Keywords: Quinazoline, Hydrazones, Hydrazide, Biological activity.

1. Introduction

Quinazoline represents a class of bicyclic heterocyclic compounds incorporating a pyrimidine system. These compounds are distinguished by their significant biological activities, rendering them of great interest. Their diverse medicinal properties have been well-documented, including remarkable effects as anticancer agents [1], antioxidants [2], anti-inflammatory agents [3,4], antimalarials [5,6], antiviral agents [7], and antimicrobial agents [8]. Hydrazones, classified as pivotal organic compounds, possess the general structure (R1R2C=N-NH2), originating from aldehydes and ketones wherein the oxygen atom is replaced by the functional group (N-NH2). Typically synthesized through hydrazine-aldehyde/ketone reactions, the C=N linkage is crucial for their biological activity. Hydrazones have gained significant attention in pharmacy due to their potent biological properties, including antibacterial [9], antifungal [10], anticancer [11], anti-inflammatory [12], antioxidant [13], antidiabetic [14], anxiolytic [15], and antimalarial activities [16]. Hydrazides, with their versatile nature, serve as valuable precursors in heterocyclic system synthesis. In medicinal chemistry, hydrazide-hydrazones continue to captivate interest due to their extensive array of biological attributes, spanning antidiabetic [17], antimalarial [18], anticancer [19], antifungal [20], antioxidant [21], anti-inflammatory, and anxiolytic [22].

2. Experimental:

All chemicals and solvents employed were sourced from Aldrich and Fluka and were used without further purification. Melting points were measured using an open capillary tube on a Stuart melting point apparatus. Infrared spectra were obtained using a Shimadzu FTIR-8100 spectrophotometer with KBr discs, while 1H NMR spectra were acquired on an MHZ spectrometer using DMSO-d6 as the solvent. Reaction monitoring and compound purity verification were conducted using thin-layer chromatography (TLC) on silica gel-coated alumina sheets (type 60 F254 Merck, Darmstadt, Germany).

2.1. Preparation of Hydrazide:

A solution of 0.01 mol of the ester (4-nitrophenyl acetate) in 20 ml of absolute ethanol was prepared. To this solution, 0.04 mol of aqueous hydrazine was added, and the mixture was heated for 4 hours. After cooling, the solution was concentrated by half. The resulting precipitate was filtered and dried [23, 24].

2.2. Preparation of Hydrazones:

Equal moles of the prepared hydrazide compound (AB1) were mixed with an aromatic substituent for benzaldehyde in 20 ml of absolute ethanol. A drop of acetic acid was added to the mixture, which was stirred continuously for 3 hours. Following this, the solution was concentrated, the precipitate was filtered, and recrystallization was carried out using ethanol [25, 26]. Physical properties of the synthesized compounds [AB2-AB8] are presented in Table 1.

2.3. Preparation of Quinazoline:

Equal moles of the hydrazone prepared with ortho-aminobenzoic acid were dissolved in 20 ml of absolute ethanol. Gradually, 3 drops of triethylamine were added with stirring, and the mixture was allowed to escalate for 6 hours in a water bath with continuous stirring. The resulting solution was then treated with 10 percent sodium bicarbonate. Filtration, drying, and recrystallization steps were performed to obtain quinazoline compounds [27, 28]. Table 1 lists the physical properties of the prepared compounds [AB23-AB29].

2.4. Biological Activity Evaluation:

Biological activity assessment was conducted using the propagation method and the Kirby-Bauer diffusion method. In the Kirby-Bauer method, 0.1 ml of bacterial suspension was spread on Mueller-Hinton agar plates and allowed to absorb for 5 minutes. Subsequently, wells of 5 mm diameter were created on each plate using a cork borer, and 0.1 ml of the prepared solutions was added to the fourth well as the control sample using DMSO. The plates were then incubated for 24 hours at 37°C [29, 30]. The diameters of inhibition zones around each well were measured in millimeters following the Prescott method.

3. Results and Discussion

3.1. FT-IR spectrum

Confirmation of the reaction involving the hydrazide derivatives [AB1] was achieved through the observation of alterations in physical characteristics such as melting point and significant color changes. The melting point was recorded at (168-170) ºC, and the product displayed a light-yellow hue. A favorable yield of 85% was obtained. Moreover, the identity of the hydrazide derivatives [AB1] was established via infrared spectra (IR) and nuclear magnetic resonance (^{1}H,^{13}C-NMR) measurements. The infrared spectrum of [AB1] revealed absorption bands at (3033) cm^{-1} for aromatic (CH) bonds, (3188) cm^{-1} for stretching (NH) bonds, and (3305) cm^{-1} and (3409) cm^{-1} for (NH_2) stretching [31]. A decline in the carbonyl group (C=O) frequency, indicating its association with [NH-NH_2] groups, was observed at (1656) cm^{-1}. The infrared spectrum also displayed bands at (1610) cm^{-1} and (1413) cm^{-1} corresponding to (C=C) aromatic bonds [32].

The identification of prepared hydrazones (AB2-AB8) was based on changes in physical properties, such as color and melting point, and supported by infrared spectra (IR) measurements. The IR spectrum displayed absorption bands corresponding to (NH) stretching (3180-3247) cm^{-1} [33], (Ar-H) stretching (3056-3084) cm^{-1}, (C=O) stretching (1660-1670) cm^{-1}, and (C=N) stretching (1600-1618) cm^{-1} [34].

The infrared spectrum of quinazoline derivatives (AB23-AB29) exhibited absorption bands corresponding to (N-H) stretching (3186-3257) cm^{-1}, (Ar-H) stretching (3058-3076) cm^{-1}, (C=O) stretching (1664-1674) cm^{-1} [35], (C=O) stretching of the quinazoline ring (1604-1616) cm^{-1}, (C=C) aromatic bond stretching (1413-1558) cm^{-1}, and (C-N) extension (1223-1267) cm^{-1}.

3.2. ^{1}H-NMR spectrum

The proton nuclear magnetic resonance (^{1}H-NMR) spectrum of compound (AB1) displayed signals at (3.725) ppm for (CH_2) protons [36], (4.31) ppm for a proton (NH_2), (9.31) ppm for a proton (NH) [37], and multiple signals within (7.53-8.57) ppm attributed to aromatic ring (Ar-CH) protons.

The proton nuclear magnetic resonance (^{1}H-NMR) spectrum of compound (AB4) indicated signals at (4.2) ppm for (CH_2) protons, (11.29) ppm for a proton (NH) [38], (8.26) ppm for a proton (N=CH), and (3.014) ppm for a proton (CH_3), along with multiple signals within (6.77-8.11) ppm related to the aromatic ring (Ar-CH) protons.

The proton nuclear magnetic resonance (^{1}H-NMR) spectrum of compound (AB25) displayed signals at (4.18) ppm for (CH_2) protons, (11.30) ppm for a (NH) proton, (7.53) ppm for a (NH) proton of the quinazoline ring, (6.80) ppm for a (CH) proton, and (3.01) ppm for a (CH3) proton, along with signals within (7.54-8.27) ppm associated with the aromatic rings (Ar-CH) [39].

3.3. ^{13}C-NMR spectrum

The carbon nuclear magnetic resonance (^{13}C-NMR) spectrum of compound (AB1) showed signals at (39.9) ppm for carbon (CH_2), (168.9) ppm for carbon (C=O), and multiple signals in the range (123.4-146.7) ppm corresponding to carbons in the aromatic ring (Ar-CH) [40].

The carbon nuclear magnetic resonance (^{13}C-NMR) spectrum of compound (AB4) revealed signals at (41.3) ppm for carbon (CH_2) [41], (151.9) ppm for carbon (CH), (172.2) ppm for carbon (C=O), and signals in the range (112.2-146.1) ppm corresponding to carbons in the aromatic ring (Ar-CH).
The carbon nuclear magnetic resonance (^{13}C-NMR) spectrum of compound (AB25) indicated signals at (41.3) ppm for carbon (CH_2), (112.3) ppm for carbon (CH) [42], (171.1) ppm for carbon (C=O), (165.3) ppm for carbon (C=O) of the quinazoline ring, and (39.3) ppm for carbon (CH_3) [43], along with signals within the range (121.8-151.9) ppm corresponding to carbons in the aromatic ring (Ar-CH).

3.6. Evaluation of the biological activity of prepared compounds:

Compounds with heterocyclic rings are characterized by different biological activity against Gram-positive and Gram-negative bacteria, so the biological activity of compounds prepared in this study was evaluated on two types of bacteria, which are as follows: Escherichia coli and Staphylococcus aureus. Spreading on Petri dishes using Mueller Huntington medium for compounds prepared at concentrations (0.01, 0.001, 0.0001 mg/ml) and the diameter of the inhibition zone was determined in millimeters [44]. The results were compared with a standard antibiotic. When comparing the effect of these compounds, it was noticed that the prepared compounds had a clear effect against the first type of bacteria compared to the other type [45]. Some of them had a clear effect against the second type of bacteria compared to the other type, which did not appear for any of the prepared compounds to affect them, as shown in tables (3). From the table below, compounds with strong efficacy and inhibition can treat diseases caused by the aforementioned studied bacteria after conducting histological and anatomical studies of the prepared compounds [46]. Antibiotic amoxicillin was used as a control sample, depending on what is used in the Ministry of Health laboratories and based on the World Health Organization examinations [47].

Table (1) shows some of the physical properties of (AB2-AB8) and (AB2-AB8).

Comp. No.	Z	Molecular Formula	M.P °C	Yield %	Color
AB2	4-F	$C_{15}H_{12}N_3O_3F$	178-180	80	White
AB3	2,3-Cl	$C_{15}H_{11}N_3O_3Cl_2$	203-205	78	Yellow
AB4	4-N$(CH_3)_2$	$C_{17}H_{18}N_4O3$	190-192	75	Red
AB5	4-Cl	$C_{15}H_{12}N_3O_3Cl$	227-229	75	White
AB6	4-NO_2	$C_{15}H_{12}N_4O_5$	240-242	72	White
AB7	4-Br	$C_{15}H_{12}N_3O_3Br$	209-211	67	White
AB8	4-OCH_3	$C_{16}H_{15}N_3O_4$	219-221	55	Brown
AB23	4-F	$C_{22}H_{17}N_4O_4F$	188-190	45	Yellow
AB24	2,3-Cl	$C_{22}H_{16}N_4O_4Cl_2$	206-208	44	Yellow
AB25	4-N$(CH_3)_2$	$C_{24}H_{23}N_5O_4$	208-210	40	Orange
AB26	4-Cl	$C_{22}H_{17}N_4O_4Cl$	232-234	42	White
AB27	4-NO_2	$C_{22}H_{17}N_5O_6$	230-232	41	White
AB28	4-Br	$C_{22}H_{17}N_4O_4Br$	250-252	40	White

AB29	4-OCH_3	$C_{23}H_{20}N_4O_4$	198-200	42	Yellow

Table (2): Results of the FT-IR spectrum (cm^{-1}) for (AB2-AB8) and (AB2-AB8).

Comp.	Z	νNH	νAr-H	νC=O	νC=N	νC=C Ar	νC-N	Others
AB_2	4-F	3180	3082	1666	1604	1512, 1400	1228	νC-F 1014
AB_3	2,3-Cl	3199	3056	1670	1612	1544, 1450	1259	νC-Cl 784
AB_4	4-$N(CH_3)_2$	3189	3087	1667	1608	1550, 1462	1283	νCH_3 2842, 2970
AB_5	4-Cl	3194	3078	1668	1613	1555, 1427	1287	νC-Cl 781
AB_6	4-NO_2	3182	3083	1670	1591	1515, 1440	1261	νNO_2 1344, 1392
AB_7	4-Br	3180	3078	1666	1606	1515, 1485	1263	ν C-Br 676
AB_8	4-OCH_3	3247	3074	1674	1604	1546, 1458	1255	ν C-O-C 1166

Comp.	Z	νN-H	νAr-H	νC=O	νC=O cycle	ν C=C-Ar	νC-N	Others
AB_{23}	4-F	3257	3072	1674	1604	1544, 1413	1234	ν C-F 1064
AB_{24}	2,3-Cl	3197	3058	1670	1616	1544, 1452	1243	νC-Cl 864
AB_{25}	4-$N(CH_3)_2$	3205	3054	1667	1613	1543, 1446	1239	νCH_3 2852, 2968
AB_{26}	4-Cl	3232	3056	1664	1614	1558, 1477	1267	νC-Cl 867
AB_{27}	4-NO_2	3186	3082	1668	1609	1515, 1446	1261	ν NO_2 1344, 1396
AB_{28}	4-Br	3184	3070	1666	1610	1515, 1487	1265	νC-Br 582
AB_{29}	4-OCH_3	3245	3076	1670	1606	1546, 1421	1249	νC-O-C 1184

Table (3): Result of the biological activity test of the selected compounds against bacterial species measured in millimeters around the agar pit loaded with chemical compounds.

Moraxella			*E. coli*			*S. pyogenes*			*S. marscence*			for bacterial species
10^{-3}	10^{-2}	10^{-1}	10^{-3}	10^{-2}	10^{-1}	10^{-3}	10^{-2}	10^{-1}	10^{-3}	10^{-2}	10^{-1}	Solution number
	Niz			niz		0	0	13				AB5
0	0	12	12	12	19	0	0	15		Niz		AB6
0	0	10		niz		0	0	12				AB23

	0	0	10	0	0	14	0	0	11	AB25
		Niz		0	0	13	0	0	10	AB26
Niz		Niz		0	0	13	0	0	12	AB27
	0	0	11	0	0	12				AB28
		Niz		0	0	12		Niz		AB29

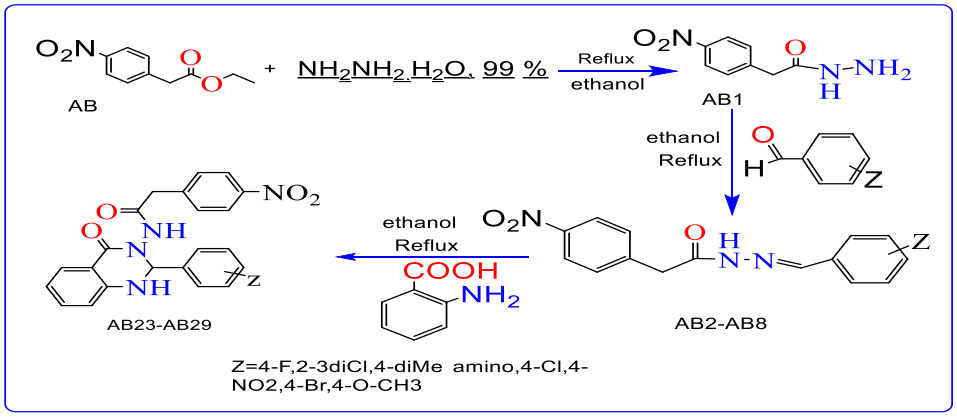

Figure (1) shows the work plan

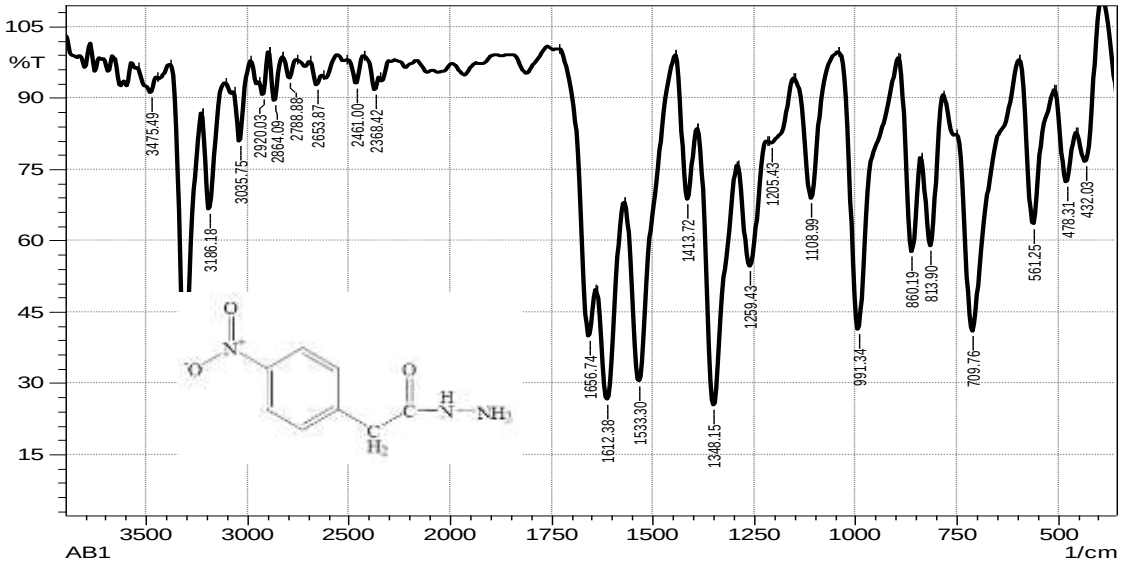

Figure (2): FT-IR of (AB1).

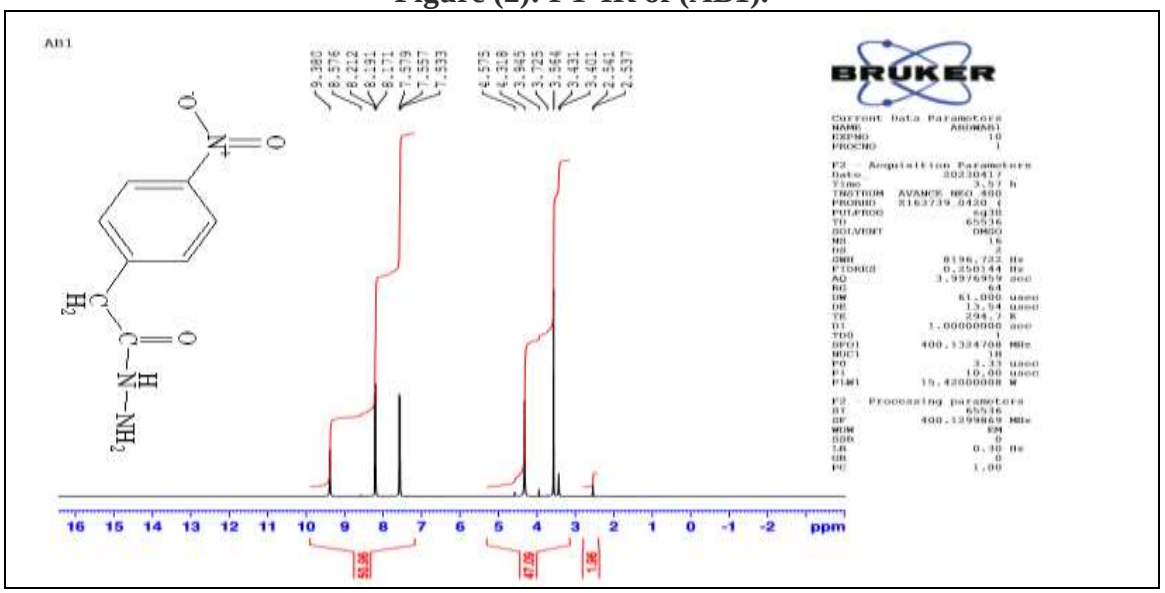

Figure (3): ^{1}H-NMR of (AB1).

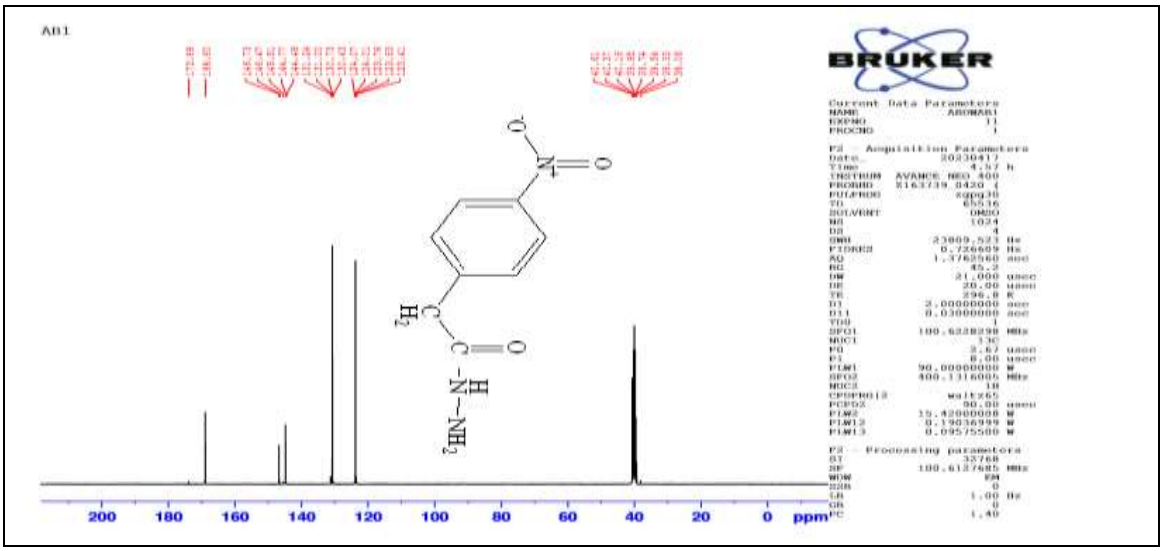

Figure (4): ^{13}C-NMR of (AB1).

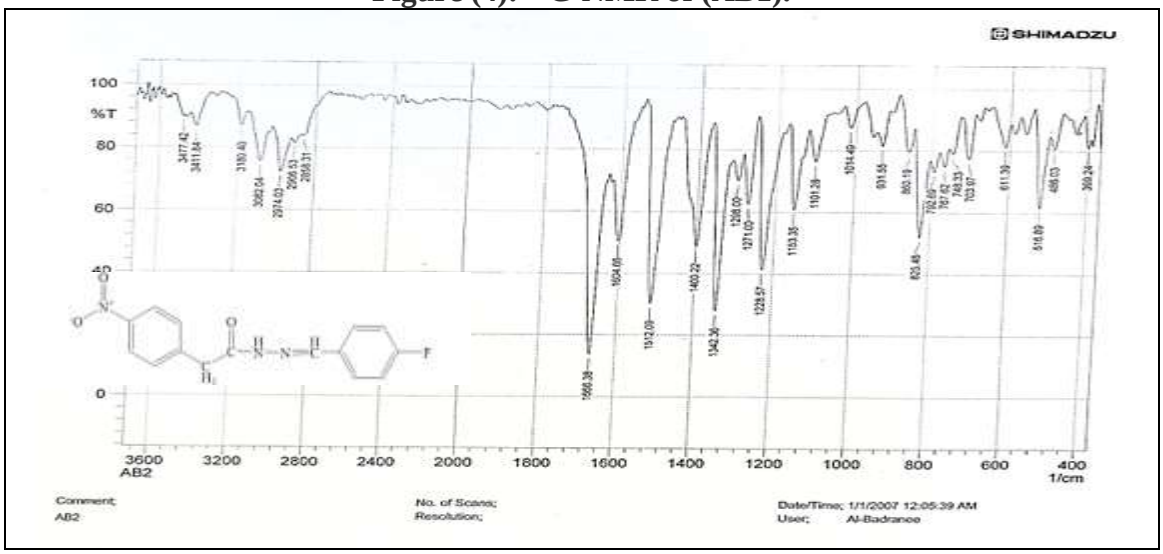

Figure (5): FT-IR of (AB2).

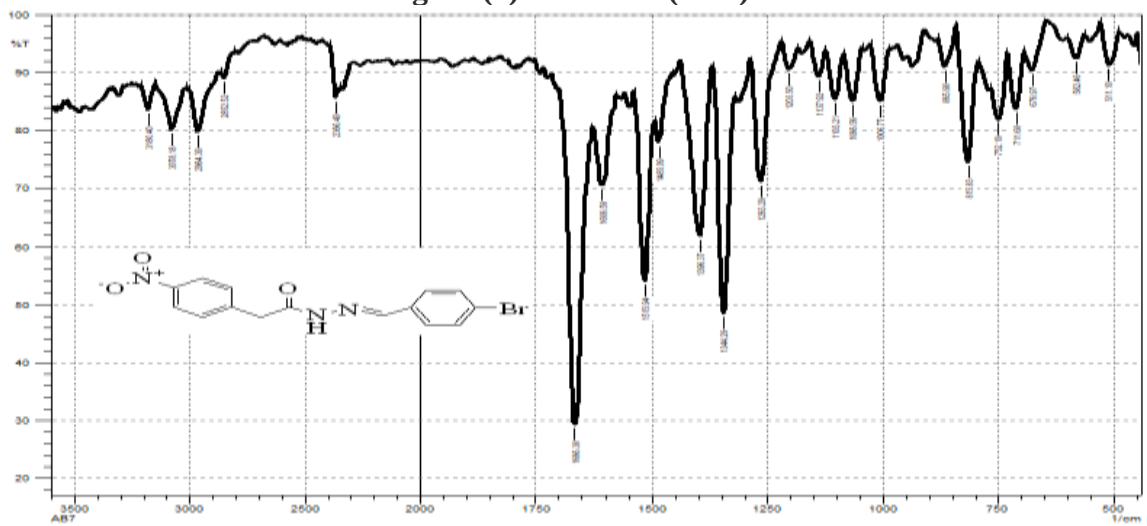

Figure (6): FT-IR of (AB7).

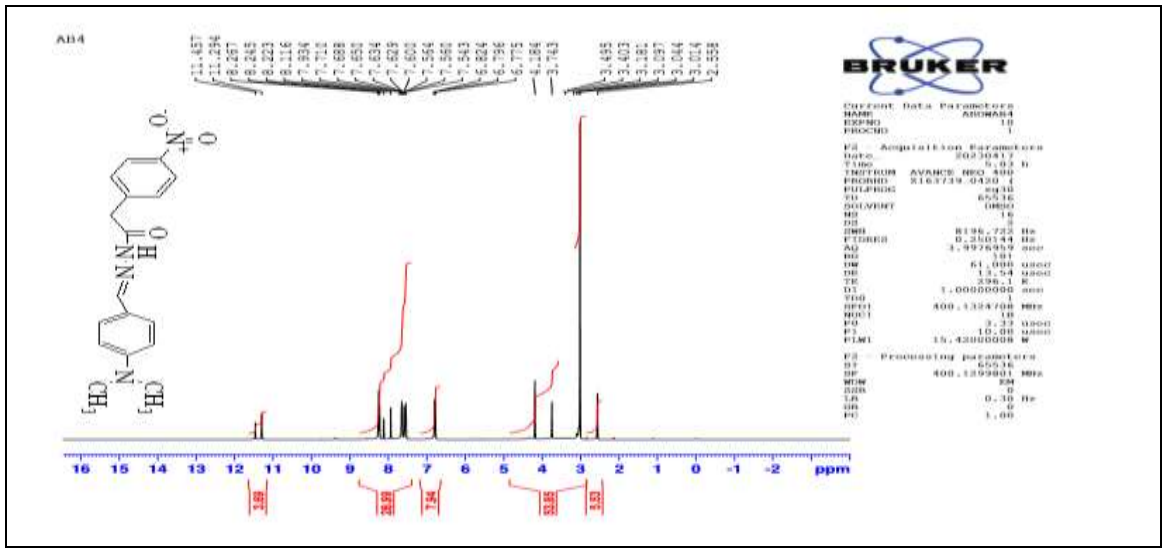

Figure (7): ^{1}H-NMR of (AB4).

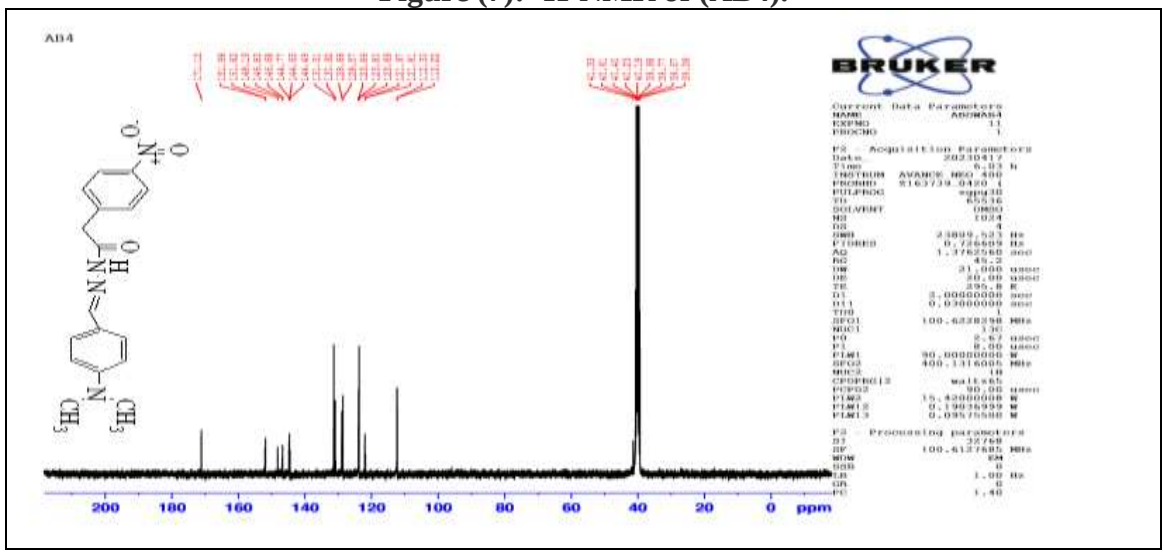

Figure (8): ^{13}C-NMR of (AB4).

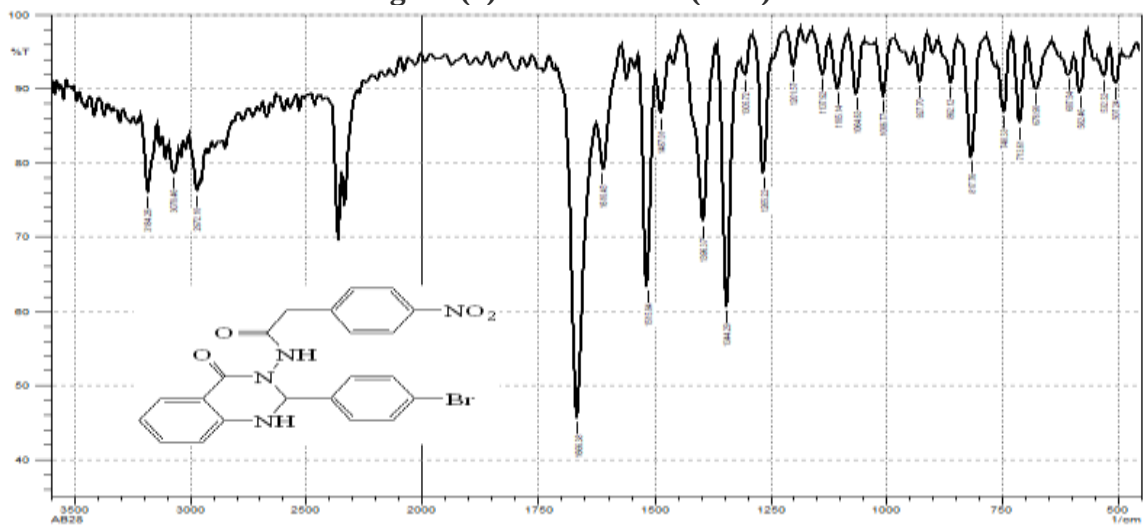

Figure (9): FT-IR of (AB28).

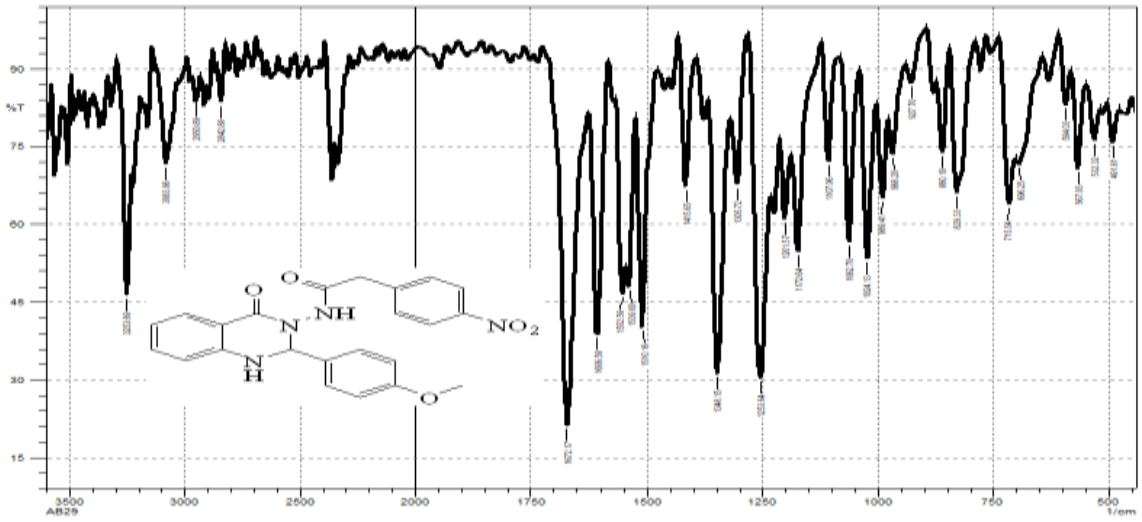

Figure (10): FT-IR of (AB29).

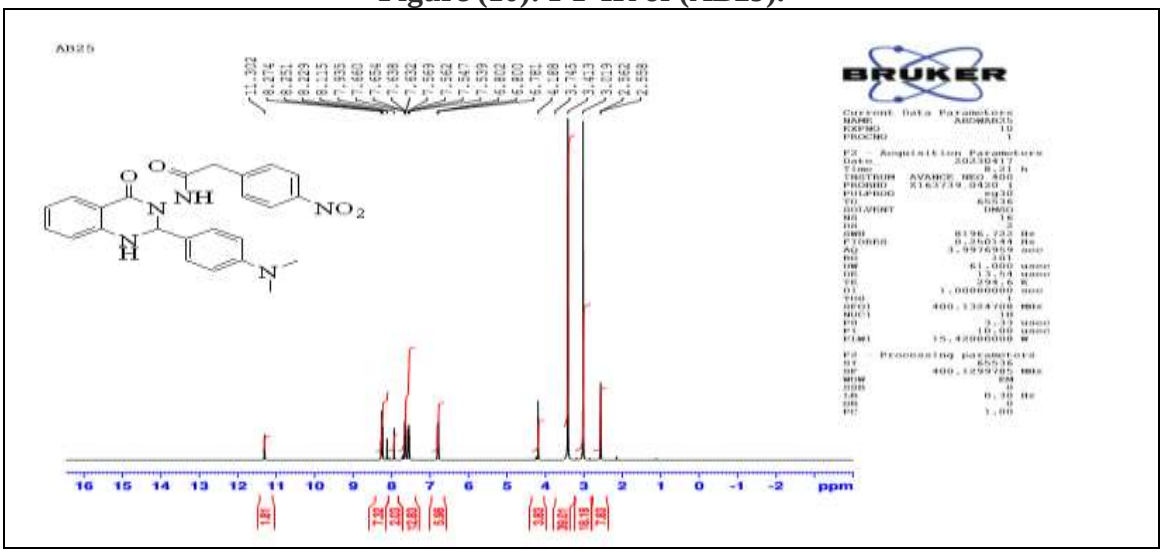

Figure (11): ^{1}H-NMR of (AB25).

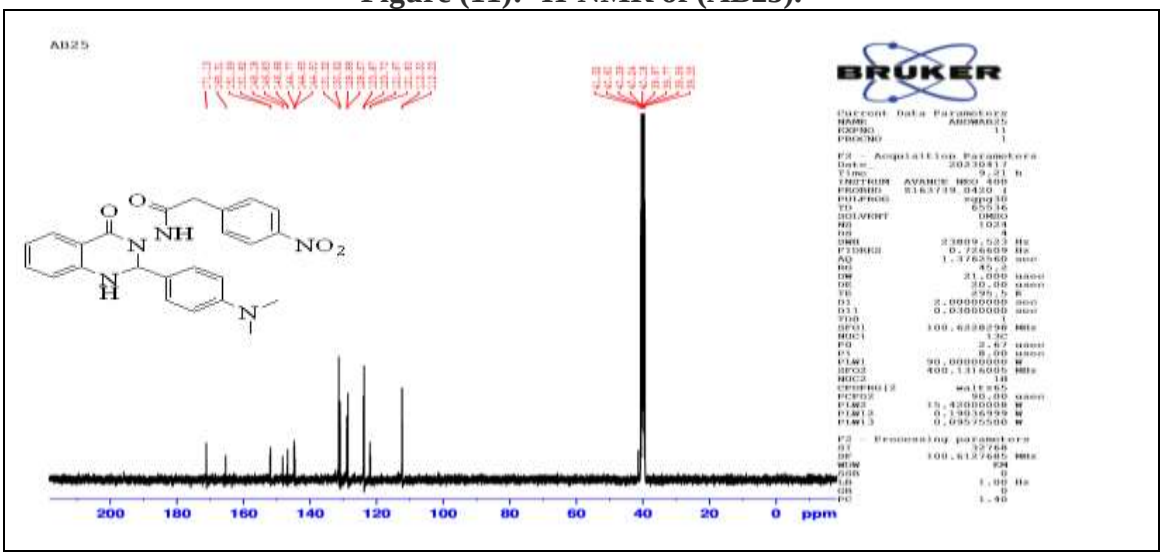

Figure (12): ^{13}C-NMR of (AB25).

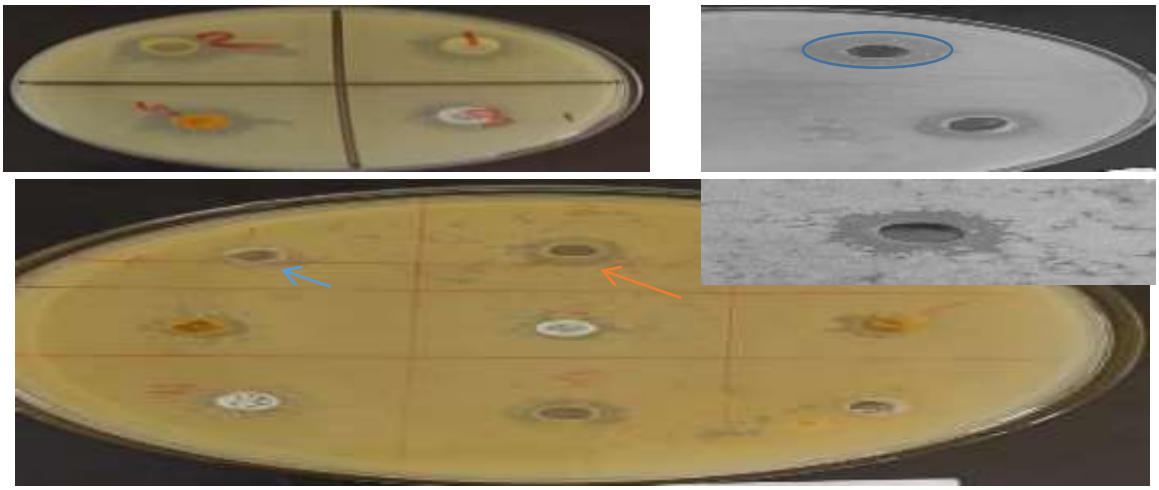

Figure (13): Evaluation of the biological activity of prepared compounds.

4. Conclusions: The accuracy and validity of the prepared compounds were confirmed through spectral and physical measurements, where the infrared spectrum proved the presence of active aggregates accurately, and this confirmation increased the nuclear magnetic resonance spectrum of the proton and carbon, which accurately agreed on the validity of the structures of the prepared compounds. These compounds are stable at laboratory temperature and do not degrade or change color. The prepared compounds showed high and good inhibitory activity against Gram-positive and Gram-negative bacteria, and the results were compared with control samples, which are antibiotics.

References

1. El-Gazzar, Y. I., Ghaiad, H. R., El Kerdawy, A. M., George, R. F., Georgey, H. H., Youssef, K. M., & El-Subbagh, H. I. (2023). New quinazolinone-based derivatives as DHFR/EGFR-TK inhibitors: Synthesis, molecular modeling simulations, and anticancer activity. *Archiv der Pharmazie*, *356*(1), 2200417.
2. Pore, A., Gaikwad, G., Hegade, S., Jadhav, Y., Mane, R., & Kumbhar, R. (2023). Analyzing the Impact of the Substituent on the Quinazolinone Schiff Base and the Interaction of the Fe (III) and Cr (III) with Different Quinazolinone Schiff Base for Antioxidant and Anti-inflammatory Activity. *Analytical Chemistry Letters*, *13*(1), 39-59. Romeo, R., Iannazzo, D., Veltri, L., Gabriele, B., Macchi, B., Frezza, C., ... & Giofrè, S. V. (2019). Pyrimidine 2, 4-diones in the design of new HIV RT inhibitors. *Molecules*, *24*(9), 1718.
3. Kothayer, H., Rezq, S., Abdelkhalek, A. S., Romero, D. G., & Elbaramawi, S. S. (2023). Triple targeting of mutant EGFRL858R/T790M, COX-2, and 15-LOX: design and synthesis of novel quinazolinone tethered phenyl urea derivatives for anti-inflammatory and anticancer evaluation. *Journal of Enzyme Inhibition and Medicinal Chemistry*, *38*(1), 2199166.
4. Luan, M. Z., Zhang, X. F., Yang, Y., Meng, Q. G., & Hou, G. G. (2023). Anti-inflammatory activity of fluorine-substituted benzo [h] quinazoline-2-amine derivatives as NF-κB inhibitors. *Bioorganic Chemistry*, 106360.
5. Charoensutthivarakul, S., Lohawittayanan, D., Kanjanasirirat, P., Jearawuttanakul, K., Seemakhan, S., Chabang, N., ... & Phanchana, M. (2023). Rational Design and Lead Optimisation of Potent Antimalarial Quinazolinediones and Their Cytotoxicity against MCF-7. *Molecules*, *28*(7), 2999.
6. Ibrahim, Z. Y. U., Uzairu, A., Shallangwa, G. A., Abechi, S. E., & Isyaku, S. (2022). Virtual screening and molecular dynamic simulations of the antimalarial derivatives of 2-anilino 4-amino substituted quinazolines docked against a Pf-DHODH protein target. *Egyptian Journal of Medical Human Genetics*, *23*(1), 119.
7. Abuelizz, H. A., Bakheit, A. H., Marzouk, M., El-Senousy, W. M., Abdellatif, M. M., Mostafa, G. A., ... & Al-Salahi, R. (2023). Antiviral activity of some benzo [g] quinazolines against coxsackievirus B4: biological screening and docking study. *Pharmacological Reports*, 1-17.
8. Patel, P. J., Vala, R. M., Patel, S. G., Upadhyay, D. B., Rajani, D. P., Damiri, F., ... & Patel, H. M. (2023). Catalyst-free synthesis of imidazo [5, 1-b] quinazolines and their antimicrobial activity. *Journal of Molecular Structure*, *1285*, 135467.
9. Zhou, Y., Zhang, S., Cai, M., Wang, K., Feng, J., Xie, D., ... & He, H. (2021). Design, synthesis, and antifungal activity of 2, 6-dimethyl-4-aminopyrimidine hydrazones as PDHc-E1 inhibitors with a novel binding mode. *Journal of Agricultural and Food Chemistry*, *69*(21), 5804-5817.
10. Şenkardeş, S., Han, M. İ., Kulabaş, N., Abbak, M., Çevik, Ö., Küçükgüzel, İ., & Küçükgüzel, Ş. G. (2020). Synthesis, molecular docking and evaluation of novel sulfonyl hydrazones as anticancer agents and COX-2 inhibitors. *Molecular diversity*, *24*, 673-689..
11. Alsaif, N. A., Bhat, M. A., Al-Omar, M. A., Al-Tuwajiri, H. M., Naglah, A. M., & Al-Dhfyan, A. (2020). Synthesis of novel diclofenac hydrazones: Molecular docking, anti-inflammatory, analgesic, and ulcerogenic activity. *Journal of Chemistry*, *2020*, 1-12..

12. Yadav, M., Sharma, S., & Devi, J. (2021). Designing, spectroscopic characterization, biological screening and antioxidant activity of mononuclear transition metal complexes of bidentate Schiff base hydrazones. *Journal of Chemical Sciences*, *133*, 1-22.
13. Karrouchi, K., Fettach, S., Anouar, E. H., Bayach, I., Albalwi, H., Arshad, S., ... & Himmi, B. (2022). Synthesis, Spectroscopic Characterization, DFT, Molecular Docking and Antidiabetic Activity of N-Isonicotinoyl Arylaldehyde Hydrazones. *Polycyclic Aromatic Compounds*, 1-13..
14. Prokopchuk, E. G., Aleksandrova, A. I., & Kravchenko, I. A. (2020). Neurotropic properties of new complex compounds of SnCl4 with salicyloyl hydrazones of benzaldehyde and 4-bromobenzaldehyde. *Фармакологія та лікарська токсикологія*, *14*(5), 308-315.
15. Karnatak, M., Hassam, M., Singh, A. S., Yadav, D. K., Singh, C., Puri, S. K., & Verma, V. P. (2022). Novel hydrazone derivatives of N-amino-11-azaartemisinin with high order of antimalarial activity against multidrug-resistant Plasmodium yoelii nigeriensis in Swiss mice via intramuscular route. *Bioorganic & Medicinal Chemistry Letters*, *58*, 128522.
16. Duong, T. H., Devi, A. P., Huynh, N. V., Sichaem, J., Tran, H. D., Alam, M., ... & Nguyen, T. C. (2020). Synthesis, α-glucosidase inhibition, and molecular docking studies of novel N-substituted hydrazide derivatives of atranorin as antidiabetic agents. *Bioorganic & Medicinal Chemistry Letters*, *30*(17), 127359.
17. Ramírez, H., Fernandez, E., Rodrigues, J., Mayora, S., Martínez, G., Celis, C., ... & Charris, J. (2021). Synthesis and antimalarial and anticancer evaluation of 7-chlorquinoline-4-thiazoleacetic derivatives containing aryl hydrazide moieties. *Archiv der Pharmazie*, *354*(7), 2100002.
18. Umapathi, A., Navya, P. N., Madhyastha, H., Singh, M., Madhyastha, R., Maruyama, M., & Daima, H. K. (2020). Curcumin and isonicotinic acid hydrazide functionalized gold nanoparticles for selective anticancer action. *Colloids and Surfaces A: Physicochemical and Engineering Aspects*, *607*, 125484.
19. Popiołek, Ł. (2021). Updated Information on Antimicrobial Activity of Hydrazide–Hydrazones. *International Journal of Molecular Sciences*, *22*(17), 9389.
20. Jabeen, M., Ahmad, S., Shahid, K., Sadiq, A., & Rashid, U. (2018). Ursolic acid hydrazide based organometallic complexes: synthesis, characterization, antibacterial, antioxidant, and docking studies. *Frontiers in chemistry*, *6*, 55.
21. Reddy, A. K., & Kathale, N. E. (2017). Synthesis and anti-inflammatory activity of hydrazones bearing biphenyl moiety and vanillin based hybrids. *Oriental Journal of Chemistry*, *33*(2), 971.
22. Pan, X., Chen, L., Xu, W., Bao, S., Wang, J., Cui, X., ... & Chen, R. (2021). Activation of monoaminergic system contributes to the antidepressant-and anxiolytic-like effects of J147. *Behavioural Brain Research*, *411*, 113374.
23. Dalaf, A. H. (2018). Synthesis and Characterization of Some Quartet and Quinary Hetero cyclic Rings Compounds by Traditional Method and Microwave Routes Method and Evaluation of Their Biological Activity. *M.Sc. Thesis, Tikrit University*, Tikrit, Iraq: 1-94 pp.
24. Dalaf, A. H., & Jumaa, F. H. (2018). Synthesis, Characterization of some 1,3-Oxazepane -4,7-Dione by Traditional and Microwave routes method and evaluation of their biological activity. *Al-utroha for Pure Science*. (8): 93-108.
25. Dalaf, A. H., Jumaa, F. H., & Jabbar, S. A. S. (2018). Synthesis and Characterization of some 2, 3-dihydroquinozoline and evaluation of their biological activity. *Tikrit Journal of Pure Science*, 23(8): 66-67.
26. Salwa, A. J., Ali, L. H., Adil, H. D., Hossam, S. A. (2020). Synthesis and Characterization of Azetidine and Oxazepine Compounds Using Ethyl-4-((4-Bromo Benzylidene) Amino) Benzoate as Precursor and Evalution of Their Biological Activity. *Journal of Education and Scientific Studies*, ISSN: 24134732. 16(5): 39-52.
27. Abd, I. Q., Ibrahim, H. I., Jirjes, H. M., & Dalaf, A. H. (2020). Synthesis and Identification of new compounds have Antioxidant activity Beta-carotene, from Natural Auxin Phenyl Acetic Acid. *Research Journal of Pharmacy and Technology*, 13(1): 40-46.
28. Dalaf, A. H., & Jumaa, F. H. (2020). Synthesis, Identification and Assess the Biological and Laser Efficacy of New Compounds of Azetidine Derived from Benzidine. *Muthanna Journal of Pure Science (MJPS)*, 7(2):12-25.
29. Saleh, R. H., Rashid, W. M., Dalaf, A. H., Al-Badrany, K. A., & Mohammed, O. A. (2020). Synthesis of Some New Thiazolidinone Compounds Derived from Schiff Bases Compounds and Evaluation of Their Laser and Biological Efficacy. *Ann Trop & Public Health*, 23(7): 1012-1031.
30. Yass, I. A., Aftan, M. M., Dalaf, A. H., & Jumaa, F. H. (Nov. 2020). Synthesis and Identification of New Derivatives of Bis-1,3-Oxazepene and 1,3-Diazepine and Assess the Biological and Laser Efficacy for Them. *The Second International & The Fourth Scientific Conference of College of Science – Tikrit University*. (P4): 77-87.
31. Salih, B. D., Dalaf, A. H., Alheety, M. A., Rashed, W. M., & Abdullah, I. Q. (2021). Biological activity and laser efficacy of new Co (II), Ni (II), Cu (II), Mn (II) and Zn (II) complexes with phthalic anhydride. *Materials Today: Proceedings*, 43, 869-874.
32. Aftan, M. M., Jabbar, M. Q., Dalaf, A. H., & Salih, H. K. (2021). Application of biological activity of oxazepine and 2-azetidinone compounds and study of their liquid crystalline behavior. *Materials Today: Proceedings*, 43, 2040-2050.
33. Aftan, M. M., Talloh, A. A., Dalaf, A. H., & Salih, H. K. (2021). Impact para position on rho value and rate constant and study of liquid crystalline behavior of azo compounds. *Materials Today: Proceedings*.
34. Aftan, M. M., Toma, M. A., Dalaf, A. H., Abdullah, E. Q., & Salih, H. K. (2021). Synthesis and Characterization of New Azo Dyes Based on Thiazole and Assess the Biological and Laser Efficacy for Them and Study their Dyeing Application. *Egyptian Journal of Chemistry*, 64(6), 2903-2911.

35. Khalaf, S. D., Ahmed, N. A. A. S., & Dalaf, A. H. (2021). Synthesis, characterization and biological evaluation (antifungal and antibacterial) of new derivatives of indole, benzotriazole and thioacetyl chloride. *Materials Today: Proceedings*. 47(17), 6201-6210.
36. Dalaf, A. H., Jumaa, F. H., & Salih, H. K. (2021). Preparation, Characterization, Biological Evaluation and Assess Laser Efficacy for New Derivatives of Imidazolidin-4-one. *International Research Journal of Multidisciplinary Technovation*, 3(4), 41-51.
37. Dalaf, A. H., Jumaa, F. H., & Salih, H. K. (2021). *MULTIDISCIPLINARY TECHNOVATION*. *Red*, *15*(A2), C44H36N10O8.
38. Dalaf, A. H., Jumaa, F. H., Aftana, M. M., Salih, H. K., & Abd, I. Q. (2022). Synthesis, Characterization, Biological Evaluation, and Assessment Laser Efficacy for New Derivatives of Tetrazole. In *Key Engineering Materials* (Vol. 911, pp. 33-39). Trans Tech Publications Ltd.
39. Alasadi, Y. Kh., Jumaa, F. H., Dalaf, A. H., Shawkat, S. M., & Mukhlif, M. Gh. (2022). Synthesis, Characterization, and Molecular Docking of New Tetrazole Derivatives as Promising Anticancer Agents. Journal of Pharmaceutical Negative Results. 13(3): 513-522.
40. Dalaf, A. H., Jumaa, F. H., & Yass, I. A. (2022, November). Synthesis, characterization, biological evaluation, molecular docking, assess laser efficacy, thermal performance and optical stability study for new derivatives of bis-1, 3-oxazepene and 1, 3-diazepine. In *AIP Conference Proceedings* (Vol. 2394, No. 1, p. 040037). AIP Publishing LLC.
41. Alasadi, Y. K., Jumaa, F. H., & Dalaf, A. H. (2022, November). Synthesis, identification, antibacterial activity and laser effect of new derivatives of bis-1, 3-oxazepene-4, 7-dione and 1, 3-diazepine-4, 7-dione. In *AIP Conference Proceedings* (Vol. 2394, No. 1, p. 040019). AIP Publishing LLC.
42. Toma, M. A., Ibrahim, D. A., Dalaf, A. H., Abdullah, S. Q., Aftan, M. M., & Abdullah, E. Q. (2022, November). Study the adsorption of cyclopentanone on to natural polymers. In *AIP Conference Proceedings* (Vol. 2394, No. 1, p. 040007). AIP Publishing LLC.
43. Hamad, A. M., Atiyea, Q. M., Hameed, D. N. A., & Dalaf, A. H. (2023). Green synthesis of copper nanoparticles using strawberry leaves and study of properties, anti-cancer action, and activity against bacteria isolated from Covid-19 patients. *Karbala International Journal of Modern Science*, *9*(1), 12.
44. Selvam, T. P., & Kumar, P. V. (2015). Quinazoline marketed drugs. *Research in Pharmacy*, *1*(1).
45. Wang, D., & Gao, F. (2013). Quinazoline derivatives: synthesis and bioactivities. *Chemistry Central Journal*, *7*, 1-15.
46. Kovács, A., Vasas, A., & Hohmann, J. (2008). Natural phenanthrenes and their biological activity. *Phytochemistry*, *69*(5), 1084-1110.
47. Martins, M. B., & Carvalho, I. (2007). Diketopiperazines: biological activity and synthesis. *Tetrahedron*, *63*(40), 9923-9932.

Solving Tri-Criteria and Tri-Objective for Total Completion Time, Total Earliness, and Maximum Tardiness Problems Using Exact and Heuristic Methods on single machine scheduling problem

Nagham M. Neamah[1,2*,]

Bayda A. Kalaf[2]

[1] *Department of Mathematics, College of Science for Women, University of Baghdad, Baghdad, Iraq*

[2]*Department of Mathematics, College of Education for Pure Science Ibn-Al-Haitham, University of Baghdad, Baghdad, Iraq*

Solving Tri-Criteria and Tri-Objective for Total Completion Time, Total Earliness, and Maximum Tardiness Problems Using Exact and Heuristic Methods on single machine scheduling problem

Nagham M. Neamah[1,2*], Bayda A. Kalaf[2]

[1] *Department of Mathematics, College of Science for Women, University of Baghdad, Baghdad, Iraq*

[2]*Department of Mathematics, College of Education for Pure Science Ibn-Al-Haitham, University of Baghdad, Baghdad, Iraq*

Abstract: A multi-criteria single-machine model is introduced in the presented work. A machine scheduling problem (MSP) for n jobs on a single machine was considered for minimizing the function of tri-criteria: total earliness$(\sum E_j)$, total completion time$(\sum C_j)$, and maximum tardiness(T_{max}), and is an NP-hard problem. In the theoretical part of this work, the mathematical formula for the addressed problem will be presented and then the importance regarding dominance rule (DR) that could be applied to the problem in order to improve good solutions will be shown. While in the practical part, two exact methods are important; a Branch and Bound algorithm (BAB) and a Complete Enumeration method are applied to solve the three proposed MSP criteria by finding a set of efficient solutions. The experimental results showed that CEM can solve problems for up tojobs. Two $n = 11$ approaches of the BAB method were applied: the first approach was BAB without dominance rule(DR), and the BAB method uses dominance rules to reduce the number of sequences that need to be considered. Also, this method can solve problems for up to $n = 2000$, and the second approach BAB with dominance rule (DR), can solve problems for up to $n = 3000$ jobs in a reasonable time to find efficient solutions to this problem. In addition, to find good approximate solutions, two heuristic methods for solving the problem are proposed, the first heuristic method can solve up to $n = 5000$ jobs, while the second heuristic method can solve up to $n = 4000$ jobs. Practical experiments prove the good performance regarding the two suggested approaches.

Keyword: Multi-Criteria, Multi-Objective Function, Exact Methods, Heuristic Methods.

1. The introduction

Sheduling problems have gotten a lot of attention in literature since 1954. The researchers started out by focusing on just one objective function[1]. The decision-maker is

required to select just one objective in practical cases. There is more study being done on multi-criteria scheduling problems today. An overview regarding multiple and binary scheduling problems was published by Nagar et al.[2]. Hierarchical and concurrent minification are the two main structures used to resolve competing criteria[3].The primary criterion is the first, and the secondary criterion is the second. In this scenario, one lowers the primary criterion and selects a table with the secondary criterion's minimum value. Pareto set will be formed in the second method, and the decision-maker will be the one with the optimal composite objective function[4]. In 1956 Smith published the first study on a topic of that type[5]. Scheduling n jobs on only one machine could only be handled in this study one job at a time, uninterrupted. At time zero, each job becomes accessible for processing, necessitating positive processing time. Also, the first and two criteria (bi-criteria) scheduling problem was actually solved by Smith, where the problem of $1//(\sum C_j, T_{max})$. In 1995, Hoogveen and Van presented an algorithm for finding all effective tables for Problem $1//(\sum C_j, F_{max})$[4]. In 2015, Zainab and Tariq studied the problem $1//(\sum C_j, \sum T_j, T_{max})$ and fined sub-problem, also solved this problem by branch and bound method. In 2017, Hafed and Tariq presented a multi-objective function $1//\sum C_j + \sum T_j + T_{max} + E_{max}$ and solved this problem by branch and bound[6]. In 2019, Hameed and Chachan attempted to solve a new multi-objective problem $1//\sum(C_j + T_j + E_j + V_j)$, they suggested the use of the BAB approach for solving the aforementioned problem. In 2020 Aseel et al provided a multi-criteria objective function $1//(\sum C_j, \sum E_j)$problem in the SMSP that is solved by BAB[7]. In 2020, Ahmed and Ali provided the problems $1//(\sum C_j, R_L, T_{max})$, $1//\sum C_j + R_L + T_{max}$ in the SMSP solved through BAB and certain heuristic approaches [8] [9]. In 2021, Anmar and Adawyia used BAB to solved the problem $1//\sum C_j + \sum T_j + E_{max}$.

The following table shows the basic problem codes that were used in the presented work.

Table(1): some basic notations and rules for the problem.

Abbreviations	Description
N	Number of jobs $\text{s.t.} N = \{1,2, \dots, n\}$, n: No. of available jobs.
p_j	Processing time of the job j.
d_j	Due date for Job j.
s_j	Slack time for Job j $\text{s.t.} s_j = d_j - p_j$.

L_j	Lateness time of job j, s.t. $L_j = C_j - d_j$.
T_j	Tardiness for job j, s.t. $T_j = max\{0, L_j\}$, T_{max}: Maximal tardiness s.t. $T_{max} = max_{j \in N}\{T_j\}$.
E_j	Earliness time for job j, s.t. $E_j = max\{0, -L_j\}$, $\sum E_j$: Total earliness time.
C_j	Completion time for job j, where $C_j = \sum_{k=1}^{j} p_k$, $\sum C_j$: Total completion time.
F_{CET}	Objective Function of $(S_{CE}M_T)$Problem, F_{SP}: Objective Function of (SP)Problem.
MOF	Multi-Objective Function, MCF: Multi- Criteria Function.
$BAB(WDR)$	Branch and Bound Method With Dominance Rules, where DRs is the Dominance Rules.
$BAB(WODR)$	Branch and Bound Method Without Dominance Rules.
SPT	**Shortest Processing Tim***:* Jobs are Sequencing in a non-decreasing order of processing times p_j (i.e. $p_1 \leq p_2 \leq \cdots \leq p_n$), this rule has been well known for minimizing $\sum C_j$ for problem 1// $\sum C_j$ [5].
EDD	**Earliest Due Date***:* Jobs are sequenced in non-decreasing order regarding their due dates $d_j (where\ d_1 \leq d_2 \leq \cdots \leq d_n)$, this rule utilized for minimizing T_{max} for problem 1// T_{max} [10].
MST	**Minimum Slack Time***:* Jobs are sequenced in a non-decreasing order regarding their slack time $s_j = d_j - p_j$ (where $s_1 \leq s_2 \leq \cdots \leq s_n$). For minimizing E_{max} with the use of this rule [4].
EFSO	**Efficient Solution** [7]: A schedule α^* is known as efficient solution or Pareto optimal or (non-dominated) If cannot found another schedule α satisfying $h_j(\alpha) \leq h_j(\alpha^*), j = 1,2,..,n$, With at least one of the above considered a strict disparity. Another way is that α^* is dominated by α [11].

This paper introduces three-criteria scheduling problems and starts with some basic scheduling concepts for multi-criteria problems. The basic rules are introduced, and the dominance rule is described in Section (1). Section (2) provides information on the original problem and the formulation and analysis of the sub-problem. In Section(4), the exact and approximate methods and algorithms for solving the two problems given in the previous section were presented, in addition to that the experimental results of the two problems were presented. In Section (4) Results and Discussion. The conclusions and lists of future works are given in Section (5).

1.1. Dominance rules in MSP[12]

The size of search tree (i.e., number of the nodes) grows as the number of (n) increases in the (BAB) approach, particularly in the branching scheme. Thus, it is necessary to decrease this size by removing irrelevant solutions or choosing intriguing ones. The problem is that while the complementary subset of the solutions is being stored, one subset of the solutions is being rejected. The goal of dominance rules is for reducing the available

research on scheduling problems. Consequently, as a process for reducing search area and shorten search period.

Definition[13]**:** The graph G depicts a finite number of the vertices or nodes V and a finite number of edges joining 2 vertices; the edge joining a vertex to itself has been referred to as the loop.

Definition[13]**:** If n vertices make up a graph that is referred to as G, then $A(G) = [a_{ij}]$ be the matrix (referred to as adjacency matrix), whose $i^{th}$and j^{th} element is 1 if there is at least 1 edge between 2 vertices v_1 and v_2 and 0 otherwise, $a_{ij} = \begin{cases} 0, \text{if } i = j \text{ or } i \nrightarrow j \\ 1, \text{if } i \rightarrow j \\ a_{ij}, \text{ otherowise} \end{cases}$.

2. The Mathematical Formulation for 1// $\left(\sum C_j, \sum E_j, T_{max}\right)$ Problem.

The problem$(S_{CE}M_T)$considered in this paper is to schedule a set of N of jobs $N = \{1,2,\dots,n\}$ on a one–machine. Every job $j, j \in N$ has an integer processed time p_j, due date d_j.Given schedule $\delta = (\delta_1, \delta_2, \dots, \delta_n)$, then for each job j calculate the completion time by $C_1 = p_1$ and $C_j = \sum_{k=1}^{n} p_{\delta_k}$ for $j = 2,3,\dots,n$. The tardiness of job j is defined by $T_j = max\left\{C_j - d_{\delta_j}, 0\right\}$ and earliness by $E_j = max\left\{d_{\delta_j} - C_j, 0\right\}$. Let $\mathcal{S}$ be a set of all of the feasible solutions (where a feasible schedule means it satisfies all the constraints of problem $(S_{CE}M_T)$ that minimizes the multi-criteria $\left(\sum C_j, \sum E_j, T_{max}\right)$, and $\delta = (\delta_1, \delta_2, \dots, \delta_n)$, is a schedule in S. The mathematical form of the problem $(S_{CE}M_T)$ may be written as:

$$\left.\begin{array}{ll} F_{CET} = Min\left\{\sum C_j, \sum E_j, T_{max}\right\} & \\ \text{s.t.} & \\ C_1 = p_{\delta_1} & \\ C_j \geq p_{\delta_j} & j = 1,2,\dots,n \\ C_j = C_{(j-1)} + p_{\delta_j} & j = 2,\dots,n \\ T_j \geq C_j - d_{\delta_j} & j = 1,2,\dots,n \\ E_j \geq d_{\delta_j} - C_j & j = 1,2,\dots,n \\ T_j \geq 0, E_j \geq 0 & j = 1,2,\dots,n \end{array}\right\} \quad (S_{CE}M_T).$$

Where δ_j indicate where job j falls in ordering δ and S specifies collection of all of the schedules. Finding the set of all of the efficient solutions to the problem $(S_{CE}M_T)$is complicated due to the fact that it is an NP-hard problem (due to the fact that the problem $1//\sum_{j=1}^{n} E_j$ is NP-hard). The aim is finding a processing order $\delta = (\delta_1, \delta_2, \dots, \delta_n)$, for

problem$(S_{CE}M_T)$ for minimizing total earliness, the total completion times, and maximal tardiness.

2.1 Sub problem of the $S_{CE}M_T$ problem.

For problem$(S_{CE}M_T)$, sub-problem can be concluded: The $1//\left(\sum C_j + \sum E_j + T_{max}\right)$ problem is referred to as the problem(SP). The objective of the problem $1 // \sum C_j + \sum E_j + T_{max}$ is to find the sequence of job processing that will minimize $\sum C_j + \sum E_j + T_{max}$. Following is a definition of this sub-problem:

Suppose that α is any machine schedule that is possible to formulate as follows for a given schedule $\alpha = (\alpha_1, \alpha_2, \dots, \alpha_n)$. Assume that α is any schedule which could be expressed in the following way for a specific schedule $\alpha = (\alpha_1, \alpha_2, \dots, \alpha_n)$:

$$\left.\begin{array}{ll} F_{SP} = Min\{\sum C_j + \sum E_j + T_{max}\} & \\ \text{s.t.} & \\ C_1 = p_{\alpha_1} & \\ C_j \geq p_{\alpha_j} & j = 1,2,\dots.,n \\ C_j = C_{\alpha_{(j-1)}} + p_{\alpha_j} & j = 2,\dots.,n \\ T_j \geq C_j - d_{\alpha_j} & j = 1,2,\dots.,n \\ E_j \geq d_{\alpha_j} - C_j & j = 1,2,\dots.,n \\ T_j \geq 0, E_j \geq 0 & j = 1,2,\dots.,n \end{array}\right\} \quad (SP).$$

Finding a processing order $\alpha = (\alpha_1, \dots, \alpha_n)$ for the jobs on one machine that minimizes the summation of total completion times, the total earliness, and maximal tardiness $\left(\sum C_j(\alpha) + \sum E_j(\alpha) + T_{max}(\alpha)\right), \alpha \in S$ (where S is the set of all of the feasible solutions), is the aim of this problem.

3.Methodology:

This section is devoted to examining the approaches for solving the problem$(S_{CE}M_T)$ and (SP). Of the exact approaches, the BAB is utilized as the main approach for solving the problem,

3.1 Exact Solution for Multi-Criteria and Multi-Objective Function Problems

A. Complete Enumeration Method(CEM)

Complete counting can be defined as a simple approach for generating all of the feasible tables and after that selects the optimal one, with regard to multi-criteria (multi-objective function) problem of n jobs, there are tables of number.$n!$

B. Branch and Bound(BAB) Approach

The scheduling problem-solving approach that sees the most use is probably the BAB approach. It is an illustration of implicit enumeration method that could identify the optimal solution by methodically reviewing sub-sets of alternatives. A search tree with nodes matching to such sub-sets describes BAB.

3.1.1 Using BAB to Solve $(S_{CE}M_T)$ and (SP) Problems

Through implicitly enumerating every solution in solution set (in other words, the testing gradually smaller sub-sets of solution set), BAB finds optimal solutions. Those subsets could be thought of as groups of solutions to smaller problems that relate to the main problem. In order to accurately find a solution that enhances the (minimum) problem, the (BAB) approach is applied. The process for (BAB) is introduced in the present study by suggesting a number of the upper and lower bounds, and a number of the dominance rules have been introduced in order to lessen the quantity of branching.

3.1.2 BAB without DRs (classic technology) for Problem$(S_{CE}M_T)$.

This approach could be summarized in the following way: the upper bound (UB) utilized depends on MST rule and lower bound (LB) for a non-serial segment per node depend on SPT rule. The steps for BAB(WODR) are:

Algorithm: BAB(WODRs) Algorithm

***ST (1)*:** Input n, p_j and d_j for $j = 1,2,\dots,n$.

***ST (2)*:** Let $\mathcal{S} = \varphi$, for any α define $F_{CET}(\alpha) = \left(\sum C_j(\alpha), \sum E_j(\alpha), T_{max}(\alpha)\right)$

***ST (3)*:** Calculate an upper bound UB of the problem $S_{CE}M_T$ by sorting the jobs in $\alpha = MST$ rule. Calculate . Set $j = 1,2,\dots,n$for $F_{CET}(\alpha)$ at the search tree's parent node. $UB = F_{CET}(\alpha) = \left(\sum C_j(\alpha), \sum E_j(\alpha), T_{max}(\alpha)\right)$

***ST (4)*:** For every node of search tree of the BAB approach and for every partial sequence π of jobs, calculate $LB(\pi) =$ cost of sequenced jobs + cost of sequence jobs that have been obtained by sequence jobs in SPT EDD rule (where $\pi = SPT$).

***ST (5)*:** Branch from each node with $LB \leq UB$.

***ST (6)*:** At the last level of search tree, get a set of solutions, if $F(\pi)$ the result is

indicated, π are added to the set $\mathcal{S}$ unless they are dominated by the efficient solutions previously obtained in $\mathcal{S}$, this process is called $\mathcal{S}$ filtering.

***ST (7)*:** Stop.

3.1.3 BAB with DRs Method for Problem $S_{CE}M_T$

This approach could be summarized in the following way: UB depend on MST rule and LB for un-sequenced part for each one of the nodes will depend upon the SPT and EDD rules. This BAB is based on DR to decrease the number of the branched(open) nodes which saves time and increases n number of solved problems. The steps of BAB(DR) are as follows:

Algorithm: BAB(WDRs) Algorithm

***ST (1)*:** Input n, p_j and d_j for $j = 1,2,\dots,n$.Find Adjacency Matrix A.

***ST (2)*:** Let $S = \varphi$, for any α define $F_{CET}(\alpha) = \left(\sum C_j(\alpha), \sum E_j(\alpha), T_{max}(\alpha)\right)$.

***ST (3)*:** Calculate an upper bound UB of the problem $S_{CE}M_T$ through sorting jobs in $\alpha = MST$ rule. Calculate Let $j = 1,2,\dots,n$for $F_{CET}(\alpha)$ .search treeat the parent node of the $UB = F_{CET}(\alpha) = \left(\sum C_j(\alpha), \sum E_j(\alpha), T_{max}(\alpha)\right)$

***ST (4)*:** For each node of the search tree of the BAB method and for each partial sequence β of jobs $\beta = MST$, compute $LB(\beta)$ =cost of sequenced jobs +cost of unsequenced jobs obtained by β.

***ST (5)*:** Branch from each node with $LB \leq UB$ and $i \rightarrow j$.

***ST (6)*:** At the last level of the search tree, get a set of solutions, if $F(\beta)$ the result is indicated, α are added to the set S unless they are dominated by the efficient solutions previously obtained in S, this process is called S filtering.

***ST (7)*:** Stop.

3.1.4 BAB Without DRs (Classic Technology) and BAB with DRs Method for Problem(SP).

For the(SP) problem, use the same BAB that is used for the$(S_{CE}M_T)$ problem, with some modifications indicated by BAB_{SP}. First, calculate UB for $(\boldsymbol{SP})$ problem s.t., $UB(\alpha = MST) = F_{SP}(\alpha) = \sum C_j(\alpha) + \sum E_j(\alpha) + T_{max}(\alpha)$, then calculate the LB of any node consisting of sequence and non-sequence parts (obtained by SPT rule) s.t., $LB(\sigma = MST) = F_{SP}(\sigma) = \sum C_j(\sigma) + \sum E_j(\sigma) + T_{max}(\sigma)$, where σ is the rule for unsequenced jobs. Repeat these steps until an optimal solution is obtained from the root.

3.2 Heuristic Methods for $S_{CE}M_T$ and(SP)Problems.

Many research academics use approximatively or heuristic algorithms to handle scheduling problems fast and efficiently since almost all of them are NP-hard and solving them with the use of a CEM and BAB technique could be time-consuming. An algorithm or strategy which searches for the optimum or nearly optimum solutions in a reasonable period of time without a guarantee of optimality or even to see how close that solution is to an optimum one in several circumstances is referred to as a heuristic(or approximation) strategy. For problems$(S_{CE}M_T)$and(SP), new approximation methods for the two problems will be proposed, and these methods are discussed in the following:

3.2.1 The First Heuristic Method for Solving$(S_{CE}M_T)$and(SP) Problems

For the first heuristic method since the SPT rule to solve the $1//\sum C_j$ problem. First, calculate the objective function using the SPT rule. Then put the third job in the second position and the other jobs are still ordered based on SPT rule and calculate the objective function, etc. until n sequences are obtained, repeat the same procedures when using the MST rule.

Algorithm: $SM - S_{CE}M_T(SP)$ Heuristic Algorithm

ST (1): input: $n, p_j \; and \; d_j, j = 1,2, \dots, n, \mathcal{S} = \varphi$.

ST (2): Arrange jobs in the SPT rule (β_1) and calculate
$F_{11}(\beta_1) = \left(\sum C_j(\beta_1), \sum E_j(\beta_1), T_{max}(\beta_1)\right); \mathcal{S} = \mathcal{S} \cup \{F_{11}(\beta_1)\}$.

ST (3): For $i = 2, \dots, n$, put the job i in the first position of β_{i-1} to get β_i and

calculate $F_{1i}(\beta_i) = \left(\sum C_j(\beta_i), \sum V_j(\beta_i), E_{max}(\beta_i)\right)$; $\alpha = \alpha \cup \{F_{1i}(\beta_i)\}$.

End;

ST (4): Arrange jobs in the MST rule (σ_1) and calculate $F_{21}(\sigma_1) = \left(\sum C_j(\sigma_1), \sum V_j(\sigma_1), E_{max}(\sigma_1)\right)$; $\mathcal{S} = \mathcal{S} \cup \{F_{21}(\sigma_1)\}$.

ST (5): For $i = 2, \ldots, n$, put the job i in the first position of σ_{i-1} to get σ_i and calculate $F_{2i}(\sigma_i) = \left(\sum C_j(\sigma_i), \sum V_j(\sigma_i), E_{max}(\sigma_i)\right)$; $\mathcal{S} = \mathcal{S} \cup \{F_{2i}(\sigma_i)\}$.

End;

ST (6): A filter set $\mathcal{S}$ to obtain a set of efficient solutions to the problem $\boldsymbol{S_{CE}M_T}$.

ST (7): Output: the set of efficient solutions $\mathcal{S}$.

ST (8): End.

Where ST=Step

3.2.2 The Second Heuristic Method for Solving$(\boldsymbol{S_{CE}M_T})$and$(\boldsymbol{SP})$Problems

The idea of the second heuristic approach is based on dominance rules and is summarized by finding a sequence sort with a minimum of p_j and d_j, which isn't inconsistent with dominance rules, and calculating objective function. $\boldsymbol{DR - S_{CE}M_T(SP)}$ algorithms can be summarized in the following steps:

Algorithm: $\boldsymbol{DR - S_{CE}M_T(SP)}$ Heuristic Algorithm

ST (1): input: $n, p_j \; and \; d_j, j = 1,2, \ldots, n.$

ST (2): Apply remark or theorem (1) to find the DRs and corresponding adjacent matrix A; $N = \{1,2, \ldots, n\}$ calculate $s_j = d_j - p_j, \forall j \in N, \mathcal{S} = \varphi$.

ST (3): Find a sequence α_1 with a non-increasing order of p_j that does not conflict with DR (matrix A), if it is more than 1 job order α_1 by s_j, then $\mathcal{S} = \mathcal{S} \cup \{\alpha_1\}$.

ST (4): Find a sequence α_2 with a non-increasing order of d_j does not conflict with the DR (matrix A), if there is more than 1 job that breaks links arbitrarily order α_2

by p_j, then $\mathcal{S} = \mathcal{S} \cup \{\alpha_2\}$.

ST (5): Find the dominant sequence set $\mathcal{S}'$ from $\mathcal{S}$.

ST (6): Calculate $F_{CET}(\mathcal{S}')$.

ST (7): Output: Effective solution set $\mathcal{S}'$.

ST (9): End.

Note that the $\boldsymbol{SM - S_{CE}M_T(SP)}$ and $\boldsymbol{DR - S_{CE}M_T(SP)}$ proposed in the previous section will be used for the problem$(\boldsymbol{SP})$.

3.4 Practical Examples of Utilizing the Proposed Methods

In this subsection, (5) randomly generated examples of p_j and d_j s.t. $p_j \in \{1,2,\dots,10\}$ and $d_j \in \{1,2,\dots,70\}$, provided that $d_j \geq p_j$, for $j = 1,2,\dots,n$.

First, let's define the following abbreviations:

ACT/S:	Average of CPU-Time per second.	EX:	Example.
Av:	Average.	NEFS:	Number of efficient Solutions.
ANEFS:	Average number of efficient solutions.	n_i :	The number of jobs, where i is the number of problems tested.
CT/S:	CPU-Time per second.	RL:	0 < Real < 1.

3.5 The Results of The Comparison of Problem $S_{CE}M_T$

The results of applying BAB(WODR), and BAB(WDR) that were compared to the CEM for the **problem** $S_{CE}M_T$ have been listed in Table (2), n = 4, 5,,,,,11

Table (2): Comparison between BAB(WODR) and BAB(WDR) with CEM for problem $S_{CE}M_T$.

	CEM			BAB(WODR)LB=SPT, UB=MST			BAB(WDR)LB=SPT, UB=MST		
X	MCF	TIME	NES	MCF	TIME	NES	MCF	TIME	NES
	$AV(F_{CET})$	ACT/S	ANEFS	$AV(F_{CET})$	ACT/S	ANEFS	$AV(F_{CET})$	ACT/S	ANEFS
4	(60.8, 24.2, 2.2)	RL	8.2	(59.0, 26.4, 2.5)	RL	7.0	(59.0,27.3,1.8)	RL	4.6
5	(90.1, 23.3, 6.5)	RL	10.2	(84.5,30.2,7.3)	RL	5.0	(100.6,20.3,10.1)	RL	4.8

6	(89.6, 23.2, 5.5)	RL	14.6	(81.5,33.7,7.4)	RL	5.6	(120.5,23.6,11.2)	RL	12.2
7	(113.4, 32.4, 9.2)	RL	36	(99.1,51.5,12.5)	RL	7.2	(126.3,22.4,12.6)	RL	22.6
8	(153.3, 26.1, 16.1)	RL	56.2	(137.4,47.9,19.1)	RL	3.8	(149.8,29.5,16.2)	RL	31.2
9	(215.1, 19.0, 24.7)	6.8	35.4	(182.5,20.8,17.9)	RL	1.2	(203.1,36.7,27.8)	RL	24.8
10	(210.6, 34.6, 20.4)	71.2	118.6	(185.3,64.8,27.3)	RL	1.6	(193.0,38.1,18.1)	RL	71.8
11	(301.8, 20.9, 35.9)	845.3	72.4	(278.4,43.4,39.7)	RL	1.2	(286.6,23.9,35.3)	RL	29.8

In Table (3) the results of applying BAB without DR and BAB with DR for **problem** $S_{CE}M_T, n = 12, \dots, 25$.

Table (3): Comparison between the BAB without DR and BAB with DR for problem $S_{CE}M_T, n = 12, \dots, 25$.

EX	BAB(WODR)			BAB(WDR)		
	MCF	TIME	NES	MCF	TIME	NES
n_5	$AV(F_{CET})$	ACT/S	ANEFS	$AV(F_{CET})$	ACT/S	ANEFS
12	(326.9,55.6,42.2)	RL	2.0	(323.7,28.2,37.7)	RL	39.2
13	(344.8,59.8,47.6)	RL	1.0	(345.8,30.8,45.6)	RL	35.8
14	(455.3,26.4,62.3)	RL	1.6	(453.0,14.9,58.1)	RL	21.6
15	(530.0,52.2,67.3)	RL	1.4	(556.8,25.4,66.8)	RL	48.6
16	(498.4,63.6,61.8)	RL	1.0	(514.4,31.1,60.9)	RL	47.0
17	(617.5,43.4,73.0)	RL	1.4	(631.9,21.4,72.7)	RL	33.2
18	(670.1,82.2,75.7)	RL	1.2	(702.0,38.0,74.0)	RL	79.6
19	(712.3,60.6,77.6)	RL	1.2	(697.1,33.4,75.7)	RL	48.2
20	(789.8,70.2,80.7)	RL	1.4	(827.9,35.5,81.7)	RL	55.4
21	(803.1,66.4,81.3)	RL	1.2	(718.3,22.8,69.2)	RL	67.2
22	(1099.1,66.8,106.8)	RL	1.2	(1032.8,39.5,100.5)	RL	40.2
23	(1187.0,54.0,107.0)	RL	1.0	(1142.3,30.8,101.2)	RL	28.0
24	(1257.2,73.6,116.6)	RL	1.0	(1271.5,33.7,115.5)	RL	50.0
25	(1454.8,51.2,125.6)	RL	1.0	(1445.1,24.5,123.6)	RL	23.2
30	(1934.4,60.2,146.6)	RL	1.0	(2393.2,28.1,148.4)	RL	9.8
40	(3302.2,78.6,199.6)	RL	1.0	(4036.1,31.6,203.0)	RL	10.6

50	(4784.6,91.0,241.0)	RL	1.0	(6188.4,29.5,247.8)	RL	13.6
100	(20597.8,96.6,542.4)	RL	1.0	(24137.7,24.5,547.2)	RL	12.4
1000	(1935453.8,0,5484.6)	194.9	1.0	(1935453.8,0,5484.6)	43.9	1.0
2000	(7639198.8,0,10912.0)	1433.1	1.0	(7711677.4,0,10976.6)	358.6	1.0
3000	-	-	-	(17299485.2,0.0,16444.2)	1290.4	1.0

In Table (4) The results of applying$SM - S_{CE}M_T$ andthat were compared to $DR - S_{CE}M_T$ the CEM for the problem $S_{CE}M_T$ have been listed in Table (4), $n = 4,5,\ldots,11$.

Table (4): Comparison between $SM - S_{CE}M_T$ and.$n = 4,5, \ldots,11$,$S_{CE}M_T$ problemfor with CEM $DR - S_{CE}M_T$

EX	CEM			$SM - S_{CE}M_T$			$DR - S_{CE}M_T$		
	MCF	TIME	NES	MCF	TIME	NES	MCF	TIME	NES
n_5	$AV(F_{CET})$	AT/S	ANES	$AV(F_{CET})$	AT/S	ANES	$AV(F_{CET})$	AT/S	ANES
4	(57.4,2.5,15.8)	RL	6.4	(60.2,25.7,2.9)	RL	5.6	(78.5,22.5,6)	RL	6.0
5	(88.2,7.2,12.3)	RL	7.2	(91.9,24.4,7.3)	RL	5.8	(112.9,26.3,15)	RL	7.0
6	(110.2,11.6,13.4)	RL	15.2	(113.7,28.9,11.3)	RL	6.8	(132.5,37,13.5)	RL	6.0
7	(128.1,14.2,10.9)	RL	25.6	(131.4,24.1,14.4)	RL	7.8	(120.5,20,13.8)	RL	4.0
8	(150.9,16, 11.8)	RL	20.8	(155.6,32.4,18)	RL	8.0	(99.7,52,0.7)	RL	3.0
9	(216.4, 25.9,8.5)	8.2	21.2	(225.3,21.3,27.7)	RL	6.8	(194.9,25.7,22.4)	RL	7.0
10	(205,18.3,12.1)	87.2	40.0	(224.5,36.5,23)	RL	10.4	(189.8,36.3,14.3)	RL	4.0
11	(301,35.5,8.3)	1800	26.8	(317.7,23.9,37.9)	RL	8.8	(296.3,25.5,35)	RL	4.0

In Table (5): The results of applying $SM - S_{CE}M_T$ an $DR - S_{CE}M_T$ that were compared to the BAB(WODR), and BAB(WDR) for the problem $S_{CE}M_T$ have been listed in Table (5), $n = 4,5,\ldots,25$.

Table (5): Comparison between $SM - S_{CE}M_T$ and$S_{CE}M_T$ problemfor BAB(WODR), and BAB(WDR)with $DR - S_{CE}M_T$, n = 4,5,…,25.

BAB(WODR)LB=SPT, UB=MST		BAB(WDR)LB=SPT, UB=MST		$SM - S_{CE}M_T$		$DR - S_{CE}M_T$	
MCF	TIME	MCF	TIME	MCF	TIME	MCF	TIME

$AV(F_{CET})$	ACT/S	$AV(F_{CET})$	ACT/S	$AV(F_{CET})$	ACT/S	$AV(F_{CET})$	ACT/S
(59.0, 26.4, 2.5)	RL	(59.0,27.3,1.8)	RL	(60.2,25.7,2.9)	RL	(78.5,22.5,6.0)	RL
(84.5,30.2,7.3)	RL	(100.6,20.3,10.1)	RL	(91.9,24.4,7.3)	RL	(112.9,26.3,15.0)	RL
(81.5,33.7,7.4)	RL	(120.5,23.6,11.2)	RL	(113.7,28.9,11.3)	RL	(132.5,37.0,13.5)	RL
(99.1,51.5,12.5)	RL	(126.3,22.4,12.6)	RL	(131.4,24.1,14.4)	RL	(120.5,20.0,13.8)	RL
(137.4,47.9,19.1)	RL	(149.8,29.5,16.2)	RL	(155.6,32.4,18.0)	RL	(99.7,52.0,0.7)	RL
(182.5,20.8,17.9)	RL	(203.1,36.7,27.8)	RL	(225.3,21.3,27.7)	RL	(194.9,25.7,22.4)	RL
(185.3,64.8,27.3)	RL	(193.0,38.1,18.1)	RL	(224.5,36.5,23.0)	RL	(189.8,36.3,14.3)	RL
(278.4,43.4,39.7)	RL	(286.6,23.9,35.3)	RL	(317.7,23.9,37.9)	RL	(296.3,25.5,35.0)	RL
(326.9,55.6,42.2)	RL	(323.7,28.2,37.7)	RL	(378.9,31.8,42.9)	RL	(396.8,27.8,46.8)	RL
(344.8,59.8,47.6)	RL	(345.8,30.8,45.6)	RL	(415.5,31.8,44.2)	RL	(429.3,30.3,47.2)	RL
(455.3,26.4,62.3)	RL	(453.0,14.9,58.1)	RL	(507.7,15.1,58.4)	RL	(515.8,14.3,58.4)	RL
(530.0,52.2,67.3)	RL	(556.8,25.4,66.8)	RL	(624.7,26.4,64.8)	RL	(641.9,22.5,65.7)	RL
(498.4,63.6,61.8)	RL	(514.4,31.1,60.9)	RL	(601.3,32.4,60.4)	RL	(628.9,30.8,62.4)	RL
(617.5,43.4,73.0)	RL	(631.9,21.4,72.7)	RL	(711.5,24.3,72.9)	RL	(739.1,21.8,72.3)	RL
(670.1,82.2,75.7)	RL	(702.0,38.0,74.0)	RL	(832.8,40.6,75.2)	RL	(859.7,35.1,76.8)	RL
(712.3,60.6,77.6)	RL	(697.1,33.4,75.7)	RL	(880.3,30.2,79.3)	RL	(917.8,24.7,79.9)	RL
(789.8,70.2,80.7)	RL	(827.9,35.5,81.7)	RL	(1039.4,31.3,89.1)	RL	(1090.8,20.6,92.9)	RL
(803.1,66.4,81.3)	RL	(718.3,22.8,69.2)	RL	(1101.7,33.1,87.0)	RL	(1133.6,31.5,91.4)	RL
(1099.1,66.8,106.8)	RL	(1032.8,39.5,100.5)	RL	(1183.6,39.7,92.8)	RL	(1253.4,31.7,94.1)	RL
(1187.0,54.0,107.0)	RL	(1142.3,30.8,101.2)	RL	(1203.4,31.4,93.3)	RL	(1224.1,26.5,96.6)	RL
(1257.2,73.6,116.6)	RL	(1271.5,33.7,115.5)	RL	(1497.2,39.4,112.7)	RL	(1560.9,33.2,113.0)	RL
(1454.8,51.2,125.6)	RL	(1445.1,24.5,123.6)	RL	(1605.0,37.2,112.7)	RL	(1673.8,35.0,116.0)	RL

Table (6) presents the results of applying $SM - S_{CE}M_T$ and problemfor $DR - S_{CE}M_T$ .n, for different $S_{CE}M_T$

Table (6): Comparison results $SM - S_{CE}M_T$ and.$n$for different $S_{CE}M_T$for problem $DR - S_{CE}M_T$

EX	$SM - S_{CE}M_T$			$DR - S_{CE}M_T$		
	MCF	TIME	NES	MCF	TIME	NES

n_5	$AV(F_{CET})$	ACT/S	ANEFS	$AV(F_{CET})$	ACT/S	ANEFS
40	(4022.5,32.7,201.1)	RL	16.4	(4568.4,23.6,224.9)	RL	16.0
60	(8577.7,32.9,298.0)	RL	18.2	(9080.7,22.1,307.6)	RL	13.0
80	(16483.9,37.1,424.9)	RL	20.8	(16093.5,27.4,445.8)	RL	13.0
100	(25917.9,38.9,544.9)	RL	21.0	(26323.7,35.2,568.4)	RL	19.0
400	(415738.1,34.3,2179.2)	1.1	34.2	(384681.3,0.3,2238.3)	RL	3.0
600	(940295.2,35.0,3258.7)	2.2	38.2	(695900.0,0.0,3266.0)	1.2	1.0
800	(1688582.7,29.4,4394.1)	3.8	39.0	(1195823.0,0.0,4279.0)	2.3	1.0
1000	(2637870.0,32.0,5487.0)	5.8	39.2	(1867334.0,0.0,5345.0)	3.4	1.0
2000	(10547780.3,30.5,10979.9)	102.3	40.2	(7711677.4,0.0,10976.6)	353.6	1.0
3000	(23709647.0,30.6,16446.7)	289.3	40.4	(17299485.2,0.0,16444.2)	1299.5	1.0
4000	(42101524.4,30.9,21895.1)	694.7	39.8	-	-	-
5000	(65994864.8,36.4,27466.0)	1348.9	40.0	-	-	-

3.6 The Results of The Comparison of Problem $S_{CE}M_T$.

The results of applying BAB(WODR), and BAB(WDR) that were compared to the CEM for the problem(SP) have been depicted in Table (7), $n = 4,5,\dots,17$

Table (7): Comparison of BAB(WDR) and BAB(DR) with CEM for problem(SP), $n = 4{:}\ 17$.

EX	CEM		BAB(WODR), LB=UB=SPT		BAB(WDR), UB=LB=SPT	
	MOF	TIME	MOF	TIME	MOF	TIME
n_5	$AV(F_{SP})$	ACT/S	$AV(F_{SP})$	ACT/S	$AV(F_{SP})$	ACT/S
4	84.2	RL	84.2	RL	84.2	RL
5	116.6	RL	116.6	RL	116.6	RL
6	141	RL	141.0	RL	141.0	RL
7	154.2	RL	154.2	RL	154.2	RL
8	189.6	RL	189.6	RL	189.6	RL
9	253.8	6.8	253.8	RL	253.8	RL
10	257.6	72.5	257.6	351.4	257.6	RL

11	348	847.9	348.0	145.8	348.0	RL
12	-	-	409.8	628.2	409.8	RL
13	-	-	418.2	1800	418.2	1.1
14	-	-	537.2	254.3	531.4	1.1
15	-	-	629	1800	629.6	97.2
16	-	-	-	-	607.4	17.0
17	-	-	-	-	718.2	RL

The results of applyingthe or fthat were compared to the CEM $DR-SP$and $SM-SP$ problem(SP) have been listed in Table (8), $n=4,5,\dots,11$

Table (8): Comparison between $SM-SP$ and $DR-SP$ with CEM for problem(SP), $n=4,5,\dots,11$.

EX	CEM		$SM-SP$		$DR-SP$	
	MOF	TIME	MOF	TIME	MOF	TIME
n_5	$AV(F_{SP})$	ACT/S	$AV(F_{SP})$	ACT/S	$AV(F_{SP})$	ACT/S
4	84.2	RL	84.2	RL	85.6	RL
5	116.6	RL	118.2	RL	117.2	RL
6	141.0	RL	147.2	RL	144.0	RL
7	154.2	RL	162.8	RL	163.8	RL
8	189.6	RL	194.0	RL	196.6	RL
9	253.8	6.8	267.0	RL	267.6	RL
10	257.6	72.5	272.4	RL	270.4	RL
11	348.0	847.9	358.4	RL	361.4	RL

Table (9) presents the results of applying $SM-SP$and $DR-SP$ for problem (SP) for problem $S_{CE}M_T$, for different n. Table (9) also shows the comparison between BAB without DR, BAB with DR, $SM-SP$and $DR-SP$ for problem (SP) for different n.

Table (9): Comparison results between the BAB without DR, BAB with DR, $SM-SP$ and $DR-SP$ for problem (SP) for different n.

	BAB(WODR),	BAB(WDR),	$SM-SP$	$DR-SP$

EX	LB=UB=SPT		UB=LB=SPT					
	MOF	TIME	MOF	TIME	MOF	TIME	MOF	TIME
n_5	$AV(F_{SP})$	ACT/S	$AV(F_{SP})$	ACT/S	$AV(F_{SP})$	ACT/S	$AV(F_{SP})$	ACT/S
4	84.2	RL	84.2	RL	84.2	RL	85.6	RL
5	116.6	RL	116.6	RL	118.2	RL	117.2	RL
6	141.0	RL	141.0	RL	147.2	RL	144.0	RL
7	154.2	RL	154.2	RL	162.8	RL	163.8	RL
8	189.6	RL	189.6	RL	194.0	RL	196.6	RL
9	253.8	RL	253.8	RL	267.0	RL	267.6	RL
10	257.6	351.4	257.6	RL	272.4	RL	270.4	RL
11	348.0	145.8	348.0	RL	358.4	RL	361.4	RL
12	409.8	628.2	409.8	RL	423.4	RL	426.2	RL
13	418.2	1800	418.2	1.1	450.4	RL	451.2	RL
14	537.2	254.3	531.4	1.1	548.0	RL	545.6	RL
15	629	1800	629.6	97.2	648.2	RL	648.4	RL
16	-	-	607.4	17.0	625.2	RL	623.8	RL
17	-	-	718.2	RL	738.6	RL	734.8	RL
18	-	-	-	-	828.6	RL	828.2	RL
19	-	-	-	-	854.8	RL	851.0	RL
20	-	-	-	-	1031.0	RL	1030.0	RL
40	-	-	-	-	3583.2	RL	3580.4	RL
60	-	-	-	-	7359.0	RL	7346.8	RL
80	-	-	-	-	13638.8	RL	13616.0	RL
100	-	-	-	-	21258.8	RL	21236.8	RL
400	-	-	-	-	312938.6	1.5	312795.4	1.8
600	-	-	-	-	697160.0	2.7	697006.6	4.0
800	-	-	-	-	1245389.8	5.0	1245259.0	9.0
1000	-	-	-	-	1941079.4	8.2	1940938.4	21.0
2000	-	-	-	-	7722685.6	46.1	7722683.0	140.8
3000	-	-	-	-	17315967.4	130.6	17315958.4	496.3

4000	-	-	-	-	30700639.2	307.1	30700633.4	1255.7

A sign (-) indicates unresolved examples.

4. Results and Discussion

Analyze the results by discussing the problem $S_{CE}M_T$:

- From Table(2), note that BAB(WODR) starts to give the minimum values for the $S_{CE}M_T$ problem compared to the results for BAB(WDR) and that CEM performs better than BAB for $n = 4{:}11$, but CEM takes a long time compared to BAB(WODR).
- Fr From Table(3), note that BAB(WDR) starts to give the minimum values for the $S_{CE}M_T$ problem compared to the results for BAB(WODR) for $n = 12{:}24$. While, BAB(WODR) starts to give the minimum values for the $S_{CE}M_T$ problem compared to the results for BAB(WDR) for $n = 25{,}3 \times 10{,}4 \times 10{,}5 \times 10, 10^2, 10^3, 2 \times 10^3$.
- om Table(4), Note that CEM performs better than $SM - S_{CE}M_T$, and $DR - S_{CE}M_T$ for problem $S_{CE}M_T$ for n=4:10, and that $SM - S_{CE}M_T$ performs better than $DR - S_{CE}M_T$.
- From Table(5), note that BAB(WODR) starts giving the minimum values for the $S_{CE}M_T$ problem compared to the results for BAB(WDR), while BAB(WDR) gives better results than $SM - S_{CE}M_T$ .Also, $SM - S_{CE}M_T$ gives better results than $DR - S_{CE}M_T$, for different n .
- From Table (6), Note that Heuristic $SM - S_{CE}M_T$ gives better results than $DR - S_{CE}M_T$ for $n = 40{,}60{,}100$. while, $DR - S_{CE}M_T$ gives better results than $SM - S_{CE}M_T$ for $n = 80{,}400{,}600{,}..{,}3000$, for problem $S_{CE}M_T$

Regarding the problem SP

- From Table(7), note that the application results of BAB(WODR), BAB(WDR), and CEM are identical, but CEM and BAB(WODR) take a long time compared to BAB(WDR). The problems are solved using the CEM method for $n = 11$, the BAB(WODR) method for $n = 15$, and the BAB(WDR) method for $n = 17$.
- From Table(8), Note that CEM gives better results than heuristic $SM - SP$ and $DR - SP$ for problem SP for $n = 4{:}11$.Also, CEM takes a long time compared to heuristic methods
- Note from Table(9), note that the application results of BAB(WODR) and BAB(WDR) are identical, BAB(WODR) takes a long time compared to BAB(WDR).

- From Table(9), note that Heuristic $DR-SP$ gives better results than $SM-SP$ for problem $S_{CE}M_T$ for different n, $DR-SP$ takes a long time compared to $SM-SP$.

5. Conclusions and Future Works

In the present study, a single multipurpose machine function (MSP) with dominance rules was considered $1//(\sum C_j, \sum E_j, T_{max})$, and from this problem can be derived a subproblem $1//(\sum C_j + \sum E_j + T_{max})$. In this paper, two techniques of BAB methods are proposed to solve the two problems $(S_{CE}M_T)$ and (SP) Problems, With and without DR, and results demonstrate the accuracy of the BAB results. Suggest 2 new heuristic methods $SM-S_{CE}M_T(SP)$andwith good efficiency for the two problems that $DR-S_{CE}M_T(SP)$ have been discussed.

In the future, it will be interesting to conduct research on the MSPs that are listed.

1) $1//Lex(\sum C_j, \sum E_j, T_{max})$.
2) $1//Lex(\sum E_j, \sum C_j, T_{max})$.
3) $1//Lex(T_{max}, \sum C_j, \sum E_j)$.

Reference

[1] P. J.-C. B. Associate Professor Vincent T'kindt, *Multicriteria Scheduling Theory, Models and Algorithms Translated*, Second Edi. Springer Berlin Heidelberg New York.

[2] H. C. JOKSCH, "CONSTRAINTS , OBJECTIVES , EFFICIENT SOLUTIONS AND SUBOPTIMIZATION IN MATHEMATICAL PROGRAMMING Author (s): H . C . JOKSCH Source : Zeitschrift für die gesamte Staatswissenschaft / Journal of Institutional and Published by : Mohr Siebeck GmbH & Co . KG S," *J. Institutional Theor. Econ.*, no. Januar 1966, pp. 5–13, 2016, [Online]. Available: http://www.jstor.org/stable/40748933

[3] B. A. Amin and A. M. Ramadan, "Novel Heuristic Approach for Solving Multi-objective Scheduling Problems," *Ibn AL- Haitham J. Pure Appl. Sci.*, vol. 34, no. 3, pp. 50–59, 2021, doi: 10.30526/34.3.2677.

[4] J. A. Hoogeveen, "Minimizing maximum promptness and maximum lateness on a single machine," *Math. Oper. Res.*, vol. 21, no. 1, pp. 100–114, 1996, doi: 10.1287/moor.21.1.100.

[5] W. E. Smith, "Various optimizers for single-stage production," *Navel Res. Logist. Q.*, vol. 3, pp. 59–66, 1956, doi: 10.1002/nav.3800030106.

[6] T. S. A. Razaq and H. M. Motair, "Solving Composite Multi objective Single Machine Scheduling Problem Using Branch and Bound and Local Search Algorithms," *Al-Mustansiriyah J. Sci.*, vol. 28, no. 3, 2017, doi: http://doi.org/10.23851/mjs.v28i3.122 Solving.

[7] A. A. Jawad, F. H. Ali, and W. S. Hasanain, "Using heuristic and branch and bound methods to solve a multi-criteria machine scheduling problem," *Iraqi J. Sci.*, vol. 61, no. 8, pp. 2055–2069, 2020, doi: 10.24996/ijs.2020.61.8.21.

[8] M. G. Ahmed and F. H. Ali, "Exact Method with Dominance Rules for Solving Scheduling on a Single Machine Problem with Multiobjective Function," *Al-Mustansiriyah J. Sci.*, vol. 33, no. 2, pp. 56–63, 2022,

doi: 10.23851/mjs.v33i2.1091.

[9] F. H. Ali and M. G. Ahmed, “Local Search Methods for Solving Total Completion Times, Range of Lateness and Maximum Tardiness Problem,” *Proc. 6th Int. Eng. Conf. ’ ’Sustainable Technol. Dev. IEC 2020*, pp. 103–108, doi: 10.1109/IEC49899.2020.9122821.

[10] T. S. Abdul-Razaq and A. O. Akram, “Local Search Algorithms for Multi-criteria Single Machine Scheduling Problem,” *Ibn AL-Haitham J. Pure Appl. Sci.*, pp. 436–451, 2017, doi: 10.30526/2017.ihsciconf.1817.

[11] D. A. Hassan, N. Mehdavi-Amiri, and A. M. Ramadan, “A heuristic approach to minimize three criteria using efficient solutions,” *Indones. J. Electr. Eng. Comput. Sci.*, vol. 6, no. 1, pp. 334–341, 2022, doi: 10.11591/ijeecs.v26.i1.pp334-341.

[12] N. M. Neamah and B. A. Kalaf, “Solving the multi-criteria: total completion time, total late work, and maximum earliness problem,” *Period. Eng. Nat. Sci.*, vol. 11, no. 3, pp. 46–57, 2023, doi: 10.21533/pen.v11i3.3559.g1288.

[13] G. Strang, *Introduction to Linear Algebra, Fourth Edition*. 2009. [Online]. Available: http://students.aiu.edu/submissions/profiles/resources/onlineBook/Y5B7M4_Introduction_to_Linear_Algebra-_Fourth_Edition.pdf

Solving an inverse Cauchy Problem for modified Helmholtz Equations depending on a polynomial expansion approximation

Shaymaa A. Flayih *, Fatima M. Aboud

[1] **Department of Mathematics, College of Science, University of Diyala**

Solving an inverse Cauchy Problem for modified Helmholtz Equations depending on a polynomial expansion approximation

Shaymaa A. Flayih *, Fatima M. Aboud

[1] **Department of Mathematics, College of Science, University of Diyala**

Abstract

The inverse problem for the modified Helmholtz equation's linked to heat conduction in fins is considered in this paper. The goal of this study is to estimate the boundary temperature and heat flow on a segment of an under-specified boundary (a portion of the outer border of a given domain) using the known Cauchy data on the other portion. Numerical solutions to this problem are found using a proposed meshless method. In order to test the stability, a noise is added to the Cauchy data.

Key words: Inverse Cauchy Problem, Preconditioned Conjugate Gradient Method (PCG), Polynomial Expansion, Modified Helmholtz Equation, and Conjugate Gradient Least Square Method (CGLS).

الخلاصة

في هذا البحث تم تناول المشكلة العكسية لمعادلة هيلمهولتز المعدلة والمرتبطة بالتوصيل الحراري في الزعانف. الهدف من هذه الدراسة هو تقدير درجة حرارة الحدود وتدفق الحرارة على جزء من حدود غير محددة (جزء من الحد الخارجي لمجال معين) باستخدام بيانات كوشي المعروفة على الجزء الاخر. تم العثور على حلول عددية لهذه المشكلة باستخدام طريقة لا شبكية مقترحة. من أجل اختبار الاستقرار، تم إضافة ضوضاء إلى بيانات كوشي

Introduction

One of the key applications in the design and optimization of inverse problems is the identification of an unknown obstacle and its resistive characteristics. This motivates us to solve an inverse Cauchy problem to get the temperature on the inner boundary of an annular region, which is governed by a modified Helmholtz equation.

In this article, we look at the invers problem, which entails estimating the temperature u at the inner boundary of an annular domain from Cauchy data on the outer boundary (boundary temperature and heat flux), under the assumption that the steady-state temperature u satisfies the modified Helmholtz equation governing the heat conduction in a fin.

$$\nabla^2 u - k^2 u = 0\,, \quad \Omega/D$$

based on the knowledge of the boundary conditions on the boundary of and the knowledge of the Dirichlet temperature data and Neumann heat flux data on the outer half of the boundary of Ω , where is the outward unit normal at Lesnic & Bin-Mohsin [1-2].These kinds of problems are ill-posed. In reality, a problem is well-posed in the sense of Hadamard if a unique, stable solution exists [3-4]. If the solution does not satisfy one of these characteristics,

the problem is ill-posed, and an inverse problem must be formulated to solve it [5]. In contrast to direct problems, the inverse problem is typically known to be more challenging to solve [6-7].

In addition, the inverse problems are unstable Hadamard, meaning that even a minor measurement error in the input data might result in a significant inaccuracy in the solution [8]. Inverse problems have recently been considered in a number of scientific fields [9]. One of the inverse problem examples is the inverse Cauchy problem, are some references to this [10-13]. In this type of problem, the boundary conditions (Dirichlet, Neumann) are only known for a portion of the boundary (the accessible portion), while the remaining portion of the boundary has no information, which makes it under-specified or inaccessible[14-15].

In order to avoid the ill-posedness of this kind of problem, a suitable algorithm must be selected for it [16]. The Cauchy problem for the Helmholtz equation has been solved using a variety of techniques over the past 20 years [17]. We will now briefly review a few of these techniques, including the truncation method, the conjugate gradient method, the meshless generalized finite difference method, the Landweber method, and the fractional Tikhonov regularization method[18-21].

In fact, the quality of approximation is significantly impacted by the direct Helmholtz equation numerical solutions' dependency on the physical parameter; for additional information [22-23]. for some approaches that have been suggested to solve the Cauchy Helmholtz equation for some large parameter k. [Jourhmane & Nachaoui, 1996] suggested an alternating algorithm based on relaxation of alternating algorithms. In [Berdawood et al, the authors demonstrated that an efficient relaxed alternating approach proved the convergence for all values of wave number k in the case of the Helmholtz equation and accelerated the convergence in the case of the modified Helmholtz equation [24].

In order to approximate the solution of a Cauchy problem for a modified Helmholtz-type equation in a bounded domain surrounded by a smooth boundary, the goal of this work is to investigate an approach based on polynomial expansion. In this work, the meshless method suggested by Rasheed et al. [Rasheed et al is used to approximate the temperature on the inaccessible inner boundary. This approach was well considered by Rasheed et al to solve an inverse Cauchy problem and by Jameel et al. in 2022 to solve a Cauchy problem Helmholtz equation [25].

The paper will be organized as follows: Basic definitions of the inverse Cauchy problem for the modified Helmholtz equation are provided in Section 2. Our suggested approximation technique is presented in Section 3. In part 4, numerically solving two separate examples of the linear system using CGLS and PCG

2- Inverse Cauchy problem for the modified Helmholtz equation

Have a look at the area with $\Omega/D \subset R^2$ where

$\Omega=\{(r,\theta): 0\leq r < 1, \quad 0 \leq \theta \leq 2\pi\}$

$D=\{(r,\theta): 0\leq r < \beta, \quad 0 \leq \beta < 1, 0 \leq \theta \leq 2\pi\}$

The domain $\Omega \subset R^2$ has as boundary $\partial\Omega = \Gamma_1 \cup \Gamma_2$ with

$\Gamma_1 = \{(r,\theta) \quad : r = \rho_e(\theta) \quad 0 \leq \theta < \beta\pi\}$

$\Gamma_2 = \{(r,\theta) \quad : r = \rho_i(\theta) \quad \beta\pi \leq \theta \leq 2\pi\}$

Where $0 < \beta < 1$, for the modified Helmholtz equation given below, we consider the following inverse Cauchy Problem:

$$\Delta u(x,y) - k^2 u(x,y) = 0 \qquad in\ \Omega/D \qquad (1)$$

$$u(\rho,\theta) = h(\theta) \qquad on\ \Gamma_1 \qquad (2)$$

$$\frac{\partial_\mu}{\partial_n}(\rho,\theta) = g(\theta) \qquad on\ \Gamma_1 \qquad (3)$$

A note is made regarding the Cauchy data $u(x,y)$ and $\partial_n u$(x,y) on the accessible domain boundary. where the functions $h(\theta)$ and g(θ) that are known. The boundary is divided in two portions, the part Γ_2 is underdetermined and the part Γ_1 is overdetermined. The inverse problem for the modified Helmholtz equation is constructed in order to find the temperature u on the underdetermined part of the boundary Γ_2.

Remembering that Rasheed et al. (2021) and Liu & Kubo (2016) provide the following expressions for the normal derivative of u, denoted by $\partial_n u$:

$$\partial_n u(\rho,\theta) = \eta(\theta)[\frac{\partial u(\rho,\theta)}{\partial \rho} - \frac{\rho'}{\rho^2}\frac{\partial u(\rho,\theta)}{\partial \theta}] \qquad (4)$$

$$\eta(\theta) = \frac{\rho(\theta)}{\sqrt{\rho^2(\theta)+[\rho'(\theta)]^2}} \qquad (5)$$

We may also express the normal derivative $\partial_n u(x,y)$ in terms of $\partial_x u$ and $\partial_y u$.

$$\partial_n u = \eta(\theta)[\cos\cos(\theta) - \frac{\rho'}{\rho^2}\sin\sin(\theta)]\,\partial_x u + \eta(\theta)[\sin\sin(\theta) - \frac{\rho'}{\rho^2}\cos\cos(\theta)]\partial_y u \qquad (6)$$

3. Approximation of the solution by polynomial expansion

The solution $u(x,y)$ can be expressed as a polynomial expansion

$$u(x,y) = \sum_{i=1}^{m}\sum_{j=1}^{i} cijx^{i-j}\,y^{j-1} \qquad (7)$$

To find cij, the coefficients u(x,y) must be determined. The highest order of the aforementioned polynomial is m-1, and the total number of these coefficients is n= $\frac{(m(m-1)}{2}$

Equation (8) allows us to determine $\partial xu(x,y), \partial yu(x,y), and\ \Delta u$

$$\partial xu(x,y) = \sum_{i=1}^{m}\sum_{j=1}^{i} c_{ij}(i-j)x^{i-j-1}\,y^{j-1} \qquad (8)$$

$$\partial yu(x,y) = \sum_{i=1}^{m}\sum_{j=1}^{i} c_{ij}(j-1)x^{i-j}\,y^{j-2} \qquad (9)$$

$$\Delta u(x,y) - k^2 u(x,y) = \sum_{i=1}^{m}\sum_{j=1}^{i} c_{ij}[(i-j)(i-j-1)x^{i-j-2}\,y^{j-1} + (j-1)(j-2)x^{i-j}y^{j-3} - k^2(x^{i-j}y^{j-1}) \qquad (10)$$

The coefficients in equation (8) c_{ij} can first be expressed as an n-dimensional vector c with the components $c_k, k = 1,\ldots\ldots n)$. When $i = 1,\ldots m$ and $j = 1,\ldots,i$ are taken into consideration, the coefficients c_ij are actually rearranged, with each index ij corresponding to one index k when k$\frac{=(i(i-1))}{2} + j$. The phrase $u(x,y)$ can be expressed as the vector at with inner product.

$$u(x,y) = [1\ x\ \ y\ \ x^2\ xy\ \ y^2\ \ x^3 x^2 y\ xy^2\ \ y^3\ \ldots\ldots][c_1 c_2 c_3\ \ldots\ldots c_n] = a^T c \qquad (11)$$

We obtain an expression for _n u by substituting (8) and (9) into (6). For each point on the accessible part of the boundaryΓ_1, the normal derivative Anu can also be expressed as the inner product of a vector e with c, where the $l-th$ component of e is given by

$$e_l = \eta(\theta)[(i-j)x^{i-j-1}y^{j-1}(\cos\cos\theta) - \frac{\rho'}{\rho^2}\sin(\theta)) + (j-1)x^{i-j}y^{j-2}(\sin\sin\theta) - \frac{\rho'}{\rho^2}\cos(\theta))] \qquad (12)$$

for those who used cij to calculate el for $l = 1,\ldots,n$, keeping the same coefficients i, j. Now, for each point in the domain, the term $u(x,y) - k^2\,u(x,y)$ can be written as the inner product of a vector d with c, where the l-th component, $l = 1,\ldots,n$, is given by

$$d_k = (i-j)(i-j-1)x^{i-j-2}y^{j-1} + (j-1)(j-2)x^{i-j}y^{j-3} - k^2(x^{i-j}y^{j-1}) \qquad (13)$$

The boundary condition (2)–(3) is verified by selecting n1 points on boundary Γ_1, say $(xi, yj) = (\mathrm{r}\cos(\theta_i), \mathrm{r}\sin(\theta_i)), and\ i = 1,2,\ldots..n_1$. We also select n_2 points in the domain Ω/D, say (x_j, y_j) and $j = 1,\ldots..,n_2$ (to meet the equation) (1),

We now have the linear system as a result $Ac = b$ (14)

Therefore, the vector b is longer. $(2n_1 + n_2) \times 1\ and\ A\ is\ (2n_1 + n_2) \times \frac{m(m+1)}{2}$ matrix provided in each case by

$$A = [a_1^T \ldots A_{n1}^T e_1^T .. e_{n1}^T d_1^T .. d_{n2}^T] \qquad b = [h(\theta_1) \ldots h(\theta_{n1}) g(\theta_1) \ldots g(\theta_{n1})\ 0\ 0] \qquad (15)$$

4 Solving the linear system

We use the well-known Preconditioned Conjugate Gradient Method (PCG) and the Conjugate Gradient Least Squares (CGLS) to solve the linear system $Ac = b$.

4.1 Algorithms of the Preconditioned Conjugate Gradient method (PCG) and the Conjugate Gradient least square method (CGLS)

We will initially define the preconditioned conjugate gradient method as an iterative approach to solving a linear system of equations. A positive definite, symmetric, $A \in R^{n,n}, Ax = b$.

Preconditioned Conjugate Gradient method (PCG)	**Conjugate Gradient least square method (CGLS)**
Algorithm 1: Preconditioned Conjugate Gradient method (PCG) **1.** let $\alpha_{k+1} = r_k^T z_k/(p_{k+1}^T w)$ **2.** **let** $\boldsymbol{x_{k+1} = x_k + \alpha_{k+1} p_{k+1}}$	**Algorithm 2: Conjugate Gradient least Square Method (CGLS)**

3. let $r_{k+1} = r_k - \alpha_{k+1} w$ **4. let $p_{k+1} = z_k + \beta_k p_k$** **5. let $\beta_k = r_k^T z_k / (r_{k-1}^T z_{k-1})$** **6. let $k = k + 1$** **7. repeat the prior actions until convergence**	**1. let** $\alpha_k = \frac{\|r_k\|_2^2}{(p_k^T A^T)(Ap_k)}$ 2. **let** $x_{k+1} = x_k + \alpha_k p_{k\nabla}$ **3. let** $r_{k+1} = A^T s_{k+1}$ **4.** $p_k = -r_k + \beta_{k-1} p_{k-1}$ **5. let** $\beta_k = \frac{\|r_{k+1}\|_2^2}{\|r_k\|_2^2}$ **6. let** $k = k + 1$ **7. repeat the prior actions until convergence**

4.2 Stopping criterion and Initial guess

For any numerical approach, it is essential to know when the algorithm can stop; hence we chose the following halting criteria:

$$\|r_i\| < Tol \tag{16}$$

$$\frac{\|r_i\|}{\|b\|} < Tol \tag{17}$$

5.1 Polynomials exact solution.

Here, we look at a Cauchy problem with an exact polynomial solution and a modified Helmholtz equation.

Example (1)

We consider the Cauchy problem for a modified Helmholtz equation with an exact solution $u(x,y) = 6x^2y^2 - x^4 - y^4$, defined in an annular domain with constant radius $\rho_e = 1 \; and \; \beta = 0.5$. This problem is over −specified on the following cases of the outer boundary

Case 1: $\Gamma_1 = \{(r,\theta)$:r(θ) ={(0.5)+(0.4(cos (θ))+0.1 (sin(2* θ))))/(1+0.7* (cos(θ)}
Case 2: $\Gamma_1 = \{(r,\theta)$:r(θ) =0.5×0.4)/sqrt(0.25 $(\cos(\theta)^2)$ + 0.16 $(\sin(\theta)^2)$)

for which we have the following Cauchy data
$h = 6x^2y^2 - x^4 - y^4$, $g = (12xy^2 - 4x^3)\cos(\theta) + (12x^2y - 3y^2)\sin(\theta)$. We study different cases for a different physical parameter =$\sqrt{100}$, $\sqrt{52}$, $\sqrt{25.5}$, $\sqrt{15}$. For the numerical computations , we take $n_1 = 100, n_r = 5$, $n_2 = 500$ and so we take m =2,……,10 .we compare the results obtained by using the both algorithms CGLS and PCG with $tol = 10^{-10}$.

Tables 1 and 2 show the results for the **first case** of the boundary for the cases k =$\sqrt{15}$, k =$\sqrt{25.5}$.

Table(1): K=$\sqrt{15}$

m	No. of Iter	Error BY CGLS	No. of Iter	Error BY PCG
2	3	9.73906051E-01	3	9.73906051E-01
3	7	8.79669444E-01	7	8.79669444E-01
4	14	1.02721781E+00	14	1.02721781E+00
5	**27**	**6.17522753E-11**	**27**	**5.38786028E-11**
6	52	3.18469866E-09	55	1.84298842E-09
7	110	2.25113365E-08	119	4.22935870E-10
8	244	3.09006110E-08	270	3.15870164E-08
9	579	3.27045307E-07	671	4.85552658E-08
10	1332	6.52945172E-04	1603	6.50824775E-04

In table.1 , we note that the best accuracy is obtained for $m = 5$, for both CGLS and PCG.

In figure 1, the domain for example 1 is given with a comparison between the exact solution and the approximate ones.

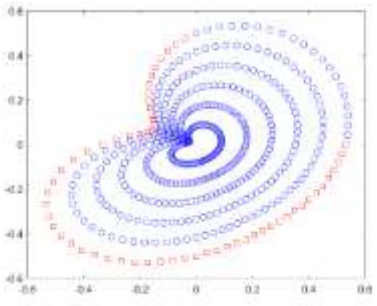

Fig.1.a: Domain

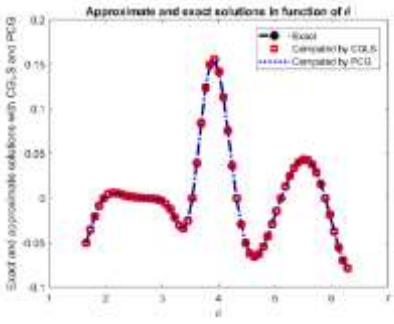

Fig.1.b: Exact and approximate solution

Figure 1: In fig.1.a the domain for Example.1. In Fig.1.b. a comparison between the exact and the approximate solutions calculated with CGLS and PCG.

The error for both CGLS and PCG is given in figure 2.

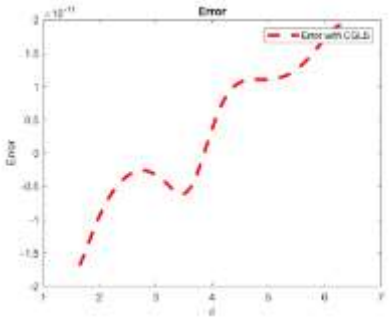

Fig.2.a Error with CGLS

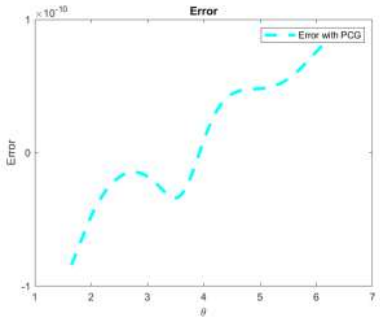

Fig.2.b Error with PCG

Figure 2: In fig.2.a the error for CGLS and in fig.2.b the error for PCG.

Table(2): $k = \sqrt{25.5}$

m	No. of iter	ERROR BY CGLS	No. of Iter	Error BY PCG
2	3	9.75178623E-01	3	9.75178623E-01
3	7	8.81066644E-01	7	8.81066644E-01
4	14	1.24563990E+00	15	1.24563990E+00
5	**29**	**5.22910876E-11**	**29**	**2.99529892E-11**
6	64	8.26849464E-11	66	3.09130694E-09
7	131	1.82353839E-08	144	9.87740857E-09
8	283	2.51246135E-08	345	2.57075318E-07
9	770	4.28457506E-06	1019	1.43427858E-04
10	1772	4.47752351E-03	1903	7.18023665E-02

For table 2, we note the same remark as table 1 . In the following the figures in which we present, the domain, a comparison between the exact solution and the approximate solution with CGLS and PCG and the error for these two methods.

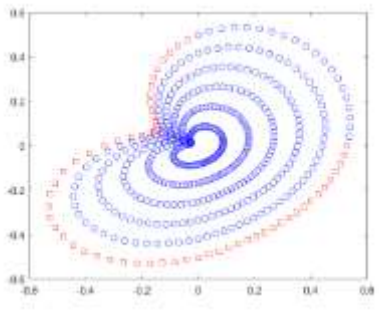

Fig.3.a: Domain

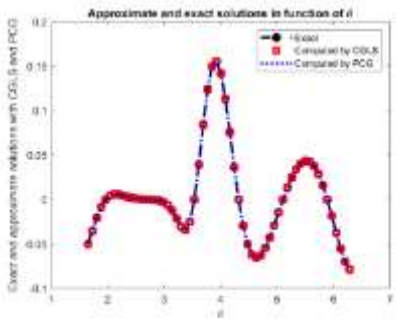

Fig.3.b: Exact and approximate solution

Figure 3: In fig.3.a the domain for Example.1. In Fig.3.b. a comparison between the exact and the approximate solutions calculated with CGLS and PCG.

The error for both CGLS and PCG is given in figure 2

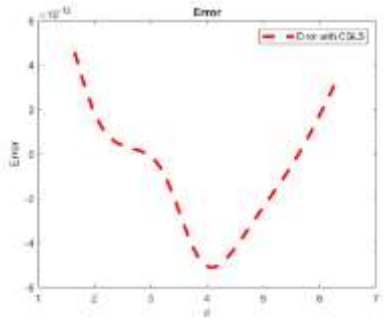

Fig.4.a Error with CGLS

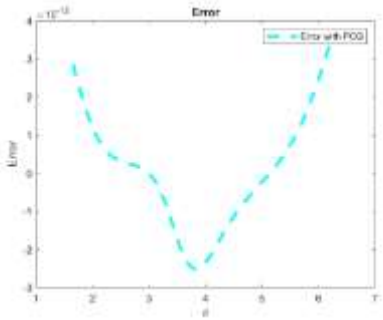

Fig.4.b Error with PCG

Figure 4: In fig.4.a the error for CGLS and in fig.4.b the error for PCG.

Tables 3 and 4 show the results that were achieved for **case 2** of the boundary for the cases $k = \sqrt{25.5}, \sqrt{52}$.

.Table(3): k = $\sqrt{25.5}$

m	No. of iter	Error BY CGLS	No. of iter	Error BY PCG
2	3	9.99558107E-01	3	9.99558107E-01
3	7	9.55310212E-01	7	9.55310212E-01
4	14	1.01862277E+00	15	1.01862277E+00
5	**29**	**5.59318029E-12**	**29**	**7.66792032E-13**
6	60	3.68183499E-10	63	5.18132718E-10

7	127	7.10992390E-09	136	1.70270745E-09
8	288	5.03971819E-08	309	2.14552063E-06
9	613	3.09162562E-05	714	3.08840693E-05
10	1633	4.04151247E-05	2003	4.45837147E-05

In table.3 , we note that the best accuracy is obtained for $m = 5$, for both CGLS and PCG.

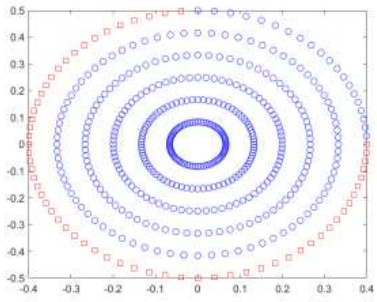

Fig.5.a: Domain

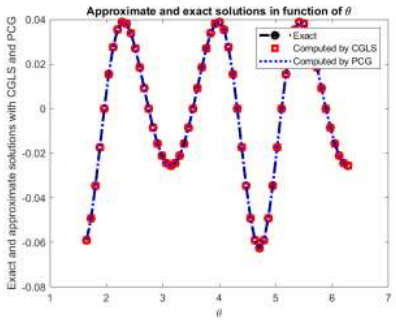

Fig.5.b: Exact and approximate Solution

Figure 5: In fig.5.a the domain for Example.1. In Fig.5.b. a comparison between the exact and the approximate solutions calculated with CGLS and PCG.

The error for both CGLS and PCG is given in figure 6

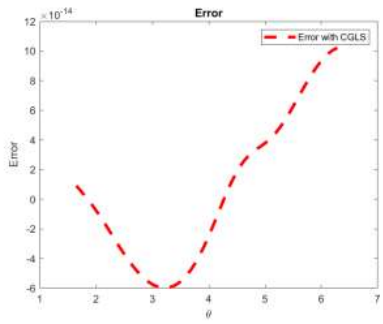

Fig.6.a Error with CGLS

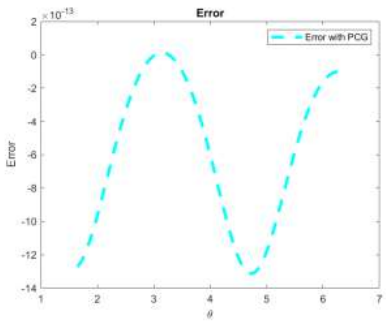

Fig.6.b Error with PCG

Figure 6: In fig.6.a the error for CGLS and in fig.6.b the error for PCG.

Table(4): k =$\sqrt{52}$

	m	No. of iter	Error BY CGLS	No. of iter	Error BY PCG
2	3		9.99638455E-01	3	9.99638455E-01
3	7		9.55431129E-01	7	9.55431129E-01
4	16		9.68936987E-01	15	9.68936987E-01
5	**32**		**1.47870984E-13**	**31**	**3.43199687E-13**
6	61		3.80264882E-11	61	1.35254817E-09
7	131		1.02373334E-09	133	2.55791415E-09
8	303		4.80568455E-09	316	8.14038323E-08
9	658		2.65454289E-06	728	2.14729247E-06
10	1231		8.19510989E-04	1403	8.24351431E-04

For table 4, we note the same remark as table 3 . In the following the figures in which we present, the domain, a comparison between the exact solution and the approximate solution with CGLS and PCG and the error for these two methods.

In the following the figures in which we present, the domain, a comparison between the exact solution and the approximate solution with CGLS and PCG and the error for these two methods.

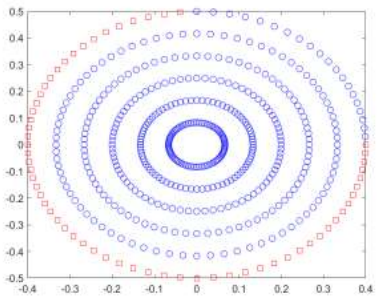

Fig.7.a: Domain

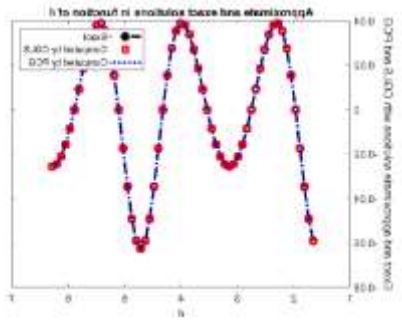

Fig.3.b: Exact and approximate solution

Figure 7: In fig.7.a the domain for Example.1. In Fig.7.b. a comparison between the exact and the approximate solutions calculated with CGLS and PCG.

The error for both CGLS and PCG is given in figure 8.

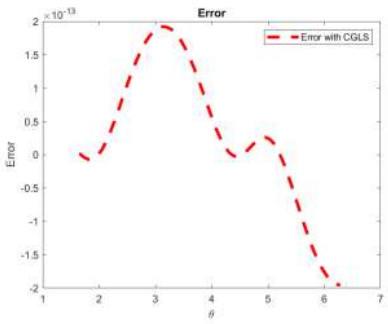

Fig.8.a Error with CGLS

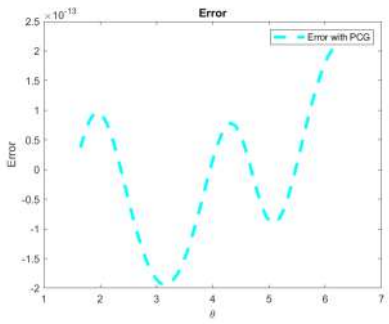

Fig.8.b Error with PCG

Figure 8: In fig.8.a the error for CGLS and in fig.8.b the error for PCG.

5.2 Non-Polynomial exact solution

Here, we examine a Cauchy problem with a non-polynomial exact solution arising from a modified Helmholtz equation.

Example (2): The Cauchy issue for a modified Helmholtz equation with an exact solution is taken into consideration $u(x) = exp(-x^2)$ defined in an annular domain with the constant radius $p_e = 1$and $\beta = 0.5$. This problem is over –specified on the following cases of the outer boundary

Case1: $\Gamma_1 = \{(r,\theta)$:r(θ) ={(0.5)+[0.4*(cos(θ))+0.1*(sin(2* θ)))]/(1+0.7* (cos(θ)}

Case 2: $\Gamma_1 = \{(r,\theta)$:r(θ) =0.5*0.4)/sqrt(0.25*(cos(θ))^2+0.16*(sin(θ))^2)

we have the following Cauchy data $h = \exp(-x^2)$, $g = -2x\exp(-x^2)\cos(\theta)$. we study different cases for a different physical parameter k . For the numerical computations, we take $n_1 = 100$, $n_r = 5$, $and\ so\ n_2 = 500$ and we take m = 2,3,4,……,15 we compare the results obtained by using the both algorithms CGLS and PCG with $tol = 10^{-12}$

Tables 5 and 6 show the results for **first case** of the boundary for the cases k =$\sqrt{15}$, k =$\sqrt{25.5}$.

Table (5): k=$\sqrt{15}$

m	No. of Iter	Error BY CGLS	No. of Iter	Error BY PCG
2	3	2.18922306E-01	3	2.18922306E-01
3	7	8.50341732E-02	7	8.50341732E-02
4	14	1.18281068E-01	14	1.18281068E-01
5	29	1.22195109E-02	30	1.22195109E-02
6	57	7.78351097E-02	57	7.78351096E-02

7	124	1.81342897E-03	139	1.81342064E-03
8	281	2.15562382E-02	343	2.15562867E-02
9	**310**	**4.00931466E-04**	**400**	**4.00586008E-04**
10	363	1.39073285E-03	442	1.39019462E-03
11	408	1.37071013E-03	509	1.36882741E-03
12	405	1.39630229E-03	581	1.29835797E-03
13	407	1.32112532E-03	584	1.30783443E-03
14	426	1.31550201E-03	565	1.31508624E-03
15	413	1.32666792E-03	452	1.50085569E-03

In table. 5, we note that the best accuracy is obtained for $m = 9$,for both CGLS and PCG.

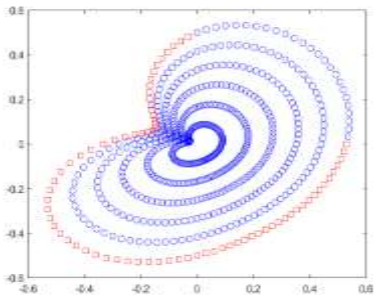

Fig.9.a: Domain

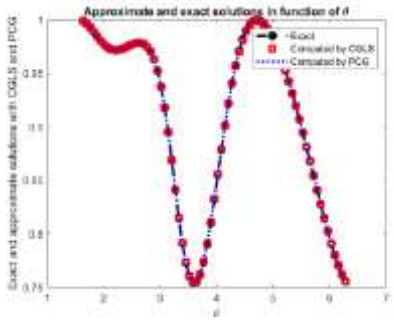

Fig.9.b: Exact and approximate solution

Figure 9: In fig.9.a the domain for Example.2. In Fig.9.b. a comparison between the exact and the approximate solutions calculated with CGLS and PCG.

The error for both CGLS and PCG is given in figure 10.

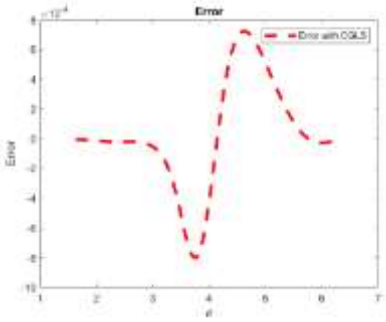

Fig.10.a Error with CGLS

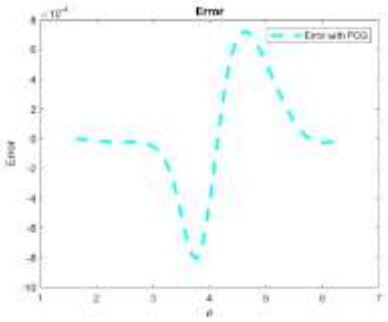

Fig.10.b Error with PCG

Figure 10: In fig..a the error for CGLS and in fig.10.b the error for PCG.

Table(6): $k=\sqrt{25.5}$

m	No. of Iter	Error BY CGLS	No. of Iter	Error BY PCG
2	3	1.70555296E-01	3	1.70555296E-01
3	7	4.42631255E-02	7	4.42631255E-02
4	14	5.13242776E-02	14	5.13242776E-02
5	28	3.58867653E-03	28	3.58867651E-03
6	59	3.09779480E-02	60	3.09779480E-02
7	130	1.02481525E-03	13	1.02481644E-03
8	248	1.25229052E-02	290	1.25228659E-02
9	**283**	**3.30076589E-04**	**233**	**5.18991030E-04**
10	298	7.10294942E-04	293	6.92124861E-04
11	266	7.44076232E-04	297	7.43990896E-04
12	290	7.49020655E-04	319	7.49018456E-04
13	284	7.45188912E-04	395	6.51084944E-04
14	309	7.18521148E-04	344	7.18513310E-04
15	311	7.20690076E-04	357	7.20584837E-04

For table 6, we note the same remark as for table 5 . In the following figures, we present the domain, a comparison between the exact solution and the approximate solution with CGLS and PCG, and the error for these two methods.

In the following figures, we present the domain, a comparison between the exact solution and the approximate solution with CGLS and PCG, and the error for these two methods.

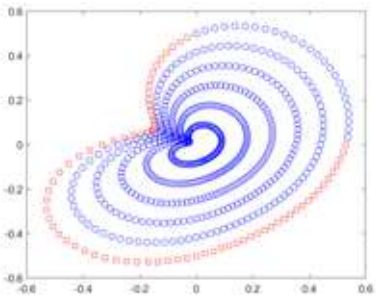

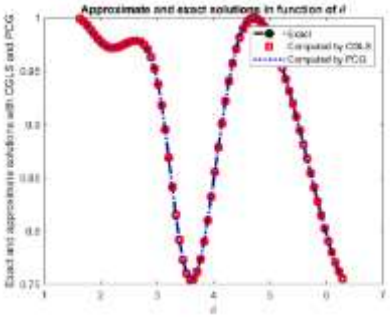

Fig.11.a: Domain	Fig.11.b: Exact and approximate solution
Figure 11: In fig.11.a the domain for Example.2. In Fig.11.b. a comparison between the exact and the approximate solutions calculated with CGLS and PCG.	

The error for both CGLS and PCG is given in figure 12.

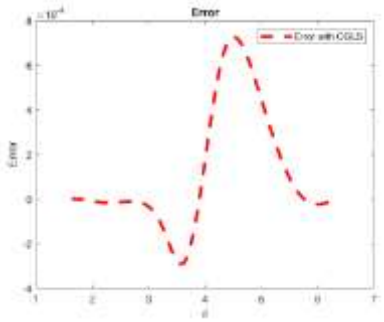	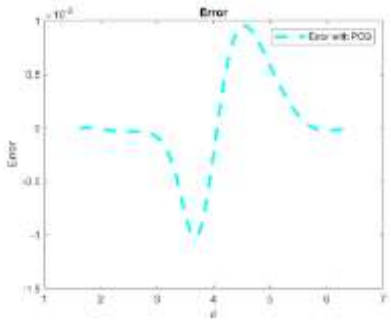
Fig.12.a Error with CGLS	**Fig.12.b Error with PCG**
Figure 12: In fig.12.a the error for CGLS and in fig.12.b the error for PCG.	

Tables 7 and 8 show the results that were achieved for **case 2** of the boundary for the cases $k=\sqrt{52}$, $k=\sqrt{100}$.

.Table (7) : $k=\sqrt{52}$

m	No. of Iter	ERROR BY CGLS	No. of Iter	Error BY PCG
2	3	1.16740998E-01	3	1.16740998E-01
3	7	1.73110297E-02	7	1.73110297E-02
4	16	1.79808788E-02	14	1.79808788E-02
5	30	1.91133785E-03	28	1.91133786E-03
6	62	5.88344291E-03	61	5.88344294E-03
7	**137**	**1.02293329E-04**	**136**	**1.02293197E-04**
8	190	1.47957911E-03	194	1.47957703E-03
9	196	3.08577828E-04	198	3.08563701E-04
10	199	3.37963537E-04	194	3.37996374E-04
11	203	3.09597055E-04	193.	3.09612452E-04

12	198	3.11453226E-04	198	3.11489884E-04
13	197	3.11073375E-04	194	3.11069280E-04
14	199	3.11359573E-04	196	3.11381173E-04
15	197	3.11470542E-04	194	3.11482196E-04

In table 7, we note that the best accuracy is obtained for $m = 7$, for both CGLS and PCG.

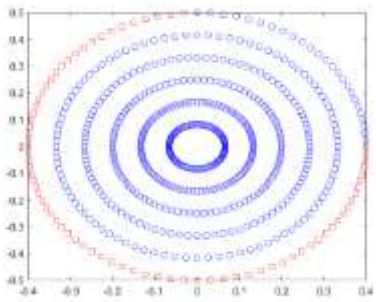

Fig.13.a: Domain

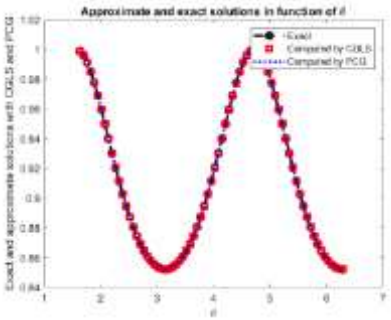

Fig.13.b: Exact and approximate solution

Figure 13: In fig.13.a the domain for Example.2. In Fig.13.b. a comparison between the exact and the approximate solutions calculated with CGLS and PCG.

The error for both CGLS and PCG is given in figure 14.

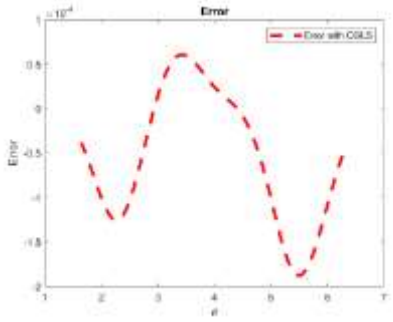

Fig.14.a Error with CGLS

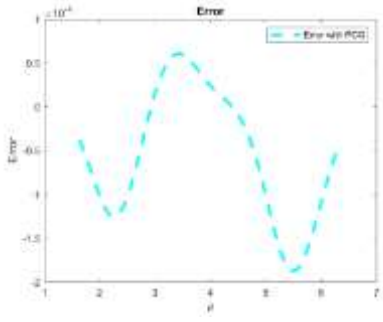

Fig.14.b Error with PCG

Figure 14: In fig.14.a the error for CGLS and in fig.14.b the error for PCG.

Table (8) : $k=\sqrt{100}$

m	No. of Iter	ERROR BY CGLS	No. of Iter	Error BY PCG
2	3	1.00846217E-01	3	1.00846217E-01
3	7	9.45579760E-03	7	9.45579760E-03
4	15	9.53529041E-03	14	9.53529041E-03
5	28	1.01538311E-03	29	1.01538311E-03
6	65	1.60483645E-03	62	1.60483632E-03
7	**154**	**3.08380102E-05**	**136**	**3.08466318E-05**
8	179	2.91056151E-04	180	2.91062154E-04
9	163	9.79980560E-05	166	9.79877960E-05
10	175	1.01537054E-04	174	1.01530971E-04
11	169	8.40815055E-05	171	8.40422657E-05
12	180	8.40425645E-05	172	8.40475172E-05
13	181	8.32397574E-05	168	8.32356726E-05
14	170	8.32378273E-05	172	8.32391710E-05
15	172	8.32134185E-05	170	8.31962562E-05

For table 8, we note the same remark as for table 7. In the following figures, we present the domain, a comparison between the exact solution and the approximate solution with CGLS and PCG, and the error for these two methods.

In the following figures, we present, the domain, a comparison between the exact solution and the approximate solution with CGLS and PCG, and the error for these two methods.

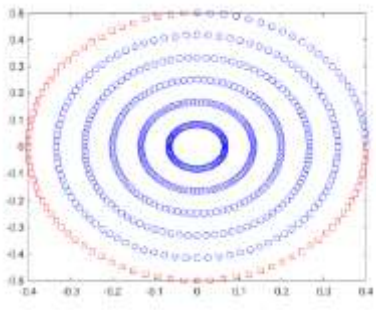

Fig.15.a: Domain

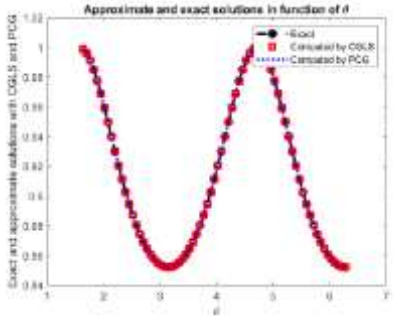

Fig.15.b: Exact and approximate solution

Figure 15: In fig.15.a the domain for Example.2. In Fig.15.b. a comparison between the exact and the approximate solutions calculated with CGLS and PCG.

The error for both CGLS and PCG is given in figure 14

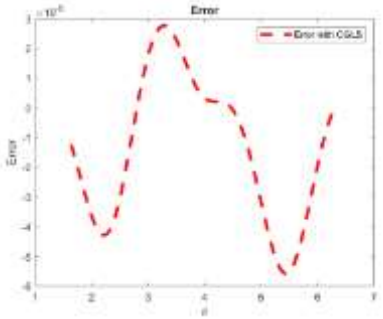

Fig.16.a Error with CGLS

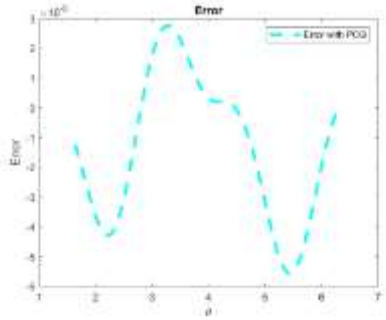

Fig.16.b Error with PCG

Figure 16: In fig.16.a the error for CGLS and in fig.16.b the error for PCG.

5.3 Stability and effect of a noise

The inverse problem is a type of issue caused by the collected (measured) data, and these data may contain errors as a result of measurement mistakes. The impact of data noise on the approximation of the answer must therefore be studied. For this, we apply noise using the following form to the Cauchy data:

$$h(\theta) = u_{ex}(\rho,\theta) + \sigma * rand$$

For some measurement, error deviation ,$\sigma = 0.1,0.01,0.05,0.001$ and for a Gaussian random error rand.

We study the perturbation of Cauchy data by noise for example 1, for a physical parameter $\sqrt{15}$,$n_1 = 100$, $n_2 = 500$ with $Tol = 10^{-10}$ and $\Gamma_3 = \{(r,\theta)$:r(θ) ={(0.5)+(0.4(cos (θ))+0.1 (sin(2θ))))/(1+0.7 (cos (θ))}

σ	No. of Iteration for CGLS	Error with CGLS	No. of Iteration for PCG	Error with PCG
Without noise	27	6.17522753E-11	27	5.38786028E-11
0.1	30	1.51541732E-01	31	1.51541732E-01
0.05	29	6.88828044E-02	29	6.88828046E-02
0.01	30	7.33304825E-04	31	7.33304770E-04
0.001	29	2.01073012E-03	31	2.01073004E-03

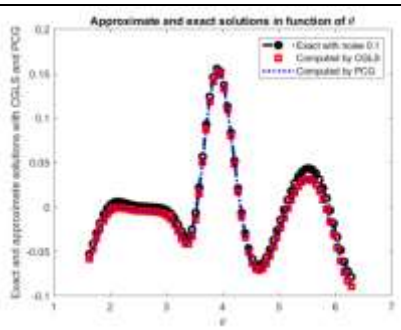

Noise parameter $\sigma = 0.1$

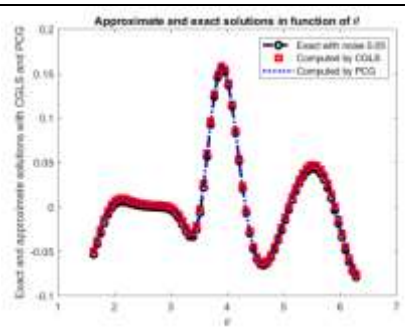

Noise parameter $\sigma = 0.05$

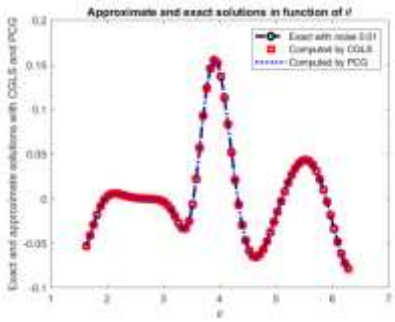

Noise parameter $\sigma = 0.01$

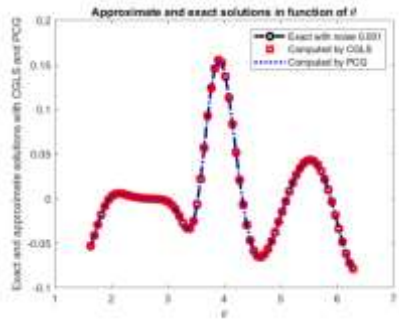

Noise parameter $\sigma = 0.001$

Figure17: Different level of noise for Example 1.

We note that for the different levels of noise, the approximate solution obtained still approaches the exact one with good accuracy and has the same geometry.

Conclusion:

In order to retrieve unknown data on a portion of the boundary from supplied data on the other accessible portion, we solve the inverse Cauchy problem of the modified Helmholtz equation. The polynomial expansion of the solution, which implies constructing a linear system, is used to transform the inverse Cauchy problem into a direct problem, which is then solved by PCG and CGLS. By resolving a few examples and contrasting the precision of PCG and CGLS, the proposed method is confirmed to be effective in overcoming the ill-posedness of the inverse Cauchy Problem. Applying noise to the Cauchy data confirm the investigation of the method's stability.

References :

1- BERNTSSON, Fredrik, et al. Robin–Dirichlet algorithms for the Cauchy problem for the Helmholtz equation. *Inverse Problems in Science and Engineering*, 2018, 26.7: 1062-1078.

2- LESNIC, Daniel; BIN-MOHSIN, Bandar. Inverse shape and surface heat transfer coefficient identification. *Journal of Computational and Applied Mathematics*, 2012, 236.7: 1876-1891.

3- FERNÁNDEZ, José R.; QUINTANILLA DE LATORRE, Ramón. Uniqueness for a high order ill posed problem. *Proceedings of the Royal Society of Edinburgh. Section A, mathematics*, 2022, 1-14.

4- BEGHINI, Marco, et al. Ill-posedness and the bias-variance tradeoff in residual stress measurement inverse solutions. *Experimental Mechanics*, 2023, 63.3: 495-516.

5- GLAGOLEV, M. V.; SABREKOV, A. F. On several ill-posed and ill-conditioned mathematical problems of soil physics. In: *IOP Conference Series: Earth and Environmental Science*. IOP Publishing, 2019. p. 012011.

6- PATEL, Dhruv V.; RAY, Deep; OBERAI, Assad A. Solution of physics-based Bayesian inverse problems with deep generative priors. *Computer Methods in Applied Mechanics and Engineering*, 2022, 400: 115428.

7- CHEN, Xudong, et al. A review of deep learning approaches for inverse scattering problems (invited review). *ELECTROMAGNETIC WAVES*, 2020, 167: 67-81.

8- Hadamard, J. (1923) Lectures on Cauchy's Problem in Linear Partial Differential Equations. Yale University Press, New Haven.

9- KUBO, Shiro. Inverse problems related to the mechanics and fracture of solids and structures. *JSME international journal. Ser. 1, Solid mechanics, strength of materials*, 1988, 31.2: 157-166.

10- NACHAOUI, Abdeljalil, et al. Some novel numerical techniques for an inverse Cauchy problem. *Journal of Computational and Applied Mathematics*, 2021, 381: 113030.

11- HERNANDEZ-MONTERO, Eduardo; FRAGUELA-COLLAR, Andres; HENRY, Jacques. An optimal quasi solution for the Cauchy problem for Laplace equation in the framework of inverse ECG. *Mathematical Modelling of Natural Phenomena*, 2019, 14.2: 204.

12- LAVRENT_EV, Mikhail Mikha_lovich; ROMANOV, Vladimir Gavrilovich; SHISHATSKI_, Serge_ Petrovich. *Ill-posed problems of mathematical physics and analysis*. American Mathematical Soc., 1986.

13- LIU, Chein-Shan; WANG, Fajie. A meshless method for solving the nonlinear inverse Cauchy problem of elliptic type equation in a doubly-connected domain. *Computers & Mathematics with Applications*, 2018, 76.8: 1837-1852.

14- MARIN, Liviu; CIPU, Corina. Non-iterative regularized MFS solution of inverse boundary value problems in linear elasticity: A numerical study. *Applied Mathematics and Computation*, 2017, 293: 265-286.

15- BUCATARU, Mihai; CÎMPEAN, Iulian; MARIN, Liviu. A gradient-based regularization algorithm for the Cauchy problem in steady-state anisotropic heat conduction. *Computers & Mathematics with Applications*, 2022, 119: 220-240.

16- MOGHADDAM, Sayyed Hamed Alizadeh, et al. A statistical variable selection solution for RFM ill-posedness and overparameterization problems. *IEEE Transactions on Geoscience and Remote sensing*, 2018, 56.7: 3990-4001.

17- YANG, Judy P.; GUAN, Pai-Chen; FAN, Chia-Ming. Weighted reproducing kernel collocation method and error analysis for inverse Cauchy problems. *International Journal of Applied Mechanics*, 2016, 8.03: 1650030.

18- YANG, Fan; ZHANG, Pan; LI, Xiao-Xiao. The truncation method for the Cauchy problem of the inhomogeneous Helmholtz equation. *Applicable Analysis*, 2019, 98.5: 991-1004.

19- MARIN, L., et al. Conjugate gradient-boundary element solution to the Cauchy problem for Helmholtz-type equations. *Computational Mechanics*, 2003, 31: 367-377.

20- HUA, Qingsong, et al. A meshless generalized finite difference method for inverse Cauchy problems associated with three-dimensional inhomogeneous Helmholtz-type equations. *Engineering Analysis with Boundary Elements*, 2017, 82: 162-171.

21- QIAN, Zhi; FENG, Xiaoli. A fractional Tikhonov method for solving a Cauchy problem of Helmholtz equation. *Applicable Analysis*, 2017, 96.10: 1656-1668.

22- DURRAN, Dale R. *Numerical methods for wave equations in geophysical fluid dynamics*. Springer Science & Business Media, 2013.

23- PFAU, David, et al. Ab initio solution of the many-electron Schrödinger equation with deep neural networks. *Physical Review Research*, 2020, 2.3: 033429.

24- BERDAWOOD, Karzan A., et al. An effective relaxed alternating procedure for Cauchy problem connected with Helmholtz Equation. *Numerical Methods for Partial Differential Equations*, 2023, 39.3: 1888-1914.

25- RASHEED, Sudad M., et al. REGULARIZED AND PRECONDITIONED CONJUGATE GRADIENT LIKE-METHODS METHODS FOR POLYNOMIAL APPROXIMATION OF AN INVERSE CAUCHY PROBLEM. *Advanced Mathematical Models & Applications*, 2021, 6.2.

Review of Hybrid Face-Based Recognition Systems

Heba jabbar hassan1,a), Mousa K. Wali1, Mohamed Ibrahim Shujaa1

Department of computer Techniques Engineering, 1

.Middle Technical University, Baghdad, Iraq

a) Corresponding author: eng.aby513@gmail.com

Review of Hybrid Face-Based Recognition Systems

Heba jabbar hassan[1,a)], Mousa K. Wali[1], Mohamed Ibrahim Shujaa[1]

[1]Department of computer Techniques Engineering, Middle Technical University, Baghdad, Iraq.

[a)] Corresponding author: eng.aby513@gmail.com

Abstract. In recent years, face recognition algorithms have made great strides thanks to the rapid development of deep learning techniques and the availability of large-scale face datasets. However, despite these developments, there are still obstacles to reaching high accuracy and durability in facial recognition systems in real-world applications. Face recognition systems that combine many modalities or algorithms are gaining popularity as a means of overcoming these challenges. The goal of this research was to compile an overview of hybrid face-based recognition systems, detailing state-of-the-art methods and their effectiveness in improving face recognition performance. First, we talk about why double-mode techniques are preferable, and what benefits they have over single-mode ones. This extensive analysis, emphasize the important parameters that affect the efficacy of several hybrid face-based identification systems and indicate their strengths and limits. We also cover obstacles and potential future research topics, such as standardized evaluation methodologies and the incorporation of explainable AI methods. Insights and suggestions for the future development of more accurate and trustworthy solutions are provided in this review, making it a great resource for researchers and practitioners working on face recognition systems.

Keywords: Biometrics; Indicators Of Individuality; Hybrid ; Face Recognition Systems; Review.

1. Introduction

Recent years have seen a surge of interest in and tremendous advancements in face recognition systems, thanks in large part to the quick development of deep learning techniques, the proliferation of large-scale face databases, and the expansion in processing capacity [1], [2]. Surveillance, access control, forensic investigation, and even HCI have all found uses for these kinds of systems. The technology behind facial recognition has come a long way., but they still have a way to go before they can reliably identify a person in a variety of settings, such as those with changing lighting, poses, expressions, and occlusions[3], [4].

In light of these difficulties, researchers have explored numerous methods for enhancing the

performance of face recognition systems. Many researchers are focusing on developing hybrid face recognition systems that incorporate features from other modalities or algorithms. When it comes to improving identification accuracy, robustness, and generalization, hybrid systems integrate the best aspects of different modalities or approaches[5], [6]. Through this research, researchers aim to familiarize readers with the state-of-the-art approaches, their contributions, and the future challenges associated with hybrid face-based recognition systems by providing a detailed analysis of these systems. Multi-modal fusion, multi-algorithm fusion, and multi-level fusion are the three categories into which we've placed these architectures. The research was conducted to better understand the potential benefits and limitations of hybrid approaches. This paper's contributions are summed up as follows.:

1. Comprehensive analysis of the prior research on hybrid systems, covering topics such as their justifications, benefits over traditional methods, and potential effects on recognition accuracy. We hope to provide scholars and practitioners with a comprehensive grasp of the state-of-the-art methods in this sector by examining the various types of hybrid systems.
2. Analysis of the integration of face images with other biometric modalities, such as fingerprints or iris, to enhance recognition accuracy. We examine various fusion strategies, including early fusion, late fusion, and decision-level fusion, and evaluate their benefits and drawbacks. Additionally, we discuss the challenges associated with multi-modal data acquisition and fusion, as well as potential solutions.
3. Exploration of hybrid systems with different facial recognition methods. Deep neural networks, local binary patterns, and sparse representation-based algorithms are discussed for hybrid systems. We examine the pros and cons of feature-level, score-level, and decision-level fusion and their effects on recognition performance.
4. Investigation of how to combine low-level pixel-based characteristics with high-level semantic representations to improve facial recognition's robustness and discriminatory power. We talk about combining matching scores or decision outputs, as well as features retrieved at various depths. We evaluate the advantages and disadvantages of multi-level fusion and suggest directions for future study.

The remaining sections of the paper are as follows: The many types of face recognition systems, such as feature-based, template-based, and model-based, are discussed in detail in Section 2.Section 3 discusses the motivations behind hybrid face-based recognition systems and presents their advantages over single-modality systems. In Section 4, we categorize the existing hybrid systems into three main groups: multi-modal fusion, multi-algorithm fusion, and multi-level fusion, providing detailed explanations of each category. Section 5 presents a comparative analysis of the strengths and limitations of different hybrid approaches. The difficulties and potential future research areas for hybrid face recognition systems are discussed in Section 6. The report finishes in Section 7, where the major findings are recapped and suggestions for future research are offered...

2. Face Recognition Systems

Identifying people by their faces, as seen in Figure (1). can be broken down into various sub-types according to the methods and processes that underpin them. The various forms of face recognition systems, such as Holistic-based approaches, feature-based methods, model-based techniques, and Hybrid-based approaches[7], [8], are discussed in detail below (see Figure (2)).

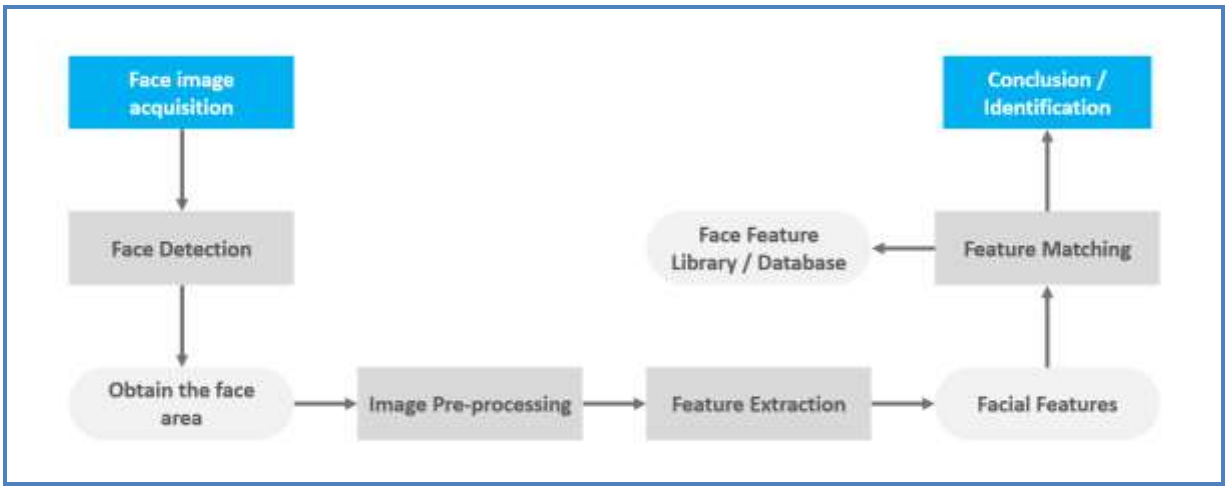

FIGURE 1. Structure for facial recognition [9].

[1] Holistic-based Approach:

The Holistic method, sometimes called the Global method, takes into account the complete face in its analysis. It analyzes the face as a whole and extrapolates features from the overall configuration of the face. This is a common application area for statistical image analysis techniques like Principal Component Analysis (PCA), Linear Discriminant Analysis

(LDA), and others like them. Then, we employ these attributes for identification or categorization. Though computationally efficient, holistic-based approaches may struggle with factors such as position, illumination, and facial expression fluctuation[10].

[2] Feature-based Approach:

The Feature-based method, also known as the local method, is concerned with the collection and evaluation of localized aspects of a person's face. This method extracts and matches individual facial features, such as the eyes, the nose, the mouth, or local texture descriptors, to carry out recognition rather than treating the face as a whole. Methods like Local Binary Patterns (LBP), Scale-Invariant Feature Transform (SIFT), Histogram of Oriented Gradients (HOG), and Convolutional Neural Networks are frequently utilized for feature extraction in this method (CNNs). While feature-based methods may withstand shifts in position and lighting, they may falter when confronted with occlusions or a lack of data[11].

[3] Model-based Approach:

The Model-based method creates a mathematical or statistical representation of the face. These models account for individual differences in the face's structure and appearance in order to facilitate identification. Active Appearance Models (AAM) are a popular model-based technique because they combine shape and appearance models to describe the face. The Elastic Bunch Graph Matching (EBGM) technique is another good illustration; it builds a 3D representation of the face that can adapt to changes in position and lighting. Although model-based techniques are robust against shifts in position and lighting, aligning face landmarks precisely can be difficult[12].

[4] Hybrid-based Approach:

The purpose of the Hybrid-based approach is to boost the efficiency of face recognition systems by utilizing a combination of different approaches. To enhance recognition precision, robustness, and generalizability, hybrid systems combine the best features of multiple methods. Using a global feature representation and local feature descriptors, for instance, a hybrid system may combine the holistic and feature-based techniques. To improve recognition accuracy, another hybrid method might combine data from different

modalities such as fingerprints and iris scans with facial photos. To overcome the shortcomings of standalone methods and attain better results in complex settings, hybrid approaches hold much promise[13], [14].

It's important to keep in mind that the lines between these methods aren't always well drawn, and that many cutting-edge facial recognition systems use a hybrid approach. Examples of deep learning-based systems that mix holistic and feature-based representations include Convolutional Neural Networks (CNNs)[15]. As a result of its capacity to mix diverse approaches or modalities, hybrid face-based recognition systems have garnered a lot of attention in recent years, and we'll be taking a look at some of these systems in the sections that follow.

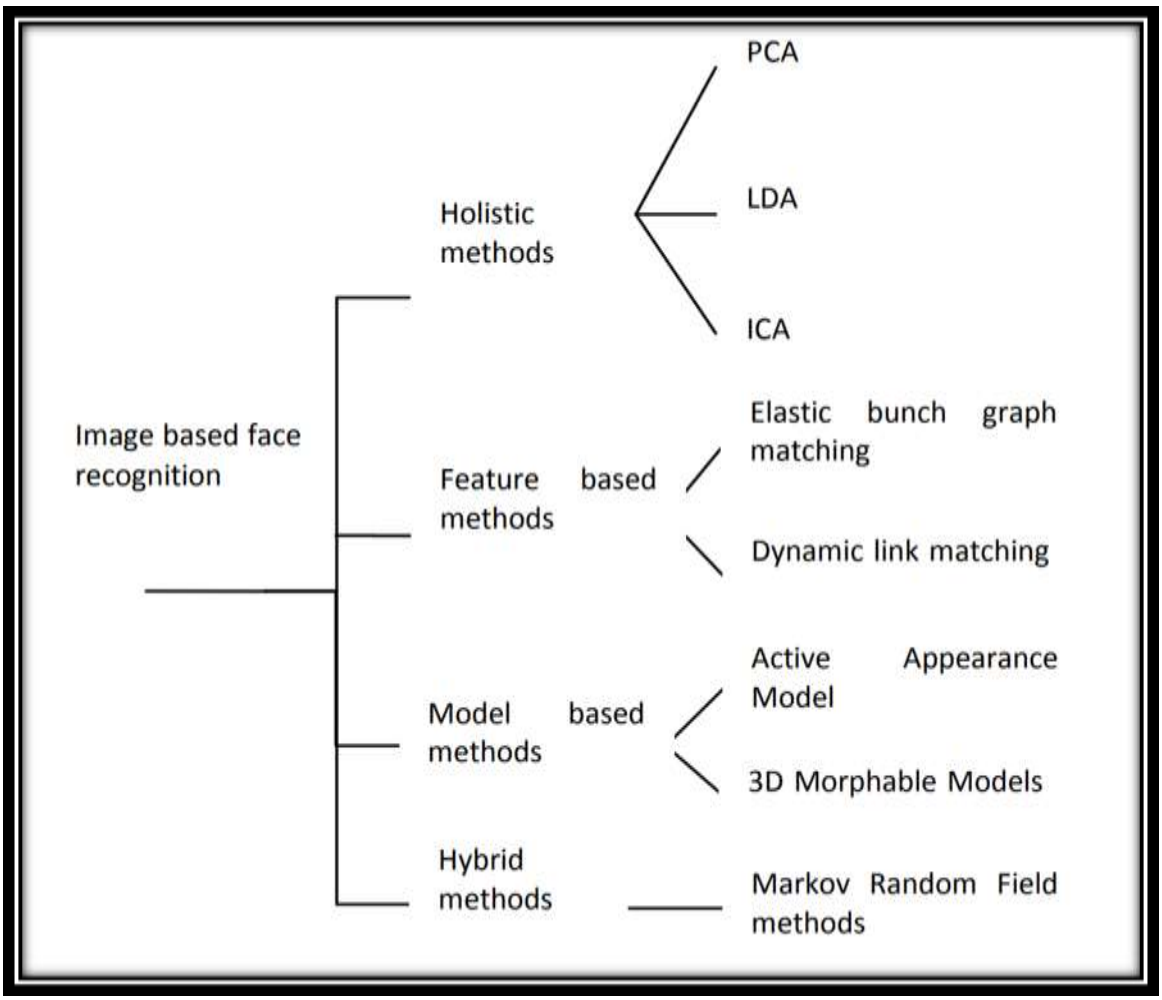

FIGURE 2. Methods for Recognizing Faces[16].

3. Hybrid Approach

Hybrid methods combine local and subspace features to reap the benefits of both approaches, which could result in better face recognition system performance. Gabor wavelets and linear discriminant analysis (HGWLDA) were employed to develop a unique method for face recognition by Fathima et al. [17]. Similarly, the size of the grayscale facial image that is an approximation is reduced. The grayscale face image goes through a series of Gabor filters, each with a distinct size and orientation. After that, they reduce the amount of space that exists within each class by employing the subspace technique known as 2D-LDA, while simultaneously expanding the amount of space that exists between the classes. For the purposes of classifying and identifying the test face image, the k-nearest neighbor classifier is utilized. Comparing each individual feature of the test face image to the features of the faces in the training set is what the recognition process entails. The experimental results suggest that the reliability of this approach remains unaffected by changes in illumination.
Experimenting with different activation functions (Softmax and Segmod) and optimization algorithms; using a convolutional neural network (CNN) architecture for feature extraction; using the histogram of oriented gradient (HOG), the scale invariant feature transform (SIFT), the Gabor, and the Canny contour detector; Benradi et al. [18] developed a novel strategy to improve face recognition accuracy when faced with variance or occlusion.Before feeding the results of a feature extraction operation using the aforementioned methods into the CNN architecture we were utilizing, we preprocessed two of our face databases (ORL and Sheffield faces).Their simulation results show that the SIFT+CNN combo performs exceptionally well, with an accuracy of up to 100% even when noise is present.

For 3D face categorization, Dutta et al. [19] employed a PICANet-based composite filter network after employing a cascaded linear convolutional network. Some of the layers that make up these networks are convolutional layers, nonlinear layers, pooling layers, and classification layers. The fundamental advantage of these networks over DCNN is the network topology's simplicity and processing efficiency. Three publicly available 3D face datasets (Frav3D, GavabDB, and Casia3D) have been used to assess the effectiveness of the proposed approach. Recognition rates of 96.7%, 87.7%, and 89.21% were attained by the system when applied to photos of faces from Frav3D, GavabDB, and Casia3D using the proposed hybrid network.

Combining probabilistic neural networks (PNNs) with enhanced kernel linear discriminant analysis (IKLDA)is the basis of a hybrid approach to face recognition proposed by Ouyang et al. [20]First, a PNN approach is used to handle face recognition problems by reducing the dimensionality of features from a sample while maintaining its relevant information. Both the efficiency and accuracy of computing are enhanced by the suggested IKLDA+PNN approach. Since they cover a wide variety of facial emotions, facial characteristics, and degrees of scale, the ORL, YALE, and AR datasets were used to evaluate the IKLDA+PNN approach to face identification. In tests on three different datasets, it was shown to attain recognition accuracies of 97.22%, 83.84%, and 99.12%, respectively.

Latent dirichlet allocation (LDA), unbiased correction for collinearity in latent classes (WCBC), and over-complete least-squares bias correction (OCLBP) were all recommended by Barkan et al [21]. Adapting the LBP method allowed for this multi-scale representation to be created. The LDA method is useful for dealing with the many-dimensionality issue. For facial recognition, the final measure learning procedure is called within class covariance normalization (WCCN).

Using high-dimensional Walsh Local Binary Patterns (WLBP) and enhanced correlation filters, Juefei et al. [22] developed a periocular-based, single-sample, alignment-robust face recognition system (WLBP). With this technology, you may quickly and easily generate new face images across a wide range of 3D rotations thanks to the 3D generic elastic model.The proposed solution outperformed state-of-the-art algorithms on the LFW database across all four assessment methods, with an accuracy of 89.6 percent.

A multi-sub-region based correlation filter bank (MS-CFB) is proposed by Yan et al. [23] as a risk-free method of gathering data for use in facial recognition systems. Each of the face's individual areas can have its own unique set of features extracted using MS-CFB. as a risk-free method of gathering data for use in facial recognition systems. Each of the face's individual areas can have its own unique set of features extracted using MS-CFB.

Through the utilization of PCA, SIFT, and Fisher vectors, Simonyan et al. [64] developed a fresh technique for recognizing people by their faces. As a solution to the problem of the Fisher vectors' large dimensionality, the authors advocate for a

discriminative dimensionality reduction. The vectors are then linearly projected onto a more convenient axis. Using dense SIFT feature descriptors and Fisher vector encoding, this method performs exceptionally well on the challenging LFW dataset in both confined and unconstrained circumstances.

Using convolutional neural networks (CNNs) and stacked auto-encoder (SAE) techniques, Ding et al. [24] the original holistic face image, the rendered frontal face using a 3D face model (representing local facial features), and uniformly sampled image patches into a multimodal deep face representation (MM-DFR) framework. The proposed MM-DFR framework uses three-layer stacked auto-encoders (SAEs) for feature compression and convolutional neural networks (CNNs) for feature extraction to construct a low-dimensional representation of the face. Comparison to the LFW database is used to gauge how well MM-object DFR detects objects. Figure 3 depicts the proposed MM-DFR structure.

An efficient pose-invariant facial recognition system is provided by Sharma et al. [25], which makes use of the PCA method and the ANFIS classifier. Principal component analysis (PCA) is used to extract features from images, and an ANFIS classifier is created to recognize images regardless of the subject's attitude. Since it is based on PCA-ANFIS, the suggested system outperforms ICA-ANFIS and LDA-ANFIS on the face recognition challenge. The ORL database is used for decision-making.

The fast facial recognition system developed by Mussa et al. [26]makes use of DCT and PCA. In order to streamline the process and get rid of extraneous data, facial traits are extracted using a genetic algorithm (GA) approach. Dimensionality reduction and feature extraction are also carried out with the aid of the DCT-PCA technique. The shortest possible Euclidean distance is used as the criterion (ED). We use many free online face databases to demonstrate the efficacy of our strategy.

Mian et al. [27] In order to efficiently and robustly recognize facial emotions, it is necessary to provide a multimodal (2D and 3D) face recognition system based on hybrid matching employing principal component analysis (PCA), support vector machine (SVM), and iterative closest point (ICP).The transformation makes it easy to adjust the 3D location of a face based on the texture of the face. The SIFT descriptor is used with a novel 3D spherical face representation (SFR) to build a rejection classifier, allowing for effective recognition even in the case of large galleries. To draw a

conclusion, we use a modification of the iterative closest point (ICP) technique. Over the whole FRGC v2 database, the system achieved a verification rate of 98.6% and an identification rate of 96.16%, making it less sensitive to and more resilient in the face of facial expressions.

Cho et al. [28] used principal component analysis, local Gabor binary pattern histogram sequence (LGBPHS), and GABOR wavelets to create a hybrid system for facial identification. The number of dimensions can be minimized via principal component analysis. For recognition, they then employ the local Gabor binary pattern histogram sequence (LGBPHS) method, which was developed to lessen the burden of the difficulties introduced by the Gabor filters. Recognition rates are shown to increase experimentally under different illumination situations compared to PCA and Gabor wavelet techniques. Using the Extended Yale Face Database B, we show that this technique is effective.

Sing et al. [29] combine principal component analysis (PCA) and Fisher linear discriminant (FLD) to create a novel hybrid approach to face representation and recognition. In order to extract local attributes from a picture, segmentation is required, while processing the full image at once will yield global characteristics. The resulting fused feature vector is then subjected to dimensionality reduction methods like principal component analysis (PCA) and Fisher linear discriminant analysis (FLD). To do this, they query the CMU-PIE, FERET, and AR databases for facial features.

SPCA–KNN Coupling Principal Component Analysis (PCA) with Kernel Neural Networks, Kamencay et al. [30]develop a novel method for facial recognition. The SPCA descriptor and the Hessian-Laplace detector are utilized for this purpose. SPCA is used for facial recognition. To locate people with similar characteristics, the KNN classifier is presented. Using the unsegmented ESSEX database, the experiment was successful 92% of the time, whereas using the segmented database, it was successful 96% of the time (700 training images).

For sequential human activity recognition, Sun et al. [31] present a CNN-LSTM-ELM hybrid deep structure that combines convolutional operations, recurrent units from the LSTM network, and the ELM classifier (HAR). On the OPPORTUNITY dataset, they tested their suggested CNN-LSTM-ELM system. Each sample represents a sequence, and there are a total of 46,495 training samples and 9894 testing samples. Models are

trained and tested on GPUs with 1536 processing cores, 1050 MHz clock speeds, and 8 GB of memory. Using a flowchart representation, Figure 4 depicts the suggested CNN-LSTM-ELM architecture.

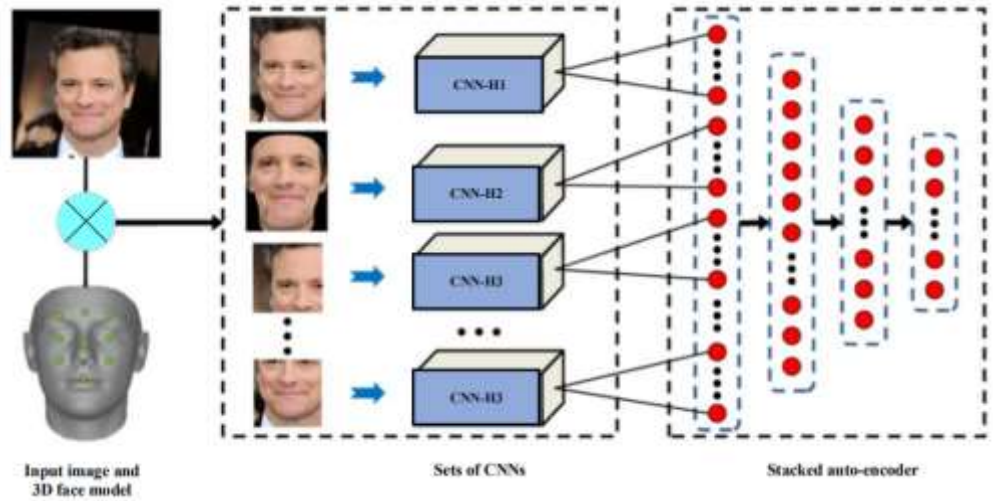

FIGURE 3. Illustration of the Multimodal Deep Face Representation (MM-DFR) Method in Action [24],

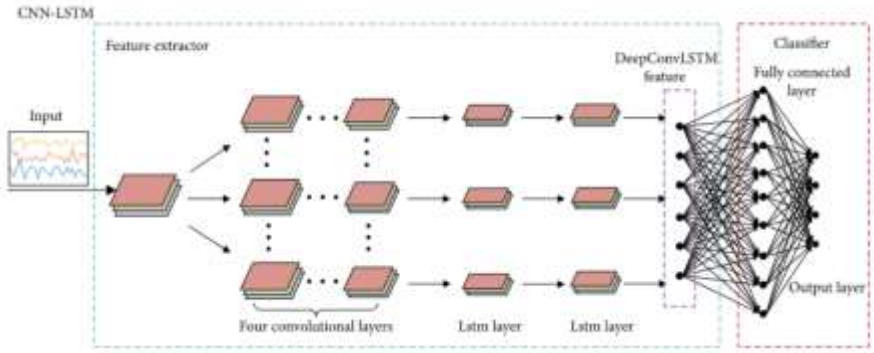

FIGURE 4. The proposed convolutional neural network LSTM ELM[31].

3.2An Overview of Hybrid Methods

The various hybrid methods are summed up in Table 3.Recognition systems have been given a boost in accuracy and speed thanks to the development of new techniques. Combining local and subspace methods produces reliable recognition and dimensionality reduction under varied lighting and expressions. It is also implied that these technologies are susceptible to noise and resistant to scale and rotation.

TABLE 1. Hybrid approaches summary.

Author	Technique Used	Database	Matching	Limitation	Advantage	Result
Benradi et al.[18]	SIFT+CNN	ORL and Sheffield	HOG	--	accuracy rate	100%
Dutta[19]	CNN+PICANet	Frav3D, GavabDB, and Casia3D.	PCA	Complexity	computationally efficient	96.93%, 87.7%, and 89.21%
Ouyang et al.[20]	IKLDA+PNN	ORL, YALE and AR	SVM	--	processing time	97.22%, 83.8% 99.12%
Fathima et al. [17]	GW-LDA	AT&T FACES94 MITINDIA	k-NN	High processing time	Illumination invariant and reduce the dimensionality	88% 94.02% 88.12%
Barkan et al., [21]	OCLBP LDA WCCN	LFW WCCN	MAP	---	Reduce the dimensionality	5.50% 9.70% 91.97%
Juefei et al. [22]	ACF and WLBP	LFW	--	Complexities	Pose conditions	89.69%
Simonyan et al. [32]	Fisher + SIFT	LFW	Mahalanobis matrix	Single feature type	Robust	87.47%
Sharma et al. [25]	PCA-ANFIS ICA-ANFIS LDA-ANFIS	ORL	ANFIS	Sensitivity-specificity	Pose conditions	96.66% 71.30% 68%
Moussa et al. [26]	DCT-PCA	ORL UMIST YALE	Euclidian distance	Complexity	Reduce the dimensionality	92.62% 99.40% 95.50%
Mian et al. [27]	Hotelling transform, SIFT, and ICP	FRGC	ICP	Processing time	Facial expressions	99.74%
Cho et al. [28]	PCA-LGBPHS PCA-GABOR	Extended Yale Face Wavelets	Bhattacharyya distance	Illumination condition	Complexity	95%
Sing et al. [29]	PCA-FLD	CMU FERET AR	SVM	Robustness	Pose, illumination, and expression	71.98% 94.73% 68.65%
Kamencay et al. [30]	SPCA-KNN	ESSEX	KNN	Processing time	Expression variation	96.80%
Sun et al. [31]	CNN-LSTM-ELM	OPPORTUNITY	LSTM/ELM	High processing time	Automatically learn feature representations	90.60%
Ding et al. [24]	CNNs and SAE	LFW	--	Complexity	High recognition rate	99%

Discussion on Hybrid Approaches in Face Recognition Systems

As a result of their potential to improve recognition performance and accuracy, hybrid approaches have attracted a lot of interest in the field of face recognition systems. These algorithms offer a comprehensive and powerful method of face identification by combining regional and holistic features. The capacity to successfully manage both local and global elements is a major benefit of hybrid systems. Unique traits are best extracted from segmented face regions using local feature-based approaches including HOG, LBP, Gabor filters, and correlation filters. Facial expressions and occlusions, however, might contribute

significant background noise that can hinder their performance. Holistic approaches, on the other hand, consider the whole face rather than just the eyes, mouth, and nose. Holistic approaches are able to capture the full representation of a face because they treat the facial image as a matrix of pixels. On the other hand, they might not distinguish between different colors or textures in an image.

Hybrid approaches can be more effective than either option alone since they combine regional and holistic approaches. Improved recognition accuracy and reliability can result from combining the strengths of local and holistic approaches. The system's adaptability to changes in illumination, facial expression, and stance is improved by utilizing both local and global features for analysis of facial recognition. When deciding on the best approach, it is vital to take into account the unique circumstances of the application. For instance, face recognition systems that employ modestly sized photos may struggle with the accuracy of local feature-based techniques. When choosing an algorithm, it is also necessary to take into account the amount of training instances that will be needed. By combining the best features of local and systemic approaches, hybrid methods provide a solution that can be adjusted to meet the needs of a given application.

Future facial recognition system research should concentrate on improving hybrid techniques. Development of 3D face recognition methods, multimodal fusion methods that mix data from different sources (such as visible and infrared pictures), and the use of deep learning (DL) methods are three intriguing avenues for further investigation. While issues with lighting and position fluctuations plague 2D face recognition, 3D data can help, and multimodal fusion techniques can boost recognition performance even further. With its better accuracy in face recognition tests and its ability to learn high-level abstractions, DL has shown considerable promise. As a result of bringing together local and global features, hybrid techniques in face recognition systems provide an effective answer. The recognition accuracy, robustness, and adaptability of such systems can all be improved by combining the best features of both approaches. To further increase face recognition, future research should continue to investigate and improve hybrid approaches, with a particular emphasis on the creation of 3D face recognition, multimodal fusion techniques, and the application of deep learning algorithms.

5. Conclusions

In conclusion, the field of face recognition systems has seen considerable developments, with many approaches and methodologies being developed and investigated. hybrid

techniques, which mix regional and holistic characteristics, have emerged as a potential direction in boosting recognition performance and accuracy. these approaches integrate regional and holistic properties. these methods offer a complete and robust solution for face identification because they capitalize on the capabilities of both locally feature-based methods and holistic representations. moving forward, the focus of future research should be on further improving hybrid approaches and exploring new directions. for example, the development of 3d face recognition techniques, multimodal fusion strategies, and the integration of deep learning algorithms are all examples of new directions that could be investigated. these advancements will contribute to the continued progress and adoption of face recognition systems in a variety of domains, including biometric authentication, security, and surveillance. they will do this by addressing the challenges posed by changing lighting conditions and changing poses, as well as by improving overall recognition capabilities.

References

[1] R. A. R. Ahmad, M. I. Ahmad, M. N. M. Isa, and S. A. Anwar, "Face recognition using assemble of low frequency of DCT features," Bulletin of Electrical Engineering and Informatics, vol. 8, no. 2, pp. 541–550, Jun. 2019, doi: 10.11591/eei.v8i2.1417.

[2] M. Z. Nasution, "Face Recognition based Feature Extraction using Principal Component Analysis (PCA)," JOURNAL OF INFORMATICS AND TELECOMMUNICATION ENGINEERING, vol. 3, no. 2, 2020, doi: 10.31289/jite.v3i2.3132.

[3] A. Elmahmudi and H. Ugail, "Deep face recognition using imperfect facial data," Future Generation Computer Systems, vol. 99, 2019, doi: 10.1016/j.future.2019.04.025.

[4] G. Yue and L. Lu, "Face Recognition Based on Histogram Equalization and Convolution Neural Network," in Proceedings - 2018 10th International Conference on Intelligent Human-Machine Systems and Cybernetics, IHMSC 2018, 2018. doi: 10.1109/IHMSC.2018.00084.

[5] S. A. Baker, H. H. Mohammed, and H. A. Aldabagh, "Improving face recognition by artificial neural network using principal component analysis," Telkomnika (Telecommunication Computing Electronics and Control), vol. 18, no. 6, pp. 3357–3364, Dec. 2020, doi: 10.12928/TELKOMNIKA.v18i6.16335.

[6] M. Gupta and Deepika, "An Efficacious Method for Face Recognition Using DCT and Neural Network," in Lecture Notes on Data Engineering and Communications Technologies, Springer Science and Business Media Deutschland GmbH, 2021, pp. 671–683. doi: 10.1007/978-981-15-8677-4_55.

[7] A. Ouyang, Y. Liu, S. Pei, X. Peng, M. He, and Q. Wang, "A hybrid improved kernel LDA and PNN algorithm for efficient face recognition," Neurocomputing, vol. 393, pp. 214–222, Jun. 2020, doi: 10.1016/j.neucom.2019.01.117.

[8] P. Vijaykumar and J. K. Mani, "Face Recognition with Frame size reduction and DCT compression using PCA algorithm," Indonesian Journal of Electrical Engineering and Computer Science, vol. 22, no. 1, p. 168, Apr. 2021, doi:

10.11591/ijeecs.v22.i1.pp168-178.

[9] X. Fu, "Design of Facial Recognition System Based on Visual Communication Effect," Comput Intell Neurosci, vol. 2021, 2021, doi: 10.1155/2021/1539596.

[10] S. Das, D. Venugopal, and S. Shiva, "A Holistic Approach for Detecting DDoS Attacks by Using Ensemble Unsupervised Machine Learning," in Advances in Intelligent Systems and Computing, Springer, 2020, pp. 721–738. doi: 10.1007/978-3-030-39442-4_53.

[11] N. A. Shnain, Z. M. Hussain, and S. F. Lu, "A feature-based structural measure: an image similarity measure for face recognition," Applied Sciences (Switzerland), vol. 7, no. 8, 2017, doi: 10.3390/app7080786.

[12] V. Riccio and P. Tonella, "Model-based exploration of the frontier of behaviours for deep learning system testing," ESEC/FSE 2020 - Proceedings of the 28th ACM Joint Meeting European Software Engineering Conference and Symposium on the Foundations of Software Engineering, no. 2, pp. 876–888, 2020, doi: 10.1145/3368089.3409730.

[13] W. H. Abdulsalam, R. S. Alhamdani, and M. N. Abdullah, "Emotion recognition system based on hybrid techniques," Int J Mach Learn Comput, vol. 9, no. 4, 2019, doi: 10.18178/ijmlc.2019.9.4.831.

[14] H. M. Shahzad, S. M. Bhatti, A. Jaffar, S. Akram, M. Alhajlah, and A. Mahmood, "Hybrid Facial Emotion Recognition Using CNN-Based Features," Applied Sciences (Switzerland), vol. 13, no. 9, May 2023, doi: 10.3390/app13095572.

[15] H. Benradi, A. Chater, and A. Lasfar, "A hybrid approach for face recognition using a convolutional neural network combined with feature extraction techniques," IAES International Journal of Artificial Intelligence, vol. 12, no. 2, pp. 627–640, Jun. 2023, doi: 10.11591/ijai.v12.i2.pp627-640.

[16] Z. Sufyanu, F. Mohamad, A. Yusuf, and A. Nuhu, "Feature Extraction Methods for Face Recognition," International journal of applied engineering research (IRAER), vol. 5, no. October, 2016.

[17] A. A. Fathima, S. Ajitha, V. Vaidehi, M. Hemalatha, R. Karthigaiveni, and R. Kumar, "Hybrid approach for face recognition combining Gabor Wavelet and Linear Discriminant Analysis," in 2015 IEEE International Conference on Computer Graphics, Vision and Information Security, CGVIS 2015, 2016. doi: 10.1109/CGVIS.2015.7449925.

[18] H. Benradi, A. Chater, and A. Lasfar, "A hybrid approach for face recognition using a convolutional neural network combined with feature extraction techniques," IAES International Journal of Artificial Intelligence, vol. 12, no. 2, pp. 627–640, Jun. 2023, doi: 10.11591/ijai.v12.i2.pp627-640.

[19] K. Dutta, D. Bhattacharjee, M. Nasipuri, and O. Krejcar, "3D Face Recognition Using a Fusion of PCA and ICA Convolution Descriptors," Neural Processing Letters, vol. 54, no. 4. Springer, pp. 3507–3527, Aug. 01, 2022. doi: 10.1007/s11063-022-10761-5.

[20] A. Ouyang, Y. Liu, S. Pei, X. Peng, M. He, and Q. Wang, "A hybrid improved kernel LDA and PNN algorithm for efficient face recognition," Neurocomputing, vol. 393, pp. 214–222, Jun. 2020, doi: 10.1016/j.neucom.2019.01.117.

[21] O. Barkan, J. Weill, L. Wolf, and H. Aronowitz, "Fast high dimensional vector multiplication face recognition," in Proceedings of the IEEE International Conference on Computer Vision, 2013. doi: 10.1109/ICCV.2013.246.

[22] F. Juefei-Xu, K. Luu, and M. Savvides, "Spartans: Single-sample periocular-based alignment-robust recognition technique applied to non-frontal scenarios," IEEE Transactions on Image Processing, vol. 24, no. 12, 2015, doi: 10.1109/TIP.2015.2468173.

[23] Y. Yan, H. Wang, and D. Suter, "Multi-subregion based correlation filter bank for robust face recognition," Pattern Recognit, vol. 47, no. 11, 2014, doi: 10.1016/j.patcog.2014.05.004.

[24] C. Ding and D. Tao, "Robust Face Recognition via Multimodal Deep Face Representation," IEEE Trans Multimedia, vol. 17, no. 11, 2015, doi: 10.1109/TMM.2015.2477042.

[25] R. Sharma and M. S. Patterh, "A new pose invariant face recognition system using PCA and ANFIS," Optik (Stuttg), vol. 126, no. 23, 2015, doi: 10.1016/j.ijleo.2015.08.205.

[26] M. Moussa, M. Hmila, and A. Douik, “A novel face recognition approach based on genetic algorithm optimization,” Studies in Informatics and Control, vol. 27, no. 1, pp. 127–134, 2018, doi: 10.24846/v27i1y201813.

[27] A. S. Mian, M. Bennamoun, and R. Owens, “An efficient multimodal 2D-3D hybrid approach to automatic face recognition,” IEEE Trans Pattern Anal Mach Intell, vol. 29, no. 11, 2007, doi: 10.1109/TPAMI.2007.1105.

[28] H. Cho, R. Roberts, B. Jung, O. Choi, and S. Moon, “An efficient hybrid face recognition algorithm using PCA and GABOR wavelets,” Int J Adv Robot Syst, vol. 11, no. 1, 2014, doi: 10.5772/58473.

[29] J. K. Sing, S. Chowdhury, D. K. Basu, and M. Nasipuri, “An improved hybrid approach to face recognition by fusing local and global discriminant features,” Int J Biom, vol. 4, no. 2, 2012, doi: 10.1504/IJBM.2012.046245.

[30] P. Kamencay, M. Zachariasova, R. Hudec, R. Jarina, M. Benco, and J. Hlubik, “A novel approach to face recognition using image segmentation based on SPCA-KNN method,” Radioengineering, vol. 22, no. 1, 2013.

[31] J. Sun, Y. Fu, S. Li, J. He, C. Xu, and L. Tan, “Sequential human activity recognition based on deep convolutional network and extreme learning machine using wearable sensors,” J Sens, vol. 2018, 2018, doi: 10.1155/2018/8580959.

Theoretical Study, Diagnostic and Biological Efficacy of Some Cyclic Pyrazoline Compounds of 5-Chloroandanone

Ibraheem Abdul Razzaq Abdullah and Khalid, A. Al-Badrany
Department of Chemistry / College of Education for Pure Sciences / Tikrit University

Theoretical Study, Diagnostic and Biological Efficacy of Some Cyclic Pyrazoline Compounds of 5-Chloroandanone

Ibraheem Abdul Razzaq Abdullah and Khalid, A. Al-Badrany
Department of Chemistry / College of Education for Pure Sciences / Tikrit University

Abstract
This research encompasses the preparatory and theoretical investigation of the computational chemistry of a series of chalcones utilizing quantum mechanics and molecular mechanics (MM2) methodologies. The investigation involves the evaluation of electronic density, total energy of the molecule, heat of formation, atomic charges, bond angles, bond lengths, and various other molecular properties. The quantum mechanics approaches employed encompass semi-empirical extended structure theory methods, including the AM1 method. Additionally, an assessment of their antibacterial activity was conducted, involving the synthesis of novel pyrazoline derivatives through the reaction of 5-chloroidanone with various benzaldehyde substitutes. The chemical identity of the synthesized compounds was established via measurements of melting point and spectroscopic techniques such as ^{1}H-NMR, ^{13}C-NMR, and FT-IR.
Keywords: Chalcones, pyrazolines, biological activity, 5-chloroidanone

1. Introduction

Heterocyclic compounds composed of five atoms, featuring two nitrogen atoms within their structure, are of interest in this study. Conversely, pyroxylene is comprised of two hydrogen atoms and possesses a double bond. Pyrrolidine, in contrast, consists of four hydrogen atoms and lacks a double bond [1, 2].

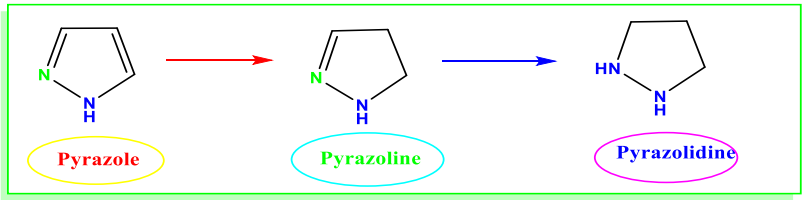

Pyrazoline and its analogues have demonstrated notable pharmacological activity across industrial, medical, pharmaceutical, and agricultural domains [3]. Furthermore, they serve as counterparts to various heterocyclic compounds such as imidazoles, thiazoles, and oxazoles. Pyrazolines, known for their stability, have incited chemists to explore structural modifications aimed at generating diverse compounds with distinct pharmacological attributes [4]. The preparation of pyrazoline involves the interaction of chalcones with hydrazine or phenylhydrazine under acidic conditions [5]. The presence of double bonds and alkyl group attachments contribute to the multiple geometries exhibited by pyrazoline [6]. Solubility variations in pyrazolines, linked to solvent polarity changes due to double bond shifts, have been investigated in the context of medicinal chemistry [7]. Notably, pyrazole derivatives have been studied since Knorr's pioneering synthesis in 1883, leading to the discovery of antipyrene and its derivatives [8]. The initial pyrazolone derivative surfaced in 1884 as a treatment for pain, inflammation, and fever, marking a significant advancement in the field. Subsequently, pyrazole derivatives have gained recognition for their efficacy as anti-inflammatory, analgesic, and antipyretic agents [9].

2. Materials and Methods

2.1. Materials Employed: All chemicals utilized in this study were procured from Fluka, Aldrich, and BDH Companies.

2.2. Instrumentation: Solids were fashioned into KBr discs and subjected to Fourier-transform infrared spectroscopy (FT-IR) analysis within the range of 400-4000 cm^-1 using a Shimadzu Infrared FT-IR-8300 instrument. Measurements were conducted at the University of Tikrit - College of Education for Pure Sciences - Department of Chemistry. In addition, proton nuclear magnetic resonance (H-NMR) and carbon-13 nuclear magnetic resonance (C13-NMR) were performed at the University of Tehran using a Bruker device and dimethyl sulfoxide (DMSO) solvent. Melting points were determined using an Electrothermal melting point apparatus. Tracking of reaction progress and product purity assessment employed 9300

fluorescently activated silica gel-G sheets (0.2mm) and various solvents, with iodine serving as revealing agent.

2.3. Preparation of Chalcone

In a 100 mL round-bottomed flask, 0.01 mol of 5-chloroidanone was dissolved in 10 mL of ethanol, followed by the addition of 10 mL of 10% NaOH solution. The mixture was stirred magnetically for 15 minutes. Subsequently, 0.01 mol of aromatic aldehyde dissolved in 10 mL of ethanol was added, and the mixture was stirred for 2-3 hours in a water bath within the temperature range of 20-40℃. Afterward, the mixture was refrigerated overnight, resulting in the appearance of a precipitate, which was then collected via filtration and recrystallized from ethanol. The progression of the reaction was monitored using thin-layer chromatography (TLC) [10, 11]. Table (1) presents selected physical properties of the synthesized compounds (IB1-IB8).

2.4. Preparation of Pyrazoline

In a round-bottomed flask with a capacity of 100 ml, equimolar quantities (0.00257 mol) of one of the chalcones were solubilized in 10 ml of ethanol. Subsequently, 0.00257 mol of hydrazine, dissolved in 5 ml of ethanol, was introduced into the solution and stirred for a duration of 10 minutes. Following this, 10 ml of a 10% sodium hydroxide solution was added to the mixture. The reaction mixture was allowed to proceed for 6-8 hours under continuous stirring. Subsequent to this reaction period, the solution was concentrated, cooled, and then gently added to crushed ice. The resulting mixture was neutralized by gradual addition of diluted hydrochloric acid (10%) until the pH reached 7. Monitoring of the reaction's progress was accomplished using thin-layer chromatography (TLC) [12, 13,14]. Physical properties of the synthesized compounds (IB9-IB16) are detailed in Table (1).

2.5. Measurement of Biological Activity

Biological activity evaluation was performed through the Agar-well diffusion method. This involved inoculating the bacterial cultures across the entire growth medium using a cotton swab. Wells were then created in the agar medium employing a sterile puncture tool with a diameter of 6 mm. Subsequently, 100 microliters of each compound were placed within these wells on separate culture plates, each harboring a distinct bacterial strain. This process was replicated across all prepared solutions, encompassing their respective concentrations and targeted bacterial strains under study. The antibacterial activity assessment was conducted on two distinct bacterial types: the gram-positive Staphylococcus citrus and the gram-negative E. coli. To ensure the effectiveness of the test, both bacterial species were initially re-cultivated and subsequently incubated in a controlled laboratory environment at 37°C for a duration of 18-24 hours. This incubation period facilitated the preparation of bacterial inoculums with a concentration of 1.5×10^8 bacterial cells per ml, calibrated against the McFarland standard set at an optical density of 0.5 [15, 16].

3. Results and Discussion

This investigation encompassed several key aspects. Firstly, the reaction involving chalcones and various reagents was undertaken to synthesize a series of heterocyclic compounds featuring pyrazoline rings. The identification of the synthesized compounds was accomplished through spectroscopic techniques, specifically Fourier-transform infrared spectroscopy (FT-IR) and proton and carbon nuclear magnetic resonance (^{1}H,^{13}C-NMR) spectroscopy. In addition, thin-layer chromatography (TLC) was employed to verify the formation of the prepared compounds. The study further delved into the biological activity of the synthesized compounds against two distinct bacterial strains, each yielding diverse responses based on their unique biological profiles.

3.1. Characterization of chalcones

The utilization of 5-chloroanedanone alongside different aromatic aldehydes in an alkaline medium (NaOH 10%) served as the foundation for generating varied chalcones and their subsequent ring structures.

Upon analysis of the FT-IR spectrum of the chalcones, distinct absorption bands were observed, such as the absorption at 3026 cm^{-1} linked to the aromatic (CH) bond stretching [17, 18]. A noticeable reduction in the frequency of the carbonyl group (C=O) of ketones was evidenced at 1696 cm^{-1}, indicating its interaction with the double bond, manifesting at 1598 cm^{-1} [19]. Moreover, absorption bands appeared at 1492 cm^{-1} and

1415 cm^{-1}, corresponding to the aromatic bond (C=C). Comparable results were found in literature references [20, 21], as in Figure (1).

When studying the 1H-NMR spectrum of compound [IB1] using DMSO-d^6 as the solvent, signals at 4.14 ppm were attributed to the (-CH_2) group adjacent to the benzene ring [22, 23], while signals at 7.12 ppm were attributed to the (β-CH) group [24, 25]. Multiple signals ranging from 7.29 to 7.92 ppm denoted the protons of the aromatic rings, and a signal at 2.49 ppm was assigned to solvent protons (DMSO-d^6) [26, 27], as in Figure (2).

Likewise, the ^{13}C-NMR spectrum of compound [IB1] showcased signals at 192.09 ppm carbonyl group, 32.47 ppm (CH_2) group adjacent to the benzene ring [28, 29], and (136.60-126.52) ppm carbons of the aromatic ring [30, 31]. Signals at 39.97-40.48 ppm were attributed to the DMSO solvent carbon, aligning closely with the literature [32, 33], as in Figure (3).

3.2. Characterization of pyrazoline

Similarly, the FT-IR spectrum of pyrazoline compounds exhibited characteristic absorption bands: C=N bond stretching at 1606-1690 cm^{-1} and N-H bond stretching at (3380-3310) cm^{-1} [34]. The spectrum also displayed bands indicative of aromatic bond (C=C) stretching at (1530-1591) cm^{-1} and (1406-1506) cm^{-1} [34]. Other features, such as aromatic (Ar-H) bond stretching, were observed within specific ranges. These results mirrored prior findings [35, 36], as illustrated in Figure (4).

3.3. Biological Activity of preparation compounds

Moving to the biological assessment, the results from the inhibition zone measurements were tabulated Table (3). Notably effective solutions were identified, such as (6, 3, and 2), showcasing efficacy against both types of bacterial species [37, 38]. The potency of the compounds diminished with lower concentrations, with the concentrated solution displaying higher effectiveness [39, 40]. In general, inhibition zones varied from 10 mm to 31 mm. Compounds lacking effectiveness were indicated as "niz" denoting the absence of inhibition zones [41].

3.4. Theoretical Study

Theoretical calculations were performed using Chem Office 12.0 software, which facilitated the determination of key engineering and physical properties for newly prepared chalcones [42]. This encompassed bond lengths, atom angle measurements, atom charges, as well as various energy variables, including LUMO, HOMO, ημ, and W. The AM1 method was utilized [43].

$\eta=1/2\ (E._{HOMO} + E._{LOMO})$……(1) $\mu=1/2\ (E._{LUMO} - E._{HOMO})$…....(2) $w= \mu 2/2\eta$ …….(3)

Upon examination of Table 6, it's evident that compounds compensated with electron-withdrawing groups, like (1, 8, 5), exhibited higher HOMO energies compared to those compensated with electron-donating groups such as (4, 6, 7). Compound (2) presented notably high values due to its NO_2 group, indicating its electrophilic behavior. These energetic relationships between HOMO and LUMO suggest enhanced electron transition processes [44, 45]. The presence of withdrawal groups effectively reduces the energy gap and increases compound stability [46].

The second set of effects, influenced by steric interactions like Van der Waals forces (attractive or repulsive) and hydrogen bonding, played a role in determining molecular stability. Various theoretical parameters were evaluated in this context, including bond lengths (C=C, C-C), atom angles (C=C-C), overlap energies (1.4 VDW and Non-1.4 VDW), heat of formation (Hf), and various energies (Stretch-Bend, Torsion, Dip-Dip, TE) [47, 48]. Notably, the steric hindrance effect was prominent in compound (IB5), as indicated by its increased 1.4 VDW and TE values. Steric hindrance led to elevated compound energy, resulting in decreased stability [49].

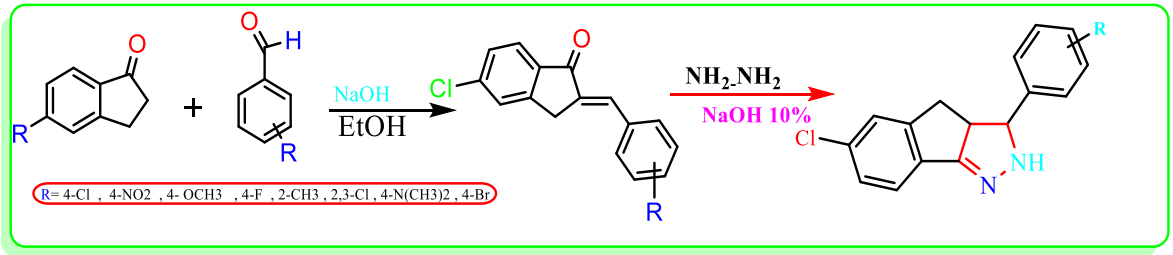

Scheme (1): Route of prepared compounds (IB_1-IB_{16})

Table (1): Physical properties of the prepared compounds (IB_1-IB_{16})

Comp.	R	Molecular formula	m.p. °C	Yield %	Color
IB_1	4-Cl	$C_{16}H_{12}Cl_2O$	208-210	72	**off white**
IB_2	4-NO_2	$C_{16}H_{10}ClNO_3$	211-209	80	**Dark brown**
IB_4	4-F	$C_{16}H_{10}ClFO$	207-205	68	**Off whit**
IB_3	4-OCH_3	$C_{17}H_{13}ClO_2$	175-173	60	**Light White**
IB_5	2,3-Cl	$C_{16}H_9Cl_3O$	192-190	83	**Whit**
IB_6	2-CH3	$C_{17}H_{13}ClO$	185-187	65	**Light White**
IB_7	4-$N(CH_3)_2$	$C_{18}H_{16}ClNO$	198-200	62	**orange**
IB_8	4-Br	$C_{16}H_{10}BrClO$	220-222	75	**Light White**
IB_9	4-Cl	$C_{16}H_{12}Cl_2N_2$	177-178	70	**white**
IB_{10}	4-NO_2	$C_{16}H_{12}ClN_3O_2$	182-180	78	**Black**
IB_{11}	4-F	$C_{16}H_{12}ClFN_2$	163-161	67	**Yellow**
IB_{12}	4-OCH_3	$C_{17}H_{15}ClN_2O$	150-148	53	**brown**
IB_{13}	2,3-Cl	$C_{16}H_{11}Cl_3N_2$	177-175	75	**Yellow**
IB_{14}	2-CH3	$C_{17}H_{15}ClN_2$	164-166	61	**Light yellow**
IB_{15}	4-$N(CH_3)_2$	$C_{18}H_{16}ClN_3$	175-177	57	**Light orange**
IB_{16}	4-Br	$C_{16}H_{12}BrClN_2$	189-190	71	**White**

Table (2): FT-IR (cm^{-1}) absorption results for chalcone derivatives [IB1-IB8]

Comp. No.	R	ν(C-H) Arom.	ν(C-H) Aliph.	ν(C=C) Olphen	ν(C=O) ν(C-Cl)	ν(C=C) Arom.	Others
IB_1	Cl	3026	2908, 2837	1598	1695, 813	1492, 1415	-----
IB_2	NO_2	3066	2937, 2802	1595	1708, 846	1454, 1421	**ν(N-O) 1344**
IB_4	F	3050	2927, 2810	1598	1697, 821	1465, 1419	**ν(C-F) 952**
IB_3	OCH_3	3058	2920, 2839	1600	1693, 815	1510, 1461	**ν(C-O) 1253**
IB_5	2,3-Cl	3065	2960, 2805	1596	1700, 827	1454, 1421	-----
IB_6	2-CH3	3062	2968, 2813	1596	1708, 875	1487, 1461	**ν(C-Cl) 738**
IB_7	4-$N(CH_3)_2$	3075	2910, 2862	1587	1679, 810	1523, 1429	**ν(C-N) 1311**
IB_8	4-Br	3062	2921, 2846	1596	1693, 813	1488, 1413	**ν (C-Br) 667**
Comp. No.	**R**	**ν(C-H) Arom.**	**ν(N-H)**	**ν(C=N)**	**ν(N-N) ν(C-Cl)**	**ν(C=C) Arom.**	**Others**
IB_9	Cl	3062	3332	1611	1030, 812	1591, 1515	-----
IB_{10}	NO_2	3070	3324	1633	1042, 815	1577, 1510	**ν (N-O) 1337**
IB_{11}	F	3028	3338	1606	1093, 835	1506, 1406	**ν (C-F) 954**
IB_{12}	OCH_3	3048	3352	1608	1071, 819	1591, 1475	**ν (C-O) 1295**
IB_{13}	2,3-Cl	3066	3310	1654	1052, 864	1588, 1466	-----
IB_{14}	2-CH3	3058	3377	1690	1100, 870	1530, 1467	-----
IB_{15}	4-$N(CH_3)_2$	3043	3365	1625	1097, 815	1557, 1415	**ν (C-N) 1317**
IB_{16}	**4-Br**	**3064**	**3380**	**1606**	**1085, 819**	**1580, 1479**	**ν (C-Br) 678**

Table (3): Result of the biological activity test of the selected compounds

E. coli			*S. citrus*			Bacteria/ number
10^{-3}	10^{-2}	10^{-1}	10^{-3}	10^{-2}	10^{-1}	IB9
12	16	20	10	14	17	IB10
16	17	26	13	19	26	IB11
0	0	11			niz	IB12
		niz			niz	IB13

16	17	28	12	13	15	IB14
		niz			niz	IB15
0	0	11			niz	IB16

*NIZ (No Inhibition Zone)

Table (4): Theoretically calculated energy variables for chalcones using the (MM2) method

Comp.	E Stretch	E Bend	E Stretch-Bend	E Torsion	E Non-1,4 VDW	E 1,4 VDW	E Dipole/Dipole	TE (kcal/mol)
1	1.002	10.3813	0.0384	-11.0449	0.1854	14.9143	-0.4074	15.0683
2	1.0958	11.1425	0.0448	-11.0655	1.3804	16.7556	-0.2623	17.1918
3	0.9701	10.3255	0.0235	-11.0856	0.2826	14.3851	-0.4080	14.4931
4	1.2056	12.7607	0.0846	-11.0644	0.6786	17.2172	-0.4584	20.4238
5	2.0178	17.3784	0.2207	-11.6040	3.0533	18.5299	1.9032	31.4994
6	1.5992	15.5491	0.1029	-6.9033	1.6604	16.2997	-0.4513	27.8567
7	1.4195	15.3926	0.3392	-13.1270	3.1812	18.0255	-0.5396	24.6913
8	1.0042	10.4450	0.0475	-11.0289	0.1202	15.0733	-0.4122	15.2490

Table (5): Theoretically computed values of the physical variables for the bases of chalcones using method (AM1)

Comp.	Charge (Coulomb)			Bond Length (Å)		Angle (Degree)	H_f
	C1	C2	C3	C═C	C—C	C1C21C3	(Kcal/Mol)
1	-0.1797	-0.044	-0.0585	1.340	1.450	131.1	23.0389
2	-0.1543	-0.0693	-0.0393	1.340	1.450	131.1	34.4711
3	-0.1829	-0.0407	-0.074	1.340	1.448	131.0	-15.1673
4	-0.1954	-0.0279	-0.0991	1.341	1.447	131.3	-8.3085
5	-0.1529	-0.0618	-0.0275	1.339	1.455	138.5	27.0839
6	-0.181	-0.0385	-0.0586	1.340	1.457	131.8	27.2942
7	-0.2091	-0.014	0.1273	1.342	1.444	131.3	38.2252
8	-0.1759	0.0473	0.0454	1.340	1.450	130.5	35.0667

Table (6): Theoretically calculated values of energy variables for chalcones using (AM1)

Comp.	HOMO (eV)	LUMO (eV)	Ƞ (eV)	μ (eV)	ω (eV)	Δ(L-H) (eV)
1	-0.3465	-0.0486	0.148	-0.197	0.131	0.297
2	-0.3749	-0.0953	0.139	-0.235	0.198	0.279
3	-0.3444	-0.0471	0.148	-0.192	0.124	0.297
4	-0.3324	-0.0398	0.144	-0.186	0.120	0.292
5	-0.3513	-0.0524	0.146	-0.201	0.138	0.298
6	-0.3409	-0.0403	0.15	-0.190	0.120	0.300
7	-0.3008	-0.0267	0.137	-0.163	0.096	0.274
8	-0.3477	-0.0502	0.148	-0.198	0.132	0.297

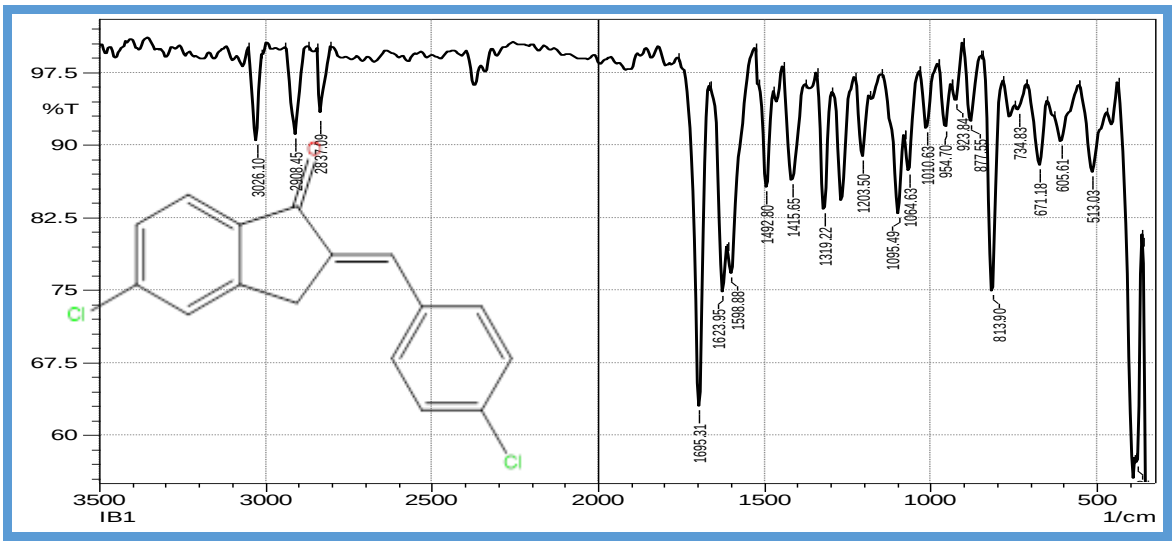

Figure (1): FT-IR spectrum of compound (IB1)

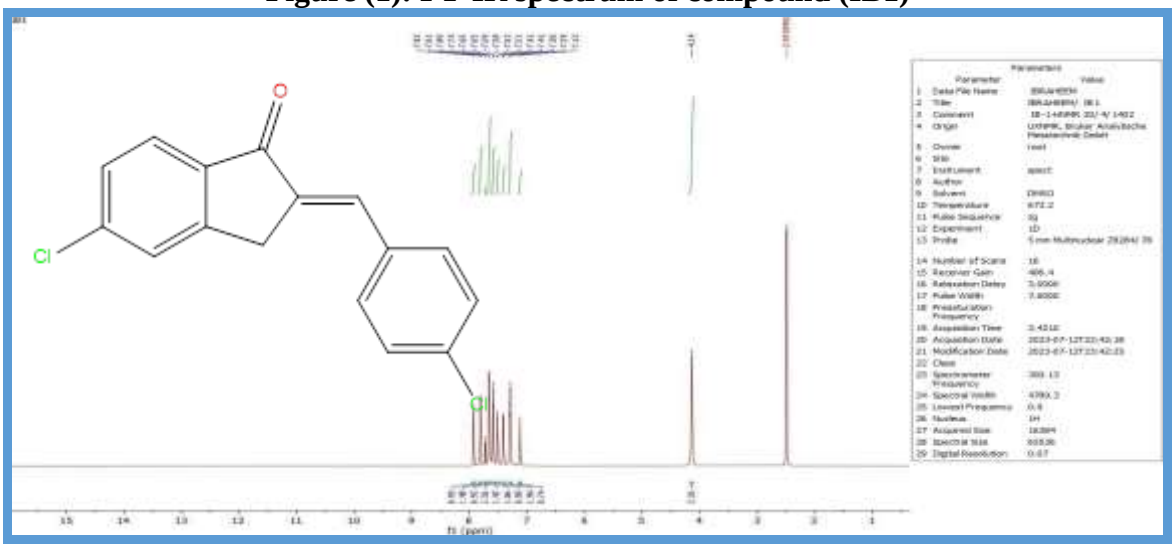

Figure (2): ^{1}H-NMR of (IB1)

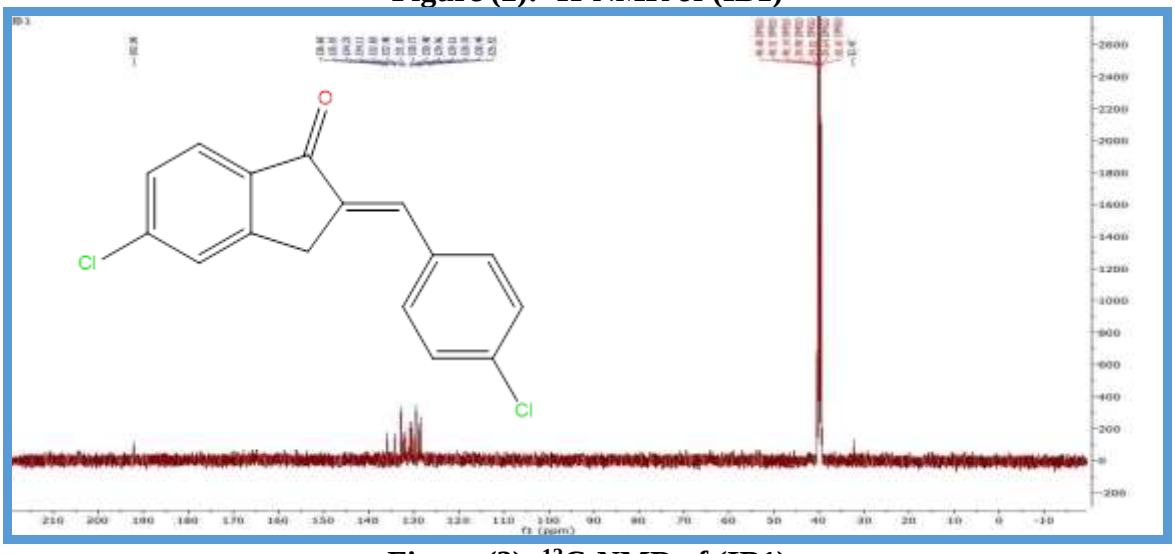

Figure (3): ^{13}C-NMR of (IB1)

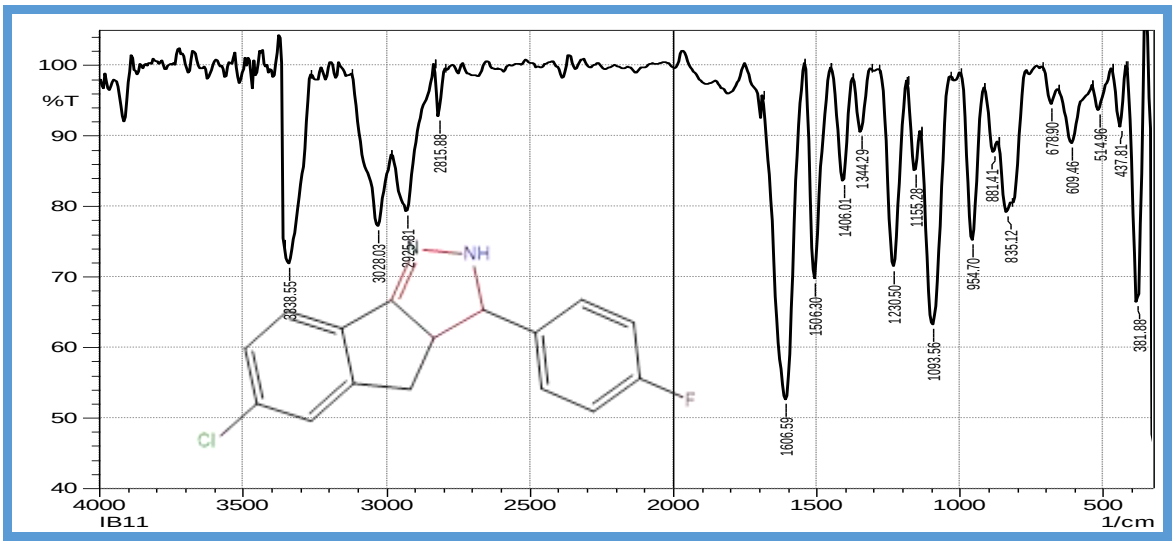

Figure (4): FT-IR of (IB11)

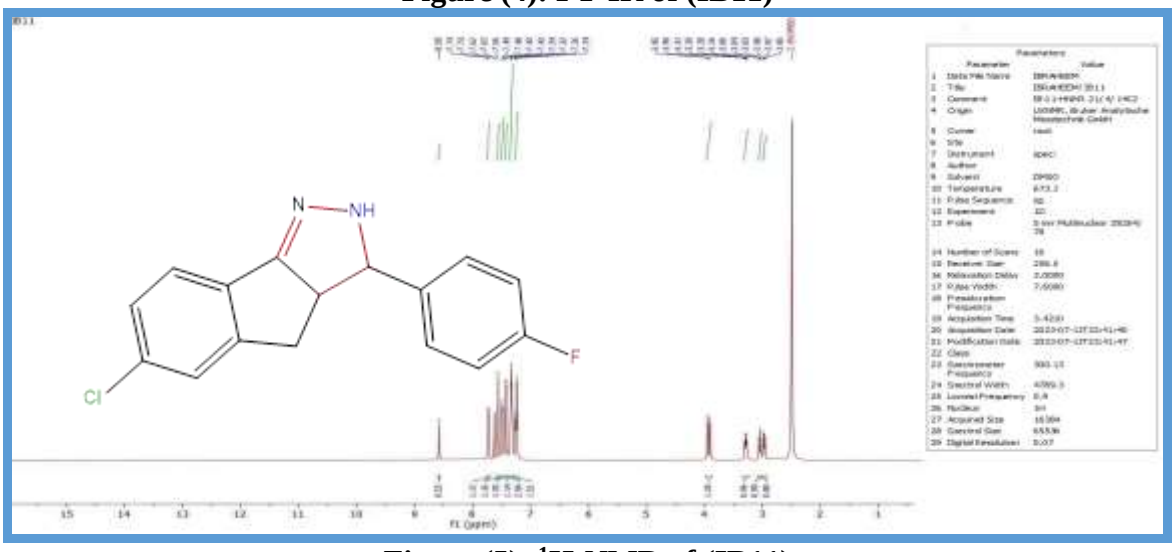

Figure (5): ^{1}H-NMR of (IB11)

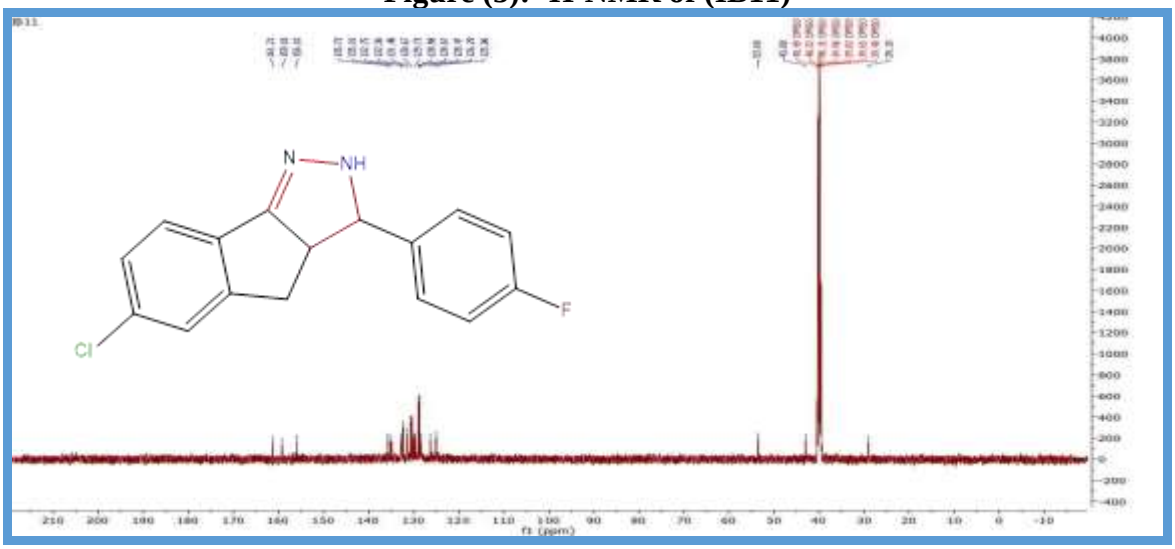

Figure (6): ^{13}C-NMR of (IB11)

4. Conclusions: High product percentages can be obtained from fresh chalcones by stirring in a 10% alkaline medium. By using chalcone as a raw material for the preparation of heterocyclic rings, a good proportion of the product was obtained, and the method is simple and easy, and the product can be obtained directly. Some of the prepared compounds showed moderate activity against the tested bacteria. The theoretical results obtained using quantum mechanics methods for chalcone compounds were

consistent with the practical part in terms of product percentage, where the compounds substituted with withdrawn groups showed more product percentage than the groups compensated with electrons pushing groups..

References:

1. Kumar, K. A., & Jayaroopa, P. (2013). Pyrazoles: synthetic strategies and their pharmaceutical applications-an overview. *International Journal of PharmTech Research*, *5*(4), 1473-1486.
2. Xu, Z., Zhuang, Y., & Chen, Q. (2023). Current scenario of pyrazole hybrids with in vivo therapeutic potential against cancers. *European Journal of Medicinal Chemistry*, 115495.
3. Singh, P., Singh, J., Pant, G. J., & Rawat, M. S. (2018). 2-Pyrazolines as biologically active and fluorescent agents, an overview. *Anti-Cancer Agents in Medicinal Chemistry (Formerly Current Medicinal Chemistry-Anti-Cancer Agents)*, *18*(10), 1366-1385.
4. Bennani, F. E., Doudach, L., Cherrah, Y., Ramli, Y., Karrouchi, K., & Faouzi, M. E. A. (2020). Overview of recent developments of pyrazole derivatives as an anticancer agent in different cell line. *Bioorganic Chemistry*, *97*, 103470.
5. Matiadis, D., & Sagnou, M. (2020). Pyrazoline hybrids as promising anticancer agents: An up-to-date overview. *International Journal of Molecular Sciences*, *21*(15), 5507.
6. Küçükgüzel, Ş. G., & Şenkardeş, S. (2015). Recent advances in bioactive pyrazoles. *European Journal of Medicinal Chemistry*, *97*, 786-815.
7. Sadeek, G. T., Saeed, Z. F., & Saleh, M. Y. (2023). Synthesis and Pharmacological Profile of Hydrazide Compounds. *Research Journal of Pharmacy and Technology*, *16*(2), 975-982
8. Chang, Jing, et al. "A Comprehensive Investigation of Hydrazide and Its Derived Structures in the Agricultural Fungicidal Field." *Journal of Agricultural and Food Chemistry* (2023).
9. Kumar, Rajnish, et al. "Synthetic Approaches, Biological Activities, and Structure–Activity Relationship of Pyrazolines and Related Derivatives." Topics in Current Chemistry ", vol.381, No.3, p.381,2023
10. Saleh, M. J., & Al-Badrany, K. A. (2023). Preparation, Characterization of New 2-Oxo Pyran Derivatives by AL2O3-OK Solid Base Catalyst and Biological Activity Evaluation. *Central Asian Journal of Medical and Natural Science*, *4*(4), 222-230.
11. Al-Bayati, R. I. (2013). Synthesis of New Chalcones and Pyrazoles Derived from Dehydroacetic Acid. *Al-Mustansiriyah Journal of Science*, *24*(2).
12. Mohamed, S. A., Hussein, M. S., & Al-badrany, K. A. (2022). Synthesis and characterization of pyrazolines and oxazapine derivatives using chalcones as precursor and evaluation of their biological activity. *Samarra Journal of Pure and Applied Science*, *4*(4).
13. Yaseen, Lina A., and Hanoy K. Al-Amood. "Preparation, Characterization, and Study of Antibacterial some new Pyrazole Derivatives." *JOURNAL OF KUFA FOR CHEMICAL SCIENCES* ", vol.**2**, No.9,2022
14. Ahsan, Mohamed Jawed, et al. "Pyrazoline Containing Compounds as Therapeutic Targets for Neurodegenerative Disorders." *ACS omega* ", vol.**7**, No.43, p.38207-38245,2022
15. Balouiri, M., Sadiki, M., & Ibnsouda, S. K. (2016). Methods for in vitro evaluating antimicrobial activity: A review. *Journal of pharmaceutical analysis*, *6*(2), 71-79.
16. Alam, Md Jahangir, et al. "A review on pyrazole chemical entity and biological activity." *Int. J. Pharm. Sci. Res* ", vol.**6**, p.1433-1442,2015
17. Ahmad, A., Sinha, R. K., Kulkarni, S. D., Lewis, P. M., Bhat, P., & Shetty, N. S. (2023). Synthesis, photophysical properties and DFT studies of chalcones and their 2-methoxy-3-cyanopyridine derivatives. *Journal of Photochemistry and Photobiology A: Chemistry*, *437*, 114494.
18. Hassan, T. G., & Omar, A. O. (2023). Synthesis, Characterization of some new Heterocyclic Compounds Derived from Chalcones Containing Schiff Bases. *Synthesis*, *32*(1), 127-137.
19. de Farias, I. F., de Oliveira Gonçalves, R., de Freitas, M. D., da Silva, F. L., de Sousa, A. F., Trevisan, M. T. S., & de Lemos, T. L. G. (2023). Synthesis, characterization and molecular docking study of pyrazolines synthesized from chalcones: Antioxidant and acetylcholinesterase activities. *Journal of Molecular Structure*, *1291*, 135961.
20. Atiya, R. N., Salih, N. A., & Adam, R. W. (2022). Preparation with Biological Study for Pyrimidine Derivatives from Chalcone. *Int J Drug Deliv Technol*, *12*(1), 174-9.
21. Yaseen, Lina A., and Hanoy K. Al-Amood. "Preparation, Characterization, and Study of Antibacterial some new Pyrazole Derivatives." JOURNAL OF KUFA FOR CHEMICAL SCIENCES ," vol.2, No.9,2022
22. Fakhry, Mariam M., et al. "Rational Design, Synthesis and Biological Evaluation of Novel Pyrazoline-Based Antiproliferative Agents in MCF-7 Cancer Cells." Pharmaceuticals ", vol.15, No.10, p.1245,2022.
23. Özdemir, Zuhal, et al. "Synthesis and studies on antidepressant and anticonvulsant activities of some 3-(2-furyl)-pyrazoline derivatives." European journal of medicinal chemistry" ,vol.42, No.32, p.373-379,2007
24. Chouiter, Mohamed I., et al. "New chalcone-type compounds and 2-pyrazoline derivatives: Synthesis and caspase-dependent anticancer activity." *Future Medicinal Chemistry* ", vol.**12**, No.6, p.493-509,2020

25. Bhirud, Jayashri D., Rajendra D. Patil, and Hemant P. Narkhede. "Sulfamic acid catalyzed synthesis of new 3, 5-[(sub) phenyl]-1H-pyrazole bearing N1-isonicotinoyl: And their pharmacological activity evaluation." Bioorganic & Medicinal Chemistry Letters," vol.30, No.23, p.127-558,2020.
26. Ahmad, Aftab, et al. "Synthesis, antimicrobial and antitubercular activities of some novel pyrazoline derivatives." *Journal of Saudi Chemical Society* ", vol.**20**, No.5, p.577-584,2016
27. Mohamed, Shifaa A., Khalid A. Al-Badrany, and Maha S. Huseen. "PREPARATION AND STUDY OF BIOLOGICAL ACTIVITY OF PYRIMIDINE COMPOUNDS DERIVED FROM 2-ACETYLPYRIDINE." Vegueta. Anuario de la Facultad de Geografía e Historia ," vol.22, p.8,2022.
28. Saleh, Jamil Nadhem, and A. Khalid. "Synthesis, Characterization and Biological Activity Evaluation of Some New Pyrimidine Derivatives by Solid Base Catalyst AL2O3-OBa." *Central Asian Journal of Medical and Natural Science* 4.4 (2023): 231-239.
29. Elkanzi, Nadia AA, et al. "Synthesis, in vitro evaluation and molecular docking of new pyrazole derivatives bearing 1, 5, 10, 10a-tetrahydrobenzo [g] quinoline-3-carbonitrile moiety as potent antibacterial agents." Journal of the Iranian Chemical Society ," vol.18, p.977-991,2021.
30. Ahsan, Mohamed Jawed, et al. "Pyrazoline Containing Compounds as Therapeutic Targets for Neurodegenerative Disorders." *ACS omega* ", vol.**7**, No.43, p.38207-38245,2022
31. Kumari, Simpal, Sarvesh K. Paliwal, and Rajani Chauhan. "An improved protocol for the synthesis of chalcones containing pyrazole with potential antimicrobial and antioxidant activity." *Current Bioactive Compounds* ", vol.**14**, No.1, p.39-47,2018
32. Al-Saheb, Rawan, et al. "Synthesis of new pyrazolone and pyrazole-based adamantyl chalcones and antimicrobial activity." *Bioscience reports* ", vol.**40**, No.9, 2020.
33. Hamd, Amera H., and Naeemah Al-Lami. "Anti-Breast Cancer Activity of Some Synthesized Pyrazole Derivatives Bearing Imidazo [1, 2a] pyridine Moiety." *Iraqi Journal of Science* (2023): 4105-4117.
34. Zhang, Yan-min-zi, et al. "Synthesis and characterization of a chalcone-derived epoxy containing pyrazoline ring with excellent flame resistance." *High Performance Polymers* 33.7 (2021): 785-796.
35. Al-Mosawi, Suha K., Hanan A. Al-Hazam, and Abbas F. Abbas. "Microwave Assisted Synthesis, Characterization and Biological Study of Some Chalcone Compounds Derived from Phenyl Isothiocyanate." (2019).
36. Dharani, S., et al. "C–H activation and subsequent C–C bond formation in rigid alkenes catalyzed by Ru (iii) metallates." *Reaction Chemistry & Engineering* 8.1 (2023): 164-174.
37. Gonelimali, F. D., Lin, J., Miao, W., Xuan, J., Charles, F., Chen, M., & Hatab, S. R. (2018). Antimicrobial properties and mechanism of action of some plant extracts against food pathogens and spoilage microorganisms. *Frontiers in microbiology*, *9*, 1639.
38. Laxminarayana, Vanaparti, Megha Balha, and Ramana Tamminana. "Preparation of novel pyrazole substituted triazole libraries and estimation of their biological activity." *ChemistrySelect* vol.**8**, No.22,2023.
39. Hassan, Tharee Gh, and Adnan O. Omar. "Synthesis, Characterization of some new Heterocyclic Compounds Derived from Chalcones Containing Schiff Bases." *Synthesis* ", vol.**32**, No.1, p.127-137,2023
40. Al-Tufah, Mohammad M., et al. "Synthesis, Characterization of Ethyl Dioxoisoindolinyl Cyclohexenone Carboxylate Derivatives from Some Chalcones and its Biological Activity Assessment." (2023).
41. Kanaan, Shaymaa, and Tagreed NA Omar. "Synthesis and Preliminary Pharmacological Evaluation of New Pyrazoline Derive from Different Heterocyclic Aldehydes." *Journal of Population Therapeutics and Clinical Pharmacology* ", vol.**30**, No.14, p.311-318,2023.
42. Barua, N., Sarmah, P., Hussain, I., Deka, R. C., & Buragohain, A. K. (2012). DFT-based QSAR Models to Predict the Antimycobacterial Activity of Chalcones. *Chemical Biology & Drug Design*, *79*(4), 553-559.
43. Baig, H., Iqbal, A., Rasool, A., Hussain, S. Z., Iqbal, J., Alazmi, M., & Saleem, R. S. Z. (2023). Synthesis and Photophysical, Electrochemical, and DFT Studies of Piperidyl and Pyrrolidinyl Chalcones. *ACS omega*.
44. Priya, M. K., Jonathan, D. R., Muthu, S., Shirmila, D. A., Hemalatha, J., & Usha, G. (2022). Structural examination, theoretical calculations, and pharmaceutical scanning of a new tetralone based chalcone derivative. *Journal of Molecular Structure*, *1253*, 132296.
45. Vadivoo, Velayutham Shanmuga, et al. "Computational and spectral discussion of some substituted chalcone derivatives." *Biointerface Res. Appl. Chem* 12 (2022): 7159-7176..
46. Farooq, Saba, et al. "In vitro Cytotoxic Activities, Molecular Docking and Density Functional Theory (DFT) Evaluation of Chalcone Derived Pyrazolines." *Chemistry Africa* ", vol.**5**, No.2, p.227-236,2022
47. . Vadivoo, Velayutham Shanmuga, et al. "Computational and spectral discussion of some substituted chalcone derivatives." *Biointerface Res. Appl. Chem* ", vol.**12**, p.7159-7176,2022.
48. Farooq, Saba, et al. "Microwave Assisted Synthesis and Antimicrobial Activities of Carboxylpyrazoline Derivatives: Molecular Docking and DFT Influence in Bioisosteric Replacement." *Polycyclic Aromatic Compounds* 42.8 (2022): 5422-5435.

49. Farooq, Saba, and Zainab Ngaini. "Synthesis of Benzalacetophenone-based Isoxazoline and Isoxazole Derivatives." *Current Organic Chemistry* ", vol.**26**, No.7, p.679-692,2022

اعادة تدوير للمخلفات النباتية

واستخدامها كسماد للنباتات

1- ا.م.د. افراح طعمه خلف جامعة سامراء/ كلية التربية

Afrah Toma Kalf AL Badry

University of Samarra / College of Education

afrah.t@uosamarra.edu.iq

2- م.م. ماردين علي عباس فتاح جامعة سامراء/ كلية التربية

Mardin Ali Abbas Fattah

University of Samarra / College of Education

Mardeen.a@uosamarra.edu.iq

3- م.م. مروان عبد الرزاق كامل الجامعة التقنية الشمالية / المعهد التقني الدور

Marwan Abdulrazzaq Kamil

Northern Technical University / Technical Institutes Al-Dour

Marwan.kamil@ntu.edu.iq

اعادة تدوير للمخلفات النباتية واستخدامها كسماد للنباتات

ا.م.د. افراح طعمه خلف جامعة سامراء/ كلية التربية

م.م. ماردين علي عباس فتاح جامعة سامراء/ كلية التربية

م.م. مروان عبد الرزاق كامل الجامعة التقنية الشمالية / المعهد التقني الدور

Recycling of vegetable waste and using it as fertilizer for plants

Afrah Toma Kalf AL Badry

University of Samarra / College of Education

afrah.t@uosamarra.edu.iq

Mardin Ali Abbas Fattah

University of Samarra / College of Education

Mardeen.a@uosamarra.edu.iq

Marwan Abdulrazzaq Kamil

Technical Institutes Al-Dour/Northern Technical University

Marwan.kamil@ntu.edu.iq

الخلاصة

اجريت الدراسة في جامعة سامراء/ كلية التربية–قسم علوم الحياة لغرض اعادة تدوير المتبقيات النباتية وتحويلها الى سماد عضوي، اذ جُمعت مخلفات النباتات من حدائق الجامعة بواسطة اكياس وتضمنت بقايا الاوراق المتساقطة بمختلف الانواع، ثم فُرزت لإبعاد الأجزاء الغير نباتية من بلاستك وغيرها.

أظهرت نتائج الدراسة ان السماد كان ذا كفاءة جيدة، مع حصول تغيرات عند البعض من صفاته الفيزيائية والكيمائية للمدة من تشرين الثاني 2022, ولغاية شهر شباط 2023، إذ سجلت تذبذبات في الاس الهيدروجيني تراوحت بين–6.5 3.5، بينما تباينت قيم التوصيلية الكهربائية ما بين 2.5–4 مايكروسيمنز/سم، في حين قيم المادة العضوية كانت –23.5 20.1%, والرطوبة تراوحت 70.5–76.4%، وسجلت نسبة N:C قيماً تراوحت ما بين 8.44–16.5. في حين سجل النتروجين نتائج ما بين 1.4–4.33%, والفسفور سجل 0.12–1.3 %.

من خلال النتائج تبين ان كفاءة الحوض في اعادة التدوير للمتبقيات النباتية جيدة فضلاً عن كونه سهل الاستخدام وغير مكلف.

الكلمات المفتاحية: اعادة تدوير، مخلفات النباتات، سماد عضوي، بلاستك، بقايا الاوراق.

Abstract

The study was conducted at Samarra University-College of Education- Department of Life Sciences for the purpose of recycling plant residues and converting them into organic fertilizer**.**

The results of the study showed that the fertilizer was of good efficiency, with changes occurring in some of its physical and chemical characteristics for the period from November 2022 to February 2023, as fluctuations were recorded in the pH ranged between 3.5-6.5, while the electrical conductivity values varied between 4-2.5 microsiemens/cm, while the organic matter values were 23.5-20.1%, the humidity ranged from 70.5-76.4%, and the N:C ratio recorded values ranging between 8.44-16.5. While nitrogen recorded results between 1.4-4.33%, and phosphorous recorded 0.12-1.3%.

Through the results, it was found that the basin's efficiency in recycling plant residues is good, in addition to being easy to use and inexpensive.

Keywords: recycling, plant waste, organic fertilizer, plastic, leaf residue.

المقدمة **introduction**

الأنشطة البشرية لها تأثير سلبي على البيئة، اذ تعد سبب لتلوث المياه، والهواء، والتربة. وبالرغم من تحقيق الثورة الصناعية نجاحاً كبيراً، إلا أنها اضافت إنتاجات هائلة من الملوثات المنبعثة للهواء والتي تكون مضرة بصحة الإنسان (WHO,2019). وقد ادت التغيرات الحاصلة بالمناخ وكذلك آثار الاحترار العالمي تأثيرات بشكال متعددة على النظم البيئية، والذي قد يتسبب بمشاكل عديدة منها سلامة الأغذية، ذوبان الجليد، وقد تنقرض بعض الحيوانات، وإلحاق اضرار بالعديد من النباتات (Marlon *et al*.,2019).

تولد مواد النفايات تأثيرًا بيئيًا، حيث إنها تتجمع عادةً في ست مجموعات خطيرة، وتكوين مواد كيميائية ضوئية والأكسدة، والاحتباس الحراري، وتعزيز الانشطة الطبيعية الناتجة عن تأثير تغير المناخ، واستنفاد الموارد اللا أحيائية، والتحمض، والتغذية، يمكن أن تؤثر مثل هذه المشكلات الرئيسية المتنوعة ذات الصلة بالمكونات على مراحل إعادة التدوير وتؤدي إلى الضغط في الحفاظ على البيئة الطبيعية (2019, **Ahmed** &Ali)

تمثل عملية إعادة التدوير معالجة المواد الملوثة، وفيها تعاد المواد الملوثة الي الشكل الخام تدريجيا وبالإمكان تصنيعها مرة أخرى, وتعتمد عملية إعادة التدوير على نوع النفايات، اذ ان بعضها لا يمكن استخدامها بشكل مباشر, كأعاده تدوير الأوراق المستخدمة لعمل مغلفات وملفات وبطاقات تهنئة وما إلى ذلك, يمكن الحصول على الطاقة بعملية اعادة التدوير عن طريق الانحلال الحراري، وهي العملية التي يتم فيها احتراق النفايات بدون أكسجين لتوليد سوائل وغازات ومركبات كثيفة (Recycling,2019) .ولقد ركزت العديد من الدراسات المتعلقة بمؤشرات جودة التربة بشكل أساسي على الخصائص الفيزيائية والكيميائية للتربة واستخدمت لنمو النبات (Zhao et al, 2021) .

يعد الكربون العضوي (SOC) في التربة احد مركباته الاساسية للزراعة, اذ يتمتع بأهمية أساسية للتخفيف من ظاهرة الاحتباس الحراري, وان أي انخفاض في نسبته تؤدي الى تأثيرات كبيرة على تركيز ثاني أكسيد الكربون في الغلاف الجوي (Matschullat et al.,2018). وان

مصدر الكربون العضوي النموذجي هو استخدام المواد الدبالية، والتي يمكن استخدامها في الأراضي الزراعية لتعزيز نمو النبات والقدرة على الاحتفاظ بالمياه وكذلك لخصائصها المبيدة للجراثيم والفطريات (Kanmaz,2019).

اذ ان الآثار الضارة للتخصيب الكيميائي المفرط تتضمن في التغذية السريعة للنباتات، وتلويث الموارد المائية سواء كانت سطحية او جوفية(Liang et al.,2013), وانبعاثات غازات الاحتباس الحراري(Zhu *et al*.,2019), ويمكن للتغييرات في نسبة الكربون / النيتروجين (C/N) تعديل التنوع الميكروبي في التربة بشكل ملحوظ (Sepehri & Sarrafzadeh,2019). ولقد بدأ استخدام الأسمدة العضوية والمعدنية، بشكل رئيسي من خلال إعادة تدوير مخلفات المحاصيل أو السماد الطبيعي أو غيرها من الكتل الحيوية، اذ يعد تطوير واستخدام الأسمدة العضوية والتي لا تعتمد على توافر الموارد المعدنية أو العمليات كثيفة الاستهلاك للطاقة واستنادًا إلى استخدام المواد المتجددة بمثابة تقدم كبير نحو الاقتصاد الدائري الذي يعيد دمج النفايات في دورة الإنتاج (Paungfoo-Lonhienne *et al*., 2019).

أن إعادة التدوير عملية تساعد في الحفاظ على المواد الخام الأساسية لاستخدامها في المستقبل، اذ يجب تحقيق أقصى استفادة من الموارد الطبيعية وصنع منتجات جديدة، كاستخراج المواد الخام عن طريق قطع الأشجار والتعدين (Environment,2020). كما ان إعادة تدوير النفايات العضوية للاستخدامات الزراعية أمرًا ضروريًا للحفاظ على إنتاجية التربة في المناطق التي تكون فيها نسبة الكربون العضوي منخفضة (Tortosa *et al*., 2014).

يعد النيتروجين(N) ضروري للكائنات الحية وهو عامل مقيد في زيادة غلة المحاصيل لإطعام سكان العالم المتزايدين (FAO,2019)، وان عنصر النتروجين هو أقل المغذيات وفرة للزراعة في أجزاء كثيرة من العالم. لذلك يعد مهم جدًا لاستقرار للمنتج (Helfrich *et al*.,2020).

يمكن إعادة استخدام النفايات الزراعية التي تحتوي على مغذيات كبيرة ودقيقة بدلاً من الأسمدة الاصطناعية لتحسين خصوبة التربة، وفي الوقت الحاضر يتم وعلى نطاق واسع استخدام السماد الزائد من الحيوانات المختلفة (كالأبقار)، والفحم الحيوي، ومخلفات المحاصيل بشكل مباشر، أو في شكل مخاليط إلى جانب الذرة والقمح، ويعد الأرز غذاءً أساسياً مهمًا، ويمكن إعادة تدوير بقاياه بطريقة مستدامة (Qian *et al*.,2022). ويمكن استخدام Biochar كتعديل للتربة، وتعزيز إمدادات المغذيات وتقليل انبعاثات غازات الاحتباس الحراري (Dong *et al*.,2021؛ Melo *et al*.,2019) . كما يمكن أن يكون الكومبوست من نفايات منزلية (سماد النفايات الحيوية) سمادًا قيّمًا ومفيدًا كمكيف للتربة، ويوفر المغذيات وكذلك المواد العضوية (Carabassa *et al*.، 2020 ؛ Awad *et al*.,2021) ومفيد للمعالجة الحيوية في التربة خاصة المتأثرة بالملح (Kalanaki et al.,2020).

من خلال النشاط الزراعي والذي قد ينتج عنه طرح مخلفات نباتية بكميات كبيرة ومتنوعة بسبب عمليات الحصاد واختلاف في المحاصيل السنوية، والتي قد تسبب في إضافة اعباء على البيئة لا سيما المناطق التي تفتقر لعملية إعادة التدوير، ولكون الدراسات قليلة في محيط عملنا.

جاءت دراستنا للبحث عن وسيلة سهلة التطبيق عملياً وبأقل تكلفة، وأمنة بيئياً لإعادة تدوير المخلفات النباتية المطروحة من الأراضي الزراعية لحماية البيئة منها.

المواد وطرائق العمل Material and Method

اجريت الدراسة في جامعة سامراء– كلية التربية– قسم علوم الحياة للفترة من **10\11\2022** الى **10\2\2023** لغرض اعادة تدوير المتبقيات النباتية وتحويلها الى سماد عضوي اذ جُمعت مخلفات النباتات من حدائق الجامعة بواسطة اكياس وتضمنت بقايا الاوراق المتساقطة بمختلف الانواع، ثم فُرزت لإبعاد الأجزاء الغير نباتية من بلاستك وغيرها.

وتم تجفيفها تماماً مع التقليب المستمر ثم سُحقت(طحنت), بعدها وضعت في حوض المعالجة. واستخدم حوض الزراعة في البيت الزجاجي (العائد لقسم علوم الحياة)، أفرغ من التربة ووضع مشبك معدني في الاسفل لتصريف السوائل الزائدة، كما ويوجد ثقب او فتحة عند القاعدة عند أحد الجوانب وذلك لتصريف المياه والسوائل الناتجة من النباتات. يبلغ عُرض الحوض **100**سم والطول المستخدم 300 سم، وضعَ قاطع خشبي بعد الـ 300 سم لحجر الاوراق بعد وضع النباتات في الحوض وتم ترطيبها بنسبة 60% من خلال إضافة 30 لتر من الماء مع التقليب بشكل مستمر (لكي نظمن الترطيب الكامل)، أستمر التقليب اسبوعياً مع ضمان الحفاظ على نسبة الرطوبة في الخليط من 50%–60% بإضافة كمية من الماء الى الخليط فيما لو كان يحتاج الى ترطيب.

أُخذت عينات منها بواقع عينة كل اسبوعين بالإضافة الى عينة المقارنة، وإجريت بعض الفحوصات عليها، ومتابعة عملية التحلل، استغرقت العملية (**6**) أسابيع لإجراء الفحوصات.

التحاليل الفيزيائية والكيميائية:

1- الأس الهيدروجيني pH :

تم عمل مستخلص مائي للعينات لغرض قياس الاس الهيدروجيني pH حسب (APHA ,2017)، إذ اخذت 100 غم من كل عينة من السماد العضوي الجاف ووزنت بميزان حساس، ثُمَّ اضيف لها 500 مل ماء مقطر بنسبة (5:1) ورجها جيداً بالهزاز لمدة ساعتين، ثم رشح المحلول واخذت له قراءات الـ pH.

2- التوصيل الكهربائي: Electrical Conductivity (EC)

تم عمل مستخلص مائي لغرض قياسها (Page,1982)، إذ تم اخذ 100 غم من كل عينة من عينة (السماد العضوي الجاف)، وأضيفت لها 500 مل ماء مقطر بنسبة (5:1) وتم رجها بصورة جيدة في الهزاز لمدة ساعتين، بعدها رشح المحلول واخذت القراءات.

3- **قياس نسبة الرطوبة:**

قيست نسبة الرطوبة وفق (Page,1982) وكما يلي:

أ- وزن الاناء فارغاً على ميزان حساس (ذو اربعة مراتب).

ب- وضعت 10 غم من كل عينة من السماد العضوي الرطب في الاناء.

ت- سجل وزن الاناء مع العينة.

ث- وضع الاناء مع العينة في فرن وبدرجة حرارة 70°م, ولمدة 24 ساعة الى ان يستقر الوزن ويثبت ، ثم سجل وزنها بعد التجفيف واستخدم لحساب الفرق القانون الآتي:

$$\text{نسبة الرطوبة} = \frac{\text{وزن العينة جافة(بالهواء)} - \text{وزن العينة (بعد التجفيف)}}{\text{وزن العينة بعد التجفيف (بالفرن)}} \times 100$$

4- **تقدير المادة العضوية Determination of Organic Matter (O.M)**:

حسبت المادة العضوية بطريقة الفقد بالترميد حسب(Page, 1982)، إذ أخذت العينات وجففت ووضعت في اواني خزفية وتم وزنها، ثم وضع الاواني مع العينات في المرمدة وعلى درجة حرارة 450 °م لمدة أربع ساعات، ثم بعد إخراجها وضعت في المجفف Desiccative إلى أن انخفضت درجة حرارتها، ثم بعد ذلك أخذ وزنها النهائي، وحسب وزن المادة العضوية وفق المعادلة التالية:

وزن الرماد = وزن الاناء مع الرماد – وزن الاناء فارغة

$$\text{الرماد} = \frac{\text{وزن الرماد}}{\text{وزن السماد الجاف}} \times 100$$

$$\text{المادة العضوية \%} = 100 - \text{الرماد \%}$$

5- **النتروجين:** قدر باستخدام مايكرو كلدال الموضحة من قبل (Jackson ,1958) ، تحضر المواد التالية:

1. حامض البوريك Boric Acid يحضر من إذابة 40 غم في لتر واحد (ماء مقطر).
2. صبغة ازرق المثيل Blue methyl تحضر من إذابة 0.2 غم في 100 مل ماء مقطر.

3. صبغة احمر المثيل Red methyl تحضر بوزن 0.125 غم من مسحوق الصبغة واذابته بـ 100 مل من كحول الايثانول.

4. هيدروكسيد الصوديوم NaOH (10N):- يحضر بإذابة 400 غم في لتر واحد من ماء مقطر.

5. حامض الهيدروكلوريك (HC1 0.014N):- يحضر من إضافة 1.16 مل في لتر واحد ماء مقطر.

أخذ 20 مل من احمر المثيل ويخلط مع 80 مل من المثيل الأزرق، ثم يؤخذ من مخلوط الصبغتين 20 مل ويكمل الى 100 مل بحامض البوريك. يتم التقدير بإضافة 5 مل من العينة +10 مل من الـ NaOH في غرفة التسخين، ويوضع 10 مل من الدليل (مخلوط البوريك) عند فوهة المكثف الى ان يتغير اللون الى الأخضر، ويتم التسحيح بعد ذلك بالـ HCI الى الوصول للون الأصلي للدليل. وتحسب نسبة النتروجين المئوية الكلية، كما ياتي:

$$\% N = \frac{\text{حجم HCl} \times \text{عيارية} \times \text{الوزن المكافئ لـ(N)}}{1000} \times \frac{\text{حجم المستخلص الكلي}}{\text{حجم المستخلص المستخدم(5ml)}} \times \frac{100}{\text{وزن العينة0.4}}$$

ويمكن اختصار هذه المعادلة، بضرب قراءة السحاحة × 0.49 ليعطي ناتج النتروجين كنسبة مئوية.

7- فسفور P :

قدر الفسفور بوضع العينة في جهاز المطياف الضوئي، وبطول موجي 882 نانومتر وتسجيل القراءة (Olsen &Sommers ,1982)، ثم حسب التركيز الكلي للفسفور.

$$\text{الفسفور (ملغم/لتر)} = \text{قراءة الجهاز} \times \frac{\text{الحجم الكلي للمحلول ب(مل)}}{\text{وزن التربة الجافة بالهواء (غرام)}} \times \frac{50}{\text{حجم المستخلص بالمل}}$$

8- التحليل الاحصائي:

حللت البيانات احصائياً، حسب اختبار دنكن، عند مستوى احتمالية 0.05 حسب (الراوي وخلف, 2000).

النتائج والمناقشة: –

1– الأس الهيدروجيني pH: –

بينت قيم الأس الهيدروجيني والموضحة في الشكل (1) انخفاض قيم الأس الهيدروجيني الى ما دون المتعادل عند التحضير وثم ارتفعت قيم الأس الهيدروجيني تدريجيا وهذا الارتفاع كان معنويا وجميعها كانت باتجاه الحامضية وأقل قيمة بلغت 3.5عند البداية لكن اصبحت في الأسبوع السادس 6.5 وهي متفقة مع نتائج الدوري (2020) والدوري (2022).

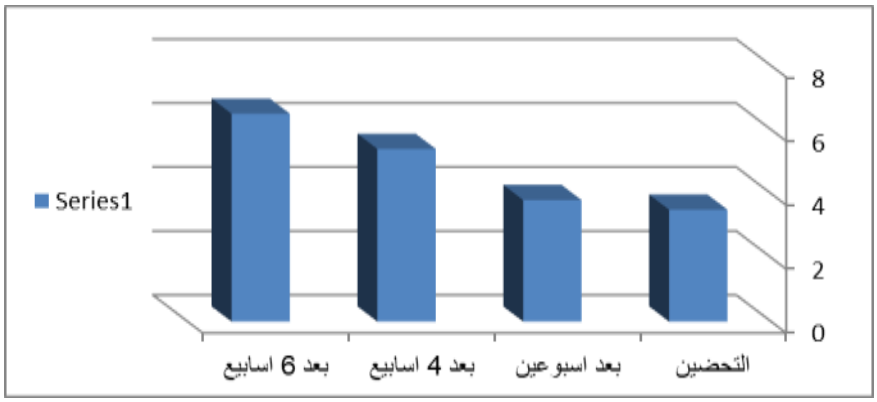

الشكل (1) يوضح الاس الهيدروجيني.

2– التوصيل الكهربائي EC: –

ان قيم التوصيل الكهربائي والموضحة في الشكل (2) قد ارتفعت عند زيادة فترة التحضين حسب اختبار دنكن عند مستوى معنوي 0.05اذا بلغت أقل قيمة 2.5 مايكروسمنز /م في حين أعلى قيمة بلغت 4 مايكروسمنز/م في الأسبوع السادس، وهي تتفق مع الرملي (2021) والدوري (2022) في تحرير الايونات المغذية خلال عمليات التحلل العضوي، وبالتالي تزداد (fang & wong,2000).

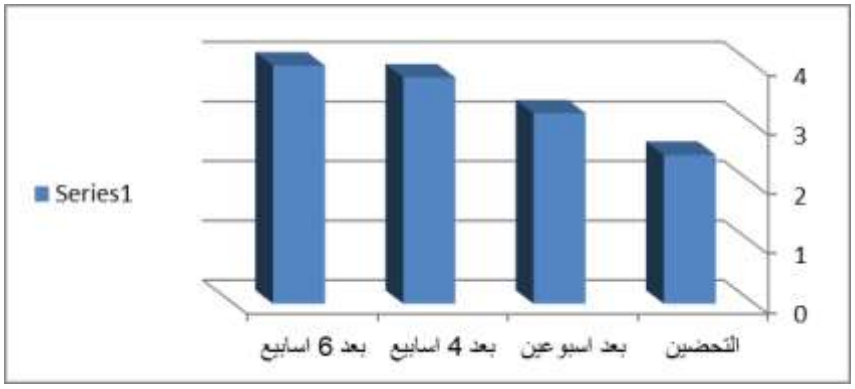

الشكل (2) يوضح قيم التوصيل الكهربائي.

3- المادة العضوية O.M.:

ان قيم المادة العضوية في بداية التحضين كانت منخفضة اذ بلغت 20.01 % ثم ارتفعت وسجلت اعلى قيمة بعد اسبوعين اذ بلغت 23.5% , فيما كانت بعد اربع اسابيع 22.2%, وبعد ست اسابيع انخفضت لتصل الى 20.2, وكما موضح في الشكل(3), ويعود سبب انخفاضها الى الزيادة الحاصلة بنشاط الأحياء المجهرية, اذ انها تحصل على الطاقة من خلال اكسده وحرق الكاربون العضوي وتحويله الى ثاني اوكسيد الكاربون وماء وبالنتيجة استهلاك المادة العضوية(Shyamala & Belagali, 2012)، واتفقت النتائج مع(الدوري, 2022).

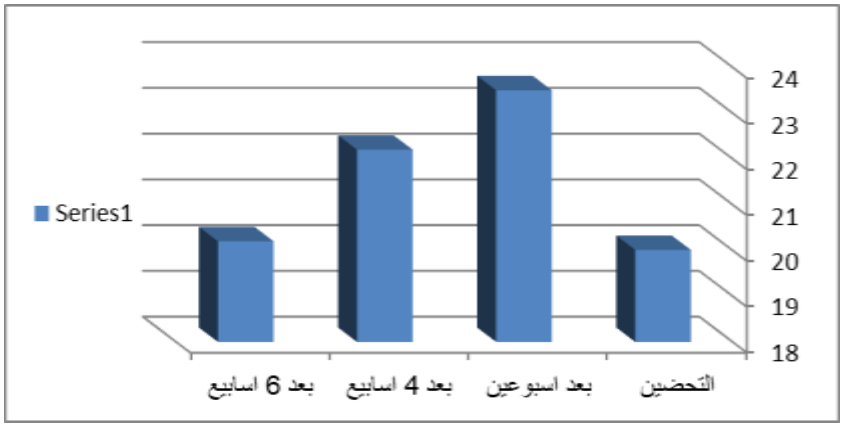

الشكل (3) يوضح المادة العضوية.

4- نسبه الرطوبة:

ان نسبة الرطوبة ارتفعت في الاسبوع الثاني والرابع كما موضح في الشكل(4), لكنها بدأت تقل بعد الاسبوع السادس, وسجلت ادنى قيمة عند التحضين اذ بلغت 70.5% , وسجلت اعلى قيمة لها عند الاسبوع الثاني اذ بلغت 76.4% ، بينما كانت بعد اربع اسابيع 73.2%, وبعد ست اسابيع انخفضت لتصل الى 73.1%, وتتفق النتائج مع الدوري (2022), ويعزى ذلك الى الزيادة الحاصلة بمعدلات التبخر والتي تحصل مع زيادة النشاط للأحياء المجهرية, علاوة على ذلك، يلعب النشاط الميكروبي دورًا رئيسيًا في تحول المواد العضوية بالسماد, وتكون بكتيريا إزالة النتروجين أكثر نشاطًا في المرحلة المحبة للحرارة، هذه الكائنات الدقيقة حساسة للتغيرات البيئية (Ma *et al*., 2018).

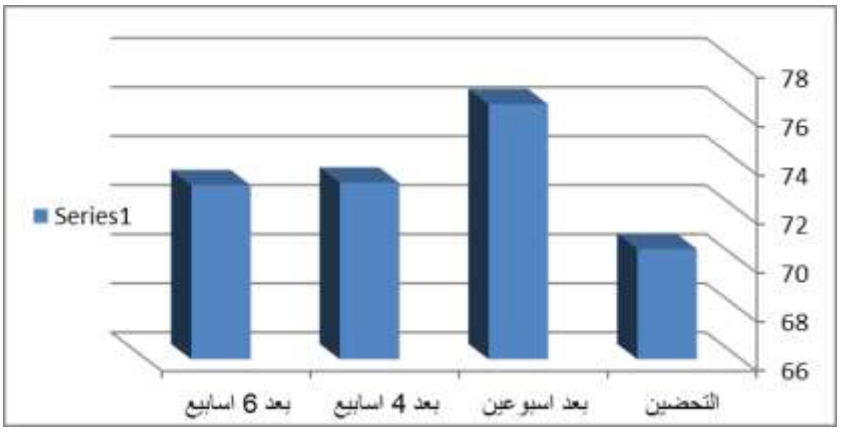

الشكل (4) يوضح نسبة الرطوبة.

5- الكاربون الى النتروجين C:N

ان نسبه C:N تختلف بالمادة العضوية وذلك حسب مصادر المواد العضوية (الاوراق بمختلف الانواع)، والتي تلعب دور مهم في التحلل الحاصل بالمادة العضوية (McCartney and Larsen,2000), وسجلت اعلى قيمة 16.5 عند التحضين, وادنى قيمة بلغت 8.44 في الاسبوع السادس من التحضين, وكما موضح في الشكل(5), و اتفقت الناتج مع الدوري(2020).

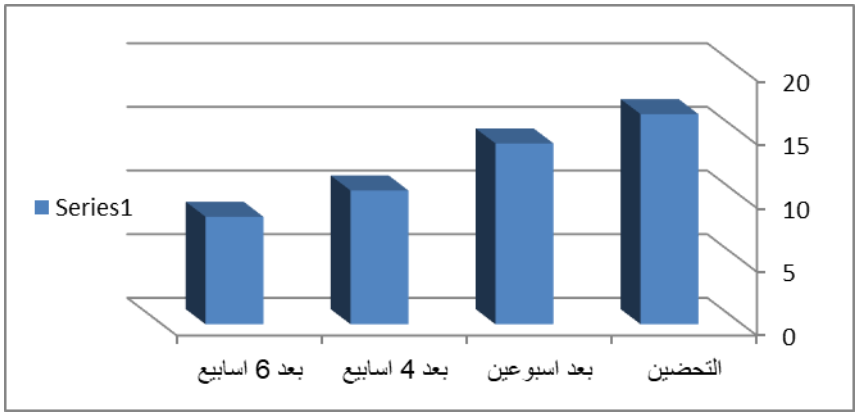

الشكل (5) يوضح قيم الكاربون.

6- اللون: color

ان اللون عند بداية التحضين يتميز بلونه الاصفر، ثم بعدها تدرج الى اللون البني الداكن عند وصولة للأسبوع السادس، أي بعد انتهاء مراحل التحلل للمخلفات وهذه النتائج تتفق مع الرملي (2021) أي وصول المنتج الى مرحلة النضج Abd Elfattah (2013).

7- النتروجين N:

ان تركيز النتروجين ارتفع مع زيادة فتره التحضين معنويا حسب اختيار دنكن عند مستوى معنوي 0.05, كما موضح في الشكل (6)، اذ بلغت اعلى نسبة 4.33 % بعد الاسبوع السادس، في حين بلغت أدنى قيمة في بداية التحضين 1.4 %، يعود سبب الارتفاع نتيجة ازدياد العمليات في التحرر اثناء التحلل الحاصل للمواد العضوية، ويعتمد النتروجين بشكل أكبر على رطوبة التربة (Goyal *et al*.,2005; Beier et al.2008). واتفقت نتائج النتروجين مع الدوري (2020) والرملي (2021).

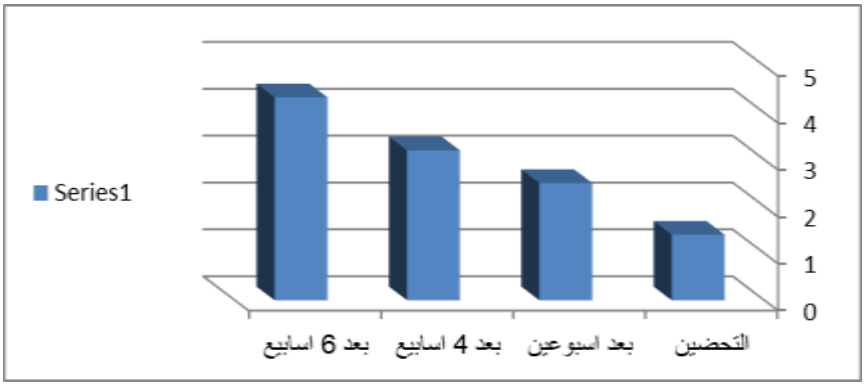

الشكل (6) يوضح قيم النتروجين.

8- الفسفور p:

بينت نتائج الفسفور الموضحة في الشكل (7)، ان قيم الفسفور ازدادت اذ بلغت 1.3 % بعد الاسبوع السادس، بعد ان كانت في الاسبوع الأول 0.12, واتفقت النتائج مع الدوري (2020) والدوري (2022),إن زيادة الفسفور تعود لانخفاض قابليته للذوبان, وقد يرجع ايضاً إلى حد كبير لزيادة الفوسفور المنبعث من المادة العضوية المتحللة, اذ يمكن للماء إذابة الفوسفور كمذيب تحت تركيز مناسب لرطوبة التربة، مما قد يزيد الفوسفور المتاح ويقلل الفسفور الكلي(Williams *et al*., 2018).

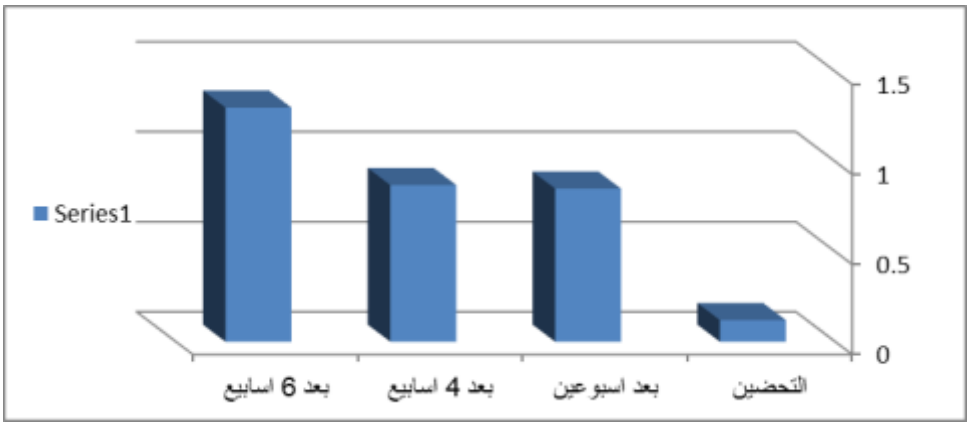

الشكل (7) يوضح قيم الفسفور.

المصادر

1- المصادر العربية:

- **الدوري، أروه كمال عطوان (2022).** اعادة تدوير متبقيات النباتات بطرق اقتصادية وامنة. رسالة ماجستير، كلية التربية للبنات، جامعة تكريت.
- **الدوري، سحر لطف الله احمد (2020).** اعادة تدوير مخلفات الاغذية وتقويمها سماداً عضوياً في تحسين نمو وانتاج محصول الطماطة. رسالة ماجستير، كلية التربية للبنات، جامعة تكريت.
- الراوي، خاشع محمود وخلف الله، عبد العزيز محمد(2000) . تصميم وتحليل التجارب الزراعية، الطبعة الثانية، مطبعة جامعة الموصل.
- **الرملي، نوري حميدي محمد (2021).** تقييم كمبوست الشوك والعاقول وسطاً وسماداً عضوياً في نمو شتلات وحاصل الطماطة. اطروحة دكتوراه، كلية الزراعة، جامعة تكريت.

2- المصادر الانكليزية:

- **Abd El-fattah.(2013).** Effect of carrier materials, sterilization method, and storage temperature on survival and biological activities of Azotobacter chroococcum inoculant, Annals of Agricultural Science, 58 (2): 111 - 118.
- **Ahmed, A.S., Ali, M. (2019).** Partnerships for Solid Waste Management in Developing Countries: Linking Theories to Realities. Habitat International 2019;28(3):467-479.
- **APHA. (American Public Health Association).(2017).** Standard Methods for the examination of water and waste water, 23th ed A. P. H. A. ,5 Fifteen street.NW. Washington. DC. USA.
- **Awad, M., El-Desoky, M. A., Ghallab, A., Kubes, J., Abdel-Mawly, S. E., Danish, S., et al. (2021).** Ornamental plant efficiency for heavy metals phytoextraction from contaminated soils amended with organic materials. Molecules 26 (11), 3360. doi:10.3390/molecules26113360.
- **Beier, C., Emmett, B.A., Peñuelas , J., Schmidt , I. K., Tietema , A., Estiarte , M., Gundersen, P., Llorens , L., Riis-Nielsen, T., Sowerby, A., Gorissen, A., (2008).** Carbon and nitrogen cycles

in European ecosystems respond differently to global warming. Science of the Total Environment 407:692–697.

- **Carabassa, V., Domene, X., and Alcañiz, J. M. (2020).** Soil restoration using compost-like-outputs and digestates from non-source-separated urban waste as organic amendments: Limitations and opportunities. J. Environ. Manag. 255, 109909. doi:10.1016/j.jenvman.2019.109909.

- **Dong,D.**
  Li, J., Ying, S., Wu, J., Han, X., Teng, Y., Zhou, M., Ren, Y., Jiang, P.(2021). Mitigation of methane emission in a rice paddy field amended with biochar-based slow-release fertilizer.Sci. Total Environ. (2021). Volume 792, 148460. https://doi.org/10.1016/j.scitotenv.2021.148460.
- **Environment,(2020).** A Forum for the Environment: Assessment of the solid waste management system of Bahir Dar town and the gaps identified for the development of an ISWM plan. Bahir Dar 2020.

- **Fang, M. and Wong, J.W.C., (2000).** Effects of Lime Addition on Sewage Sludge Composting Process. Water Research 15, 3691–3698.
- **FAO,(2019).** The state of food security and Nutrition in the world 2019. http://www.fao.org/3/19553EN/i9553en.pdf.
- **Goyal, D. S.K. Dhull, and K.K. Kapoor. (2005).** Chemical and biological changes during composting of different organic wastes and assessment of compost maturity. Bioresour. Technol. 96(14):1584-1591.
- **Helfrich, M., Nicolay, G., Well, R., Buchen-Tschiskale, C., Dechow, R., Fuss, R., Gensior, A., Paulsen, H.M., Berendonk, C., Flessa, H., (2020).** Effect of chemical and mechanical grassland conversion to cropland on soil mineral N dynamics and N2O emission. Agr. Ecosyst. Environ. 298, 106975**.**
- **Jackson, M.L. (1958).** Soil Chemical Analysis. Prentice Hall, Inc. Englewood Cliff, N.J. USA. P.225-276.

- **Kalanaki, M., Ritzema, H., Bamshad, R., Jones, E., and Fazilatnia, M. (2020).** Application of bio-desalinization for reclamation of salt-affected soil under composted cow manure and deficit irrigation with saline water. Paddy Water Environ. 18 (2), 469–479. doi:10.1007/s10333-020-00795-7.

- **Kanmaz, E.O., (2019).** Humic acid formation during subcritical water extraction of food by-products using accelerated solvent extractor. Food Bioprod. Process. 115, 118e125. https://doi.org/10.1016/j.fbp.2019.03.008
- **Liang, B., Zhao, W., Yang, X., Zhou, J., (2013).** Fate of nitrogen-15 as influenced by soil and nutrient management history in a 19-year wheatemaize experiment. Field Crop. Res. 144, 126e134. https://doi.org/10.1016/j.fcr.2012.12.007.
- **Ma, S.S., Fang, C., Sun, X.X., Han, L.J., He, X.Q., Huang, G.Q., (2018).** Bacterial community succession during pig manure and wheat straw aerobic composting covered with a semi-permeable membrane under slight positive pressure. Bioresour. Technol. 259, 221-227.
- **Marlon JR, Bloodhart B, Ballew MT, Rolfe-Redding J, Roser-Renouf C, Leiserowitz A, et al. (2019).** How hope and doubt affect climate change mobilization. Front. Commun. 4:20. doi: 10.3389/fcomm.2019.00020

- Matschullat, J., Reimann, C., Birke, M., dos Santos Carvalho, D., the GEMAS Project Team, (2018). GEMAS: CNS concentrations and C/N ratios in European agricultural soil. Sci. Total Environ. 627, 975e984. https://doi.org/10.1016/ j. scitotenv.2018.01.214
- **McCartney, D.M. and Larsen, K. L., (2000).** Effect of C: N Ratio on Microbial Activity and N Retention: Bench-scale Study Using Pulp and Paper Biosolids. Volume 8, 2000 - Issue 2, Pages 147-159. https://doi.org/10.1080/1065657X.2000.10701760.
- **Melo, T.M.,** Michael Bottlinger, Elke Schulz, Wilson Mozena Leandro, Sérgio Botelho de Oliveira, Adelmo Menezes de Aguiar Filho, Ali El-Naggar, Nanthi Bolan, Hailong Wang, Yong Sik Ok, Jörg Rinklebe. (2019). Management of biosolids-derived hydrochar (Sewchar): effect on plant germination, and farmers' acceptance.J. Environ. Manag.(2019).Volume 237, Pages 200-214. https://doi.org/10.1016/j.jenvman.2019.02.042.
- **Olsen, S.R. & Sommers, L.E., (1982).** Phosphorus. In: Page, A.L., Ed., Methods of Soil Analysis Part 2 Chemical and Microbiological Properties, American Society of Agronomy, Soil Science Society of America, Madison, 403-430.
- **Page A. L. (1982).** Methods of soil analysis, part 2: chemical and microbiological properties. 2nd ed. (Madison, WI, USA: American Society of Agronomy and Soil Science Society of America).
- **Paungfoo-Lonhienne, C., Redding, M., Pratt, C., Wang, W.,(2019**). Plant growth promoting rhizobacteria increase the efficiency of fertilisers while reducing nitrogen loss. J. Environ. Manag. 233, 337e341. https://doi.org/10.1016/ j.jenvman.2018.12.052
- **Qian, L.,** Feng, L. , Hongbo, L., Lingen, W., Breda, M., Shaosheng, J**.(2022).**Rice vs. Wheat: does staple food consumption pattern affect food waste in Chinese university canteens? *Resour. Conserv. Recycl*.(2022). Volume 176, 105902. https://doi.org/10.1016/j.resconrec.2021.105902.
- **Recycling, (2019).** The Third International Conference on Waste Management, Waste Hierarchy - Step Up & Go Green 2019 (Lansink's Ladder) (recycling.com).
- **Sepehri, A., Sarrafzadeh, M.H., (2019**). Activity enhancement of ammonia-oxidizing bacteria and nitrite-oxidizing bacteria in activated sludge process: metabolite reduction and CO2 mitigation intensification process. Appl. Water Sci. 9 https:// doi.org/10.1007/s13201-019-1017-6.
- **Shyamala, D.C., Belagali, S.L., (2012).** Studies on variations in Physicochemical and biological characteristics at different maturity stages of municipal solid waste compost, Int. J. of Environmental Sciences, 2 (4), Pp. 1984-1997.
- **Tortosa, G., Alburquerque, J.A., Bedmar, E.J., Ait-Baddi, G., Cegarra, J., (2014).** Strategies to produce commercial liquid organic fertilisers from "alperujo" composts. J. Clean. Prod. 82, 37e44. https://doi.org/10.1016/j.jclepro.2014.06.083.
- **Wang, L., Li, Y., Prasher, S.O., Yan, B., Ou, Y., Cui, H., Cui, Y., (2019).** Organic matter, a critical factor to immobilize phosphorus, copper, and zinc during composting under various initial C/N ratios. Bioresource Technology. https://doi.org/10.1016/j.biortech.2019.121745.
- **Wang, L., Li, Y., Prasher, S.O., Yan, B., Ou, Y., Cui, H., Cui, Y., (2019).** Organic matter, a critical factor to immobilize phosphorus, copper, and zinc during composting under various initial C/N ratios. Bioresource Technology. https://doi.org/10.1016/j.biortech.2019.121745.
- WHO. *Air Pollution*. WHO. Available online at: http://www.who.int/airpollution/en/ (accessed October 5, 2019).

- **Williams, M. R., King, K. W., Duncan, E. W., Pease, L. A., & Penn, C. J. (2018).** Fertilizer placement and tillage effects on phosphorus concentration in leachate from fine-textured soils. *Soil and Tillage Research*, 178, 130–138.
- **Zhao, X., Tong, M., He, Y., Han, X., & Wang, L. (2021).** A comprehensive, locally adapted soil quality indexing under different land uses in a typical watershed of the eastern Qinghai-Tibet Plateau. Ecological Indicators, 125, 107445.doi:10.1016/j.ecolind.2021.107445.
- **Zhu, E., Deng, J., Wang, H., Wang, K., Huang, L., Zhu, G., Belete, M., Shahtahmassebi, A., (2019).** Identify the optimization strategy of nitrogen fertilization level based on trade-off analysis between rice production and greenhouse gas emission. J. Clean. Prod. 239, 118060. https://doi.org/10.1016/ j. jclepro.2019.118060.

استخدام المصب العام وتقييم مياه خلال دراسة الملوثات العضوية واللاعضوية قبل وبعد محطة المعالجة ومقارنتها بالمحددات العالمية

المدرس المساعد:

بان خليل علي / مديرية تربية ذي قار/ العراق

Using the public estuary and evaluating its water during the study of organic and inorganic pollutants before and after the treatment station and comparing them with international standards.

Assistant Lecturer: -Ban Khalil Ali / Dhi Qar Education Directorate/Iraq

Summary

The study included collecting water samples from two stations located on the general downstream river, one of which was an untreated station and the other was treated to study organic and inorganic pollutants, and their suitability was evaluated by comparison with international standards, whereas samples were taken during the period 2022-2023 (April represents the spring season, July represents the summer season, October represents the fall season, and January represents the winter season) to observe the locational and temporal changes of the river. Temperature, PH, electrical conductivity, total dissolved solids, suspended solids, salinity, turbidity, dissolved oxygen, chloride, carbonates, sulfates, phosphates, nitrates, phenols, pesticides, fecal coliform bacteria, bicarbonates, hardness, oils greases, sodium, sodium adsorption rate, and concentrations of some heavy metals were measured. The results showed the abundance of pollutants and the influence of river water on the climate of the southern rugged region before treatment. However, the station that treated the water proved efficient in eliminating all pollutants except pH, dissolved oxygen, nitrates, fecal coliform bacteria, and some heavy elements such as copper, lead, and iron, as their percentages were high and required further treatment

استخدام المصب العام وتقييم مياه خلال دراسة الملوثات العضوية واللاعضوية قبل وبعد محطة المعالجة ومقارنتها بالمحددات العالمية

المدرس المساعد:- بان خليل علي / مديرية تربية ذي قار/ العراق

المخلص :-

تضمنت الدراسة جمع نماذج مياه من محطتين تقعان على نهر المصب العام أحداهما محطة غير معالجة والأخرى تم معالجتها لدراسة الملوثات العضوية واللاعضوية وقيمت مدى صلاحيتها عن طريق المقارنة بالمحددات العالمية حيث أخذت العينات عند الفترة 2022-2023[نيسان ليمثل موسم الربيع وتموز ليمثل موسم الصيف وتشرين الأول ليمثل موسم الخريف وكانون الثاني ليمثل موسم الشتاء]لملاحظة التغيرات الموقعية والزمينه للنهر.وتم قياس درجة الحرارة ,الأس الهيدروجيني ,التوصيلية الكهربائية ,المواد الصلبة الذائبة الكلية,المواد الصلبة العالقة,الملوحة ,العكورة ،الأوكسجين المذاب,الكلوريد ,الكاربونات ,الكبريتات, الفوسفات,النترات ,الفينولات ,المبيدات الحشرية,بكتريا القولون البرازية ، البيكاربونات, العسرة, الزيوت والشحوم,الصوديوم, نسبة امتزازالصوديوم وتراكيزبعض العناصرالثقيلة وبينت النتائج كثرت الملوثات وتأثرمياه النهربمناخ المنطقة الوعرة الجنوبية قبل المعالجة ولكن في المحطة التي عالجت أثبتت كفائتها في التخلص من الملوثات كافه عدا الاس الهيدروجيني والاوكسجين الذائب والنترات وبكتريا القولون البرازية وبعض العناصرالثقيلة النحاس والرصاص والحديد كانت قيمها مرتفعة تتطلب المزيد من المعالجة .

المقدمة :- Introduction

يعد الماء الصالح للشرب ضروري لجميع الكائنات الحية في ظل التطورات التي يشهدها العالم لكن نلاحظ في السنوات العشرالأخيرة أزداد تلوث البيئة المائية بالملوثات السامة وتأثيرها على الكائنات الحية [1] وربما تزداد بمستويات تفوق المستويات الطبيعية بسبب كثرت المخلفات الصناعية ومخلفات المجاري التي تدخل للجسم عن طريق الماء بصورة مباشره[2].أذ تعد مياه الانهارمصدرا مهم للمناطق الجافة التي تعتمد بصورة رئيسية على تلك الأنهارلمياه الشرب والزراعة والصناعة [3] لكن عدم معالجتها وصرف مياه الصرف الصحي فيها واستخدامها لتوليد الطاقة الحرارية وطرحها بشكل متدفقات حارة [4]ورمي مياه البزل الزراعي بشكل مباشرمن دون معالجه مما يجعلها ذات تلوث عالي وملوحة مرتفعة بالإضافة الى العوامل المناخية الذي شهدها العراق خلال الفترة الأخيرة (كالرياح والعواصف الترابية وقله الأمطار) التي تعد ربما سبب في زيادة التلوث [5] هذا ماجعلها في تردى مستمر بنوعيه المياه[6] وعدم وجود حلول لتوفير مياه نظيفة حيث كانت أكثرالأمراض المنقولة عن طريق المياه الملوثة وبينت ذلك تصريحات وزارة الصحة لهذه السنة وبالأخص الكوليرا,التيفوئيد, الامبيبا إشارة الى ذلك تقارير وزارة البيئية لعام (2020-2023)أن التلوث البكترولوجي تراوح بين المحافظات (90% - 30%)وهذا يفوق المحددات العراقية لمياه الشرب[7] . زيادة التلوث اكثرأسبابه السياسات المائية للدول المجاورة للعراق ونذكرعلى وجه الخصوص بعد قيام تركيا بأنشاء السدود الضخمة على نهري دجلة الفرات وقله الاطلاقات المائية[8] وتسريب مياه الصرف الى المياه السطحية وعدم نصب المشاريع الضرورية لتدويرالمياه والتخلص من التلوث باستمرارهذا ماجعلها تفقد خواصها الفيزيائية [9] مع تضررمساحات شاسعة من المناطق الوسطى والجنوبية بسب أرتفاع نسبة الملوحة [10] بالتالي توثرعلى جميع الكائنات الحية وهذا ماجعلنا نعيش في أزمة حقيقية مع الماء وقلة الكميات المتوفرة للاستخدام البشري ولم تعد تتناسب مع عدد السكان واحتياجاتهم للحيوانات والزراعة [11]وقد بدات محافظة ذي قارتدرك أهمية هذه المخاطر بعده هجره المناطق الزراعية وجفاف الاهوار.

نبذه عن النهر الثالث:- أن مشروع النهرالثالث من المشاريع الاروائية الكبرى المساهمة بصورة فعاله في إصلاح الأراضي الزراعية وهومن مرتكزات البني التحتية لها بتصريف مياه البزل للاراضي الزراعية بعيدا الى البحرأكمل انجازه عام 1992 بطول حوالي(665) كم من بداية منطقة الاسحاقي في بغداد حتى ينتهي بخورالزبير بالبصرة. وله أهميه في التخلص من المياه المالحة وخفض تراكيزالاملاح التي تقدرسنويا ب(80) مليون طن وتحسين نوعيه مياه النهرين من خلال شبكة من المبازل التي تنتهي بمجرى المصب العام المسوول عن توجه هذه المياه الشديدة الملوحة الى منطقة الخليج العربي ويتم عبرفتحات السايفون تحت نهرالفرات في الناصرية ونتيجة للاختلاف الحاصل في مناسيب المصب العام عن مناسيب الارض في الناصرية مما يؤدي احيانا الى حصول تاثيرسلبي لكيفية التخلص من الأملاح حيث ان فتحات السايفون لا تستطيع ان تمرر كافه التصاريف التي تطلقها قناة المصب العام والتي كانت بمقدار $220m^3/S$ ألانها قادرة على أن تمررتصاريف لاتزيد عن $140\ m^3/S$ وهذا يعود الى ضعف الإمكانيات المستعملة لتصريف المياه لذلك النهربحاجه ألى أعادة تأهيل .يعتبرالنهرالثالث من التجارب والمحاولات التي جأت بسب قله المياه لكنها صالحة فقط لري الأراضي الزراعية لذلك يجب الاهتمام

بمواصفاتها النوعية لانها موردا مهم ومغذي جيد لمحافظة ذي قارأذا تم معالجه ملوحة مياه والتخلص من أثارالملوثات فيه بالإضافة الي تمتع المحافظة بأزدياد الكثافة السكانية والشحة الحاصلة للمياه[12-15].أن مياه النهرتقع ضمن الصنف الرابع (Poor)والصنف الخامس (Very poor) وأنهاغيرصالحة لمياه الشرب بسب كثرت الملوثات العضوية واللاعضوية فيها وكذلك للماشية والدواجن بالاضافة لكونها غير صالحة للزراعة [16] فقط المحاصيل التي لها القدرة العالية لتحمل الملوحة الشديدة وبينت نتائج الدراسة من خلال الفحوصات قبل المعالجة وبعدها أن مياه النهرغيرقادرة على التنقية الذاتية (Self purification) بسب كثرت الملوثات وارتفاع الجهد العضوي[17] .

الملوثات العضوية :-

أنها ملوثات كيمياوية سامه عالية الخطورة أثارها سيئة على الماء في جميع الدول التي تعاني الإهمال تتراكم في النظام البيئي تهدد صحة الانسان تنتج غالبا من مياه الصرف الصحي الغيرمعالجة بالاضافة الى زيادة السكان جعل المياه الداخلة غيرقادرة على التنقية الذاتية لزيادة الملوثات وكثرت عمليات الاحتراق مثل غاز الكلورأوالغازات الأخرى وهذا ماأكدته الدراسات السابقة في المناطق التي شهدت زيادة النموالسكاني وكثرت المخلفات الزراعية والمنزلية [18] . للتلوث العضوي مصادر عديدة (Organic pollution sources) كالصناعية وسببها كثرت توليد الطاقة الكهربائية والحراريه بالقرب من النهروهذا ماشهدته محافظة ذي قاروالتوسعة فى بناء المنشأت الصناعية أما الزراعية ونذكرالمنطقة التي تم الدراسة عليها وانتشارالحياة الريفية بالقرب منها وكثرت أستعمال الاسمدة الثلاثية والمبيدات الكيميائية وبالتالي تنتقل الى المياه واهمها واخطرها على الاطلاق مصادر الصرف الصحي عن طريق رمي المخلفات ومياه المجاري دون معالجة وأحتوائها على المغذيات النباتية وبالتالي أزدهارالطحالب كما شهدت الآونة الأخيرة أنتشارأعداد هائلة من الطحالب [19].

الملوثات اللاعضوية:-

مسووله عن تغيرطعم وطبيعة الماء التي تزداد أثارها بزيادة تركيزها القادم من ذوبان المركبات والأملاح اللاعضوية أهمها وأخطرها تراكيزالعناصرالثقيلة ويقصد بها المعادن التي تحتوي كثافة أكثر من(5g/mL) [20] تتواجد في المياه بصورة طبيعيه من جراء العمليات الجيولوجية كالصخوروالترسبات ومياه الامطار المحملة بهذه العناصروفي بعض الاحيان يكون نشاطها بشري من الصناعات البترولية أو المبيدات أوطرح الفضلات المنزلية حيث أصبحت تتراكم هذه المعادن في المياه والرواسب وهذا مابينته الدراسات انتشارتلك العناصر في السلاسل الغذائية لذلك أصبح من الضروري مراقبة التلوث بانتظام وتكون بعض العناصر(النحاس ,الخارصين ,المغنيسيوم ,الكروم , الكوبلت , النيكل, الحديد, المنغنيز, الزنك) لها حاجة ضرورية لوظائف الجسم الطبيعية ومعظم الفعاليات الانزيمية لكن بالحدود المسموح بها اما بقية العناصر (السيزيوم,الرصاص ,الزئبق, الفضة ,الكاميوم) أثارها خطيرة وسامه لانها لأتحلل تبقى عالقة وتكمن خطورتها بتراكمه داخل الكبد والكلى[21] أن تراكم المعادن الثقيلة وأنتشارها مرتبط بعدد من

العوامل البيئية (الملوحة ,درجة الحرارة والحموضة ,الصلابة, الرقم الهيدروجيني) التي يوزع تركيزها ودورانها وانتقالها بين الطبقات المائية.

أثارتلوث المياه على الانسان:-

هناك أرتباط وثيق بين صحة الانسان والمياه النظيفة وأخطرالأمراض المعدية التي تدمرصحته تنتقل من تلوث المياه التي تبدأ بالقي والغثيان والاسهال وهي البلهارزيا , الملاريا, الكوليرا,ألتهاب الكبد الوبائي, والتفوئيد وغيرها وصولا الى الأمراض المستعصية نتيجة الاشعاعات مثل الأورام السرطانية المنتشرة من تلوث المياه لاتوجد أرقام دقيقه توضح عدد الإصابات ودقتها وسجل صيف (2023) في محافظة ذي قارأمراض عديدة مرتبطة بتلوث المياه وعملت لجنة الصحة والبيئة باستمرارعلى حماية الانسان لان نسبة كبيرة من المشاكل الصحية التي يعاني من الانسان تعود الى المياه الملوثة [22].

الجزء العملي وطرائق العمل:- Experiment Part

وصف محطات الدراسة :-

قسمت منطقة الدراسة إلى محطتين الاولى [تقع هذه المحطة عند دخول المصب العام لمحافظة ذي قار أنها واقعه ضمن منطقة صحراوية لا يوجد فيها أي نشاط زراعي قريب من النهرلكن على بعد حوالي35 كم لاحظنا أحاطتها ببعض الأراضي المزروعة بالحنطة والشعير وهناك انبوب صرف صحي محمل بالملوثات يصب بالنهروأخذت العينات من النهرمباشرتنا من دون اي معالجة] أما المحطة الثانية [أنها محطة تابعة لشركة تعمل على تنقية المياه ومعالجتها تقع على أطراف منطقة الفجرعلى بعد 20 كم] .

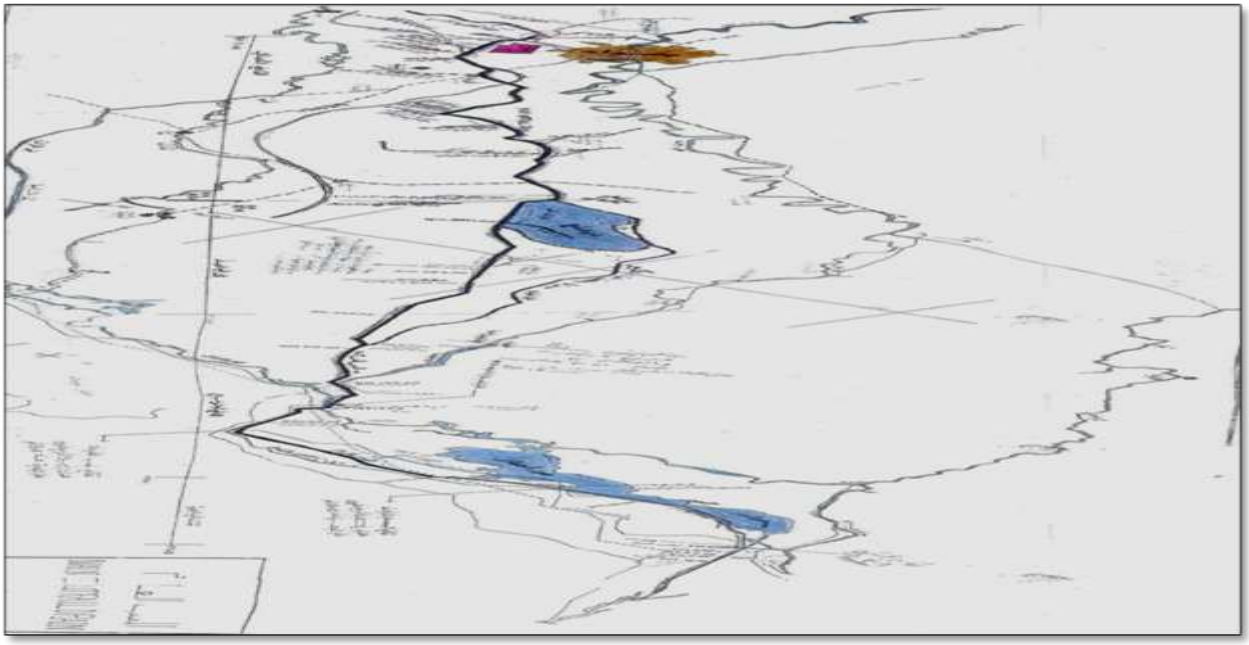

شكل(1) يوضح خريطة المصب العام

جمع عينات الدراسة:-

غسلت جميع الأدوات الزجاجية والبلاستيكية بمسحوق التنظيف والماء المقطرعده مرات ثم وضعت الأدوات في حوض يحتوي على حامض HCl المخفف بتركيز (10%) لمدة يوم كامل ثم غسلت بالماء المقطروجففت بفرن تتراوح درجة حرارة [$70\text{-}60c^0$] وجمعت عينات المياه ابتداء من شهرنيسان 2022 ولغاية شهركانون الثاني 2023 من الطبقة السطحية للنهربعمق (30cm) سم وعلى بعد (1-3m)من حافة النهربواقع ثلاث مكررات واخذ المعدل الكلي للقراءات واستخدمت القناني المصنوعة من البولي أثيلين سعة (5L) واغلقت فوهات القناني بصورة محكمة لمنع دخول الهواء بعد أن تأكد بمجانسة قناني الجمع بماء العينة قبل ملئها وأضافه بضع قطرات من مادة الكلوروفورم كمادة حافظة [23]وقمنا بتسجيل المعلومات اللازمة على كل قنينة واحتفظنا بالعينات في درجة حرارة منخفضة لحين الوصول للمختبروبعد الانتهاء من الفحوصات غُسلت القناني جيدا وجُففت لحين أخذ عينات أخرى .

تحضيرالمحاليل القياسية :-

تم تحضير المحاليل القياسية باذابة الغرامات اللازمة من كل مادة في لتر من الماء المقطر واستعملت لأجراء الفحوصات اللازمة .

الفحوصات العضوية واللاعضوية للنهر(الفيزيائية والكيميائية)

قيست درجة حرارة الماء باستخدام المحرارالزئبقي والحقلي المدرج (100-0)م ^{0} وكررت العملية عدة مرات للتأكد من القراءة أما الأس الهيدروجيني تم قياسه بجهازpH-meter والتوصيل الكهربائي للماء تم قياسه باستخدام جهاز التوصيل الكهربائي الحقلي من صنع شركة Hanna عند درجة حرارة25.وقيست العكورة لعينات المياه باستخدام جهاز قياس العكورة Turbidity meter والمحلول المخصص للمعايرة وبالمدى المطلوب وبوحدة NTU واستخدامت طريقة الإنبعاث الذري اللهبي لحساب(Na)وحساب قيم الSAR باستخدام المعادلة المقترحة من مختبر الملوحة الأمريكي في عام(1953) كم في المعادلة التالية :[24]

$$SAR = \frac{[Na^{+1}]}{[Ca^{+2} + Mg^{+2})/2]^{1/2}}$$

حيث أن تراكيزالأيونات تكون مقاسه بوحدات (ملي مكافئ / لتر).أما الملوحة حسبت بدلاله التوصيلية الكهربائية والمعادلة المذكورة في(Golterman.et.al,1978).وقيست المواد الصلبة العالقة الكلية(TSS)والمواد الصلبة الذائبة الكلية (TDS) بترشيح (100) مل من العينات وجمع الراشح في دورق معلوم الوزن ثم وضع في حمام مائي حتى الجفاف عند درجة حرارة (103-105) لمدة ساعتين ثم يبرد ويوزن بدقة . اما الاوكسجين المذاب (Do) بجهاز قياس الاوكسجين المذاب حقليا. أماالعسرة الكلية قدرت بالتسحيح مع محلول 2Na- EDTA تركيزه (0.01N) مع استخدام (EBT) كدليل وقيس الكلوريد بطريقة التسحيح باستعمال نترات الفضة وبالطرق القياسية [15].

وتم قياس البيكاربونات بالتسحيح مع محلول حامض الكبريتيك القياسي (0.02N)ودليل الفينولفثالين كدليل لقياس تركيز الكاربونات ودليل المثيل البرتقالي كدليل لقياس تركيز البيكاربونات وأيون الكبريتات($So_4^{=}$) بطريقة الكدرة Turbidimetric Mothedوقيست أيونات النترات(No_3^{-})والفوسفات (Po_4^{-3}) والفينولات باستخدام جهاز المطياف الضوئي وكانت النتائج(بمغلم /لتر) والسيانيد تم قياسه بالتقطير والقياس اللوني اما الزيوت والشحوم عينت باستخلاصها واستعمل الكلوروفورم كمذيب,وقيست بكتريا القولون البرازية Fecal Coliformبطريقة العدد الأكثر احتمالا(MPN) الموضحة من قبل منظمة الصحة العامة الامريكية(APHA,2003)[25].وقيست تراكيز أيونات العناصر الثقيلة بطريقة الانبعاث الذري اللهبي باستعمال جهاز Flame photometer من صنع شركة Jeanouy بعد معايرة الجهاز بالمحاليل القياسية المصنعة من قبل الشركة وفحصت حسب الطرق المذكورة في (APHA,2003)[15].

النتائج :- Results

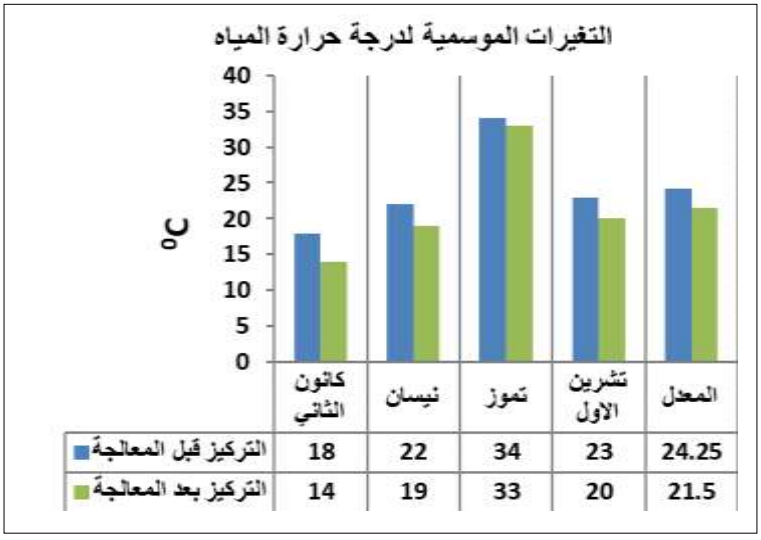

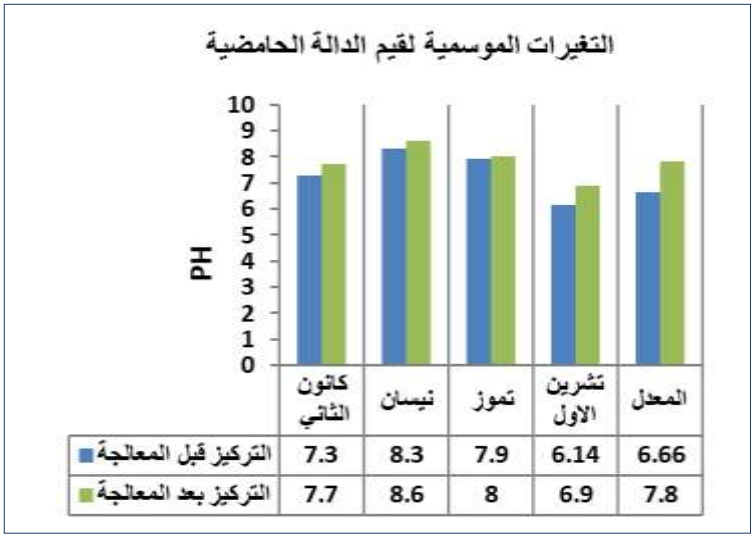

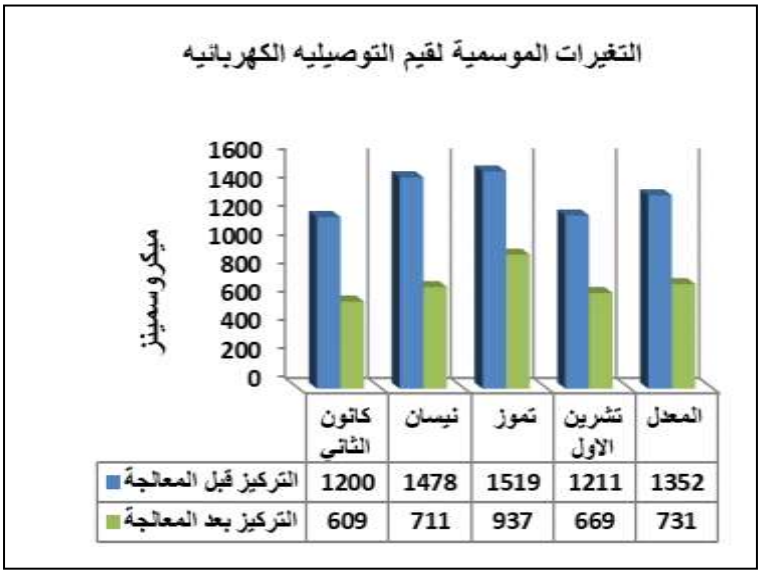

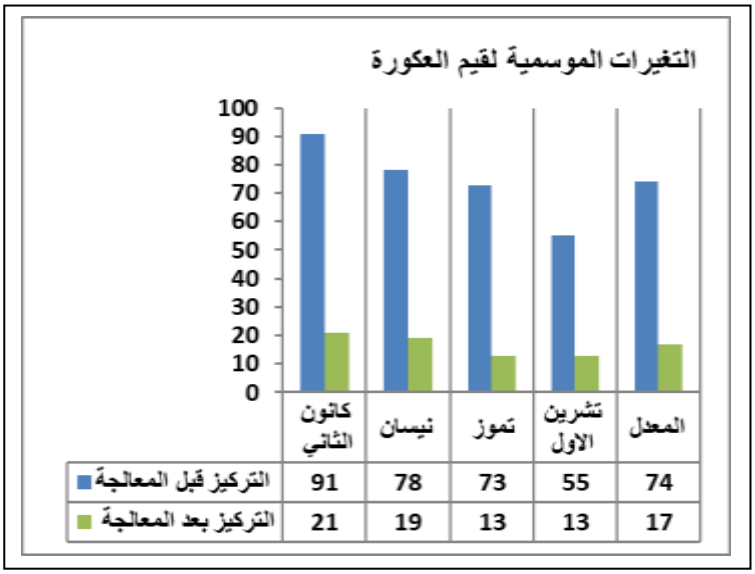

التغيرات الموسمية لقيم الملوحة

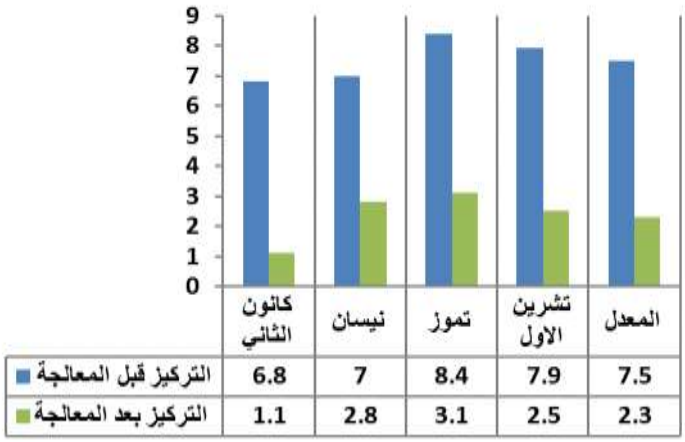

	كانون الثاني	نيسان	تموز	تشرين الاول	المعدل
التركيز قبل المعالجة	6.8	7	8.4	7.9	7.5
التركيز بعد المعالجة	1.1	2.8	3.1	2.5	2.3

التغيرات الموسمية للمواد الصلبة الذائبة

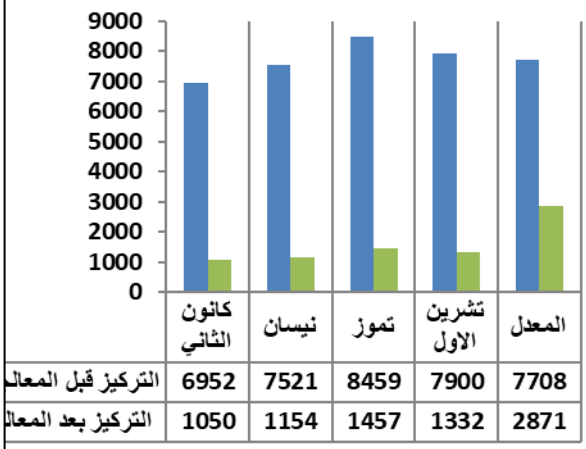

	كانون الثاني	نيسان	تموز	تشرين الاول	المعدل
التركيز قبل المعالجة	6952	7521	8459	7900	7708
التركيز بعد المعالجة	1050	1154	1457	1332	2871

كفاءة محطة المعالجة في أزالة البيكاربونات (HCO_3^{-1})

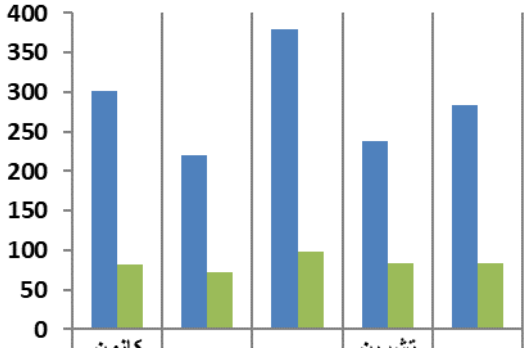

	كانون الثاني	نيسان	تموز	تشرين الاول	المعدل
التركيز قبل المعالجة	301	220	380	238	284
التركيز بعد المعالجة	81.8	72.4	97.7	83.5	83.7

كفاة محطة المعالجة في أزالة (DO)

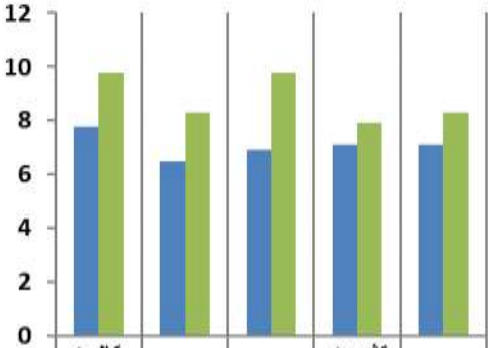

	كانون الثاني	نيسان	تموز	تشرين الاول	المعدل
التركيز قبل المعالجة	7.8	6.5	6.9	7.1	7.1
التركيز بعد المعالجة	9.8	8.3	9.8	7.9	8.3

كفاءة محطة المعالجة في أزالة أيون الفوسفات $(PO_4)^{-3}$

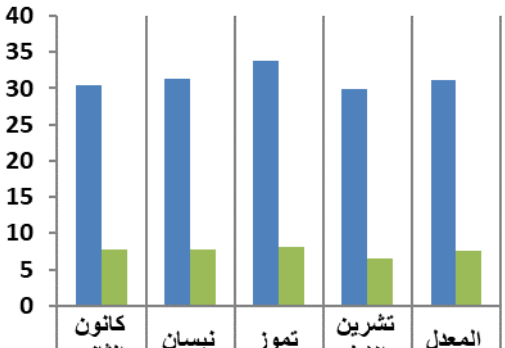

	كانون الثاني	نيسان	تموز	تشرين الاول	المعدل
التركيز قبل المعالجة	30.4	31.3	33.7	29.9	31.1
التركيز بعد المعالجة	7.7	7.8	8.1	6.5	7.5

كفاءة مجطة المعالجة في أزالة أيون الكبريتات $(SO_4)^{-2}$

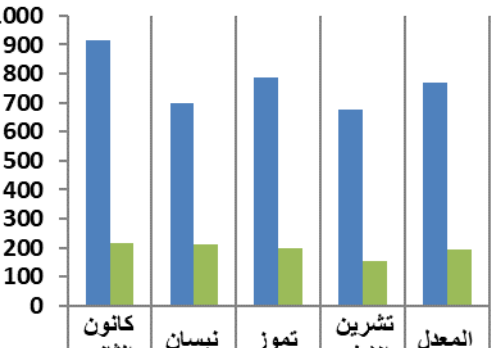

	كانون الثاني	نيسان	تموز	تشرين الاول	المعدل
التركيز قبل المعالجة	914	699	785	676	769
التركيز بعد المعالجة	214	211	200	154	195

كفاءة محطة المعالجة في أزالة أيون الكلوريد $(Cl)^-$

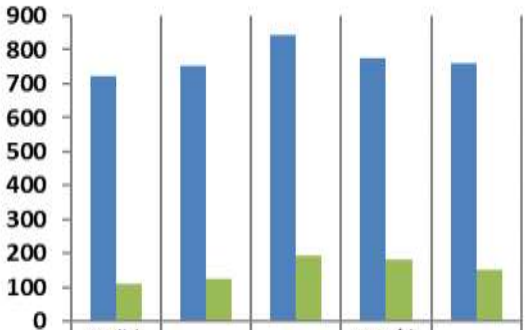

	كانون الثاني	نيسان	تموز	تشرين الاول	المعدل
التركيز قبل المعالجة	721	753	842	775	760
التركيز بعد المعالجة	112	124	192	183	152

كفاءة محطة المعالجة في أزالة أيون النترات $(NO_3)^-$

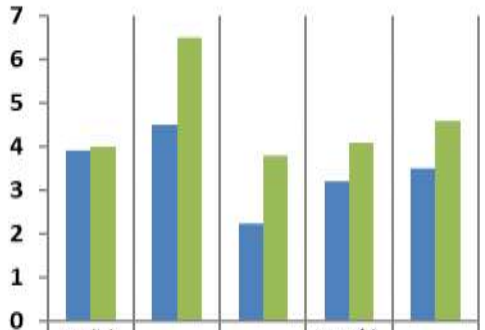

	كانون الثاني	نيسان	تموز	تشرين الاول	المعدل
التركيز قبل المعالجة	3.9	4.5	2.24	3.2	3.5
التركيز بعد المعالجة	4	6.5	3.8	4.1	4.6

التغيرات الموسمية للمواد الصلبة العالقة

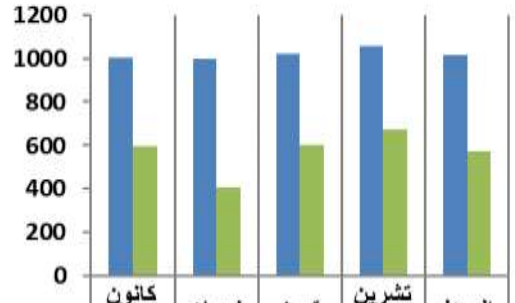

	كانون الثاني	نيسان	تموز	تشرين الاول	المعدل
التركيز قبل المعالجة	1002	996	1021	1056	1018
التركيز بعد المعالجة	598	406	603	675	570

كفاءة محطة المعالجة في أزالة العسره الكلية (TH)

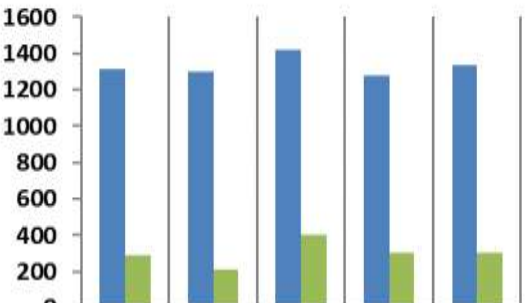

	كانون الثاني	نيسان	تموز	تشرين الاول	المعدل
التركيز قبل المعالجة	1315	1300	1420	1275	1335
التركيز بعد المعالجة	287	215	402	303	301

كفاءة محطة المعالجة في أزالة المبيدات الحشريه

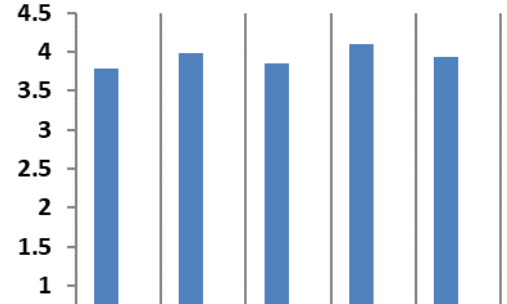

	كانون الثاني	نيسان	تموز	تشرين الاول	المعدل
التركيز قبل المعالجة	3.78	3.99	3.85	4.1	3.93
التركيز بعد المعالجة	0.022	0.036	0.035	0.045	0.034

كفاءة محطة المعالجة في أزالة التلوث بالفينولات

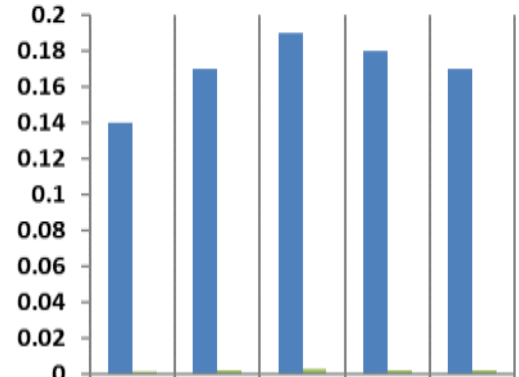

	كانون الثاني	نيسان	تموز	تشرين الاول	المعدل
التركيز قبل المعالجة	0.14	0.17	0.19	0.18	0.17
التركيز بعد المعالجة	0.0018	0.0024	0.0028	0.0022	0.0023

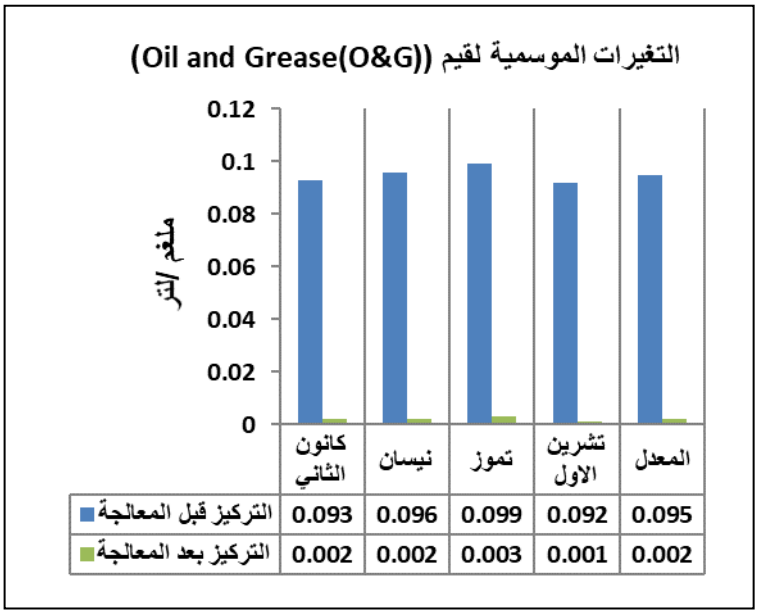
التغيرات الموسمية لقيم (Oil and Grease(O&G))
ملغم/لتر
0.12
0.1
0.08
0.06
0.04
0.02
0
كانون الثاني
نيسان
تموز
تشرين الاول
المعدل
التركيز قبل المعالجة 0.093 0.096 0.099 0.092 0.095
التركيز بعد المعالجة 0.002 0.002 0.003 0.001 0.002

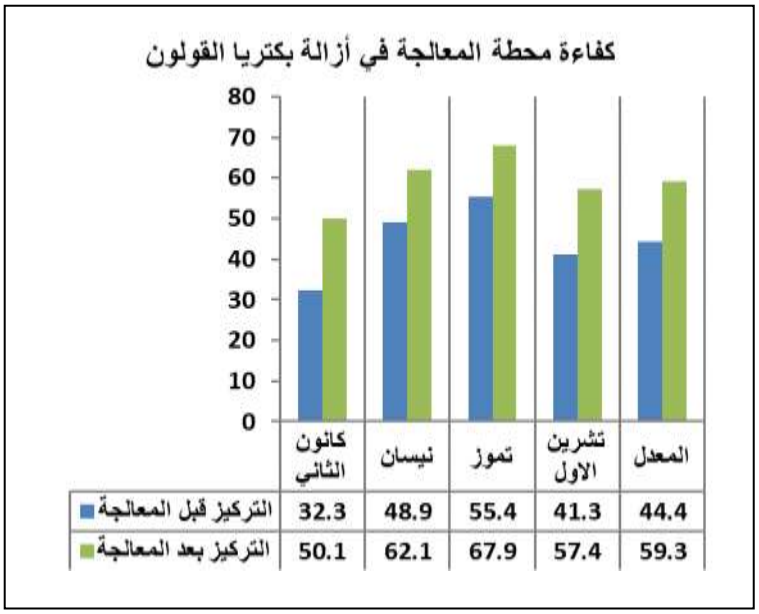
كفاءة محطة المعالجة في أزالة بكتريا القولون
80
70
60
50
40
30
20
10
0
كانون الثاني
نيسان
تموز
تشرين الاول
المعدل
التركيز قبل المعالجة 32.3 48.9 55.4 41.3 44.4
التركيز بعد المعالجة 50.1 62.1 67.9 57.4 59.3

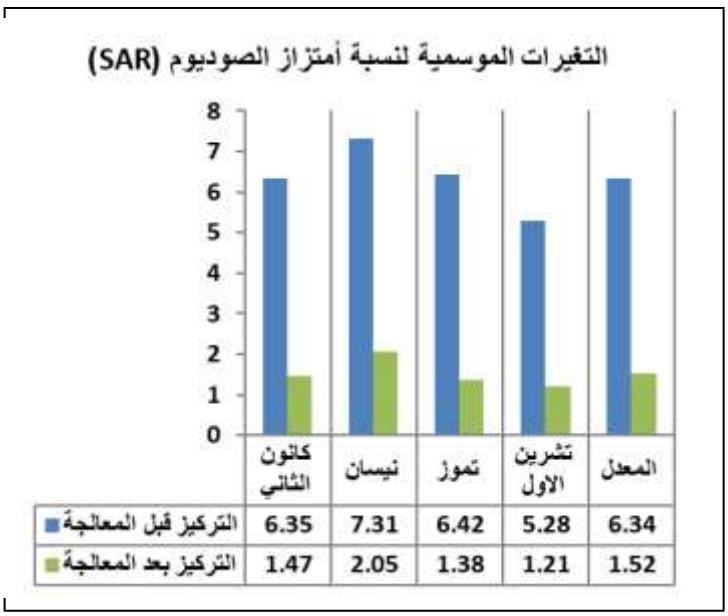
التغيرات الموسمية لنسبة أمتزاز الصوديوم (SAR)
8
7
6
5
4
3
2
1
0
كانون الثاني
نيسان
تموز
تشرين الاول
المعدل
التركيز قبل المعالجة 6.35 7.31 6.42 5.28 6.34
التركيز بعد المعالجة 1.47 2.05 1.38 1.21 1.52

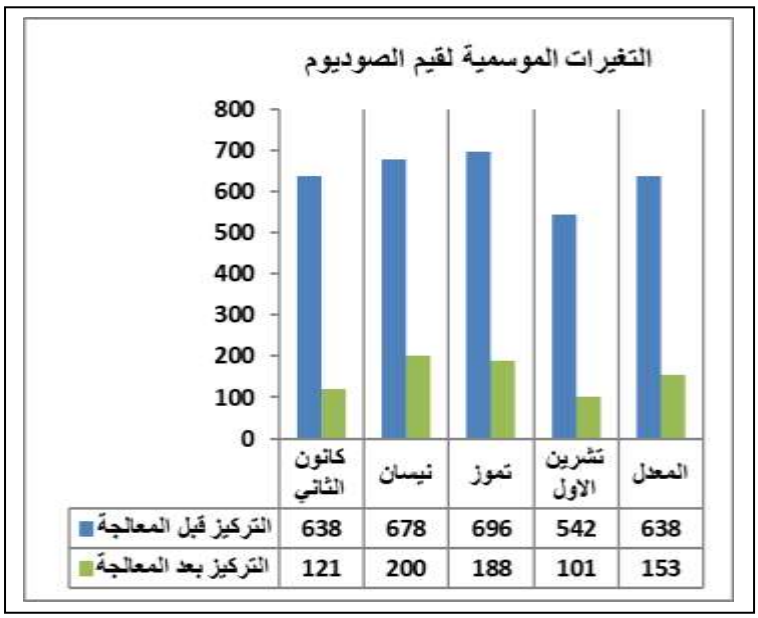
التغيرات الموسمية لقيم الصوديوم
800
700
600
500
400
300
200
100
0
كانون الثاني
نيسان
تموز
تشرين الاول
المعدل
التركيز قبل المعالجة 638 678 696 542 638
التركيز بعد المعالجة 121 200 188 101 153

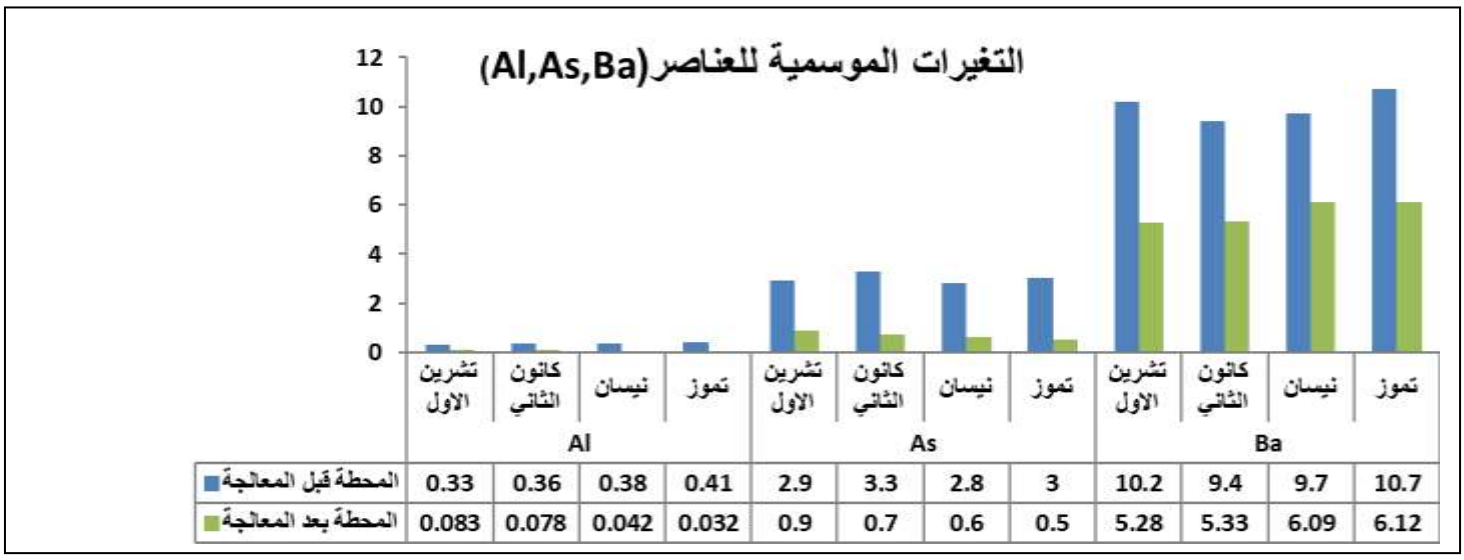
التغيرات الموسمية للعناصر(Al,As,Ba)
12
10
8
6
4
2
0
Al
As
Ba
تشرين الاول
كانون الثاني
نيسان
تموز
المحطة قبل المعالجة 0.33 0.36 0.38 0.41 2.9 3.3 2.8 3 10.2 9.4 9.7 10.7
المحطة بعد المعالجة 0.083 0.078 0.042 0.032 0.9 0.7 0.6 0.5 5.28 5.33 6.09 6.12

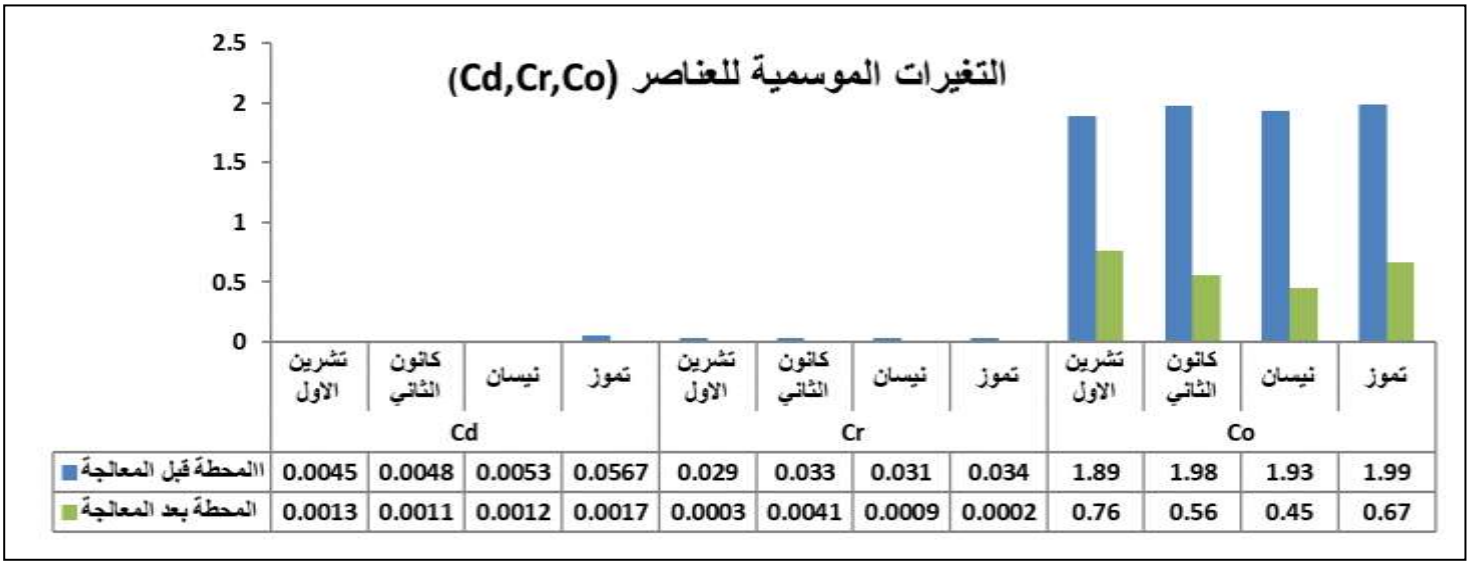

	Cd				Cr				Co			
	تشرين الاول	كانون الثاني	نيسان	تموز	تشرين الاول	كانون الثاني	نيسان	تموز	تشرين الاول	كانون الثاني	نيسان	تموز
المحطة قبل المعالجة	0.0045	0.0048	0.0053	0.0567	0.029	0.033	0.031	0.034	1.89	1.98	1.93	1.99
المحطة بعد المعالجة	0.0013	0.0011	0.0012	0.0017	0.0003	0.0041	0.0009	0.0002	0.76	0.56	0.45	0.67

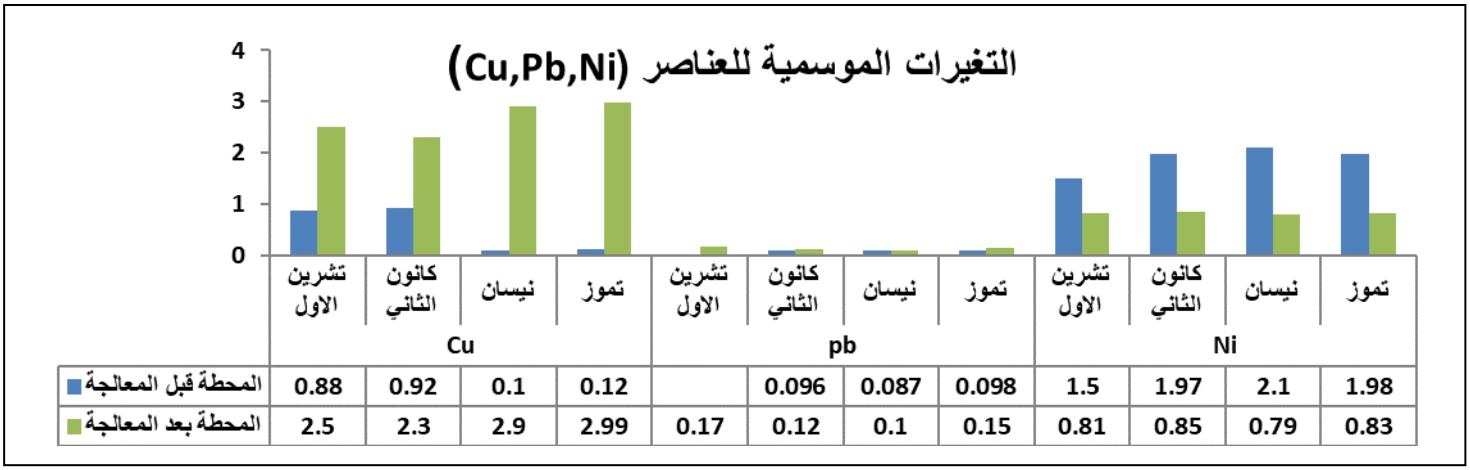

	Cu				pb				Ni			
	تشرين الاول	كانون الثاني	نيسان	تموز	تشرين الاول	كانون الثاني	نيسان	تموز	تشرين الاول	كانون الثاني	نيسان	تموز
المحطة قبل المعالجة	0.88	0.92	0.1	0.12		0.096	0.087	0.098	1.5	1.97	2.1	1.98
المحطة بعد المعالجة	2.5	2.3	2.9	2.99	0.17	0.12	0.1	0.15	0.81	0.85	0.79	0.83

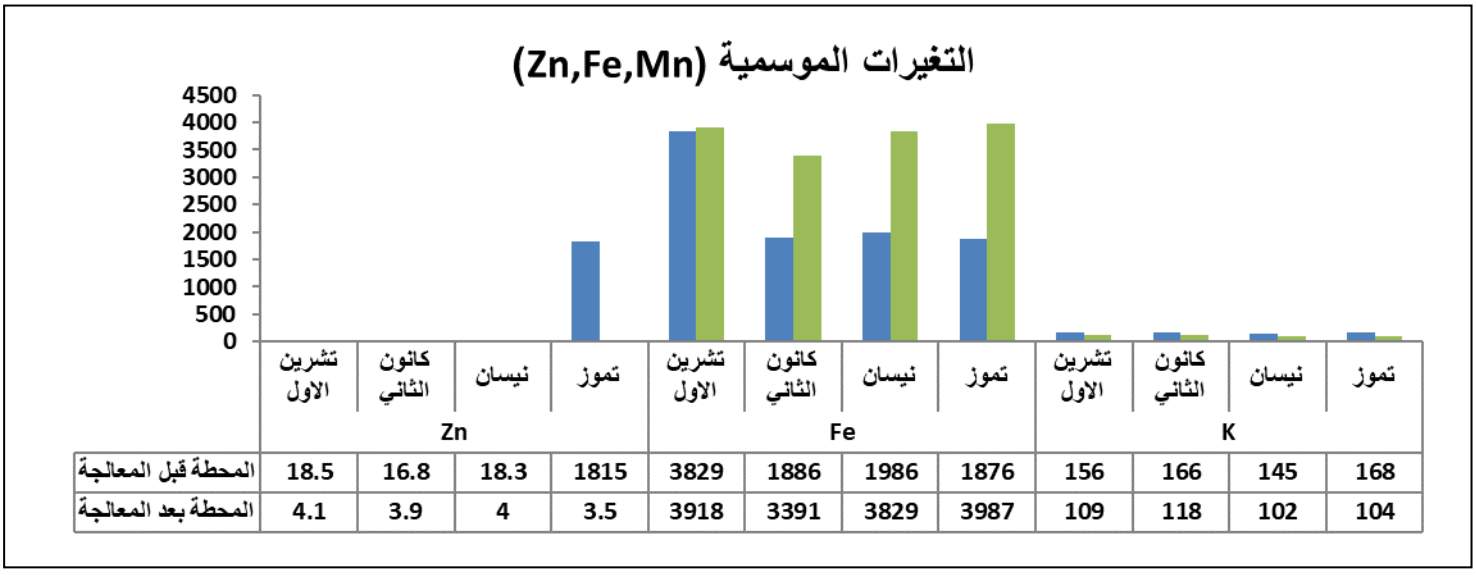

	Zn				Fe				K			
	تشرين الاول	كانون الثاني	نيسان	تموز	تشرين الاول	كانون الثاني	نيسان	تموز	تشرين الاول	كانون الثاني	نيسان	تموز
المحطة قبل المعالجة	18.5	16.8	18.3	1815	3829	1886	1986	1876	156	166	145	168
المحطة بعد المعالجة	4.1	3.9	4	3.5	3918	3391	3829	3987	109	118	102	104

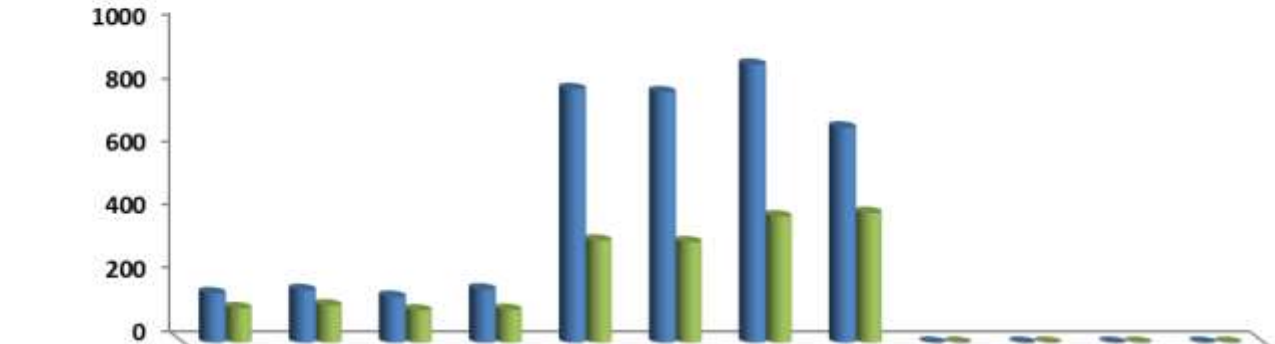

	تشرين الاول	كانون الثاني	نيسان	تموز	تشرين الاول	كانون الثاني	نيسان	تموز	تشرين الاول	كانون الثاني	نيسان	تموز
	K				Mg				Se			
المحطة قبل المعالجة	156	166	145	168	799	789	876	678	0.0038	0.0056	0.0076	0.0098
المحطة بعد المعالجة	109	118	102	104	322	317	398	409	0.0001	0.0001	0.0003	0.0002

أما بقيه الفحوصات كانت منعدمة تماما وهيالسيانيد(Cyanides) والزئبق (Mercury)و(PCB)و(VOCs)

المناقشة :- discussions

أظهرت نتائج الدراسة أن درجة حرارة الماء تراوحت قبل المعالجة بين (18^0C) في فصل الشتاء و(34^0C) في فصل الصيف وبعد المعالجة (14^0C)في فصل الشتاء و(33^0C) في فصل الصيف وهذا يعود إلى طبيعة مناخ العراق حيث يكون المناخ حار جاف صيفا وبارد ممطرشتاءا وربما أن يكون سببا هو أمتلاك الماء سعة حرارية عالية مما يجعل مياه النهرقادرة للاحتفاظ بحرارته رغم تذبذب حرارة المحيط [26].

ونلاحظ من خلال القيم أن المياه العراقية تتميز بالقاعدية الخفيفة وهي ضرورية لنشاط البكتريا اثناء عمليات التهوية حيث كانت أقل قيمه لPH قبل المعالجة(6.14) في فصل الخريف وأعلى قيمة (8.3) في فصل الربيع اما بعد المعالجة فكانت اقل قيمه(6.9) في فصل الخريف وأعلى قيمة (8.6) في فصل الربيع حيث يتراوح الحدالمفضل لمياه الشرب بين (7-8.5) القيم العالية في فصل الربيع تعود نتيجة أعتدال درجة الحرارة فيتشجع النشاط الاحيائي وتقوم بتحررغاز(Co_2) وتحلل البيكاربونات أما ألقيم الواطئة في فصل الخريف كانت تعود الى قلت نشاط الاحياء أوارتفاع تركيزغاز(Co_2) وتفاعلة مع الماء وتكوين حامض الكاربونيك الذي بدورة يدفع الداله الحامضية نحوتقليل القاعدية [27] .

وأقل قيمة سجلت قبل معالجة التوصيلية الكهربائية EC هي (1200)ميكروسيمنز/سم في فصل الشتاء وأعلى قيمة (1519) ميكروسيمنز/سم في فصل الصيف هذا مايثبت أنها عالية الملوحة جدا أما بعد

المعالجة أقلها(609) ميكروسيمنز/سم في فصل الشتاء وأعلاها(937) ميكروسيمنز/سم خلال فصل الصيف القيم العالية تعود الى ارتفاع درجات الحرارة الذي تؤدي الى تبخرالمياه وبالتالي زيادة تركيزالأملاح أما الانخفاض يرجح الى تخفف تراكيزالاملاح بالإمطار المتدفقة [28] .

ونتائج دراسة العكورة قبل المعالجة أقل قيمة سجلت هي (55) ملغم/لترخلال فصل الخريف أما اعلى قيمه (91) ملغم/لترخلال فصل الشتاء وبعد أجراء المعالجة أقل قيمة مسجلة هي (13) ملغم/لترخلال فصل الخريف واعلى قيمه (21)ملغم/لترخلال فصل الشتاء الارتفاع أسبابه سقوط الأمطار وزيادة حركة الترسبات مع تيارالماء وبالتالي تزداد حركة المواد العالقة لوجود الطحالب والمواد العضوية لان العكورة تزداد قيمتها بأزدياد المياه الجارية أما الانخفاض يعزى الى أنخفاض مناسيب المياه [29].

وسجلت المواد الصلبة الذائبة الكلية قبل المعالجة أقلها (6952) ملغم/لترخلال موسم الشتاء وأعلاها (8459) ملغم/لترخلال موسم الصيف بينما بعد المعالجة أقلها (1050)ملغم/لترخلال الشتاء وأعلاها (1457) في فصل الصيف التراكيزالعالية تعود الى زيادة نسبة المواد اللاعضوية الذائبة خلال موسم الصيف والاحتمال الاكثر يعود لذوبان الأملاح الذي يرتفع بارتفاع درجات الحرارة أما التراكيز المنخفضة في فصل الربيع نتيجة انخفاض درجة الحرارة وتاكسد المواد العضوية وترسب اللاعضوية [30].

أما نتائج دراسة الملوحة (Salinity) قبل المعالجة أقل قيمة كانت في فصل الشتاء(6.8) غم/ لترالذي تعود أسبابها الى نزول الامطار وأرتفارع مناسيب النهروأعلى قيمة (8.4)غم/ لترفي فصل الصيف وذلك يعود الى زيادة المبازل وانخفاض مياه النهرأما بعد المعالجة نلاحظ نسبة الملوحة انخفضت بشكل كبيروكانت اقلها في فصل الشتاء (1.2)غم/لتر وأعلاها في فصل الصيف (3.1)غم/ لتر[31].

ونتائج الأوكسجين الذائب Dissolved Oxygen قبل المعالجة أعلى قيمة (7.8) ملغم/ لترخلال موسم الشتاء وأقل قيمة (6.5) ملغم/ لترخلال موسم الربيع أما بعد المعالجة نلاحظها أرتفعت أعلى مما كانت عليه لتصبح (9.8) غم/ لترفي فصل الشتاء و(7.2)غم/ لترفي فصل الصيف والقيم العالية خلال موسم الشتاء تعزى الى انخفاض درجة حرارة المياه وكثرت ذوبان الغازات تتناسب عكسيا مع درجة حرارة الماء وهذا مايوكد أرتفاع قيمه الاوكسجين المذاب نسبة للتهوية الجيدة والخلط الدائم أمّا القيم الواطئة في فصلي الربيع والصيف تعود الى قله منسوب المياه وكثرت عمليات التحلل العضوي نظرا لارتفاع درجة الحرارة والحاجة العليا لاستهلاك الاوكسجين المذاب خلال هذه العمليات [32]

وبينت نتائج ايون البيكاربونات (HCO_3^{-1}) قبل عملية المعالجة اقل قيمة (220) ملغم /لترخلال موسم الربيع وربما يعود السبب الى أنخفاض درجات الحرارة واعلى قيمة (380) ملغم/لترخلال موسم الصيف و تعزى الى ارتفاع درجة الحرارة وبالتالي ارتفاع تركيز(CO_2) وبعدها سوف يتكون حامض الكاربونيك الذي يولد أيون البيكاربونات (HCO_3^{-1}) عند تفككه وهذا ينطبق مع العديد من الدراسات بوجود علاقة

طردية بين أيون البيكاربونات ودرجة الحرارة أوربما أزدهارالنباتات في الصيف حيث توثرعلى كمية غاز(CO_2) الموجود في الجو وبالتالي تثبيت الكاربون أما بعد المعالجة قلت قيمه البيكاربونات لتصبح (72.4) ملغم /لترفي فصل الربيع وأعلى قيمة (97.7) ملغم /لترفي فصل الصيف [33].

أعلى تركيزلأيون الكبريتات (SO_4^{-2}) في العينات قبل معالجتها (914) ملغم/لترفي فصل الشتاء والذي تعزى أسبابه الى كثرت الغبارونوع الطبيعة الجبسية للترب الرسوبية المليئه بالنهرالذي تكون أهم مصادرالكبريتات في المياه وأقل قيمة كانت (676) ملغم/ لترخلال موسم الخريف وقد تعود لنوعيه مياه المبازل وجرف هذا التركيز أما بعد معالجة نلاحظ أن أعلى تركيزسجل في فصل الشتاء(241) ملغم/لترواقل تركيز في فصل الخريف (154) ملغم/لترو انخفاض تركيزايون الكبريتات في محطات المعالجة قد تكون أسبابه عمليات الترسيب وتأكسد البعض منه في الأحواض الخاصة بعمليات التهوية بفعل استهلاكها من قبل البكتريا الهوائية [34] .

ونتائج أيون الفوسفات (PO_4^{-3}) قبل المعالجة اقل تركيز(29.9) ملغم/ لترخلال موسم الخريف وقد تكون أحد أسباب قله التركيزهوالالتصاق العالي لهذا الايون بدقائق التربة ويكون مهم لأغراض الزراعة لمحصولي الحنطة والشعيراوأستهلاكه من قبل الهائمات النباتيه وأعلى تركيز(33.7) ملغم/لترخلال موسم الصيف وربما أسباب القيم العالية تعود الى تحلل الهائمات النباتيه وطرح الفضلات وكثرت أستخدام المنظفات والمساحيق الحاوية على مركبات الفسفورأما بعد معالجة الفوسفات كان أقل تركيز(6.5) ملغم/ لترخلال موسم الخريف وأعلى تركيزسجل في فصل الصيف (8.1) وهذا الانخفاض بعد عملية المعالجة أسبابه عمليات الترسيب المتكررة [35].

كانت النتائج للنترات (NO_3^{-1}) قبل المعالجة أقل قيمة (2.24) ملغم /لترخلال موسم الصيف وأعلى قيمة (4.5) ملغم/ لترخلال موسم الربيع والقيم العالية للنترات نتيجة للاضافات الزراعية أمّا القيم الواطئة تعزى الى ازدياد أعداد الهائمات النباتية التي تعمل على أستهلاك النترات وأعتبرها مغذيات من قبل الخلايا النباتيه أما بعد المعالجة فتركيز أيون النترات أرتفع ليصبح أقل تركيز (3.8) ملغم /لترفي فصل الصيف وأعلى قيمة (6.5) ملغم/ لترفي فصل الربيع وربما الزيادة في تركيزأيون النترات بعد المعالجة تعود الى تأكسد البعض من المركبات الحاويه على النتروجين وتحويلها الى نترات وبالإضافة الى عمليات التهوية التي تعمل على أكسدة المركبات وتحويلها الى نترات [36].

سجلت النتائج لأيون الكلوريد (Cl^{-1})قبل المعالجة أقل قيمة (721) ملغم/ لترخلال موسم الشتاء يعود لانخفاض درجة الحرارة وقلة عمليات تبخرالمياه أوكون الكلوريفقد من جراء العمليات الفيزوكيمياوية والبايولوجية وأعلى قيمة (842) ملغم/ لترخلال موسم الصيف يعود للارتفاع الى زيادة معدلات التبخرنسبة لارتفاع درجات الحرارة أمابعد عملية المعالجة تبين أن تركيزالكلوريد أنخفض ليصبح أقل(112) ملغم/ لترخلال موسم الشتاء وأعلى قيمة (183) ملغم/ لترخلال موسم الصيف [35].

قبل معالجة العسرة الكلية Total-Hardness أقل قيمة مسجلة (1275) ملغم/لترخلال موسم الخريف سببها انخفاض تركيزكل من ايونات الكالسيوم والمغنيسيوم في المياه وأعلى قيمة (1420) ملغم/لترخلال موسم الصيف وهذا قد يعود الى كمية التصاريف وانخفاض المناسيب أو طرح الفضلات الزراعية في المياه وبعد معالجة العسرة قلت التراكيزلتصبح أقل تركيز (215) ملغم/لترخلال موسم الربيع وأعلى تركيز(402) ملغم/لترخلال موسم الصيف[35].

أما تراكيزللمواد العالقة Total suspended solids قبل المعالجة أعلها (1056)ملغم /لترفي فصل الخريف وأقلها (996) ملغم /لترفي فصل الربيع أما بعد المعالجة قل التركيز ليصبح أعلى تركيز(675) ملغم /لترفي فصل الخريف وأقل تركيز(406)ملغم /لترفي فصل الربيع والأرتفاع في تراكيزالمواد الصلبة العالقة نتيجة زيادة الفضلات الصلبة والمطروحات السائلة أما الانخفاض نتيجة ترسب المواد الصلبة في حوض الترسيب[36].

سجلت أعلى قيمة للفينولات قبل المعالجة(0.19)ملغم /لترفي فصل الصيف وأقل قيمة كانت (0.14) في فصل الشتاء لكن بعد عمليات المعالجة قلت لتصبح ضيئلة تماما وكانت أعلى قيمه حوالي(0.0028)ملغم /لترفي فصل الصيف وأقل قيمة (0.0018) في فصل الشتاء ولاتوجد اي تاثيرات ضارة تذكرمنها [37] .

وبينت المبيدات أعلى قيمة (4.1)ملغم /لترفي فصل الخريف وأقل قيمة(3.78) ملغم /لترفي فصل الشتاء أما بعد معالجة المبيدات قلت التراكيز لتصبح أعلى قيمة(0.045)ملغم /لترفي فصل الخريف وأقل قيمة(0.022) ملغم/لترفي فصل الشتاء يكمن الضررفي كونها مركبات حلقية بطيئة التحلل ذات سمية عالية هذا يوكد الإسراف في استخدام الأسمدة النتروجينية والفوسفاتيه في مراحل مختلفة لزيادة النموالمحاصيل الزراعية في فصل الخريف أما قلتها في فصلي الشتاء نتيجة سقوط الامطاروالجرف المستمر لهذه الأسمدة [38] . وقيمة لبكتريا القولونFaecal coliform سجلت أدنى تركيز (32.3) خلال موسم الشتاء وأعلى قيمة (55.4) خلال موسم الصيف وبعد أجراءعمليات المعالجة أعلى قيمه كانت خلال موسم الصيف(67.9) وأقلها في موسم الشتاء لتسجل (50.1) لوحظ أن القيم المرتفعه توكد انعدام الكلورين وارتفاع درجات الحرارة لتوفرظروف ملائمة لنمو البكتريا والمغذيات الذائبة في الماء ولايحد من نموها موسم انما مرتبط زيادتها ونقصانها بحسب الوسط الذي توفر لها كافه الظروف فلذلك يجب أجراء عمليات ترشيح دقيقة في محطات التصفية والابتعاد عن أضافه المواد الكيماوية [39].

والزيوت والشحوم قبل المعالجة Oil and Grease سجلت ادنى قيمة(0.092)ملغم/لترفي فصل الخريف وأعلى قيمة كانت (0.099) ملغم/لترفي فصل الصيف أما بعد المعالجة نلاحظ أقل قيمة كانت (0.001) ملغم/لتر في فصل الخريف أما أعلى قيمة سجلت (0.003)ملغم/لتر في فصل الصيف الزيادة تعزى الى تاثيرالمخلفات المنزلية ومخلفات الشركات النفطية عن طريق رميها مباشرة بالنهرمن دون جدوى أما القيم الوأطئه تعود الى عمليات التخفيف وتحويل الدهون من مستحلبه الى طافية [40].

أما نتائج عنصر الصوديوم(Na^{+1}) قبل المعالجة أقل قيمة (542) ملغم/لتر خلال موسم الخريف بينما أعلى قيمة سجلت في فصل الربيع (678) ملغم /لتر وبعد عمليات المعالجة كانت القيمه الاقل في فصل الخريف(101) ملغم/لتر والأعلى في فصل الربيع (200) ملغم/لتر الانخفاض أسبابه الى حصول عمليات التخفيف نتيجة ارتفاع مناسيب المياه أوأستهلاكة من قبل الاحياء أما الارتفاع يعود الى التاثيرات الزراعية للاراضي المحيطة بالنهر [41].

ونتائج دراسة نسبة امتزاز الصوديوم Sodium Absorption Ratio قبل المعالجة أقلها (5.28) ملغم/لتر خلال موسم الخريف وأعلاها سجلت في فصل الربيع (7.31) ملغم /لتر وبعد المعالجة كانت القيمه الاقل في فصل الخريف(1.21) ملغم/لتر والأعلى في فصل الربيع (2.05) ملغم/لتر تكون العلاقه طرديه بين أيون الصوديوم ونسبة الامتزاز وتبين ان مياه النهر ذات صوديوم عالي يتفق مع العديد من الدراسات [41].

أما تراكيز العناصر الثقيلة قياساتها بعد المعالجة ضمن الحدود المسموح بها (Al,As,Ba,Cr,Co,Ni,Zn,Mn,K,Mg,Se) والعناصر الاخرى فقيمتها كانت العكس مرتفعة بعد معالجتها وانها ذات خطورة (Pb,Cu,Fe) والانخفاض أسبابه نشاط الأحياء المجهرية التي تسحب كمية مختلفة من المعادن وهذا ماأكدته الدراسات الحديثة أرتباط الطحالب والعناصر الثقيلة وكيفيه سحبة من الماء وأدمصاصة وميل هذه العناصر لعمليتي الادمصاص أوالامتصاص مع الرواسب [42].

مدى صلاحية مياه النهر للشرب :-

اعتمدت المواصفات القياسية لمياه الشرب على أهم العناصر المكونة له وقيمت مدى صلاحية مياه النهر مع المواصفات المقترحة من قبل منظمة الصحة العالمية وكانت نتائج المحطة بعد المعالجة أنها مقبوله نوعا ما وتحتاج القليل من الكفاءة [43].

الصفة	الحد الادنى	الحد الاقصى	الحدود القياسية
pH	**6.9**	**8.6**	8.5 -6.5
TDS	**1050**	**1457**	500-1500
Turbidity	**21**	**13**	0-25
DO	**7.9**	**9.8**	5 <
l/Cl mg	**122**	**192**	250
l/SO4 mg	**154**	**241**	250
l/NO_3 mg	**3.8**	**6.5**	45
l/PO_4 mg	**6.5**	**8.1**	0.4
l/Na mg	**101**	**200**	200

جدول (2) يمثل مقارنة قيم بعض المحددات البيئية لمياه النهر بعد المعالجة مع المعايير العالمية

الاستنتاجات :-

1-لاحظنا أرتفاع ملوحه النهروالدالة الحامضية (PH) فيها أكثر من7 أمانسبة الاوكسجين الذائب فيه أكبرمن 5 ملغم /لتروهذا مايجعلها ذات تهويه جيدة وانها ضمن المدى الطبيعي لنمو الأحياء .

2- تلوث محطة المعالجة بالبكتريا البرازية وهذا لايعطي مياه صالحة مما يستدعي أضافه كميات هائلة من الكلورللقضاءعلى نموالأحياء الدقيقة .

3- لاحظنا زيادة في تركيزأيون النترات بعد المعالجة وله اثركبيرفي أعادة تكوين الاوكسجين في الماء وخلق ظروف سامة للبيئة المائية أما تركيز الفوسفات اكثر من الحدود المسموحة يعود لمروره بمناطق زراعية واسعة معرضه للأسمدة والمغذيات النباتية.

4- مستويات التلوث العضوي واللاعضوي في محطة المعالجة تكاد ان تكون معدومة ويتطلب الامرفقط زيادة المعالجات وكفاءة أكثرفي العمل للتخلص من العوالق والشوائب واي مشاكل أخرى .

التوصيات :-

1- تأسيس صناديق استثمارية تختص بانشاء محطات معالجة أكثركفاءة على المصب العام والاستفادة منها لأغراض الزراعة والاستهلاك البشري ووضع قوانين صارمة للمطروحات الملوثة .

2- أنشاء محميات على النهرلتربية الدواجن والاسماك محاطة باشجارقادرة على تحمل الملوحة ودائمة الخضارمثل الكالبتوزلاهميتها في تقليل التلوث .

3- عدم هدرمياه النهرالى البحربل تغير مساره الى الصحراء الجنوبية بين البصرة والناصرية والاستفادة من الثروة المائية ومعالجتها بالطرق الحديثة للتغلب على شحة المياه .

4- استخدام الطاقة الشمسية في تحليه مياه النهرباعتبارها طاقة اقتصادية نظيفة متجددة لاتتطلب المزيد من الوقود والجهد .

5- أجراء مسح شامل ودراسات أكثرعمقا لهذا النهرللتعرف على كمية التلوث الحاصلة والتخلص منها.

المصادر (References)

1- السعدي ,حسين علي ,(2002)"علم البيئة والتلوث",وزارة التعليم العالي والبحث العلمي ,جامعة بغداد ,ص(48).

2- صبحي عبد الستار حسن, صادق الغنيماوي,حسين الزاملي , (2016)" تقيم كفاءة محطة معالجة مياه الصرف الصناعي في شركة واسط العامة للصناعات النسيجية "مجلة كلية التربية /جامعة واسط. العدد(27)

3- حسين عبد الواحد اكطامي, (2020)"مشكلة شحة المياه في محافظة البصرة واثرها في البيئة والتنمية " مجلة دراسات تربوية .العدد(52) .

4-حمدان باجي نوماس ,مروة فريد عودة كاظم , (2018)"الخصائص النوعية لمياه شط العرب قرب محطات توليد الطاقة الكهربائية وصلاحيتها للاستخدامات المختلفة "مجلة الخليج العربي,المجلد (46).المجلد (1)العدد(2)

5-Ali.A.A, Brian. G. J and Samuel .M,(2019)" Spatiat- temporal analysis of Aerosol Index (AI) distribution and some climatic factors study from Iraq" Modeling Earth Systems and Environment 5(1)pp: 203-216.

6- أبراهيم عبد الكريم,تحسين علي زيدان ,وهران سعود ,(2009) "دراسة بعض الملوثات البكترية في مياه نهرالفرات وبحيرتي الحبانية والثرثار"مجلة جامعة الانبارللعلوم الصرفة.المجلد (3),العدد (3).

7- أحصائيات وزارة البيئة , "التلوث البكتريولوجي" لعام(2023) تقاريرغيرمنشورة .قسم السيطرة النوعية

8-Khalid .J.S, (2017)" Effects of Neighbouring Countries Policies on the Future of Water Resources in Iraq " Journal of the collegeof Basic Education, University of Babyion,(36) .

9- عبد الله تركي حميد , (2013) "الضررالبيئي وتعويضة في المسؤولية المدنية " منشورات الحلبي الحقوقية لبيروت ,ص87 .

10- جليل كامل غيدان ,أحمد عبد سلمان , (2014)" الاثارالاقتصادية لتلوث المياه في العراق " دراسة تابعة لكلية الادراة والاقتصاد /جامعة واسط

11-Nadhir Al- Ansari, Nahla .A and Jan .L, (2021)"Water scarcity:Problems and possible solutions" Journal of Earth Sciences and Geotechnical Engineering ,11(2),pp:243-312 .

12- الركابي ,حسين يوسف والخفاجي ,باسم يوسف وخلف ,وسن فاضل,(2013) " دراسة كمية ونوعية للهائمات في المصب العام عند مدينة الناصرية ,جنوب العراق .مجلة علوم ذي قار, العدد (4) المجلد (1).ص 42.

13- صادق صاحب منشور, (2018) "أستخدام بعض الأدلة البيئية في تقيم صلاحية مياه المصب العام واستخدامها كبديل عن نهرودجلة الفرات ".

14- نصير فاضل خضير, (2020) "أستراتيجية مقترحة لاستخدام مياه المصب في الزراعة "دراسة تابعة لوزارة الموارد المائية /دائرة المصب العام .

15- سعد شهد محمد العمري , (2010)" تقييم لنوعية مياه نهرالمصب العام في محافظة ذي قار" ,رسالة ماجستير لجامعة ذي قار.كلية العلوم.

16- محمد رضا عبد الامير ,رياض الطحان ,صفا مهدي عبد الكاظم, (2013)"تأثير التغيرات الزمنية والموقعية في بعض الخصائص الكيميائية لمياه المصب العام في محافظة بابل "مجلة الفرات للعلوم الزراعية المجلد (5).العدد(4) .ص481-487 .

17- فاطمة الزهراء كريم , حازم عزيز(2022) "التلوث البيئي لمياه النهر في الحلة والكوفة " رسالة ماجستير /كلية العلوم / جامعة الكوفة . .

18 -Nayana .S and Ritu. S, (2017) “Effects of chemical fertilizers and pesticides on human health and environment” Areview, International journal of agriculture, 10(6) ,pp:675-680.

19-محمد ضاري الشبلي , (2006) "استخدام المعدات الميكانيكية والتكنولوجية الوسيلة المتقدمة للقضاء على الأدغال المائية ".مجلة عطاء الرافدين. ,العدد (14).

20-Ail.H.Ghawi, (2017)”Using Natural Coagulant To Remove Turbidity And Heavy Metal From Surface Water Treatment In Iraq,International Journal of Engineering Technology .ISSN:2456-1851.Volume(2).Issue (1),p.p 551-563.

21-غفران فاروق جمعة,رياض حسن الانباري, (2018)" تقيم التلوث بالعناصرالثقيلة في الأراضي الزراعية الواقعة في منطقة جسرديالى" المجلة العراقية لبحوث السوق وحماية المستهلك ,المجلد (2).العدد(3).

22-Aqrawi.A.M,(1993)” Implication of Sea-level fluctuations ,sedimentation and neotectonics for the evolution of the marshlands of southern Mesopotamia” ,Quaternary proccedings. (3).pp:17-26.

23-APHA,(American Public Health Association).(2003).Standard methods for examination of water and waste water ,20th Ed Washington, DC ,USA.

24- شيماء عبيس حسين المعموري ,(2017)"تقيم كفاءة محطة تصفية مياه الشرب في مجمع حي الحسين/قضاء الحمزة الغربي".مجلة جامعة بابل للعلوم الصرفة والتطبيقية .المجلد (25). العدد (6).

25- عقيل عباس الشريفي, (2014) "التلوث المحتمل لبعض العناصر الثقيلة وبعض العوامل البيئية لمياه جدول بني حسن في محافظة كربلاء المقدسة "رسالة ماجستير لكلية التربية –جامعة كربلاء.

26-Hart,A.I.and Zabbey.N, (2005)”Physio-chemistry and benthic fauna of Woji Creek in lower Nigeria Delta “Nigeria.Environ.Ecol.23(2):pp:361-368.

27-Wilson.I and A. Floey,(2003).” Water quality of rivers in the Jordan catchment .Areport forming part of the requirements for state of rivers reporting”.Part2 (DPIWE) .Tasmania.

28-Wetzel.R.G, (2001)Limnology, Lake and river Ecosystims.3rd ed .Academic pres,An Elseveir imprint ,Sanfrancisco, New York ,London.

29-Dybas.C,(2003)“Common water measurement “USGS wetar resources,70(3) PP:306-1070.

30- Abd alsattar .A.A and Aassal.S.A,(2015)”Water quality assessment, and suitability for irrigation purposes of lesser zab river,northern iraq”, University of Mosul,(56),(3).2199-2187p.مجلة العراقية للعلوم

31- محمد تركي خثي ,(2011) "دراسة تأثيرمشروع المصب العام على الصفات الفيزيائية والكيمياوية للتربب المحاذية له وتقييم مياهه لأغراض الري من خلال دراسة بعض الخصائص الفيزيائية والكيميائية لمياه ورواسب النهر في مدينة الناصرية ومقارنتها بالمحددات العالمية " جامعة ذي قار/ كلية العلوم , المجلد (2).العدد(3)

32- حسين ,فلاح حسن ,(2000)" الواقع البيئي لمحافظة بابل لعام 2000“ الندوة العلمية الاولى عن التلوث البيئي لمحافظة بابل /كلية العلوم/ جامعة بابل ,ص5-17 .

33-Weiner.E.R,(2000)”Application of environmental chemistry ” Lewis Puplshers, London. New York.

34-Ghazali, D.and Zaid, A,(2013) “Etude de la qualite physico- chimique et bacteriologique des eaux de la source Ain Salama –Jerri (Region de Meknes-Maroc)”.LARHYSS Journal . (12).ISSN:1112-3680.

35-Abdalaziz.Y.T,Abdulhafedh.M.A and AL-Taay,(2018)”Asssessment of Drinking Water Quality in Mosul University by using WQI Model” Volume(13)Issue (2) pp:185-198,ISSN:1992-0849.

36-Mohammad.R, Satria. F,(2015)” The fluctuation impacts of BOD, COD and TSS in Surabaya’s Rivers to environmental impact assessment (EIA) sustainability drinking water treatment in Surabaya City” International Journal of ChemTech Research (8) ,pp:143-151.

37-Agency for Toxic Substances and Disease Registry (ATSDR), (2008) .Toxicological Profile for phenol ,Atlanta, GA:U.S, Department of Health and Human Services, Public Health Service .

38- فداء الروابدة ,علي الخرابشة ,(2020) " الاستخدام الامن للمبيدات الكيمياوية وأجراءات السلامة العامة ". دراسة عن تصنيف المبيدات واثارها على البيئة ,جامعة الدول العربية ,المنطقة العربية للتنمية الزراعية .

39-عبد العزيزيونس الصفاوي ,ريم عدنان الشنونة ,(2013) " دراسة بيئية وبكتريولوجية لنوعية المياه الجوفية لشرق الموصل " وقائع الموتمرالبيئي الثاني لكلية علوم البيئة وتقناتها.جامعة الموصل (11) 28-27

40- نامق حسين ,اسماعيل ,(2010) " تعويض الاضرار البيئية عن أستخراج النفط واثاره على البيئة " دراسة عن أثارالنفط ومخلفاتة والقوبات المفروضة ,مجلة كلية القانون للعلوم ,جامعة السليمانية . .

41- Mikkelsen.Rand Camberato.J, (1995).”Potassium,Sulfur,limeand micronutrient fertilizers. In: Rechcigl,Soil amendments and environment quality” .Chelesa,England ,Lewis publisher.

42-Sreenath.B, Mohammad .P and Raffaele .M,(2019) “ Sustainable technologies for water purification from heavy metals : review and analysis.” Chemical Society Reveiews ,48(2)pp:463-487.

43-Healey.M.N, (2014) ,”A baseline assessment of water quality in the Gambia River and the potential for community –based monitoring in the Gambia ,West Africa “,Saint Marys University,Science in Applied,1-117p.

Synthesis, Identification heterocyclic derivatives (seven membered) from 2,3-di Chloroaniline and study the biological activity for them

[a] Hussein A. ; [b] Shaimaa A. Bahgat

[1] Ministry of Education, Directorate of Education

AL-Qadisiyah, Diwaniyah, Iraq

[2] Department of Chemistry, College of Education,

University of Al-Qadisiyah, Iraq

Email: shaimaa.adnan@qu.edu.iq

Synthesis, Identification heterocyclic derivatives (seven membered) from 2,3-di Chloroaniline and study the biological activity for them

[a] Hussein A. ; [b] Shaimaa A. Bahgat

[1] Ministry of Education, Directorate of Education AL-Qadisiyah, Diwaniyah, Iraq

[2] Department of Chemistry, College of Education, University of Al-Qadisiyah, Iraq

Email: shaimaa.adnan@qu.edu.iq

Abstract

This study in focus was centered on the synthesis of heterocyclic compounds incorporating a seven-membered ring, specifically 1,3-oxazepine. The initial phase of the synthesis involved the preparation of azo compound (1) through the coupling of the diazonium salt of 2,3-dichloroaniline with 4-bromoacetophenone in an alkaline alcoholic medium. This was then succeeded by the reaction of azo compound (1) with 4-nitroaniline and 4-methoxyaniline in absolute ethanol, employing glacial acetic acid as a catalyst, resulting in Schiff base derivatives (2) and (3) respectively. Subsequent to this, Schiff base (2) was reacted with phthalic anhydride and maleic anhydride, as well ass succinic anhydride in a dehydrate benzene environment, leading to the formation of heterocyclic seven-membered compounds (4), (5), and (6) respectively. Lastly, Schiff base (3) was subjected to reaction with phthalic anhydride and maleic anhydride, as well as succinic anhydride in a dry benzene, resulting in the synthesis of heterocyclic seven-membered compounds (7), (8), and (9) respectively. Each of these synthesized compounds underwent characterization via FT-IR and 1H-NMR spectroscopic analysis, and the progress of reactions was monitored through Rf and TLC techniques. Melting points were recorded as part of the characterization process. Additionally, an investigation into the biological activity of these compounds was conducted against both positive and negative bacterial strains.

keywords: Schiff bases, oxazepine, azo compounds

Introduction

Heterocyclic compounds have shown a great deal of significance in the synthesis of a lot of pharmaceutical drugs [(1)]. This has increased its importance in the field of biology [(2)] , due to its participation in important biochemical processes and the formation of basic substances such as DNA and RNA, in living cells [(3)]. Heterocyclic compounds have been associated with many anaesthetics and sedatives as basic materials for many biomolecules, anti-inflammatories [(4),] antibacterial, antivirals, antiepileptics, and others. One of these important compounds is the heterocyclic oxazepine ring. Azo compound widespread compounds used as dyes in addition to their uses in the pharmaceutical industry [(5)]. azo compound can be

differentiated by functional group –N=N– the azo group which can be carry on both ends alkyl or aryl group [6] . aromatic azo compounds used widely in the chemical industries as dyes, food additives, and as initiators in free radical reaction and in drugs industry [7]. Schiff bases, prevalent and significant in the realm of coordination chemistry due to their mixed donor systems, first found recognition in the 19th century, with their synthesis reported by Schiff in 1884. The preparation of these imines was facilitated through the condensation of primary amines with an aldehyde or ketone under specific conditions[8] , Schiff bases, due to their relatively straightforward preparation, synthetic versatility, and the unique properties of the C=N group, are regarded as exceptional chelating agents. It has been discovered that their metal complexes display noteworthy biological activities. Oxazepine is a heterocyclic compound featuring a ring that is seven-membered that incorporates two heteroatoms - nitrogen and oxygen [9]. These oxazepine compounds are considered to hold biological as well as medical relevance, and possess various pharmaceutical implementations. Moreover, one of their chemical derivatives, the heteropolymer, has demonstrated a significant role in combating cancer, exhibiting efficacy against fungi and bacteria. Certain oxazepine derivatives have also been purported as medicinal drugs utilized in disease treatment [9,10].

Materials

Fourier-transform infrared (FTIR) spectra, going from 400 to 4000 cm-1, were shown on a SHIMADZU FTIR-8400S Fourier transform instrument using samples prepared in a KBr disk. The determination of melting points was executed using a Stuart apparatus, located in the UK. Both 13C-NMR and 1H-NMR spectral analyses were conducted using a Fourier transition Bruker spectrometer, working at 400MHz, with deuterated dimethyl sulfoxide (DMSO-d6) serving as the solvent. These measures were performed at the Department of Chemistry, Kashan University, Iran.

Methods

Synthesis Azo Derivative (1) [11,12]

The diazonium salt was prepared by dissolving (0.01 mol) of the amino compound 2,3-dichloroaniline in a solution consisting of 60 ml of distilled water and 4 ml of concentrated HCl. The solution were cooled to (0-5) °C inside an ice bath add to it a resolve of 20 mL Distilled water (0.01 mol ,0.7 g) of sodium nitrite ($NaNO_2$), eventually added with continuous stirring, left then for (20) minutes at a temperature of (0-5)°C to end the dizoziation method. Gradually, Then add the formed diazonium salt to the component solution from (0.01 mol ,0.797 ml) of 4-bromoacetophenone and 1 g of sodium hydroxide dissolved in 130 ml of distilled water and left the mixture for two hours with continuous stirring at PH = 6 to get a black precipitate that is washed with distilled water and then recrystallized with ethyl alcohol.

Synthesis Schiff base compounds (2,3) [13,14]

The compounds (2,3) Schiff base was prepared by reacting (0.0026 mol) of compound (1) dissolved in 10 ml ethanol absolute and put three glacial acetic acid drops with (0.3201 g, 0.0026 mol) of 4-nitroaniline (compound 2) and 4-methoxyaniline (compound 3) in (10 ml) of ethanol absolute and reflux at (78 ^{0}C) for (12 – 24 hr) , the solution is then allowed to settle at ambient temperature for 12 to 24 hours, after which the precipitate is recrystallized using methanol.

Synthesis oxazepine derivatives (4 ,5 ,6)[15]

An amalgamation was formed that incorporated 0.001 mol of compound (2) in a medium of 25 ml benzene, further supplemented with an equivalent quantity of 0.001 mol of each - phthalic anhydride as well as maleic anhydride, and succinic anhydride. This confluence was then treated under reflux conditions for a span of 28 hours, maintaining a constant thermal environment of 80°C. Post-reflux, the solution was allocated a resting period of 24 hours without interference. Subsequently, it was subjected to a filtration process and the extracted product was subjected to recrystallization, employing ethanol as the medium.

Synthesis oxazepine derivatives (7 ,8 ,9)[16]

In this procedure, 0.001 mol of compound (3) was dissolved in 25 ml of benzene. Subsequently, 0.001 mol of each of phthalic anhydride, maleic anhydride, and succinic anhydride were added to the solution. After that, this mixture was refluxed for 30 hours at 80°C. The solution was left to stand uninterrupted for 24 hours after the reflux process was finished. After filtering the solution, the result reconstituted using ethanol.

Preparation of Microbiology Culture Median

250 mL of distilled water were used to dissolve 10 g of nutrition agar to create a nutrient agar medium.. The mixture was then subjected to sterilization in an autoclave at 170 ℃ for a duration of 25 minutes. After the sterilization process, the medium was allowed to cool to a temperature of 37 °C, upon which it was poured into Petri dishes, thus rendering it suitable for bacterial streaking. The bacteria strains used, specifically Staphylococcus aureus as well as Escherichia coli, were isolated from a hospital environment. These strains were subsequently cultured on the prepared plates, which were then incubated at a constant temperature of 37 °C for duration of 24 hours to facilitate the growth of the bacteria.

Scheme1 : Prepare of some oxazepine derivatives

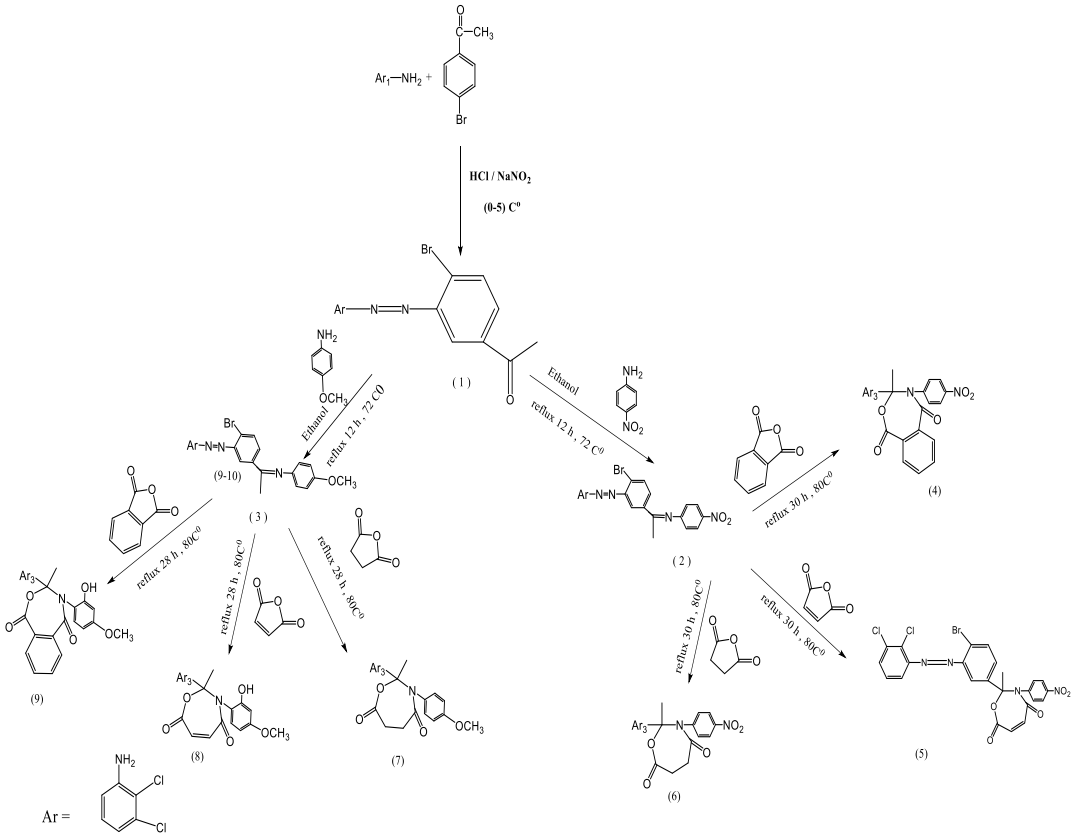

Schem1: prepare of some oxazepine derivatives

Results and Discussion

Compound 1

FT-IR spectrum data for compound (1) demonstrate band at 1712 cm^{-1} for (C=O) ,1635 cm^{-1} for (C=C) ,3070cm^{-1} for(Ar-H) ,2995 cm^{-1} for (C-H) of (CH_3) ,1440 cm^{-1} for (N=N) .^{1}H NMR (DMSO) spectrum data of compound (1) show 1.9 ppm (S , 3H , CH_3 allyl) , 7.7-7.8ppm (S ,6H , Ar-H) , . The ^{13}C- NMR (DMSO) data of spectrum compound (1) show : 27 (C_{14}) , 197 (C_{13}) , 136 ($C_{1\,,\,7}$) ,130 (C_{18} , 115-132 ($C_{aromatic}$).

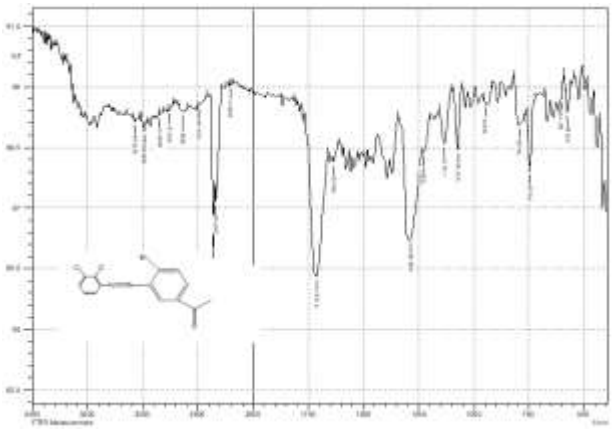

Fig. 1: FT-IR of compound 1

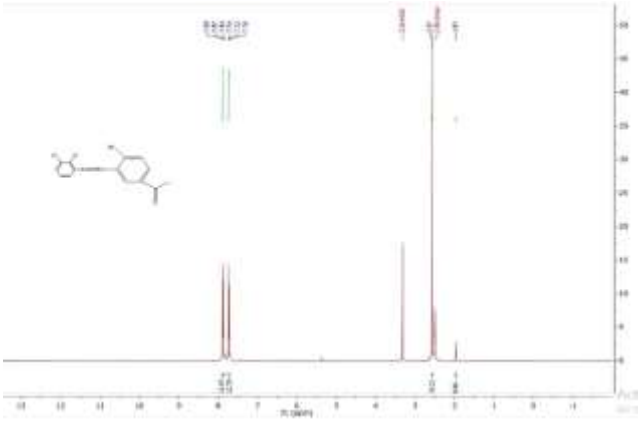

Fig. 2: ^{1}HNMR of compound 1

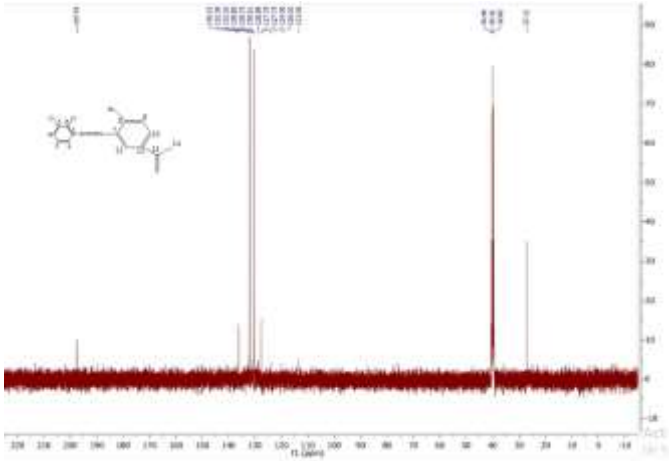

Fig. 3: ^{13}CNMR of compound 1

Compound 2

The Fourier-Transform Infrared (FT-IR) spectroscopic examination of compound (2) demonstrated specific absorbance bands at 1658 cm-1 attributed to (C=N), 1416 cm-1 assigned to (C=C), 3000 cm-1 ascribed to (Ar-H), 2800 cm-1 for (C-H) of (CH3), and 1440 cm-1 for (N=N) vibrations. The signals from compound (2)'s proton nuclear magnetic resonance (1H NMR) spectral data appeared at 2.1 ppm (singlet, 3H, CH3), 3.3 ppm (singlet, 3H, OCH3), and between 6.6-7.9 ppm (multiplet, 10H, Ar-H).. The Carbon-13 Nuclear Magnetic Resonance (13C-NMR) spectrum inside DMSO for the said compound exhibited peaks at the following chemical shifts: 27 (C13), 55 (C20), 132.1 (C2, 3), 132.9 (C10, 7), 131 (C14), and within the range of 114-130 (Caromatic).

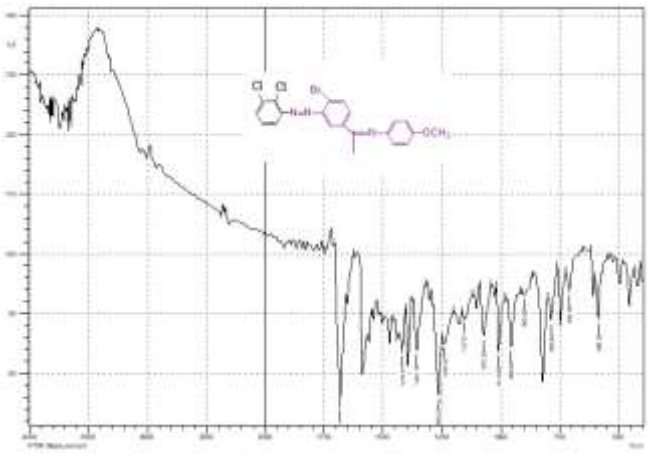

Fig. 4: FT-IR of compound 2

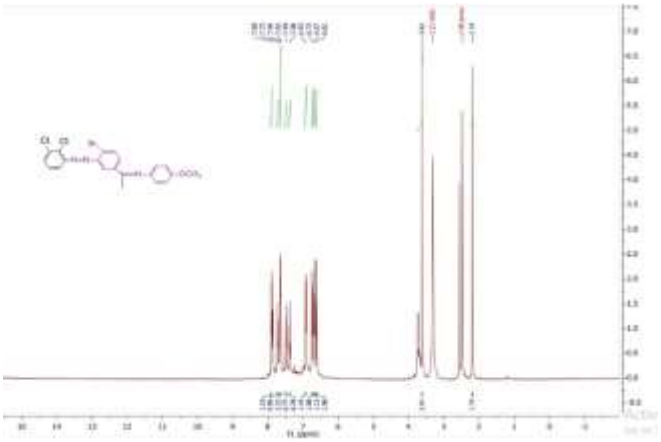

Fig. 5: ^{1}HNMR of compound 2

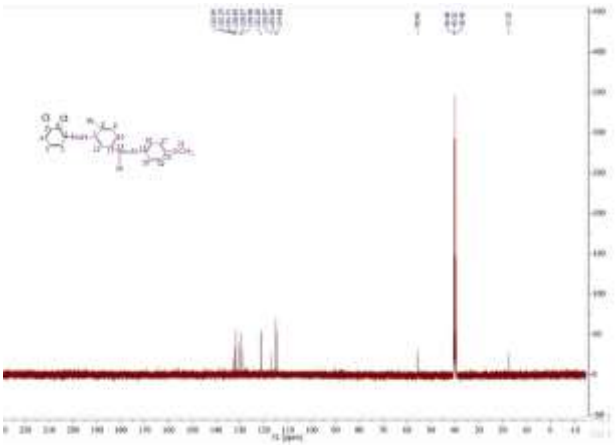

Fig. 6: ^{13}CNMR of compound 2

Compound 3

FT-IR spectrum data to compound (1) express band at 1681 cm^{-1} for (C=N) ,1620 cm^{-1} for (C=C) ,3008cm^{-1} for (Ar-H) ,2964 cm^{-1} for (C-H) of (CH_3) ,1398 cm^{-1} for (N=N). ^{1}H NMR (DMSO) spectrum data of compound (3) make 2.9 ppm (S , 3H , CH_3) , 7.2-7.9ppm (M ,10H , Ar-H) , . The ^{13}C- NMR (DMSO) spectrum data of compound (3) express: 15 (C_{20}) , 149 (C_{13}) , 135 (C_{18}) , 114-134 ($C_{aromatic}$) .

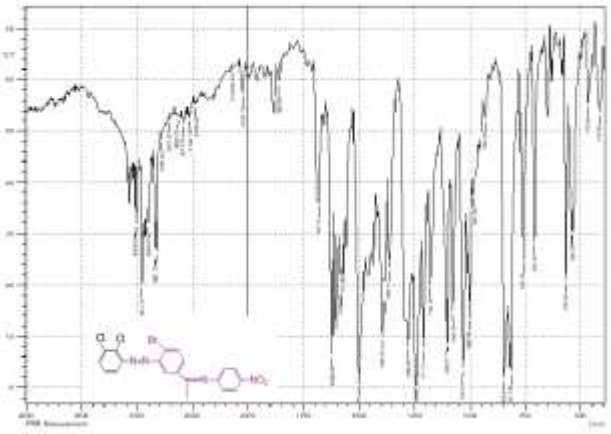

Fig. 7: FT-IR of compound 3

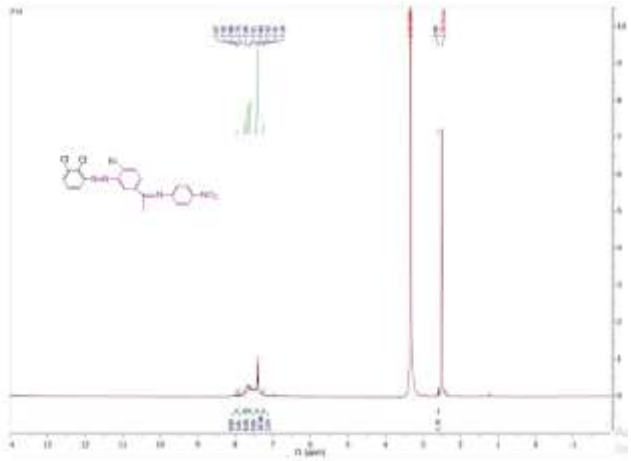

Fig. 8: ^{1}HNMR of compound 3

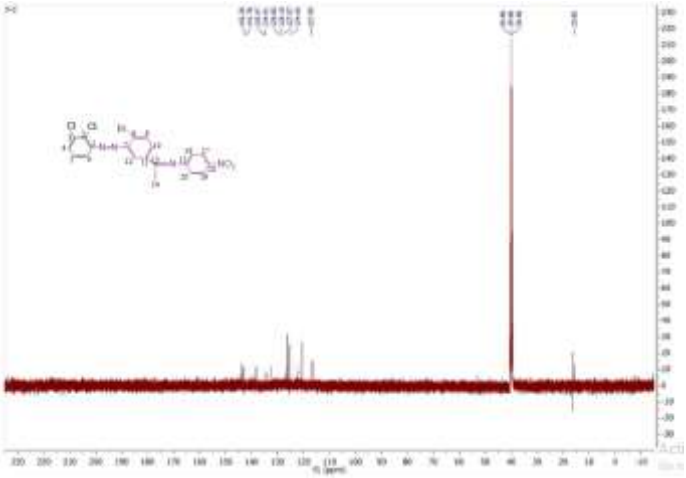

Fig. 9: ^{13}CNMR of compound 3

Compound 4

FT-IR spectrum data for compound (4) ex express and at 3000cm^{-1} for(Ar-H) , 2839 cm^{-1} for (C-H) of (CH_3) , 1700 cm^{-1} (C=O) amid , 1600 cm^{-1} for (C=C) , (1180) cm^{-1} for (C-O-C) and 1257 cm^{-1} for (C-N) of oxazepine . ^{1}H NMR (DMSO) spectrum data for compound (4) show 2.5 ppm (d , 3H , CH_3) ,3.6ppm (q ,

CH) , 6.5-7.8ppm (M ,14H , Ar-H) . The ^{13}C- NMR (DMSO) spectrum data of compound (4) make: 27 (C_{26}) , 55 (C_{13}) , 166-170 ($C_{14\,,\,17}$) , 151($C_{1\,,\,7}$) , 144 ($C_{2\,,\,3}$) ,134 (C_8) , 139 (C_{14}) , 114-132 ($C_{aromatic}$) .

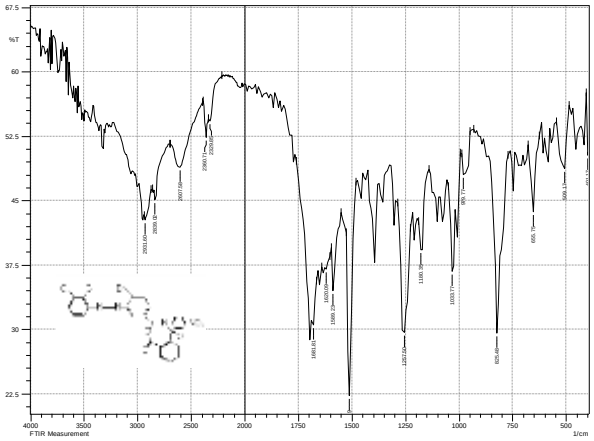

Fig. 10: FT-IR of compound 4

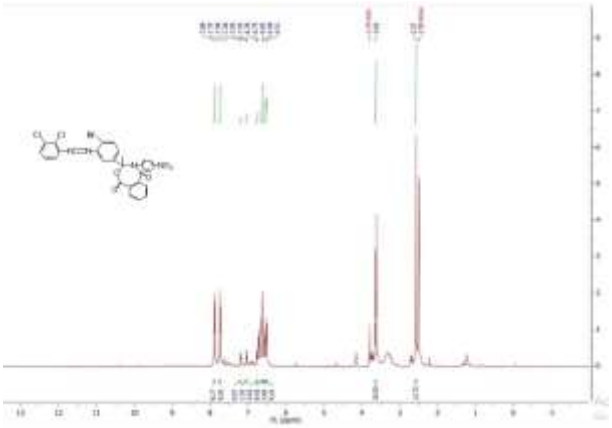

Fig. 11: ^{1}HNMR of compound 4

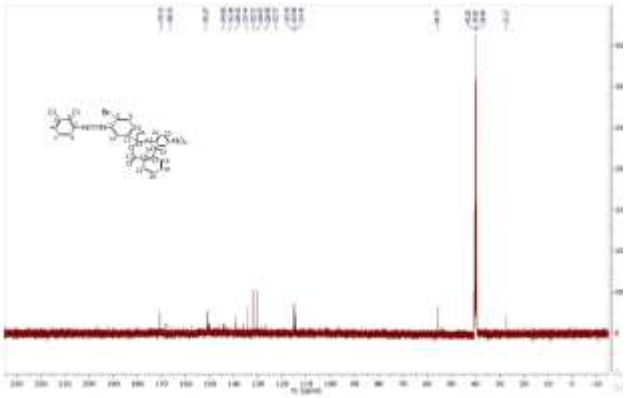

Fig. 12: ^{13}CNMR of compound 4

Compound 5

FT-IR spectrum data for compound (5) demonstrate band at 3170 cm^{-1} for(Ar-H) , 2970 cm^{-1} for (C-H) of (CH_3) , 1624 cm^{-1} (C=O) amid , 1458 cm^{-1} for (C=C) , (1180) cm^{-1} for (C-O-C) and 1157 cm^{-1} for (C-N) oxazepine.^{1}H NMR (DMSO) spectrum data for compound (5) express 1.2 ppm (S , 3H , CH_3) , 4.2 ppm (S ,4H , CH=CH) , 7-7.7ppm (S ,10H , Ar-H) , . The ^{13}C- NMR (DMSO) data spectrum compound

(5) show : 14 (C_{24}) , 61 (C_{13}) , 129($C_{15,16}$) , 142($C_{1,7}$) , 168,169($C_{14,17}$) , 137(C_{21}) , 135(C_8) , 114 – 131 ($C_{aromatic}$) .

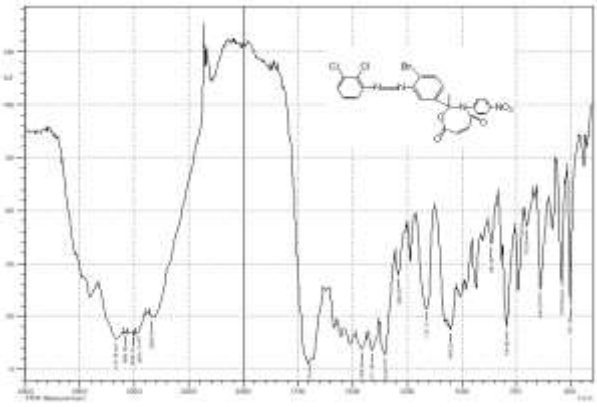

Fig. 13: FT-IR of compound 5

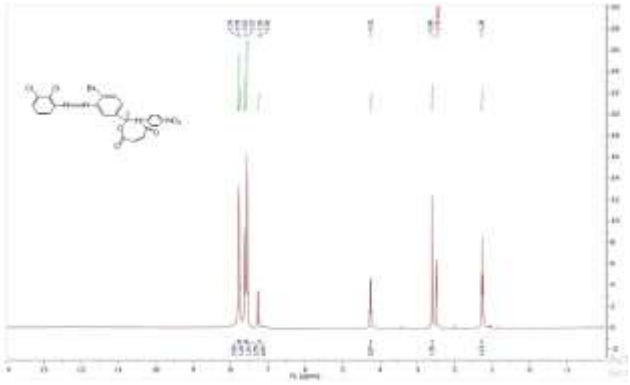

Fig. 14: HNMR of compound 5

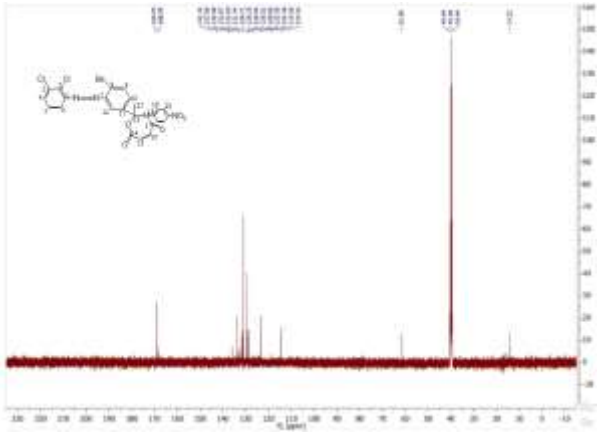

Fig. 15: ^{13}CNMR of compound 5

Compound 6

FT-IR spectrum data for compound (6) express band at 3170 cm^{-1} for(Ar-H) , 2970 cm^{-1} for (C-H) of (CH_3) , 1700 cm^{-1} (C=O) amid , 1580 cm^{-1} of (C=C) , (1180) cm^{-1} for (C-O-C) and 1157 cm^{-1} for (C-N) for oxazepine . ^{1}H NMR (DMSO) spectrum data of compound (6) make 1.2 ppm (S , 3H , CH_3 allyl) ,

3.79,3.72 ppm (t ,4H , CH_2-CH_2) , 6. 8-7.9ppm (M ,10H , Ar-H) . The ^{13}C- NMR (DMSO) spectrum data of compound (6) express : 14(C_{24}) , 55,73 ($C_{15,16}$) , 22 (C_{13}) , 167,175 ($C_{14,17}$) , 114-135 ($C_{aromatic}$) .

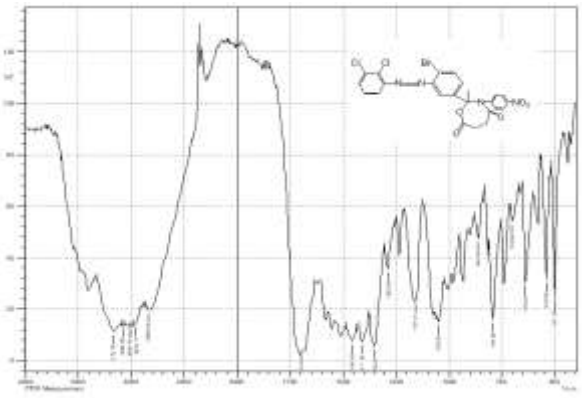

Fig. 16: FT-IR of compound 6

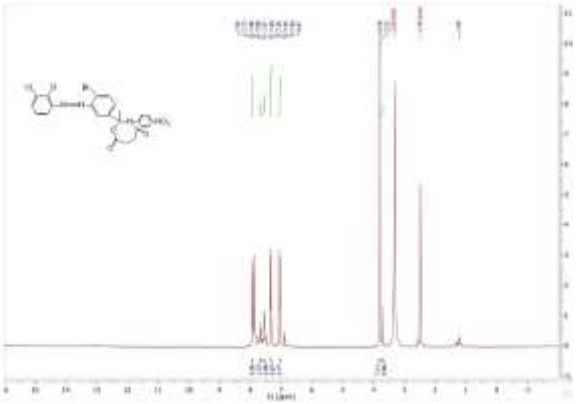

Fig. 17:^{1}HNMR of compound 6

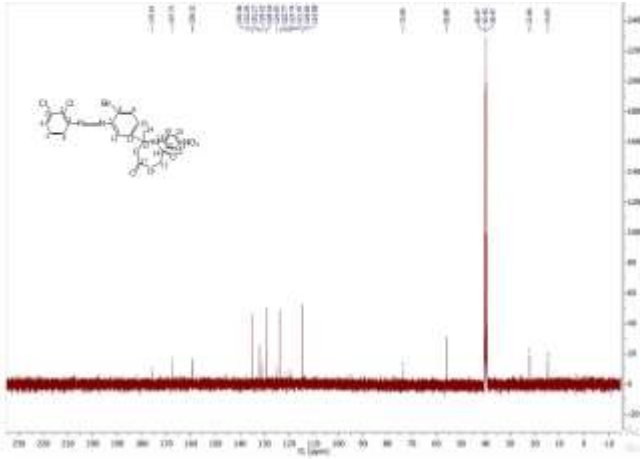

Fig. 18:^{13}CNMR of compound 6

Compound 7

FT-IR spectrum data for compound (7) demonstrate band at 3065 cm^{-1} for (Ar-H), 2970 cm^{-1} for (C-H) of (CH_3), 1624 cm^{-1} (C=O) amid, 1458 cm^{-1} for (C=C), (1180) cm^{-1} for (C-O-C) and 1157 cm^{-1} for (C-N) for oxazepine. ^{1}H NMR (DMSO) spectrum data of compound (7) make 1.2 ppm (S , 3H , CH_3) , 1.99 ppm

(S , 3H , OCH_3) , 5.4 ppm (T ,4H , CH_2-CH_2) , 6.5-7.7ppm (S ,10H , Ar-H) , . The ^{13}C- NMR (DMSO) spectrum data of compound (7) express: 163,169 ($C_{14,17}$), 16(C_{24}), 59(C_{10}), 77,69($C_{15,16}$), 100-155 ($C_{aromatic}$)

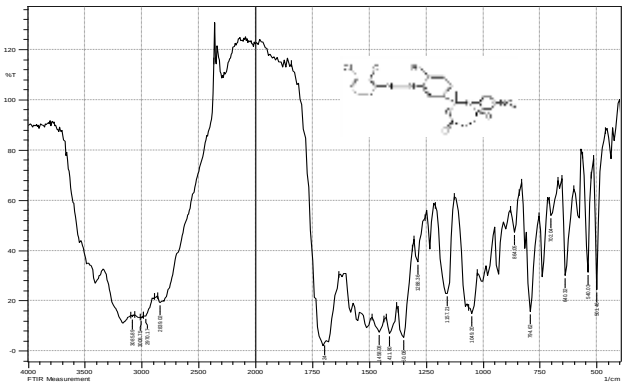

Fig. 19: FT-IR of compound 7

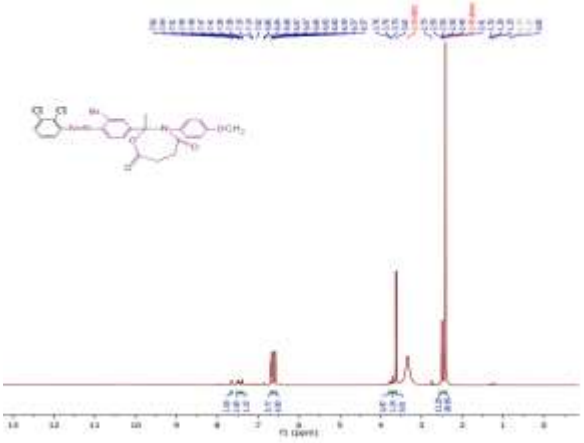

Fig. 20: ^{1}HNMR of compound 7

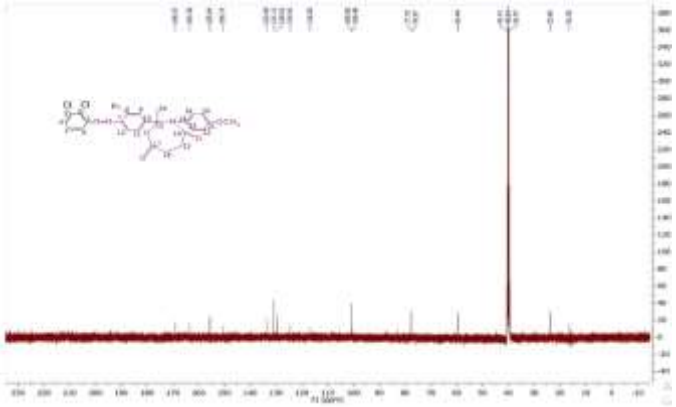

Fig. 21: ^{13}CNMR of compound 7

Compound 8

FT-IR spectrum data for compound (8) demonstrate band at 3162 cm^{-1} for (Ar-H), 2930 cm^{-1} for (C-H) of (CH_3), 1712 cm^{-1} (C=O) amid, 1512 cm^{-1} for (C=C), (1172) cm^{-1} for (C-O-C) and 1030 cm^{-1} for (C-N) for oxazepine. ^{1}H NMR (DMSO) spectrum data of compound (8) express 2 ppm (S, 3H, CH_3), 2.55 ppm (S, 3H, OCH_3), 5.5 ppm (d ,2H, CH_2=CH_2), 6.1-7.8ppm (M ,10H, Ar-H), The ^{13}C- NMR (DMSO) spectrum data of compound (8) make: 166,167 ($C_{14,17}$) , 21(C_{24}) , 55(C_{13}) , 27(C_{25}) , 140($C_{15,16}$) , 101-158 ($C_{aromatic}$)

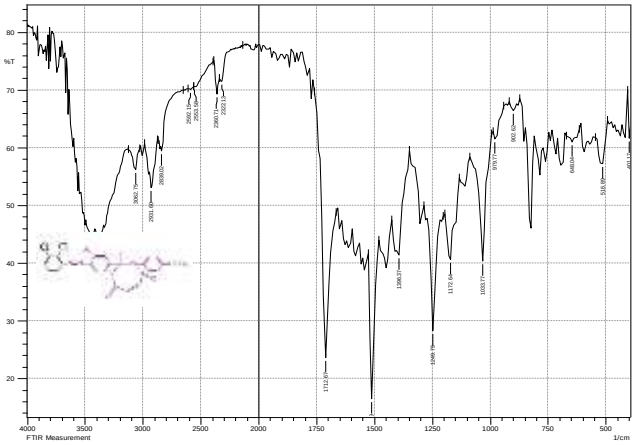

Fig. 22: IR of compound 8

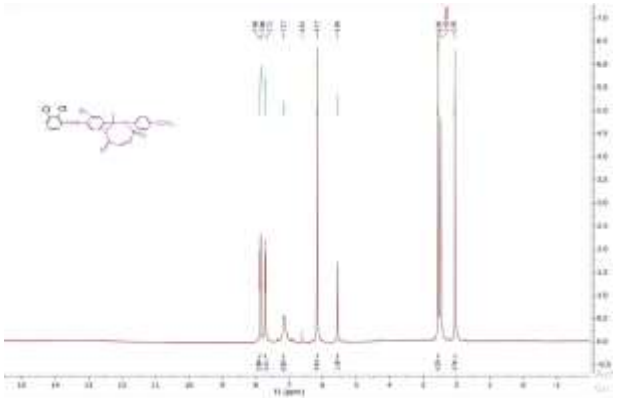

Fig. 23: ^{1}HNMR of compound 8

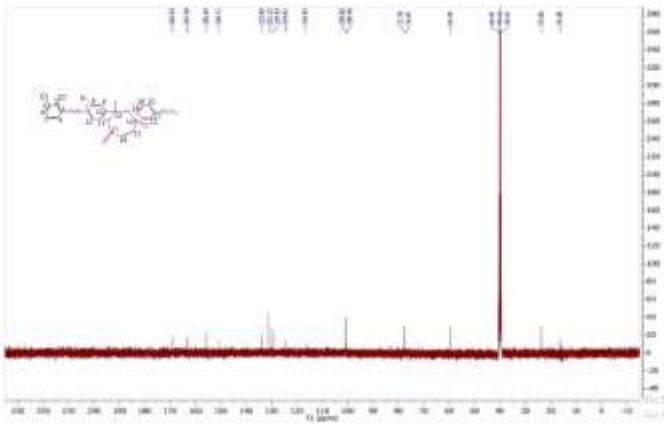

Fig. 24: ^{13}CNMR of compound 8

Compound 9

The Fourier-Transform Infrared (FT-IR) spectroscopic investigation of compound (8) depicted characteristic absorption bands at 3062 cm-1 corresponding to (Ar-H), 2931 cm-1 designated for (C-H) of (CH3), 1712 cm-1 (C=O) amide, 1635 cm-1 representing (C=C), 1180 cm-1 ascribed to (C-O-C), and 1049 cm-1 attributed to (C-N) for oxazepine. Spectral study of the proton nuclear magnetic resonance (1H NMR), structured in DMSO for compound (9), presented resonances at 1.2 ppm (singlet, 3H, CH3), 1.99 ppm (singlet, 3H, OCH3), and a range of 6.5-7.7 ppm (multiple, 10H, Ar-H). The Carbon-13 Nuclear Magnetic

Resonance (13C-NMR) spectral data, made in DMSO for compound (9), demonstrated peaks at the following chemical shifts: 154,167 (C14,17), 21 (C28), 27 (C28), 54 (C13), and a range of 101-136 (C aromatic).

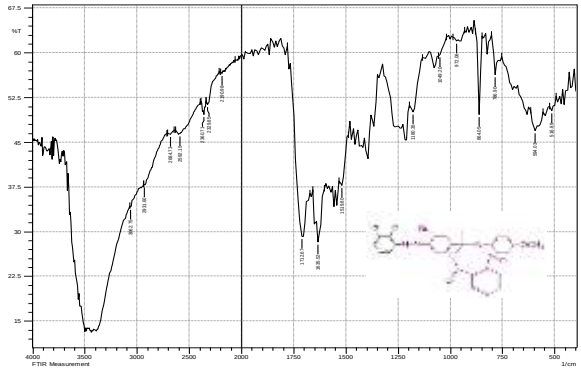

Fig. 25: FT-IR of compound 9

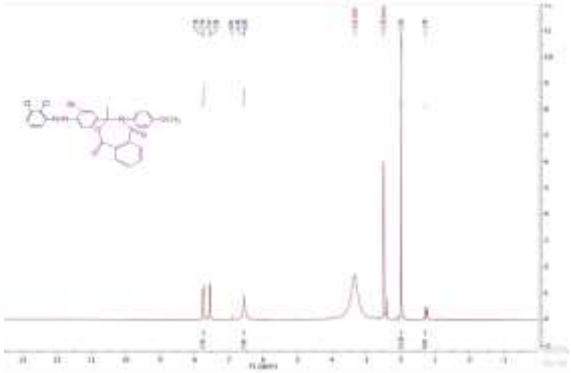

Fig. 26:^{1}HNMR of compound 9

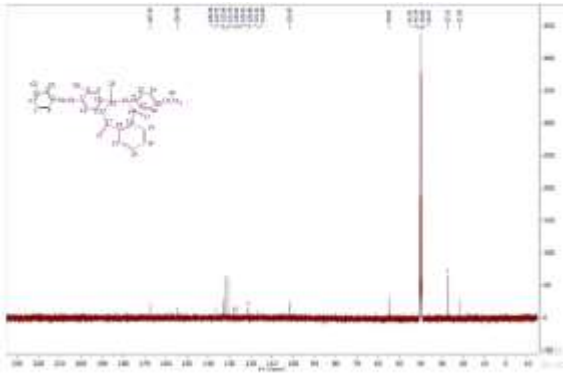

Fig. 27:^{13}CNMR of compound 9

Conclusion

It may be inferred from the aforementioned research that the synthetic chemicals significantly inhibit the growth of the bacteria Escherichia coli and staphylococcus aurous. The findings of the antibacterial activity are displayed in fig. 28. The compounds that showed promising action were (3,4,6,9) and (9,10)

against staphylococcus aurous and Escherichia coli,

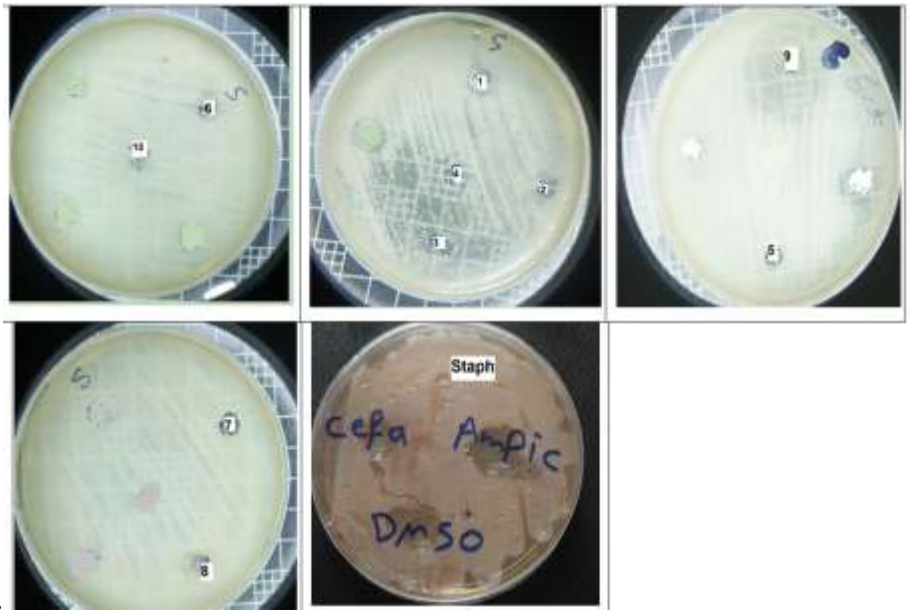

respectively.

Fig. 28: Biological activity of compound prepared against *Staphylococcus Aurous*

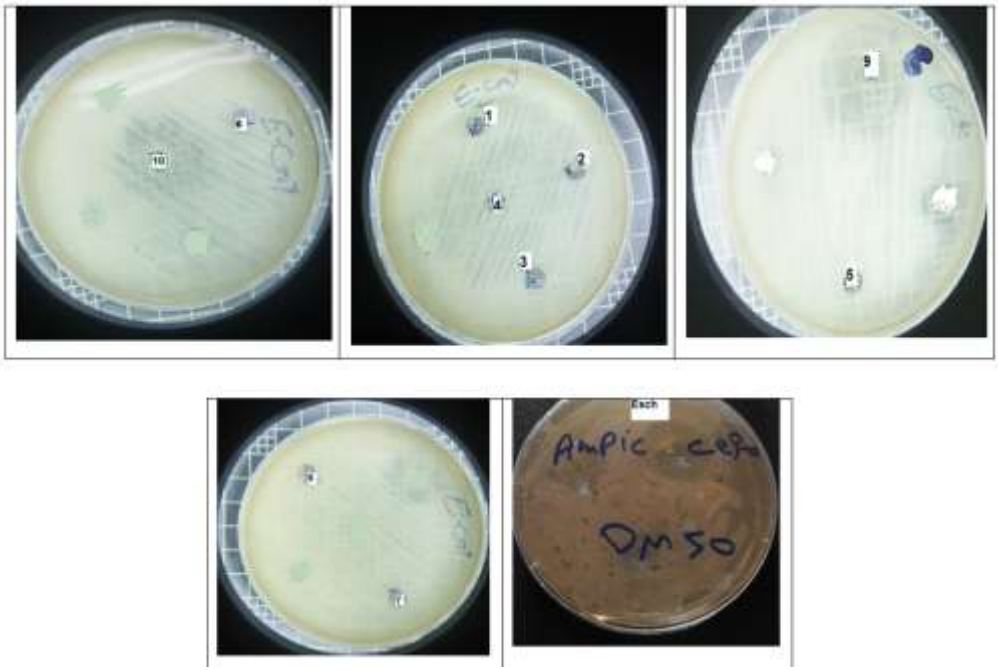

Fig. 29: Biological activity of compound prepared *Escherichia Coli*

Table 1: Activity is classified based on the extent of inhibition

Compounds NO.	**Bacterial species**	
	Staph. Aureus	*E. coli*
3	++	+

4	++	_
5	+	+
6	++	_
7	_	+
8	_	+
9	+++	+++

Activity is classified based on the extent of inhibition. Inactivity, denoted as "No inhibition", implies no observable effect. "Slightly active" is designated by "+" and corresponds to an inhibition measurement ranging between 5-10 mm. "Moderately active", symbolized as "++", refers to an inhibition measurement within the range of 11-20 mm. A significantly active state, represented as "+++", corresponds to inhibition measurements exceeding 20 mm, indicating good activity.

Table 2: Preparation of Some Oxazepine Derivatives

No.	Name of comp.	M.F	M.W	M.P(C°)	R.f	Color	%
1	1-(4-bromo-3-((2,3-dichlorophenyl)diazenyl)phenyl)ethan-1-one	$C_{13}H_{11}BrN_4O_2$	335.16	95	-	Dark brown	67
2	1-(2-bromo-5-(2-((4-nitrophenyl)imino) -2-yl)phenyl)-2-(4-nitrophenyl)diazene	$C_{21}H_{16}BrCl_2N_4O_2$	507.19	serum	0.12	Dark brown	85
3	1-(2-bromo-5-(2-((4-methoxyphenyl)imino) -2-yl)phenyl)-2-(2,3-dichlorophenyl)diazene	$C_{22}H_{19}BrC_{l2}N_3O$	492.22	serum	0.57	Dark brown	91
4	3-(4-bromo-3-((2,3-dichlorophenyl)amino)phenyl)-4-(2,3-dichlorophenyl)-3-methyl-3,4-dihydrobenzo[e][1,3]oxazepine-1,5-dione	$C_{28}H_{17}BrCl_4N_2O_3$	651.16	180	0.11	Dark brown	79
5	2-(4-bromo-3-((2,3-dichlorophenyl)amino)phenyl)-3-(2,3-dichlorophenyl)-2-methyl-2,3-dihydro-1,3-oxazepine-4,7-dione	$C_{24}H_{15}BrCl_4N_2O_3$	601.10	172	0.52	Dark brown	91
6	-(4-bromo-3-((2,3-dichlorophenyl)amino)phenyl)-1-(N-(2,3-dichlorophenyl) formamido)ethyl	$C_{23}H_{17}BrCl_4N_2O_3$	591.10	140	0.21	Dark brow	85

						n	
7	3-(4-bromo-3-((2,3-dichlorophenyl)amino)phenyl)-4-(4-hydroxy-6-methylpyrimidin-2-yl)-3-methyl-3,4-dihydrobenzo [e][1,3]oxazepine-1,5-	$C_{28}H_{23}BrCl_2N_4O_4$	630.32	149	0.42	Dark brown	70
8	2-(4-bromo-3-((2,3-dichlorophenyl)amino)phenyl)-3-(4-hydroxy-6-methylpyrimidin-2-yl)-2-methyl-2,3-dihydro-1,3-oxazepine-4,7-dione	$C_{24}H_{21}BrCl_2N_4O_4$	580.26	166	0.031	Dark brown	65
9	22-(4-bromo-3-((2,3-dichlorophenyl)amino)phenyl)-3-(4-hydroxy-6-methylpyrimidin-2-yl)-2-methyl-1,3-oxazepane-4,7-dione	$C_{24}H_{23}BrCl_2N_4O_4$	582.28	150	0.77	Dark brown	80

References

1- R.A Ghafil, N Alrazkb, N.M Aljamali," Synthesis of Triazole Derivatives via Multi Components Reaction and Studying of (Organic Characterization, Chromatographic Behavior, Chem-physical Properties)" Egypt. J. Chem. , vol(63), pp.4163-4174, (2020) .

2- Allamy, A. K. N., & Mejbel, S. A. (2022). Preparation, characterization and biological activity of some new seven-membered heterocyclic compounds. World Journal of Advanced Research and Reviews, 15(1), 662-678..

3- Salim Jasim, S. (2018). Synthesis and Characterization of Some Bis-1, 3 Oxazepine-4, 7-dione and 1, 3–Diazepine-4, 7-dione Derivatives. Kirkuk University Journal-Scientific Studies, 13(2), 149-165.

4- Khder, A. M., Sh, M. K., & Al-Jawady, M. (2022). Synthesis of some heterocyclic compounds derived from ortho-carboxybenzaldehyde. Egyptian Journal of Chemistry, 65(1), 143-150.

5- Hussein, M. S., Al-Lami, N., & Al-Jeilawi, O. H. R. (2022). Design, Synthesis of Imidazolone and Oxazepine Derivatives Bearing Imidazo (2, 1-b) Thiazole along with its Antimicrobial Activity. Chem. Methodol., 6(4), 319-330.

6- Salih, N., Salimon, J., & Hussien, H. (2021). Synthesis, characterization and in vitro antibacterial activity of novel 1, 2, 4-triazine and 1, 2-diazepine derivatives. hemoglobin, 18, 21.

7- Muhiebes, R. M., & Al-Tamimi, E. O. (2021). Chemical Methodologies.

8- Fino, R., Lenhart, D., Kalel, V. C., Softley, C. A., Napolitano, V., Byrne, R., ... & Popowicz, G. M. (2021). Computer-Aided Design and Synthesis of a New Class of PEX14 Inhibitors: Substituted 2, 3, 4, 5-Tetrahydrobenzo [F][1, 4] oxazepines as Potential New Trypanocidal Agents. Journal of Chemical Information and Modeling, 61(10), 5256-5268.

9- Sulyman, Z. H., & Ahmed, N. G. (2020). Synthesis of New Oxazepine and Thaizolidine Compounds derived from Pyrimidine-2 (1H)-one. Journal of Education and Science, 29(2), 186-200.

10- A Ahmed, A., & G Ahmed, N. (2020). Synthesis of Some New Benzoxazepine Compounds Form Derivatives of Schiff Bases. Journal of Education and Science, 29(1), 218-232.

11- Salim Jasim, S. (2018). Synthesis and Characterization of Some Bis-1, 3 Oxazepine-4, 7-dione and 1, 3–Diazepine-4, 7-dione Derivatives. Kirkuk University Journal-Scientific Studies, 13(2), 149-165.

12- Jabbar, S. A. S., Jumaa, F. H., & Mawlood, H. Q. (2015). Synthesis and Characterization of some bis 1, 3-Oxazepine and 2, 3-Dihydroquinozoline derivatives. Tikrit Journal of Pure Science, 20(2), 110-120.

13- Uçan, S. Y., Uçan, M., & Mercimek, B. (2005). Synthesis and characterization of new Schiff bases and their cobalt (II), nickel (II), copper (II), zinc (II), cadmium (II) and mercury (II) complexes. Synthesis and Reactivity in Inorganic, Metal-Organic and Nano-Metal Chemistry, 35(5), 417-421.

14- Abbas, S. F., Tomma, J. H., & Ali, E. T. (2021). Synthesis And Characterization Of New Schiff Bases And Their 1, 3-Oxazepines Derived From Phthalic Anhydride. Systematic Reviews in Pharmacy, 12(2), 260-265.

15- Al-Tufah, M. M., Al-Badrany, K. A., & Jasim, S. S. (2021). Synthesis and antibacterial evaluation of some New 1, 5-Benzooxazepines derivatives. Systematic Reviews in Pharmacy, 12(3), 270-285.

16- Jahandar Lashaki, M., Hajinasiri, R., Hossaini, Z., & Nami, N. (2022). Ag/KF/CP@ MWCNTs Catalyzed Green Synthetic Pathway for Bio-Active New Thiazolopyrimidines and Oxazolopyrimidines. Polycyclic Aromatic Compounds, 1-19.